COHESIN DYNAMICS DURING MEIOTIC PROPHASE

a thesis submitted for the degree of

Doctor of Philosophy

2013

SARAH TESTORI

Imperial College London

MRC Clinical Sciences Centre

DECLARATION OF ORIGINALITY

I, hereby, declare that the work presented in this thesis is my own and has not been submitted in any form for another degree or diploma at any other university. Information derived from the published work of others has been acknowledged in the text and a list of references is given.

Signed: Date:

COPYRIGHT DECLARATION

ACKNOWLEDGEMENTS

First and foremost I'd like to thank my supervisor Fadri Martinez-Perez for his endless enthusiasm, encouragement and patience, and for his constant assurance that, "It will work!" in the face of my overwhelming scepticism. Likewise my thanks go out to everyone in the Meiosis Group, for their technical and moral support, as well as for providing some much needed lab entertainment. In particular I'd like to give massive thanks to Jim Lightfoot for starting me off on the cohesin project and teaching me how to behead worms like a ninja. I owe you, man. Huge gratitude also goes out to Olly Crawley, who joined me on the WAPL project, for his unflappable optimism, and for always being there with tea and biscuits when needed. Finally, thanks to my friends and family for always being there for a few at the end of the day. Cheers!

ABSTRACT

For faithful segregation during meiosis, chromosomes must be physically linked by both sister chromatid cohesion (SCC), provided by cohesin, and at least one crossover (CO). In mitosis, cohesin is dynamically associated with chromatin and this has been shown to be crucial for the repair of DSBs. Although DSBs are purposely made to start meiotic recombination, it is unknown if meiotic cohesin is dynamically associated with chromatin. However, cohesin loss or degradation is thought to be involved in the high incidence of aneuploidy observed in human eggs. In *Caenorhabditis elegans* (*C. elegans*), the cohesin loader SCC-2 remains associated with the axial element of meiotic chromosomes following the completion of S-phase, hinting that cohesin may be reloaded during meiotic prophase. To confirm this, I investigated if depleting SCC-2 by RNAi after entrance into meiotic prophase had an effect on cohesin association with chromosomes. This revealed loss of the cohesin subunit REC-8 from late prophase nuclei, suggesting that without reloading cohesin is removed from chromatin. Furthermore, *scc-2* RNAi also resulted in the impairment of chiasmata, raising the possibility that cohesin reloading plays a role in CO formation or in chiasma maintenance. Two key mediators of cohesin removal are known to operate during the G2 phase of the mitotic cell cycle: the presence of DSBs and the cohesion anti-establishment factor Wapl1. Here I show for the first time that WAPL-1 modulates the cohesiveness of complexes containing the meiosis-specific kleisins COH-3 and COH-4. Furthermore, cohesin complexes containing different kleisins are differentially modulated by DSBs, and only REC-8-containing cohesin complexes can undertake the repair of DNA damage. Finally, I have developed several genetic tools to allow the visualization of cohesin turnover during meiosis. These findings show the exceptional complexity of cohesin dynamics during meiotic prophase, as well as demonstrating roles for cohesin outside of the provision of SCC.

TABLE OF CONTENTS

LIST OF TABLES

LIST OF FIGURES

LIST OF ABBREVIATIONS

9-1-1	Rad9-Rad1-Hus1 complex (C. elegans HPR-9, MRT-2 and HUS-1)
AE	Axial element
APC	Anaphase promoting complex
ATP	Adenosine 5'-triphosphate
BSA	Bovine serum albumin
CE	Central element
CGC	Caenorhabditis Genetics Centre
cM	CentiMorgan
CO	Crossover
D-loop	displacement loop
DAPI	(4', 6-diamidino-2-phenylindole)
DIG	Digoxigenin
DNA	deoxyribonucleic acid
dHJ	Double Holliday junction
dNTP	deoxyribonucleotide triphosphate
DSB	double stranded break
dsDNA	Double stranded DNA
dsRNA	Double stranded RNA
dpy	Dumpy
DTC	Distal tip cell
EMS	Ethylmethane sulphonate
EDTA	Ethylenediaminetetraacetic acid
FISH	Fluorescence in situ hybridization
FITC	Fluorescein isothiocyanate
g	Grams
GFP	Green fluorescent protein
Gys	Grays
him	High incidence of males
hr	Hours
HR	Homologous recombination
HRR	Homologue recognition region

ID	Inside diameter
L4	Larval moult 4
l	Litres
LB	Lysogeny broth
MI	Meiosis I
MII	Meiosis II
M9	Salt buffer
M	Molarity
min	Minutes
ml	Millitres
mm	Millimetre
mRNA	Messenger RNA
MRX	Mre11-Rad50-Xrs2 complex
NCO	Non-crossover
NE	Nuclear envelope
ng	Nanogramme
NGM	Nematode growth media
NHEJ	Non-homologous end-joining
NBRP	National Bioresource Project
OD	Outside diameter
ON	Overnight
OP50	Attenuated E. coli strain
PBS	Phosphate buffered saline
PBST	Phosphate buffered saline Tween
PC	Pairing Centre
PCR	Polymerase chain reaction
PFA	Paraformaldehyde
rDNA	Ribosomal DNA
RNA	Ribonucleic acid
RNAi	RNA interference
rpm	Revolutions per minute
RT	Room temperature
SC	Synaptonemal complex

SCC	Sister chromatid cohesion
sec	Seconds
SD	Standard deviation
SEI	Single end invasion
SMC	Structural maintenance of chromosomes
SNP	Single nucleotide polymorphism
SPB	Spindle Pole Body
sqt	Squat (short and rolls)
SSC	Saline-sodium citrate buffer
SSCT	Saline-sodium citrate tween buffer
ssDNA	Single stranded DNA
ssRNA	Single stranded RNA
SYTO12	Vital dye
TAE	Tris base, acetic acid and EDTA buffer
Tm	Melting temperature
TZ	Transition zone
unc	Uncoordinated
ZMM	Zip1-Zip2-Zip3-Zip4-Msh4-Msh5-Mer3 complex
mg	Microgram
ml	Microlitres
mm	Micrometres
mM	Micromolar
°C	Degree centigrade

CHAPTER 1: INTRODUCTION

1.1 Background

A cell contains in its nucleus the information that allows it to produce every protein it will need, giving it the capacity to grow, divide and responsed correctly to external stimuli. This information is stored as DNA, which is tightly packaged to form chromosomes, allowing DNA molecules that would otherwise be metres long to fit into a nucleus only a few microns in diameter. Cells must be able to maintain this information with almost perfect fidelity and pass it from one generation to the next. In order to do this, chromosomes must be replicated along their entire length, creating two identical copies, known as sister chromatids, which are then separated equally into two daughter cells. For the process of chromosome segregation to occur faithfully, sister chromatids must be held together from the completion of DNA replication until their separation on the mitotic spindle, a function that is performed by a protein complex known as cohesin, which associates with DNA to provide sister chromatid cohesion (SCC). Therefore, a crucial aspect of the mitotic cell cycle is the regulation of SCC, culminating with the sudden destruction of the cohesin complex at anaphase onset to allow segregation of sister chromatids into the daughter cells.

In sexually-reproducing organisms, another more complex cell division program called meiosis occurs. This is because these organisms carry two copies of each chromosome, which are known as homologous chromosomes or homologues, and therefore in order to maintain the chromosome number constant across generations the homologues need to be separated during gamete formation. Thus, when two gametes fuse, the resulting cell contains a complete complement of chromosomes, half from each parent, providing diversity in populations and driving evolution. In order to ensure that gametes receive a single copy of each chromosome, meiosis consists of a single round of DNA replication that is followed by two successive rounds of chromosome segregation. Homologues are separated during the first division and then sister chromatids are partitioned in the second meiotic division. In order for this

segregation pattern to occur, homologous chromosomes must pair with one another and at least one inter-homologue crossover event must be formed during meiotic recombination. Inter-homologue crossovers events, together with sister chromatid cohesion, provide a temporary link between homologous chromosomes, which is required for their correct orientation on the first meiotic spindle. The selective destruction of cohesion in non-centromeric regions allows the separation of the homologues towards opposite poles of the forming daughter cells at meiosis I, while ensuring that sister chromatids migrate together. Then, the dissolution of the remaining sister chromatid cohesion at meiosis II releases the sister chromatids, resulting in their ordered separation. It is therefore essential to life that the cohesin complex is tightly regulated throughout mitosis and meiosis.

Cohesin also has a vital role in the repair of DNA damage, the formation of inter-homologue crossovers in meiosis, and in the regulation of gene expression in differentiated cells. It is therefore, unsurprising that perturbing cohesin function can have serious deleterious effects, including impaired chromosome segregation and an inability to effectively repair DNA damage, both of which are implicated in the pathology of many cancers. When chromosome segregation is impaired in meiosis this can lead to the formation of aneuploid gametes, which is thought to be the leading cause of miscarriages and birth defects in humans. Therefore understanding the regulation of sister chromatid cohesion is not only key to furthering our knowledge of the fundamental events of cell division and consequently life, but may also lead to insights which have an impact on treatment of human disease. Despite this, there are many questions regarding the cohesin cycle, especially in meiosis, that remain unanswered.

1.2 Meiosis

Meiosis is the specialized mode of cell division that results in the formation of gametes. It is characterized by a single round of genome duplication followed by two consecutive rounds of chromosome segregation resulting in cells with a haploid chromosome complement. The first meiotic division is reductional and

separates homologous chromosomes from one another, whereas the second meiotic division is equational and separates sister chromatids, in a manner reminiscent of mitosis. Meiosis is an essential process for all sexually-reproducing organisms. It involves the exchange of genetic material between parental chromosomes, creating diversity, and results in the creation of haploid gametes from diploid precursors. To do this, the mitotic cycle is highly modified and numerous meiosis-specific events occur. During prophase of meiosis I, homologous chromosomes pair, align and synapse, before undergoing crossover recombination, thereby exchanging genetic material. This exchange between the two DNA molecules, along with sister chromatid cohesion (SCC) creates a physical link between homologous chromosome pairs, known as chiasmata, and it promotes proper segregation of the homologous on the meiotic spindle at metaphase I (Zickler and Kleckner, 1999). At the first meiotic division only cohesion at the pericentromeric region of chromosome is maintained, while cohesin on the chromosome arms is lost. This facilitates the separation of homologues at anaphase I. At anaphase II the remaining pericentromeric cohesin is lost enabling sister chromatids to segregate. The cohesin complex therefore has an essential role that is specific to meiosis in addition to those functions critical to mitosis (See Fig. 1 for a summary of the key events of meiosis).

1.2.1 Clinical relevance of meiosis

The study of meiosis is of great significance medically as it is highly error prone in humans, particularly in females where aneuploidy originated during meiosis is thought to be the leading cause of spontaneous abortions, and causes genetic abnormalities and sterility in high frequencies. Analysis of human karyotypes from embryos at various developmental stages reveals the extent to which meiosis fails to occur properly. It is not possible to generate data accurately earlier than 6 weeks of gestation, however, between 6 and 20 weeks of gestation aneuploidy was detected in a staggering ~35% of clinically recognised spontaneous abortions. Later in pregnancy abnormal karyotypes were also high

a ~4% of stillbirths, and ~0.3% of live births, carrying an abnormal karyotype (Hassold and Hunt, 2001).

The vast majority of aneuploidies are incompatible with life, however there are five trisomies that can be tolerated. Trisomy 21, known as Down's syndrome, and trisomies of the sex chromosomes, Kleinfelter's syndrome (XXY) and Triple X syndrome (XXX) all have very high survivabilities, though cause an array of disorders with varying severities. Turner's syndrome (XO) in which one X chromosome is missing presents another configuration of aneuploidy that can be tolerated to adulthood. Trisomies of chromosomes 13 and 18, called Patau syndrome and Edwards syndrome respectively, however have a very poor prognosis, with more than 80% of children with trisomy 13 dying in the first year, and even lower survival for infants with trisomy 18. In the case of Down's syndrome it has been long acknowledged that the incidence rises with increasing maternal age (Hassold et al., 2007; Yoon et al., 1996). It is unclear how and why there are such high levels of nondisjunction in human meiosis, but hopefully continuing study of this topic can yield insights that may lead to treatment of conditions such as human infertility, as well as illuminating the mechanisms underlying a fundamental biological process.

1.2.2 *C. elegans* as a model organism for investigating meiosis

Research into meiosis in humans poses two major difficulties; the ethical barriers to working with human tissues, and the scarcity of human meiotic cells, in particular oocytes. In addition to this, in females, meiotic prophase I begins in the embryo at around 5 months post implantation, after which time the oocytes are arrested, going on to complete meiosis I and II at ovulation and fertilization, greatly limiting the window of study. For this reason, it is necessary to employ the use of a number of divergent model organisms, through which evolutionarily conserved meiotic processes can be investigated. One such organism is the nematode *C. elegans*, first proposed as a model organism by Sydney Brenner in 1974 (Brenner, 1974). *C. elegans* has the advantages of many model organisms: it is fast growing, providing an easily maintainable stock of

animals which are highly amenable to molecular techniques. In addition to this, the adult worms have two large compartmentalised germline syncytia in which hundreds of nuclei are undergoing meiosis. An exceptional feature of the *C. elegans* germline is that it is arranged in such a way as to provide a complete time course of meiosis, so the stage of meiosis that a nucleus is undergoing can be identified by its position within the gonad.

Most *C. elegans* individuals carry two X chromosomes and are self-fertilising hermaphrodites, a feature that enables large numbers of animals to be generated rapidly. Early in its lifecycle, the worm produces sperm which is stored in a sack called the spermatheca. Later on in development, sperm production is switched to production of oocytes, which are fertilised as they are pushed through the spermatheca. Males, of genotype XO, exist in the population at very low frequencies (about 0.1% of the population) due to missegregation of the X chromosome during meiosis.

The germline can be segmented into four distinct zones based upon position and the cytological features of the nuclei within them (Fig 2). The distal tip of the germline contains a pool of undifferentiated, mitotically-dividing nuclei that provides a flow of nuclei that will differentiate into spermatocytes and oocytes. Once these mitotically-dividing nuclei have moved sufficiently far from the stem cell at the tip of the germline, they undergo meiotic S-phase. The mitotic tip of the germline is followed by a region known as transition zone, which corresponds to the leptotene/zygotene stages of meiotic prophase I, when chromosome pairing occurs. The third germline zone corresponds to pachytene, in which meiotic recombination is completed yielding inter-homologue crossover events. The fourth zone of the germline comprises nuclei at the stages of diplotene and diakinesis, with chromosomes undergoing substantial compaction and revealing the resolved bivalent structure. Finally, fertilisation triggers the meiotic divisions.

The meiotic pathways that are analogous between humans and *C. elegans* are becoming increasing well characterised, and in the following sections there will

be an outline of the current understanding of the mechanisms and regulation of meiosis and where possible, details of the peculiarities of this model organism's meiotic cycle will be included.

1.2.3 Initiation of Meiosis

To begin meiosis, key regulatory genes must be expressed causing cells to transition from the G1 phase of the mitotic cell cycle into the meiotic program. The exact mechanism by which this is achieved varies across organisms. In the unicellular *Saccharomyces cerevisiae* (*S. cerevisiae*) entry into meiosis is triggered by changes in the nutritional content of their environment. At the onset of meiosis, signals such as an increase in nitrogen (Kassir et al., 1988) or decrease in glucose (Gray et al., 2008) cause the transcriptional regulation of two genes; IME1, a transcription factor, and IME2, a Ser/Thr kinase. Transcription of these genes triggers entry into meiosis with the initiation of DNA replication and expression of later meiotic genes (Honigberg and Purnapatre, 2003). Multicellular organisms have developed more diverse mechanisms by which to initiate meiotic entry. In *C. elegans* a single primordial stem cell, or distal tip cell (DTC), found at the distal tip of the germline, proliferates mitotically. This cell promotes mitotic proliferation in the adjacent region of the germline by GLP-1/Notch signalling, inhibiting differentiation and creating a somatic niche. As nuclei are physically pushed away from the tip by DTC proliferation, they move through a signalling gradient, and the decreasing levels of GLP-1/Notch initiate entry into the meiotic cell cycle (Crittenden et al., 2003). In mice, intrinsic factors such as the RNA-binding protein DAZL enables postmigratory germ cells to respond to the vital extrinsic inducer, retinoic acid (RA), initiating meiosis (Bowles et al., 2006; Lin et al., 2008).

1.2.4 Meiotic S-phase

As with mitosis, the onset of meiosis, begins with DNA replication. However, meiotic S-phase takes place more slowly than its mitotic equivalent in yeast (Williamson et al., 1983), *C. elegans* (Jaramillo-Lambert et al., 2007) and mammals (Sung et al., 1986). The reasons for this are not fully understood,

however, it may be that chromosomes need to acclimatise in preparation for meiosis-specific events, such as the inter-homologue repair necessary for CO formation. In support of this, the length of pre-meiotic S-phase in *S. cerevisiae* is significantly reduced if recombination is prevented from occurring (Cha et al., 2000). Similarly, blocking meiotic replication, in yeast, prevents double-strand break formation, and delaying replication of a chromosomal region delays break formation in that particular segment (Borde et al., 2000). However, this is not universal for all organisms. In *S. pombe* delay or inhibition of DNA replication has no effect on DSB formation (Murakami and Nurse, 2001). In *C. elegans* different regions of the genome replicate at different times from one another. In particular, the X chromosome, which is more heterochromatic than the autosomes during meiosis, replicates much later in S-phase (Jaramillo-Lambert et al., 2007). In mitosis, genetically inactive heterochromatin replicates late during S phase, in mammalian cell culture (Dutrillaux et al., 1976; Holmquist et al., 1982). These data suggest that chromatin modifications and DNA topology influence replication timing.

For the proper segregation of chromosomes in the meiotic divisions, it is critical that sister chromatid cohesion (SCC) is established during S-phase. This holds sister chromatids together, providing the tension necessary to enable correct chromosome orientation at metaphase I. This will be discussed in detail in the later sections of this chapter.

1.2.5 Homologous chromosome pairing

As mentioned earlier, the first meiotic division is reductional, separating homologous chromosomes from one another rather that sister chromatids, as would be the case in mitosis. In order that this occurs, it is vital that each chromosome locates and pairs with its homologous partner. The manner in which this is achieved is still a matter of lively debate and diverse mechanisms have been elucidated in different organisms.

A physical characteristic often associated with homologue pairing, is the formation of a chromosome bouquet (Scherthan et al., 1996). The telomeres of chromosomes are restricted in a tight cluster on the nuclear envelope. This is thought to confine the area in which chromosomes are present, thereby improving the chances of homologues locating one another (Rockmill and Roeder, 1998). The bouquet structure itself is conserved in many model organisms, however, there are differences in the mechanisms by which it is formed amongst the different species. For example, in mammals, initially centromeric regions attach to the nuclear envelope and the telomeres are subsequently gathered in. In *S. pombe* however, the bouquet is directly linked to the spindle pole body (SPB). This SPB attachment leads to dynein driven oscillations in which the nucleus is pulled back and forth across the cell (Davis and Smith, 2006). The importance of the bouquet is given further credence by the fact that mutations affecting its formation cause aberrant pairing. In addition to this, they cause polypolar and mislocalised spindles, indicating that there are high levels of signalling between chromosomes and the SPB. However, recent investigations in budding yeast show that pairing is actually promoted by telomere-led chromosome movement, while the bouquet per se contributes little to pairing (Lee et al., 2012). Furthermore, in many organisms full pairing requires the initiation of meiotic recombination, since mutations that affect DSB formation and recombination affect the ability of homologous chromosomes to locate their partners (Loidl et al., 1994).

In *C. elegans* the link between pairing and a polarised configuration of chromosomes during early meiotic prophase has long been recognised. Analysis of mutants lacking the worm homologue of the Chk2 kinase showed that chromosomes failed to acquire the characteristic clustered formation typical of the transition zone of the germline, and that there was an concurrent failure of homologue pairing, suggesting a mechanistic link between the two events (MacQueen and Villeneuve, 2001). Recently, the asymmetric organisation of chromosomes in the transition zone has been implicated as analogous to the chromosome bouquet in other organisms. The polarisation of chromosomes in *C. elegans* has been shown to be actively driven by the molecular attachment of

their ends to the nuclear envelope via a protein bridge comprised of the SUN-1 and ZYG-12 proteins. This bridge spans the nuclear envelope and allows cytoskeletal forces to be transmitted to the chromosomes, moving them around inside the nucleus, facilitating the homology search (Minn et al., 2009; Penkner et al., 2009; Sato et al., 2009). However, unlike the bouquet configuration in most other organisms, in *C. elegans* only a single chromosomal end attaches to the nuclear envelope. This is mediated through specific chromosomal regions, known as the pairing centres (PC), which interact with four related proteins containing two zinc-finger domains which bind to the PC in a sequence-specific manner (Phillips et al., 2009). These movements bring different chromosomes into close proximity with one another enabling homology to be assessed. Once homologues have found their partner, the interaction is stabilised by the formation of the synaptonemal complex (Harper et al., 2011; Wynne et al., 2012).

1.2.6 Synapsis

An obvious cytological feature of meiosis is the synaptonemal complex (SC). It is a supramolecular proteinaceous structure, which localises between homologous pairs of chromosomes, in a process known as synapsis. Electron microscopy (EM) reveals the SC to be a "zipper-like" assembly that bridges homologues, holding them 100nm apart (Moses et al., 1975). It is thought that the SC stabilises the alignment between homologous chromosomes and provides a scaffold upon which to load the recombination proteins required at the later stages of meiosis. The SC is comprised of two major components, the axial element (AE) and the central element (CE). Linear arrays of chromatin loops are anchored to the AE that forms along the length of sister chromatid pairs. As meiosis proceeds the AEs of homologous chromosomes converge with the CE connecting the two (Bardhan, 2010).

In *S. cerevisiae* the AE is consists of Red1 (Smith and Roeder, 1997) and Hop1 (Hollingsworth et al., 1990). Homologues of these two proteins have been discovered in other organisms, although there is a degree of divergence across

species. In *C. elegans, him-3* was the first identified Hop1 homologue (Zetka et al., 1999), but in addition to this there are three *him-3* paralogues: *htp-1*, *htp-2* (Couteau and Zetka, 2005; Martinez-Perez et al., 2008; Martinez-Perez and Villeneuve, 2005) and htp-3 (Goodyer et al., 2008; Severson et al., 2009), which have some functionally analogous roles and some roles which are distinct from Hop1. Formation of the AE on chromosomes takes place early in prophase I and requires that the cohesin complex is loaded onto chromatin (Klein et al., 1999), with components of the AE interacting directly with the cohesin subunits SMC1 and SMC3 in mice (Eijpe et al., 2000). A recent study in *C. elegans* has shown that HTP-3 and cohesin are dependent on one another for their loading, reinforcing the connection between the AE and cohesin.

Once homologous chromosomes, with their AE proteins associated, locate their partners, the interaction between them is stabilised by proteins linking the two AEs. The loading of CE "zips" the AEs together, creating the tripartite SC. In budding yeast the protein responsible for this is Zip1 (Sym et al., 1993). In *C. elegans* the proteins that comprise the CE are the SYP proteins (Colaiacovo et al., 2003; MacQueen et al., 2002; Smolikov et al., 2007; Smolikov et al., 2009). Synapsis initiates at the PCs and the SC polymerises along the length of chromosomes in a highly processive manner that can even link non-homologous chromosomes of varying lengths (MacQueen et al., 2005). In *S. cerevisiae*, plants and mammals the induction of DSBs is required for the initiation of SC assembly (Zickler and Kleckner, 1999). However, in both *C. elegans* and *Drosophila* SC formation is independent of recombination (Dernburg et al., 1998; MacQueen et al., 2002; MacQueen et al., 2005). In *C. elegans* this is possibly due to the PCs stabilising the interaction between homologous chromosomes (Colaiacovo et al., 2003; Dernburg et al., 1998; MacQueen et al., 2005).

1.2.7 Recombination

A striking difference between mitosis and meiosis is the programmed generation of DSBs throughout the genome in meiotic prophase I. This is the initial step required for meiotic recombination (Sun et al., 1989). A number of

these DSBs will go on to form double Holliday junctions and ultimately be resolved as COs. At least one CO is required per homologue pair as they provide the basis for chiasmata, the physical link between homologous chromosomes that become visible towards the end of meiotic prophase I. However, more recombination events are initiated than COs formed, so many DSBs are repaired by pathways that do not yield COs.

There are two key essential consequences of the formation of COs. Firstly, the DNA molecules of homologous chromosomes become tethered to one another, and around these linkages crucial remodelling events can occur, leading to the breakdown of the SC and ultimately the alignment of chromosomes on the metaphase plate. Secondly, the exchange of genetic material between chromosomes creates new allele combinations in the gametes, ensuring genetic variation in each subsequent generation, driving population diversity and consequently evolution.

(See Fig. 3 for a summary of the events and key proteins involved in recombination)

1.2.7.1 DSB generation

Recombination begins with the generation of DSBs by the highly conserved type II topoisomerase-like protein Spo11 (Bergerat et al., 1997; Keeney et al., 1997; Sun et al., 1989). Spo11 is thought to act as a dimer, with the two molecules of Spo11 binding covalently to DNA breaking each strand simultaneously (Bergerat et al., 1997; Keeney et al., 1997; Keeney and Neale, 2006). A number of additional auxiliary proteins have been discovered, involved in the signalling, recruitment and stabilisation of Spo11 at the DSB site, and involved in the further processing of the break. The action of Spo11 preferentially targets DSBs to restricted regions of the genome, known as recombination hotspots (Gerton et al., 2000; Symington et al., 1991). Hotspot usage varies between individuals, and is thought to be influenced by sequence identity, chromatin structure, DNA topology and condensation (Baudat et al., 2010; Buard et al., 2009; Robine et al., 2007). In worms, global crossover distribution has been shown to be affected by

mutations in the chromatin factor, X non-disjunction factor 1, *xnd-1*, probably by altering the pattern of histone modifications (Wagner et al., 2010). In addition to this, condensin affects the distribution of DSB and ultimately CO location (Mets and Meyer, 2009; Tsai et al., 2008) and, finally, the AE protein HTP-3 is required not only for cohesin loading, but also for the formation of DSBs, demonstrating a link between the three processes of AE assembly, cohesin loading and DSB formation, in *C. elegans* (Goodyer et al., 2008; Severson et al., 2009).

1.2.7.2 DSB resection

In order for a DSB to be processed as a CO product, the Spo11 covalently bound to the DNA, must be removed from the break site (Bergerat et al., 1997; Keeney et al., 1997). This requires the MRX complex, comprised of Mre11, Rad50 and Xrs2, and consequently, if these components are missing there is an accumulation of unprocessed Spo11 "breaks" (Alani et al., 1990; Tsubouchi and Ogawa, 1998). The initial step of processing Spo11 DSBs involves endonucleolytic cleavage of the DNA behind the bound Spo11 molecules, releasing Spo11 bound to a short oligonucleotide (Neale et al., 2005). The MRX complex and Sae2/Com1 are required for this cleavage step (Alani et al., 1990; McKee and Kleckner, 1997; Prinz et al., 1997; Tsubouchi and Ogawa, 1998). After this initial step, the dsDNA on either side of the break site is resected 5' to 3', resulting in overhanging ssDNA. The protein believed to be responsible for this is the exonuclease Exo1 (Tsubouchi and Ogawa, 2000; Zakharyevich et al., 2010).

1.2.7.3 Strand invasion

Once resection has taken place, strand exchange proteins can bind to the ssDNA, forming helical nucleoprotein filaments. These structures, once stabilised, produce single end invasions (SEIs), which carry out the search for a homologous target sequence and catalyse strand exchange (Hunter and Kleckner, 2001).The invasion by ssDNA of a neighbouring chromosome causes the formation of a displacement loop (D-loop). This process initially requires

replication protein A (RPA) (Sung and Robberson, 1995), which is then displaced by two RecA-like strand exchange proteins, which produce the nucleoprotein filaments capable of carrying of homology search. These are the meiosis-specific recombinases Dmc1 and Rad51, which function both in mitosis and meiosis (Aboussekhra et al., 1992; Bishop et al., 1992; Shinohara et al., 1992). In *C. elegans*, where there is no Dmc1 homologue, and Rad51 appears to carry out the roles of Dmc1 (Alpi et al., 2003; Rinaldo et al., 1998).

1.2.7.4 Partner choice

In order for chiasmata formation to occur it is essential that inter-homologue COs are generated. Therefore, there must be a repair bias in meiosis, whereby interhomologue strand invasion is promoted and inter-sister repair inhibited, with the inverse being true in mitosis. In yeast, interactions between Dmc1 and the Mnd1-Hop2 complex, play a key role in ensuring that strand invasion occurs between homologues (Henry et al., 2006). In addition to the role of strand exchange proteins in partner choice, the AE component Hop1 is involved in a checkpoint-like mechanism ensuring interhomologue repair occurs. A key role of Hop1 is to prevent non-homologous synapsis (Latypov et al., 2010), but in addition to this it has been shown that its phosphorylation by the checkpoint kinases Mec1 and Tel1 is required to ensure inter-homologue recombination in meiosis (Carballo et al., 2008). In *C. elegans*, the AE component and Hop1 homologue HTP-1 has also been proposed to prevent the repair of meiotic DSBs between sister chromatids, probably by promoting a bias towards inter-homologue repair, thus ensuring chiasmata formation (Martinez-Perez and Villeneuve, 2005).

1.2.7.5 ZMM crossover pathway

Once a SEI has been stabilised, the DSBs can be re-ligated to form a double Holliday junction (Schwacha and Kleckner, 1995). This is then thought to be cleaved in an asymmetric manner by an, as yet, unknown resolvase finalising the CO event. Key for these processing steps are a group of interacting proteins collectively known as the ZMM complex. This complex is composed of Zip1-4,

Msh4, Msh5 and Mer3. The consequence of lacking any of these proteins is a situation where the quantity of DSBs that are generated is normal, but the number of COs that result is severely reduced (Borner et al., 2004). Mer3 with the Msh4-Msh5 heterodimer functions to promote or stabilise strand invasion, with the helicase Mer3 thought to be involved in assisting strand invasion between Dmc1 or Rad51 coated ssDNA (Mazina et al., 2004), while Msh4-Msh5 appear to stabilise the Holliday junction by mobilising progenitor Holliday junctions away from the point of strand exchange in an ATP-dependent manner (Snowden et al., 2004). With homologous chromosomes now physically joined by a CO, and held together by SCC, the stage is set for the meiotic divisions to occur. This will be discussed in detail later in this chapter, however, first I will briefly outline some further aspects of recombination and the repair pathways used in meiosis.

1.2.7.6 Crossover interference

The phenomenon of crossover interference refers to a chromosome-wide process whereby CO events are prevented from occurring nearby one another. A model in which transmission occurs along the SC has been suggested (Shinohara et al., 2003), however, interference has been observed before the formation of the SC (Fung et al., 2004). Another model proposes that changes in the physical state of the chromosomes occur once a recombination intermediate becomes committed to forming a CO rather than NCO. Chromosomes must be under physical stress for COs to be formed and once a recombination intermediate has been fated to become a CO this stress is relieved in the flanking regions of the chromosome, thereby inhibiting further CO formation (Borner et al., 2004). More research into this area will be required in order to elucidate the mechanism by which interference is achieved.

1.2.7.7 Non crossover pathway of DSB repair

Crossover formation requires the stabilisation of SEIs by the ZMM complex. In the absence of this stabilising force the invading strand is thought to be unable to maintain an interaction with its homologous duplex and after a small amount

of DNA synthesis, the 3' overhang becomes dissociated from the homologue and reassociates with the 5' end of the original DSB. This process is known as synthesis-dependent strand annealing (SDSA), and in this way, a NCO is formed (Allers and Lichten, 2001; Lichten, 2001). The NCO outcome of DNA repair can be promoted by facilitating strand displacement that causing the SEI to be destabilised. The RTEL1 helicase has been shown to do this (Barber et al., 2008), and indeed in *C. elegans rtel-1* mutants CO numbers are higher than wild-type, as most DSBs are repaired as COs (Youds et al., 2010).

1.2.7.8 ZMM-independent crossover pathway

In addition to the ZMM repair pathway, evidence exists for CO pathways which are independent of the ZMM complex. For example, in yeast and *Arabidopsis* mutants lacking ZMM components, some residual COs are still formed. This is also the case in mutant mice lacking the MLH1 protein, which is required for ZMM COs (Borner et al., 2004; Holloway et al., 2008; Mercier et al., 2005). The endonuclease Mus81 seems to be required for most ZMM-independent repair (de los Santos et al., 2003), however, in yeast mutants lacking both MUS81 and components of the ZMM pathway a few COs still persist, suggesting the presence of a third CO repair pathway (de los Santos et al., 2003). In *S. pombe* by contrast, all COs appear to require MUS81 for their repair (Boddy et al., 2001), and in *C. elegans* the reverse appears to be true, with the vast majority of COs eliminated in ZMM pathway mutants (Zalevsky et al., 1999).

1.2.7.9 Non-homologous end joining (NHEJ) pathway

Another way in which DSBs can be repaired is by non-homologous end joining (NHEJ) (Moore and Haber, 1996), requiring the combined action of the Ku proteins (Doherty and Jackson, 2001) and DNA ligase IV (Wilson et al., 1997). This repair pathway can take place in the absence of a homologous template. In NHEJ, ends of a DSB or even ends from different breaks are ligated directly to one another, with some genetic information being lost in the process. For this reason it is preferable for cells to use a HR repair pathway. A deleterious

outcome of NHEJ is the formation of chromosome fusions and translocations when repair takes place between DSBs on different chromosomes.

In mammalian cells, NHEJ takes place throughout the cell cycle. This is not the case in yeast however, where NHEJ is highly redundant and HR is greatly favoured (Daley et al., 2005). The use of the NHEJ pathway in *C. elegans* is limited to G1 arrested, non-cycling somatic cells, in which sister chromatids are not present to use as a repair template (Clejan et al., 2006). In *C. elegans* it has recently been shown that use of the NHEJ pathway is inhibited by the Fanconi anaemia complex during meiosis (Adamo et al., 2010). However, if repair cannot be undertaken by HR, as is the case in the absence of RAD-51, the NHEJ pathway becomes activated in the germline, resulting in the formation of disordered chromosome masses at diakinesis (Martin et al., 2005).

1.2.8 Meiotic divisions

The events outlined above, the formation of COs together with SCC in the flanking regions, provide a physical link between homologous chromosomes, known as chiasmata. These can be visualised subsequent to SC disassembly and chromosome condensation and the structure that is created by a pair of homologous chromosomes attached by one or more chiasmata is known as a bivalent. The proper segregation of chromosomes requires that these bivalents must be correctly aligned on the metaphase plate of the first meiotic division. Then at anaphase I onset, SCC must be selectively released allowing homologues to be pulled to opposite poles of the forming daughter cells. In organisms with monocentric chromosomes this is achieved by protecting SCC around the centromeres but removing it from the chromosome arms (Hauf and Watanabe, 2004; Kitajima et al., 2004; Kitajima et al., 2006). In the case of *C. elegans*, which has halocentric chromosomes, an analogous strategy is employed. The bivalents produced in prophase I have an asymmetric cruciform shape, with a pair of long and short arms (Nabeshima et al., 2005). SCC is lost from the short arms, but maintained on the long arms, with the same resulting effect: the homologues segregate to opposing poles. During the second meiotic division all remaining

SCC is lost and this allows sister chromatids to migrate to opposite spindle poles. In order for the segregation of chromosomes to occur, clusters of proteins form a dynamic structure known as the kinetochore, which functions to regulate the attachment of microtubules to the meiotic chromosomes. Unlike mitosis, during metaphase I sister chromatids are co-oriented rather than bi-oriented so that sisters migrate together to the same spindle pole. The regulation of this process will be discussed in detail later in the chapter.

1.3 Cohesin

The accurate segregation of sister chromatids to opposite poles of the cell during division is one of the most fundamental processes of life. For this to occur, sister chromatids must be physically connected from their synthesis in S-phase until their eventual separation at mitosis or meiosis. Before the onset of the anaphase to metaphase transition the kinetochores on each sister chromatid are attached to microtubules which pull the chromosomes in towards opposite spindle poles (Martinez-Perez et al., 2008; Riedel et al., 2006). Cohesin is believed to counteract these opposing forces preventing the sisters from being prematurely pulled apart. Without the pairwise alignment of chromatids on the mitotic spindle successful segregation of chromosomes would not be possible (Nicklas, 1988). The crucial juxtaposition of chromosomes, mediated by the cohesin complex results from an adherent property known as sister chromatid cohesion (SCC).

1.3.1 Cohesin complex

In mitosis the cohesin complex is comprised of two structural maintenance of chromosomes proteins (SMC); Smc1 and Smc3, and two non-Smc proteins; the α-kleisin Scc1 (also known as Mcd1 or Rad21), and Scc3 (known in mammalian cells as SA1 and SA2) (Nasmyth and Haering, 2009). The structure of both SMC proteins is that of a 50nm intermolecular antiparallel coiled coil, forming a rod shape with a hinge domain and nucleotide-binding domain (NBD) at either end (Haering et al., 2002; Hirano and Hirano, 2002). SMC1 and SMC3 interact at

their hinge domains, leading to the formation of V-shaped heterodimers with their nucleotide binding domains (NBDs) at the end of each coiled arm (Melby et al., 1998). The NBD of SMC1 is bound to the N-terminal of SCC1 whereas that of SMC3 is bound to its C-terminal, creating a huge tripartite ring, consistent with electron micrographs of the cohesin complex (Anderson et al., 2002; Haering et al., 2002). Mutations in any one of these genes results in the precocious separation of sister chromatids, highlighting the now canonical role of the cohesin complex: adhering replicated sister chromatids from S-phase until anaphase. This is further supported by the observation that SCC1 dissociates from the SMCs at the metaphase to anaphase transition and that this is dependent on the anaphase promoting complex (APC). The mechanism by which this is achieved involves a cysteine protease known as separase (Esp1) which is cleaves SCC1, thereby triggering its dissociation from chromatin (Uhlmann et al., 1999). Unsurprisingly, the activation of separase is tightly coordinated with the progression of the cell cycle, through the destruction of its inhibitor, known as securin (Pds1) (Ciosk et al., 1998). A fourth cohesin subunit, SCC3 binds within Scc1's C-terminal separase cleavage fragment. Mutations in Scc3 also lead to the precocious separation of sister chromatids and it has been shown that the association of Smc3, Scc1 and Scc3 with chromatin are all interdependent on one another (Toth et al., 1999). This has led to an established view of the cohesin complex as containing a pair of Smc subunits and two non-Smc components: SMC1 and SMC3, and SCC1 and SCC3, respectively (Fig 4A).

1.3.2 SCC mechanism

The known function of cohesin to adhere sister chromatids together from replication until anaphase, and the elucidation of the complex's structure as a large proteinaceous loop have led to the proposal of a number of theories as to the mechanism of its action. The most widely accepted is the "embrace" model, which suggests that the ring structure of the complex topologically entraps the two strands of DNA which are produced during S-phase, thereby linking sister chromatids (Fig. 4B). In support of this model is this observation that cleavage of either Smc1 or Scc1, or the DNA itself results in the release of cohesin from a

circular mini-chromosome *in vivo* (Gruber et al., 2003; Ivanov and Nasmyth, 2005). Furthermore, by using site-specific crosslinking to form a covalently closed, or "static", version of the cohesin ring it has been shown that the circular mini-chromosome DNA remains dimerized, even after denaturation (Haering et al., 2008). In addition, interruption of the hinge domain of the complex prevents cohesin from associating with DNA, suggesting that a transient dissociation of the hinge domain between Smc1 and Smc3 is required for the loading of cohesin onto chromatin, also supporting this model (Gruber et al., 2006). It is therefore believed that the switch from an open to a stably closed conformation of the ring enables cohesin to encompass the DNA and in so doing generates a cohesive force. This force is maintained until anaphase when the action of separase results in to cleavage of Scc1, breaking the ring an abolishing the entrapment (Uhlmann et al., 1999).

(See Fig. 4C for a summary of the events of the cohesin cycle)

1.3.3 Cohesin loading

The initial step in forming SCC is loading of the cohesin complex onto chromatin and it appears likely that this involves the transient opening of the complex, allowing it to encircle chromatin, rather than de novo assembly of cohesin around DNAs. The evidence for this is: firstly, that cohesin complexes not associated with chromatin also exist as a ring (Gruber et al., 2003), secondly, most of the cohesin that disassociates from chromosomes in prophase exists as a soluble complex until its reassociation during telophase (Hauf et al., 2005), and thirdly, preassembled cohesin complexes are present in *Xenopus* eggs in order to establish SCC in the cleavage divisions (Losada et al., 1998). The evidence suggests that ATPase activity associated with the Smc NBDs is required for cohesin loading. In transgenic yeast expressing mutant forms of Smc1 or Smc3 which can bind but not hydrolyse ATP as a result of mutations in their Walker B domain, cohesin rings are formed but do not stably associate with chromosomes (Arumugam et al., 2003). There is evidence that the site of this transient opening is at the interface of the Smc1 and Smc3 hinge domains.

When amino acid sequences encoding FKBP12 and FRB, which bind to one another in the presence of rapamycin only, are inserted into the hinge domains of Smc3 and Smc1 respectively, SCC can only be established in the absence of rapamycin. In addition to this, yeast cells in which Smc3's C terminus is fused to Scc1's N terminus or Scc1's C-terminus is fused to Smc1's N terminus remain viable, indicating that it is not the interface between the α-kleisin and the Smc's NBDs that are the point of entry during cohesin loading (Gruber et al., 2006).

Cohesin's association with chromosomes requires several factors, the most important of which is the Scc2/Scc4 complex, known also as Nipbl/Mau2 or adherin. It is required for cohesin loading, but not assembly, at all sites in the genome in *S. cerevisiae*, *S. pombe*, *Xenopus* and in mammalian cells and as such mutations in Scc2 or Scc4 cause major defects in SCC (Michaelis et al., 1997). In yeast, scc2 mutants also have partial defects in loading of condensin (Cortes-Ledesma and Aguilera, 2006; D'Ambrosio et al., 2008) and SMC5/6 complexes (Lindroos et al., 2006). Small amounts of Scc2/4 complexes have been immunoprecipitated with cohesin subunits, indicating that they physically interact, albeit transiently, with one another at some stage. It has been suggested that ATP hydrolysis at the NBD may cause a conformational change, temporarily disconnecting Scc1 from the Smc heads and thereby allowing DNA entrapment, and that Scc2/4 promote this process (Arumugam et al., 2003).

In yeast, the localisation of cohesin across the genome appears not to be random. High density mapping using ChIP has shown that the highest abundance of cohesin is found in the pericentric regions with a less robust enrichment at specific intergenic arm regions. The cohesin association in these arm regions are found at 2.5 to 35kb intervals and usually span 0.8 to 1kb (Blat and Kleckner, 1999; Lengronne et al., 2004; Tanaka et al., 1999). This pattern of cohesin localisation could result from complexes becoming stably associated at their loading sites, or from the rings being translocated subsequent to loading. Both possibilities have been implicated in two conflicting studies. In one, Scc2/Scc4 binding sites largely colocalize with those of cohesin (Kogut et al., 2009), while an earlier study suggests that Scc2/Scc4 initially loads cohesin but

it is subsequently moved along DNA fibres to other sites by RNA polymerases during gene expression (Lengronne et al., 2004). A more recent study has shown that cohesin initially has an unstable interaction with DNA at docking sites and this requires ATP binding. Subsequently, ATP hydrolysis stabilises the association and this allows translocation of cohesin rings up to 20kb from the docking site. In mutants in which Smc1 or Smc3 are defective in ATP hydrolysis, this dynamic behaviour is lost and cohesin remains static at the docking sites (Hu et al., 2011). Finally, it has recently been proposed that in yeast the association of Scc2 with centromeres requires the presence of a full cohesin ring, which triggers the association of Scc2 with the Ctf19 complex, allowing the centromeric loading of cohesin, which then spreads onto the flanking pericentromeric regions (Fernius et al., 2013).

In *Xenopus* egg extracts association of both Scc2/4 and the cohesin complex is dependent on the formation of the pre-replication complex (pre-RC) (Gillespie and Hirano, 2004). Scc2/4 forms stable complexes with Cdc7/Drf1 kinase (DDK) (Takahashi et al., 2008), as well as with cohesin and these are in turn recruited to the MCM complex where DNA synthesis is initiated (Gillespie and Hirano, 2004), indicating that the role of the Scc2/Scc4 complex is twofold: to recruit cohesin to chromatin and to allow entrapment of chromatin by the cohesin ring. However, in yeast Scc2/4 complexes have not been found to associate with pre-RCs (Eckert et al., 2007). Also, the finding that a large fraction of cohesin in G2 HeLa and NRK cells has a residence of less than 30 minutes indicates that cohesin must frequently interact with chromatin long after pre-RCs have been disassembled (Gerlich et al., 2006). This linkage between pre-RCs and cohesin loading may be specific to a short stage of the vertebrate cell cycle.

1.3.4 Cohesin establishment

The correct localization of cohesin to chromatin is not sufficient to establish SCC. In G2 or M phase yeast cells, Smc1/3 and α-kleisin subunits associate with chromatin but fail to establish cohesion, even in the presence of pre-existing

SCC (Haering et al., 2004; Lengronne et al., 2006; Strom and Sjogren, 2005). A striking inference we can draw from this is that there can be little or no turnover of cohesin complexes after SCC has been established.

An essential step in the establishment of cohesion is the acetylation of a pair of lysines (K112 and K113) within Smc3's NBD, by the fork-associated acetyltransferase Eco1 (Rolef Ben-Shahar et al., 2008; Unal et al., 2008). These residues are highly conserved among eukaryotes, and their equivalents have been found to be acetylated in human tissue culture cells (Zhang et al., 2008b). Acetylation of Smc3 can occur independently of DNA synthesis in *Xenopus* egg extracts, however cohesion is not established, suggesting that both the passage of the replication fork and Smc3 acetylation by Eco1 are required to generate cohesion (Higashi et al., 2012). It has been proposed that these two events generate a transient conformational change of the cohesin complex, allowing the entrapment of sister chromatids (Remeseiro and Losada, 2013). The acetylation of Smc3 is maintained until anaphase, at which point deacetylation is carried out by the action of Hos1. This step can only take place once cohesin has been liberated from chromatin by Scc1 cleavage by separase (Beckouet et al., 2010). Smc3 that has not been deacetylated cannot establish cohesion in the subsequent S-phase indicating that *de novo* Smc3 acetylation during DNA replication is required for the establishment of SCC. Deacetylation of Smc3 in post-replicative cells by Hos1 overexpression leads to a reduction in SCC, indicating that acetylation may actively stabilize cohesion (Borges et al., 2010). Other proteins have been shown to stabilize cohesion, and these will be discussed in the next section. In vertebrates, a complex between Pds5 and Sororin, which is coupled to the Smc3 acetylation cycle is also required for the stabilization of cohesin chromatin interactions. Sororin appears to act as an antagonist of Wapl (a third protein that acts to modify cohesin association with DNA) by displacing it from Pds5, an interaction that promotes the disassociation of cohesin and chromatin (Nishiyama et al., 2010).

1.3.5 Cohesin maintenance

Cohesion must be maintained throughout the cell cycle until the metaphase to anaphase transition. The mechanism for regulating the maintenance of SCC is complex and varies across different organisms. Both Wapl and Pds5 have been implicated in the homeostasis between the establishment and anti-establishment of the cohesiveness of cohesin. It has been shown that the localisation of cohesin and Pds5 on chromatin are interdependent and that Scc1 recruits Pds5 to chromosomes in G1, with its cleavage causing the dissociation of Pds5 from chromosomes at anaphase, suggesting a role in maintaining SCC (Panizza et al., 2000). In fact, in the fission yeast *Schizosaccharomyces pombe* (*S. pombe*), Pds5 is essential for the stable association of cohesin with replicated chromosomes and authorizes cohesion establishment by allowing Eco1-mediated neutralization of cohesion anti-establishment (Vaur et al., 2012).

However, there is also evidence that Pds5 and Wapl are part of an anti-establishment pathway. Deleting Wapl can bypass the requirement for Eco1 (Nasmyth, 2011). In *S. cerevisiae*, loss of Wapl leads to modest cohesion defects (Rolef Ben-Shahar et al., 2008; Rowland et al., 2009). This is distinct from Pds5, which is essential for cell viability, with its inactivation in postreplicative cells leading to loss of SCC (Hartman et al., 2000; Panizza et al., 2000). In addition to this, Pds5 and Wapl form a subcomplex that binds to cohesin promoting its removal from chromatin (Kueng et al., 2006; Rowland et al., 2009). In vertebrate cells there are two isoforms of Pds5, Pds5A and Pds5B, both of which have been shown to associate with the cohesin complex (Losada et al., 2005; Sumara et al., 2000). Depletion of either Pds5A or Pds5B lead to defects in cohesion similar to, but milder than, the effects observed with Scc1 depletion. In *Xenopus* egg extracts chromosomes assembled without Pds5A or Pds5B appeared to have looser cohesion at the centromeres, but cohesion is unaffected in the arms and surprisingly, these chromosomes retain an unusually high level of cohesin (Losada et al., 2005). It seems then, that Pds5 regulates cohesion maintenance both positively and negatively, explaining the varied and complex phenotype observed in Pds5 mutants in different organisms. Finally, in a recent study in *S. cerevisiae*, it has been shown that Wapl is the only factor preventing

G2-expressed cohesin from establishing SCC, showing that it's role is not restricted to anti-establishment activity during DNA replication, but extends to cohesion maintenance outside of S phase (Lopez-Serra et al., 2013).

1.3.6 Cohesin removal / dissolution

The timely release of cohesion is equally important for the correct segregation of chromosomes, as its establishment and maintenance. The disassociation of cohesin, in most eukaryotic cells, takes place in two phases of mitosis, in the prophase and anaphase pathways. In the prophase pathway the majority of cohesin is lost, with a small but essential complement retained at the centromeres. Disassociation is partly achieved by the phosphorylating action of Plk1 and aurora B at the C-terminus of Scc3, which presumably causes a topological change that opens the cohesin ring. The effect of phosphorylation by these two proteins is modest however, as most cohesin disassociates in their absence (Hauf et al., 2005). The binding of Wapl to Psd5 appears more crucial as its depletion from mammalian cells causes most cohesin to remain on chromosome arms (Gandhi et al., 2006). The phosphorylation of sororin by the mitotic kinase CDK1, as well as the phosphorylation of Scc3, triggers the Wapl-dependent removal of cohesion (Dreier et al., 2011). The phosphorylation of sororin disrupts its interaction with Pds5, and this allows Wapl to bind to Pds5 and remove cohesin from chromosome arms (Nishiyama et al., 2010). Sgo1 maintains sororin binding to Pds5 and cohesin through PP2A-dependent dephosphorylation. As hypophosphorylated sororin binds antagonistically with Wapl to Pds5, this dephosphorylation of sororin by Sgo1/PP2A protects cohesion at the centromeres enabling the bipolar attachments of the spindles to sister chromatids (Liu et al., 2013).

Once all of the chromosomes are aligned on the metaphase plate, the removal of the remaining cohesin triggers the onset of anaphase, whereby the mitotic spindle can pull sister chromatids apart into the two forming daughter cells. This final set of cohesin removal is irreversible and results from the proteolytic cleavage of the α-kleisin, Scc1, by a conserved cysteine protease called separase

at two related recognition sites (Uhlmann et al., 1999; Uhlmann et al., 2000; Waizenegger et al., 2000). This cleavage breaks the ring thereby abolishing SCC and enabling sister chromatid segregation. Regulation of this process is crucial, as premature cleavage would lead to chromosome missegregation and as such for the majority of the cell cycle separase is bound by an inhibitor called securin. Just before the onset of anaphase, securin is ubiquitinated by the anaphase-promoting complex or cyclosome (APC/C), triggering its destruction and thus freeing separase (Cohen-Fix et al., 1996; Funabiki et al., 1996; Zou et al., 1999). In addition to this, Scc1 cleavage is regulated by phosphorylation of separase recognition sites by the Polo-like kinase Cdc5 (Alexandru et al., 2001). To ensure that all chromosomes have been correctly attached to the mitotic spindle, there is a means of surveillance, known as the spindle assembly checkpoint, which acts as a potent inhibitor of the APC/C, and so prevents premature removal of cohesin.

The reason why a prophase pathway is required is unclear. It may be that it facilitates chromatin deconcatenation by TopoII, or perhaps the large soluble pool of cohesin created is required for rapid reassociation of cohesin with chromatin during telophase, which would not be possible if all cohesin was disassociated by separase cleavage.

1.3.7 Role of cohesin in DNA damage and double strand break repair

DNA damage is a constant threat to the integrity of the genome, and in particular DSBs whereby by chromatids are broken, pose a major challenge to the survival of a cell. Once a DSB has been detected, a number of checkpoints become activated and the cell cycle arrests, providing time for the damage to be repaired (Sjogren and Nasmyth, 2001). The mode of repair is dependent on the stage of the cell cycle, with non-homologous end joining (NHEJ) used in G1 and homologous recombination (HR) used in G2. In the case of homologous recombination, the sister chromatid is used as a template to repair the break. This results in the damage being repaired with very high fidelity, however, it can only be used subsequent to S-phase when a sister chromatid is present

(Szostak et al., 1983). In G1 when there is no sister template to use, the cell must resort to NHEJ in which the broken ends of the break are ligated directly to one another. However, this frequently leads to loss of some genetic material, eroding the genome (Wilson et al., 1997).

Cohesin plays a key role in responding to DNA damage. Mutants of all cohesin subunits display hypersensitivity to ionizing radiation (IR) in yeast and mammals, as do *Eco1* mutants, indicating that cohesion establishment is required for the DNA damage response (Sjogren and Nasmyth, 2001). It is likely that cohesin facilitates repair because cohesion keeps sister chromatids in close proximity promoting the correct sequence to be used as a donor template for repair. When the levels of cohesin in tetraploid yeast were reduced to that of a single copy, a significant increase in homologous chromosome directed HR, rather than sister chromosome recombination was detected (Covo et al., 2010). The fact that cohesin promotes the use of the sister as a template and inhibits use of the homologue is thought to reduce the risk of non-allelic recombination.

In response to DSBs cohesin becomes localized to and highly enriched at break sites, forming expanded cohesin domains spanning 50-100kb (Strom et al., 2004; Unal et al., 2007). This is dependent on Scc2/Scc4, as well as other DNA damage response factors, including Mre11, Mec1 and Tel1 (Atm/Atr), and phosphorylation of histone H2AX (Unal et al., 2004). Loading was shown to occur outside of S-phase, strongly suggesting that the cohesin was being loaded *de novo* (Strom and Sjogren, 2005; Unal et al., 2004). This form of cohesin loading is termed damage-induced cohesion (DI-cohesion). Surprisingly, a recent study in *S. cerevisiae* has shown that, in addition to DSBs triggering cohesin reloading, DNA breaks also promote dissociation of S-phase-loaded cohesin. This damage-induced disassociation requires separase and yeast expressing a separase resistant Scc1 protein have reduced DSB resection and the efficiency of repair is compromised, even when Scc1 is loaded in response to DNA damage (McAleenan et al., 2013). It therefore appears that both cohesin loading and removal are necessary for effective DNA damage repair, and one could speculate that reloading is require to reinforce cohesion moving the

damage DNA closer to its template, and then removal is required to allow access to the repair machinery and to facilitate resection.

In addition to this, Smc1 participates in a signal-transduction pathway that leads to a checkpoint response to DNA damage. The Atm kinase is activated in response to IR, phosphorylating important cell-cycle targets, including two serines of Smc1, and these modifications are important for the S-phase DNA-damage checkpoint. Interestingly, Smc1 and Smc3 might associate with DNA-damage-response proteins such as Atm, Nbs1, Blm and the breast cancer tumour suppressor Brca1 (Yazdi et al., 2002). Furthermore, it is thought that DNA damage prevents Wapl from inhibiting cohesion formation. Scc1 undergoes several post-translational modifications, which through the action of Sororin and Eco1 promote dynamic cohesin to become cohesive (Heidinger-Pauli et al., 2009). In addition to this, post-translational modifications to Smc3 also reinforce genome-wide cohesin at pre-existing cohesin sites . Finally, Scc1 is SUMOylated in response to DSBs and this is essential for establishment of DNA damage-induced cohesion (McAleenan et al., 2012). We can therefore see that cohesion functions in an intricate and highly regulated manner, in order to respond the DNA damage.

1.3.8 Regulation of gene expression and its clinical relevance

In addition to the canonical role of cohesin, it has also been demonstrated that cohesin plays a key role in the regulation of gene expression. The first evidence for this came from genetic studies in *Drosophila*, where the dosage of the cohesin loading factor Nipped-B affected the regulation of particular homeobox genes (Rollins et al., 1999). Subsequently, it was discovered that the developmental disorder, Cornelia de Lange Syndrome, was caused by mutation in Nipbl, the human homolog of Nipped-B (Strachan, 2005). In addition to this, heterozygous mutations in cohesin subunits and co-factors, as well as cohesin-modifying enzymes result in developmental abnormalities (Deardorff et al., 2012; Strachan, 2005; Vega et al., 2005; Zhang et al., 2009). The observation

that cells from NIPBL heterozygous individuals did not show defects in chromosome segregation when cultured, led to the suggestion that lack of cohesion was not the cause of the developmental defects in Cornelia de Lange Syndrome patients, but rather cohesin's function in gene regulation might be responsible (Strachan, 2005). A number of studies have demonstrated that cohesin has both roles related to and independent from cell division. Depletion of cohesin from post-mitotic neurons in *Drosophila* caused neurons to show defective axon pruning resulting from deregulated expression of the ecdyson receptor (Pauli et al., 2008; Pauli et al., 2010). Further evidence from *Drosophila* proposes that Nipped-B and Pds5 directly regulate gene transcription by controlling the quantity of cohesin that binds to DNA (Gause et al., 2010; Misulovin et al., 2008; Schaaf et al., 2009). In addition to this, deletion of the cohesin subunit Rad21 in mouse thymocytes leads to dysregulation of transcription at the T cell receptor alpha locus, which is required for thymocyte differentiation (Seitan et al., 2011).

In mammalian cells cohesin commonly colocalizes with the site-specific zinc finger DNA binding protein CTCF, which defines the boundaries between active and inactive chromatin domains (Parelho et al., 2008; Rubio et al., 2008; Wendt et al., 2008). CTCF enriches cohesin at specific binding sites, though is not required for its loading. This has been shown to control transcription at the H19/IGF2 (insulin-like growth factor 2) locus by enabling CTCF to insulate promoters from distant enhancers (Wendt et al., 2008). It has been proposed that as well as being able to attach chromatin fibres in *trans*, cohesin may also be able to facilitate interaction in *cis*, thereby regulating long-range interactions between enhancers and promoters. Such loops have been implicated in crosslinking studies at the IFNG locus in T cells, and have been shown to be cohesin dependent (Hadjur et al., 2009). Finally, it has been suggested that the recruitment of cohesin to the CTCF sites of the V and J segments of the immunoglobulin genes in pro B cells, may aid contraction of the locus and in so doing promote gene rearrangement (Degner et al., 2009).

1.4 Meiotic cohesin

Meiotic cohesin has several differences that make it distinct from its mitotic counterpart. Most apparent, is the presence of meiosis-specific cohesin subunits. A meiosis specific α-kleisin was first discovered in *S. pombe,* in which a mutation in *Rec8* caused cells to exhibit SCC defects specific to meiosis (Molnar et al., 1995). Subsequently, it was shown that in *S. cerevisae* that meiotic cohesin complexes had the α-kleisin Scc1 substituted by Rec8, but all other components remained the same (Klein et al., 1999). Rec8-containing cohesin complexes have now been identified across all phyla (Pasierbek et al., 2001). In *C. elegans* two further meiosis-specific complexes have been identified, in which REC-8 is substituted with either the COH-3 or COH-4 (Severson et al., 2009) and a further complex containing the α-kleisin COH-1 has been implicated in both meiosis and mitosis, though little is known of its function (Mito et al., 2003; Pasierbek et al., 2001). The occurrence of multiple meiosis-specific cohesin subunits is not a *C. elegans*-specific phenomenon. In mice an SMC1 paralogue, SMC1β (Revenkova et al., 2001), and an additional α-kleisin, Rad21L (Ishiguro et al., 2011; Lee and Hirano, 2011) are all present during meiosis. It is therefore possible, by combining different combinations of subunits, to create 16 distinct cohesin complexes and this may provide a flexibility that allows different meiotic specific functions to be carried out by different cohesin complexes.

It has been demonstrated that the mitotic kleisin Scc1 and meiotic kleisin Rec8 have divergent sequences and that this has led to functional differences. As previously mentioned, Scc1 is phosphorylated at serine 83 by Chk1, promoting damage-induced SCC. In Rec8 this serine is absent and therefore Rec8 cannot establish DI-cohesion, however this function can be engendered in Rec8 by introducing a serine in the equivalent position as Scc1 (Heidinger-Pauli et al., 2008). This illustrates how the divergent forms of cohesin subunits can result in specific complex functions. Elucidating how cohesin complexes with different subunit compositions function in order to regulate the different events of meiotic chromosomes remains an important topic for future research.

1.4.1 Meiotic cohesin loading

At the onset of meiotic S-phase, cohesin must be loaded on to chromatin in order to ensure the correct segregation of chromosomes in the meiotic divisions. As previously mentioned, in mitosis the loading of cohesin on to DNA is carried out by the Scc2/Scc4 complex. However, until recently it had not been demonstrated that this same complex played a role in cohesin loading in meiosis. In our lab an EMS mutagenesis screen led to the generation of an *scc-2* null allele with a single C to T substitution at position 382 of the cDNA. This mutation is predicted to create an early STOP codon after 127 amino acids, hugely truncating the protein. The mutant homozygous worms are viable, presumably due to a maternally provided complement of *scc-2* mRNA and/or protein and as a result have enabled us to study the role of SCC-2 in meiosis and formally demonstrate that it is responsible for cohesin loading in *C. elegans* meiosis. The *scc-2(fq1)* mutant displays aberrant meiotic chromosome structure, with fine and disordered strands of chromatin rather than the thick, defined tracts characteristic of wild-type pachytene nuclei. Furthermore, the numbers of chromatin bodies present in diakinesis oocytes are indicative of a cohesion defect and indeed, a cytological investigation revealed that none of the cohesin subunits are loaded to meiotic chromosomes in *scc-2 (fq1)* mutants (Lightfoot et al., 2011).

In wild-type meiosis, we have seen that SCC-2 co-localizes with the axial element throughout prophase. This suggests that in addition to its role loading cohesin in S-phase it may also function to reload cohesin elsewhere in meiosis, perhaps in response to programmed DSBs, in a situation akin to the mitotic response to DNA damage. With the *scc-2* mutant it is not possible to separate meiotic defects due to a requirement for S-phase loading, and those due to a requirement for reloading at other stages of meiosis. In addition to this, it is impossible to dissect out whether the phenotypes that we see in the mutant are solely due to problems during meiosis or also due to cohesin loading defects that take place in the pre-meiotic divisions. Addressing the potential role of SCC-2 during meiotic prophase will be an important aim of this thesis.

1.4.2 Roles of meiotic cohesin in prophase I

As previously stated, meiotic chromosomes are organized as linear arrays of chromatin loops, anchored to the axial element (AE) that forms along the length of sister chromatid pairs. This is assembled upon a cohesin topoisomerase II core. There is evidence that Rec8 is involved in the AE biogenesis and SC formation. Rec8 localizes to the axes of meiotic chromosomes and is required for normal axis assembly (Chan et al., 2003; Klein et al., 1999). In *C. elegans* HTP-3 localization to AE is dependent on the presence of all meiosis-specific kleisins, REC-8 and it's paralogs COH-3 and COH-4 (Severson et al., 2009). In mouse, however, this is not the case and loss of Rec8 does not disrupt AE formation, but this may indicate functional redundancy with Rad21, which also localizes to the SC in mice (Xu et al., 2004). In fact two recent studies demonstrate that different forms of Rad21 are present in mouse meiosis (Ishiguro et al., 2011; Lee and Hirano, 2011), and mice lacking both Rec8 and Rad21L fail to load AE components (Llano et al., 2012). In yeast, Rec8 is also required for loading of the CE to form a mature SC, and in plants the Rec8 homologue *SYN1* is required for the completion of synapsis (Bai et al., 1999; Cai et al., 2003; Klein et al., 1999). In *C. elegans, rec-8* mutants show a delay in SC assembly (Pasierbek et al., 2001), whilst *Rec8* mice apparently form normal SCs, but this is loaded between sister chromatids instead of homologous chromosomes (Xu et al., 2005).

In budding yeast, ChIP-chip experiments have shown that there is a dynamic localization of Spo11 to meiotic chromosomes and that this is dependent on the presence of Rec8. *rec8* deletion mutants have impaired Spo11 binding and DNA analysis showed a reduction in DSB formation (Kugou et al., 2009). There is also evidence that Rec8 also plays a role in the formation of COs downstream of DSB formation. In yeast *rec8* deletion mutants there is a 20-40 fold reduction in inter-allelic recombination measured at two loci on chromosome III, which cannot be attributed to a decrease in DSBs at these sites (Klein et al., 1999). In *C. elegans* mutations in both *rec-8,* and the REC-8 loader TIM-1, lead to diakinesis oocytes with 12 univalents, indicating that they are not competent to form COs at all (Chan et al., 2003).

As meiotic recombination occurs after DNA replication, sister chromatids are present throughout the process. In this context, repair of DNA damage during mitosis occurs preferentially between sister chromatids, whereas in meiosis this recombination is usually biased to occur between chromatids from homologous chromosomes, rather than between sister chromatids (Zickler and Kleckner, 1999). In *S. cerevisiae,* Rec8, together with Red1/Hop1/Mek1 are the only known meiosis-specific axis components and it is therefore expected that SCC plays a role in homolog versus sister partner bias (Schwacha and Kleckner, 1997). This idea is also attractive because SCC must be locally compromised at CO sites in order to allow chromatids to move away from their sisters and towards their homologue, enabling strand exchange. For a CO to occur this exchange at the DNA level must be accompanied by one at the structural, axis level. This loosening of cohesion should not be necessary either at breaks destined to be NCO or at sites of inter-sister recombination, where it might even prove inhibitory (Kleckner, 2006). Indeed Rec8 is absent at chiasmata and local separation of sisters can be seen at CO sites (Eijpe et al., 2003). Thus, there is a conflict between the necessity for cohesion globally and cohesin loss at CO sites. In yeast, evidence bears out this theory: Rec8 promotes sister-bias, presumably via its cohesive function, with Red1 and Mek1 kinase acting to counteract this effect and promote a homolog bias (Kim et al., 2010b).

Investigation of the *scc-2(fq1)* mutant in worms has revealed additional roles for cohesin during meiotic prophase. The mutants displayed an extensive accumulation of *spo-11*-dependent recombination intermediates during meiosis, as indicated by extensive staining of RAD-51, with not only much higher numbers of foci but also short tracts of staining in mid/late pachytene, indicating that cohesin plays a role in DNA damage repair in meiosis, as has been previously reported (Brar et al., 2009; Klein et al., 1999; Lightfoot et al., 2011).

1.4.4 Regulation of meiotic cohesion

It is clear that meiotic cohesin plays a role in regulating some key events in meiosis, but how meiotic cohesin itself is regulated throughout meiosis, allowing it carry out these functions, remains largely unknown. Are the same key players, namely Eco1, Psd5 and Wapl, that are involved in regulating mitotic cohesin carrying out the same roles in meiosis? There is a paucity of data on the role of Eco1 in meiosis. However, a study in fission yeast has shown that acetylation of Smc3 by Eco1 is required for mono-orientation of chromosomes at meiosis I, and may be the target for regulation of kinetochore orientation and that the Hos1 paralogue, Clr6 or Hos2, functions to deacetylate Smc3, antagonising Eco1's function, in a manner similar to mitosis (Kagami et al., 2011).

A little more is known of Pds5's function in meiosis. An early study in *S cerevisiae*, indicates that Pds5 is unable to load onto meiotic chromosomes, that Rec8 loading is independent of Pds5 and that mutation of Pds5 leads to premature separation of sister chromatids (Zhang et al., 2005). However, a more recent study has contradictory findings. It finds that Pds5 colocalizes with cohesin along the length of meiotic chromosomes, and that in a meiosis-conditional null allele of *Pds5*, Rec8 remains bound to chromosomes with only minor defects in SCC. In this context, sister chromatids rather than homologues synapse and DSBs are formed but are not repaired efficiently and meiotic chromosomes undergo hypercondensation. This suggests that Pds5 modulates Rec8 activity to facilitate changes in chromosome morphology required for homologue synapsis, DSB repair, and meiotic chromosome segregation (Jin et al., 2009). Similarly to this study, in *C. elegans*, the Pds5 mutant has a modest defect in meiotic SCC (Wang et al., 2003). Finally, in *Drosophila*, lack of Pds5 results in an open chromatin structure consistent with a role in SCC. This is suppressed in the absence of DSBs, suggesting that Pds5 is required to maintain the structure of meiotic chromosomes subsequent to DSB formation. In addition to this, Pds5 mutants fail to activate the ATR checkpoint (Barbosa et al., 2007).

Finally, initial evidence hinted that there might be a prophase pathway in effect in meiosis. A study in which cohesin quantity was assessed by indirect immunofluorescence and ChIP found that the amount of chromosome bound Rec8, Scc3 and Smc1 was reduced in metaphase I compared to prophase I cells, suggesting that a subset of meiotic cohesin was being removed from the chromosomes between these two stages (Yu and Koshland, 2005). It is unknown whether Wapl is responsible for any cohesin removal in meiosis. In yeast it has been shown that spore viability is not compromised by lack of Wapl indicating that Wapl's function in meiosis is not essential for chromosome segregation, however this does not preclude a role for Wapl in other aspects of meiotic chromosome behaviour (Lopez-Serra et al., 2013). Indeed, our current state of knowledge as to the roles of cohesin's regulation during meiosis is slim and inconsistent. Establishing the mechanisms through which cohesin dynamics are modulated throughout meiosis and what role these dynamics play provide a challenge for future investigations into the coordination of meiotic events.

1.4.5 Maintenance and release of centromeric cohesin

Once COs and SCC have been established, creating temporary physical links, chiasmata, that connect homologs, cohesin must be disassociated from chromosomes in two steps, firstly allowing homologue segregation at meiosis I, and then sister chromatid segregation in meiosis II. In organisms with monocentric chromosomes this is achieved by removing cohesin by separase-mediated cleavage of Rec8 along the chromosome arms but not at the centromeres. Similarly to mitosis, this in driven by a phosphorylation-dephosphorylation pathway affecting cleavage of the α-kleisin. Casein-kinase-1 (CK1) and the Cdc7 kinase phosphorylate multiple sites causing targeted cleavage of Rec8 via separase, with phosphomimetic mutants of Rec8 rendered cleavable even in the absence of CK1 and Cdc7 (Katis et al., 2010). In order to protect centromeric cohesin until metaphase II, Rec8 must be protected from phosphorylation. This is achieved through the association of Sgo1 with the protein phosphatase 2A (PP2A), which antagonises the phosphorylating activity of CK1 (Kitajima et al., 2006; Riedel et al., 2006). In a recent screen for genes

with 'anti-shugoshin' activity in *S. pombe,* a casein kinase orthologue, Hhp2, has been identified. Hhp2 is required for Rec8 cleavage and can counteract the ability of Sgo1-PP2A to protect centromeric Rec8. This reinforces the model that there is a balance between Rec8 phosphorylation and dephosphorylation that is regulated by Sgo1-PP2A in order to that cohesin is lost in a stepwise manner in meiosis (Ishiguro et al., 2010). In humans Sgo2 is phosphorylated by Aurora B kinase, inducing the binding of Sgo2 to phosphatase PP2A. This is recruited to centromeres where it is thought to dephosphorylate Rec8 protecting it from cleavage by separase, suggesting that a similar mechanism to Sgo1 may be utilised (Tanno et al., 2010). This allows the resolution of chiasmata at meiosis I, resulting in two cells with dyad chromosomes. The remaining cohesin is then lost at the anaphase to metaphase transition in meiosis II, allowing sister chromatid separation and the formation of four haploid cells.

C. elegans has holocentric chromosomes, however, the mechanism for executing the stepwise release of SCC during meiosis is functionally analogous to the system employed in organisms with monocentric chromosomes. The *C. elegans* Aurora B kinase, AIR-2, is thought to function similarly to CK1. Depletion of AIR-2 by RNAi has been shown to prevent chromosome separation at both anaphase I and II, and AIR-2 is capable of phosphorylating REC-8 at a major amino acid in vitro (Rogers et al., 2002). While it is assumed that phosphorylation of REC-8 by AIR-2 is responsible from rendering it cleavable by separase *in vivo*, this has never been formally demonstrated.

LAB-1 and HTP-1 are two axial element components of *C. elegans* meiotic chromosomes that appear to carry out a role similar to that of SGO1 and 2. Both are progressively restricted to the long arms of the asymmetric bivalents, which is the region in which SCC needs to be protected during anaphase I, and both proteins appear to restrict AIR-2 to the short arms of the bivalents until homologs separate at anaphase I. Evidence for this lies in the fact that in *htp-1* mutants AIR-2 localises to both long and short arms of bivalents, implicating HTP-1 in preventing binding of AIR-2 to regions in which SCC must be protected (Martinez-Perez et al., 2008). A similar defect is observed in the bivalents of

worms lacking LAB-1 (de Carvalho et al., 2008). Recently, it has been shown that LAB-1 directly interacts with the protein phosphatase GSP-1 and its paralogue GSP-2, thus antagonizing AIR-2 phosphorylation and promoting sister chromatid cohesion in a comparable manner to PP2A (Tzur et al., 2012). Both *htp-1/2* and *lab-1* mutants have premature separation of sister chromatids during the first anaphase I, illustrating their role in the protection of SCC (de Carvalho et al., 2008; Martinez-Perez et al., 2008).

1.4.6 Kinetochore co-orientation

In addition to this stepwise loss in cohesion, for proper segregation it is vital that the chromosomes are correctly oriented on the metaphase plate at meiosis I and II. In meiosis I, homologues must be mono-oriented so that the microtubules are pulling maternal and paternal kinetochore pairs in opposite directions, whereas in meiosis II the situation is akin to mitosis, with bioriented chromosomes so that microtubules are pulling sister kinetochores in opposite directions. For this too, cohesin is required. The physical connection provided by the CO and SCC in bivalent chromosomes provides resistance to the microtubules pulling the bivalent apart. This is necessary to stabilize correct kinetochore microtubule connections and thus the correct orientation (Nicklas, 1997). Mutations in *Rec8 S. pombe* and *Arabidopsis* lead to biorientation of sister kinetochores in meiosis I, suggesting that cohesin connects sister kinetochores in a way that promotes their mono-orientation (Chelysheva et al., 2005). As it is essential that cohesion is maintained until all chromosomes are bioriented, lagging chromosomes inhibit cohesion destruction through a process known as the spindle assembly checkpoint (SAC) (Nasmyth and Schleiffer, 2004).

1.4.7 Clinical relevance of meiotic cohesin

What is the clinical relevance of meiotic cohesin? As mentioned earlier this incidence of Trisomy 21 rises with increasing maternal age and the gradual degradation of the cohesin complex through the exceptionally long period of prophase arrest in humans has been implicated. Recent findings in mice lacking SMC1β show that male mice are sterile owing to an arrest in meiosis at

pachytene, whereas in females meiosis is highly error prone but continues until metaphase II (Revenkova et al., 2004). SMC1β -deficient oocytes, on the other hand can develop up to metaphase II, but female mice are also sterile and this is due to massive levels of aneuploidy. Furthermore, the SMC1β deficient oocytes from one-month-old females appear almost normal in meiosis I, but from two-month old litter mates, the oocytes manifest unpaired univalents, and this increases in incidence with the age of the female mutant mice. A surprising observation was that chiasmata were predominantly localized in the distal region, and the number of bivalents in meiosis I was decreased in the older mutant mice, although the pattern of recombination was found to be similar to that seen in wild-type mice (Hodges et al., 2005).

More recent studies have used conditional knock-out mice for SMC1β, in which the SMC1β protein is produced only during foetal development, as the SMC1β gene is knocked out after the neonatal period. In these mice fertility was not affected, suggesting that meiotic cohesin is sufficiently robust for cohesion throughout the life of foetal oocytes. Therefore, if cohesin is subject to age related degradation no regeneration of cohesion could be expected to occur (Revenkova et al., 2010). It should be noted that this does not preclude a role for cohesin turnover in early prophase, as the oocytes have already entered dictyate arrest at the time at which SMC1β is knocked out.

It has been demonstrated that an-age related reduction of REC8 occurs in mice and humans (Chiang et al., 2010; Garcia-Cruz et al., 2010; Lister et al., 2010). Further to this, it has been revealed that chiasma resolution was triggered by enzymatic disruption of REC8, supporting the hypothesis that degradation of the cohesin complex contributes to reduced numbers of chiasmata or premature separation of sister chromatids (Tachibana-Konwalski et al., 2010). It therefore appears likely that gradual degradation of cohesin over time may be a contributing factor to the maternal age effect. These observations demonstrate that investigating the regulation and functions of cohesin in meiosis is not only a fascinating area of research, but also has the potential to advantage medical interventions in the future.

1.5 Aims and Objectives

The initial aim of this project was to continue characterising the functions of the cohesin loader SCC-2 during meiotic prophase, and to investigate if reloading of meiotic cohesin occurs after S-phase. To extend the data obtained from the *scc-2* mutant previously isolated in our lab, I sought to deplete SCC-2 by RNAi, thereby creating a situation in the germline in which two populations of nuclei existed: those which had cohesin loaded prior to the knockdown, and those which underwent S-phase subsequent to RNAi knockdown. In particular, I wished to see what effect this would have on the DNA damage response. However, the data from these experiments strongly suggested that cohesin reloading and removal played an important role in other aspects of meiosis. I therefore, set about developing novel tools to investigate cohesin reloading, in particular by using the recently developed technique for creating single copy insertion transgenic *C. elegans* strains. In consort with this, I undertook to investigate whether WAPL plays a role in cohesin removal in meiosis. Hopefully, this project will further our understanding of the fundamental processes of meiosis, in particular the role of cohesin dynamics on the events of meiotic prophase I.

Figure 1. A schematic diagram of the major events of meiosis.

Chromosomes replicate generating sister chromatids that are held together through cohesion. The homologues pair and the SC forms between them, stabilising the interaction. DSBs are generated during early meiotic prophase and some are subsequently processed to form CO, which together with SCC provide the basis of a physical linkage holding the homologous together, known as chiasmata. Chiasmata become visible in late prophase once SC disassembly and chromosome remodelling have occurred. At this stage the homologous chromosomes attached by chiasmata is known as a bivalent. The stepwise removal of cohesin during the meiotic divisions allows the separation of the homologues at anaphase I and sister chromatids at anaphase II.

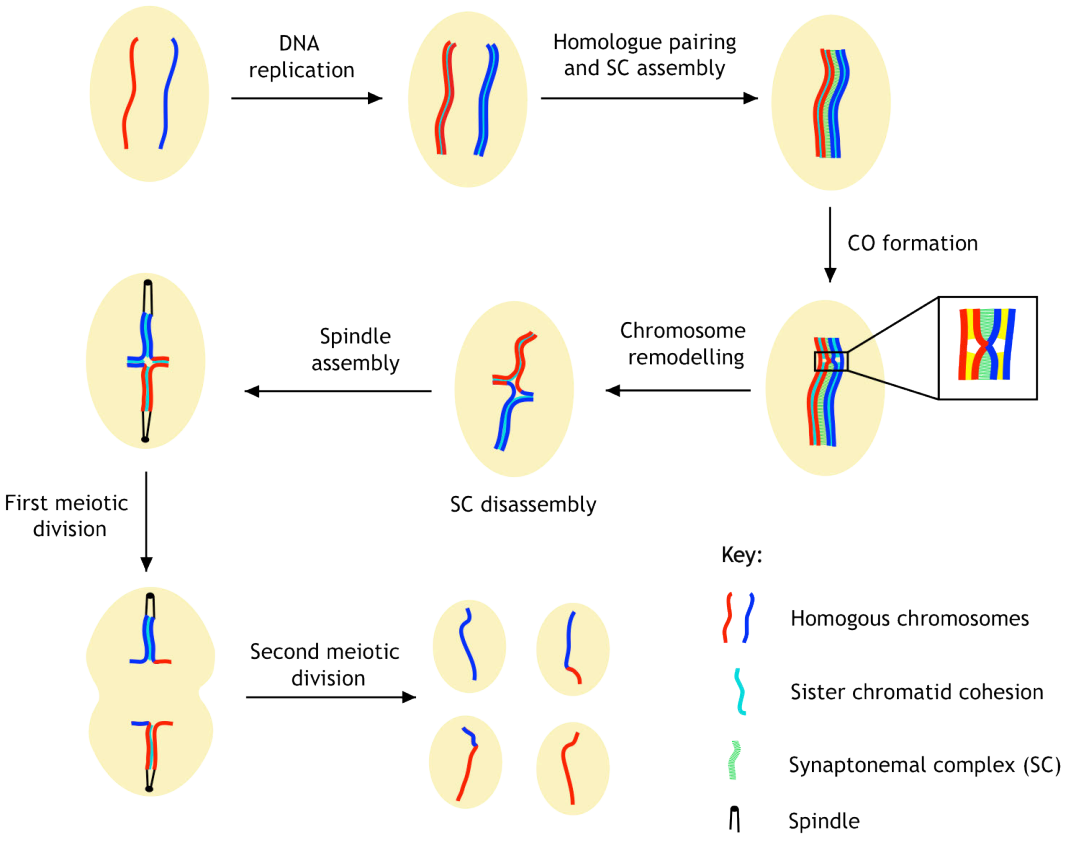
DNA replication
Homologue pairing and SC assembly
CO formation
Chromosome remodelling
SC disassembly
Spindle assembly
First meiotic division
Second meiotic division
Key:
Homogous chromosomes
Sister chromatid cohesion
Synaptonemal complex (SC)
Spindle

Figure 2. A diagram of a dissected *C. elegans* germline

The germline displays a complete time-course of meiosis in which stages are cytologically discernible by observing nuclei chromosome morphology.

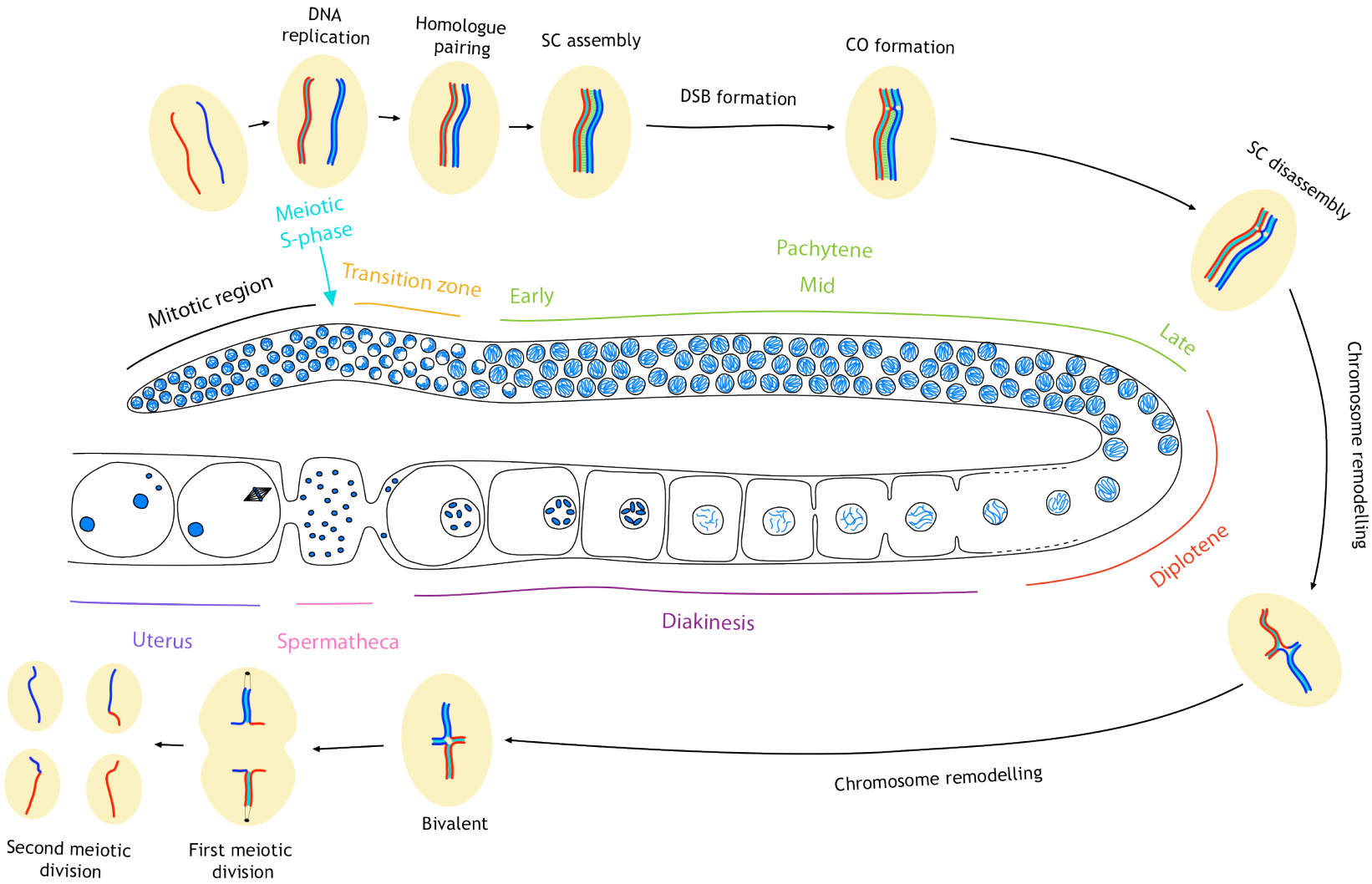
DNA replication
Homologue pairing
SC assembly
DSB formation
CO formation
SC disassembly
Meiotic S-phase
Mitotic region
Transition zone
Early
Pachytene
Mid
Late
Diplotene
Diakinesis
Chromosome remodelling
Uterus
Spermatheca
Bivalent
Chromosome remodelling
Second meiotic division
First meiotic division

Figure 3. A summary of the DSB repair pathway used in meiosis for interhomologue recombination.

The main proteins involved at each step are indicated

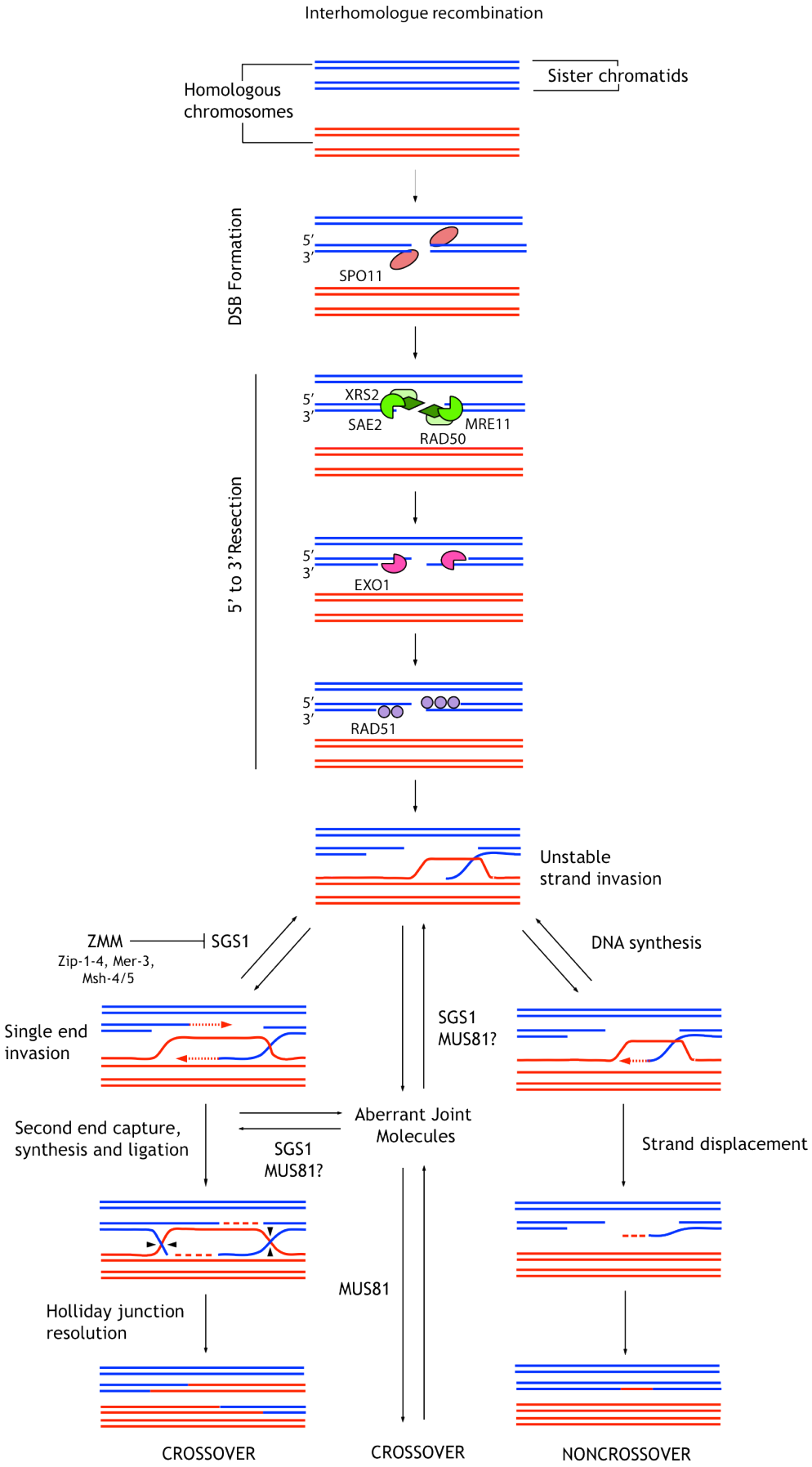
Interhomologue recombination
Homologous chromosomes
Sister chromatids
DSB Formation
5′
3′
SPO11
5′ to 3′ Resection
XRS2
SAE2
MRE11
RAD50
EXO1
RAD51
Unstable strand invasion
ZMM
Zip-1-4, Mer-3, Msh-4/5
SGS1
DNA synthesis
Single end invasion
SGS1 MUS81?
Second end capture, synthesis and ligation
Aberrant Joint Molecules
SGS1 MUS81?
Strand displacement
MUS81
Holliday junction resolution
CROSSOVER
CROSSOVER
NONCROSSOVER

Figure 4. Diagrams of the cohesin complex

(**A**) The cohesin complex with its associated proteins.

(**B**) The "embrace" model of SCC.

(**C**) The cohesin cycle. Cohesin is loaded through the SCC2/SCC4 complex prior to and during S-phase. ECO1 establishes cohesion via acetylation of SMC3 and PDS5 binding. Cohesin in reloaded in response to DSBs by Scc2/Scc4 and becomes cohesive. Cohesin is dissociated through WAPL's interaction with PDS5 in prophase and through separase cleavage of SCC1 during the metaphase to anaphase transition.

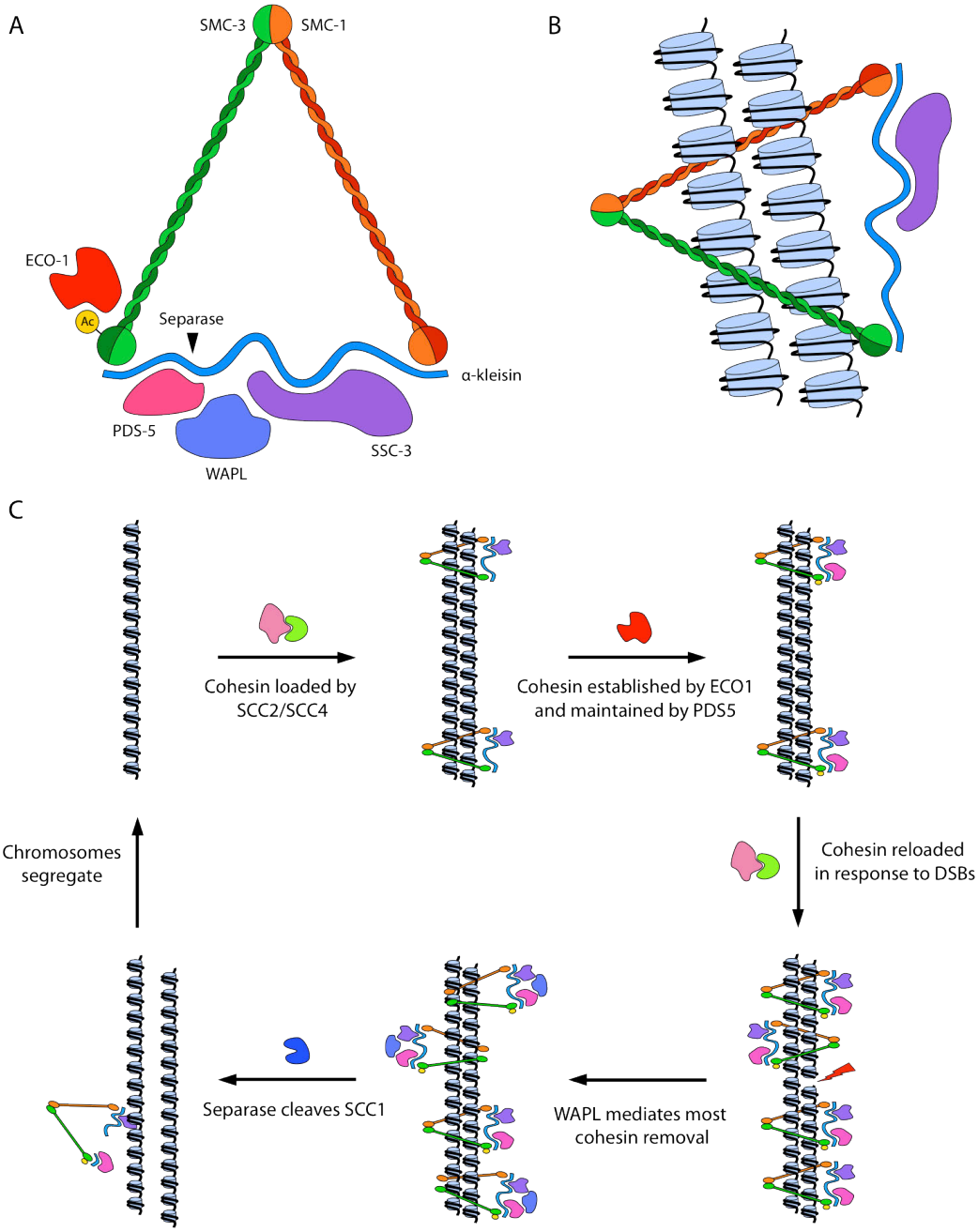
A
SMC-3
SMC-1
ECO-1
Ac
Separase
α-kleisin
PDS-5
SSC-3
WAPL
B
C
Cohesin loaded by
SCC2/SCC4
Cohesin established by ECO1
and maintained by PDS5
Cohesin reloaded
in response to DSBs
WAPL mediates most
cohesin removal
Separase cleaves SCC1
Chromosomes
segregate

CHAPTER 2: MATERIALS AND METHODS

2.1 *C. elegans* general methods

2.1.1 General growth conditions

C. elegans strains were maintained on Nematode Growth Media (NGM) plates seeded with either OP50 (Brenner, 1974), or for RNAi experiments, HT115 (DE3) attenuated *E. coli strains.* Media and solutions are described in Table 1. *C. elegans* Bristol strain (N2) was used as wild type controls and all strains were maintained at 20°C, unless otherwise stated. To prevent the population from starving and to provide a constant source of animals from all stages of the life cycle, worms were transferred to a freshly seeded plate every 2-3 days. Starved strains were prevented from becoming desiccated by wrapping parafilm around the plate, and in this way worms were viable for several months.

A list of all the strains used in this study is provided at the end of this chapter.

2.1.2 Handling and observation of *C. elegans*

Animals were manipulated using a fine crafted pick made from Platinum wire (Sigma-Aldrich Platinum wire diameter 0.25 mm, Product number: 349402-250MG) welded onto the end of a glass Pasteur pipette. Animals were observed using a Leica MZ75 bench stereoscope or with a Leica MZ16F florescence stereoscope for transgenic worms with visible fluorescent markers.

2.1.3 Maintaining male stocks

Male stocks were maintained by picking 3 to 6 male worms with 1 to 3 L4 stage hermaphrodites to a single NGM plate. This ensures that hermaphrodites

are mated while they were still young adults, resulting in the production of up to 50% of males in the F1 progeny.

2.1.4 Maintaining meiotic mutants

C. elegans meiotic mutants are difficult to maintain, as homozygous strains often have low viabilities. Compounding this, meiotic mutants often have compromised genomic integrity allowing the introduction of novel mutations into the genome when strains are kept as homozygous stocks. Therefore, meiotic mutations were maintained in heterozygousity, by using reciprocal translocations that carried visible markers to balance meiotic mutations. From these strains homozygous animals could be obtained, as heterozygous and homozygous animals were easily identifiable on the plates by their visible translocation markers.

2.1.5 Cleaning of *C. elegans* strains

C. elegans strains occasionally became contaminated with moulds and/or bacteria (different than *E. coli* OP50), which could affect the regular growth of the animals. Uncontaminated cultures were restored by washing with Bleaching Solution. Animals and eggs were washed from their contaminated plate with M9 and pipetted in Falcon tubes containing 10ml of Beaching solution (Table 1). Falcon tubes were left on a nutator for 10 min or until the adult animals had dissolved, leaving no carcasses visible. The worm eggs were pelleted by centrifuging for 1 min at 900 x g in a bench top centrifuge and washed 3 times with 10 ml of H_2O and. Finally the egg pellet was re-suspended in 500 μl of M9 and the eggs were transferred onto fresh OP50 seeded NGM plates. After 12-18 h, the larvae hatched to produce a clean culture.

2.1.6 Freezing of *C. elegans* strains

A practical, if surprising property of *C. elegans* is that it can be frozen and stored in -80°C freezers, or liquid nitrogen, for many years (Brenner, 1974). The early stages of worm development survived the freezing process best, so

plates containing large amounts of L1 and L2 were used for the creation of frozen strain stocks. Worms from three plates were washed off using M9 and placed onto a 15 ml falcon tube. This solution was mixed with freezing solution in a 1:1 ratio and 1 ml of this mixture was pipetted into a 3 ml cryotube (Fisher), producing six vials in total. These were immediately transferred to a -80°C freezer. Five vials were stored at -80°C, while 1 test vial was thawed the following day to ensure the strain survived the freezing process.

Table 1: Media and solutions for general growth conditions

Name	Composition	Use
NGM	3 g NaCl 2.5 g Bactopeptone 20 g Agar H_20 up to 1 l 1 ml 1M $MgS0_4$ 1 ml 1M $CaCl_2$ 1 ml 1M Cholesterol (5 mg/ml in EtOH) Autoclave and add 25 ml Potassium Phosphate (1 M, pH 6.0) Dispense into 60 mm petri dishes	Growth media for *C. elegans* strains
B-Broth	10 g Bactotryptone 5g NaCl dH_2O up to 1 l	Growth media for OP50 bacteria primary inocule
M9	5.8 g Na_2HPO_4 3.0 g KH_2PO_4 0.5 g NaCl 1.0 g NH_4Cl dH_2O up to 1liter	Short-term preservation of *C. elegans* in liquid.
Freezing Solution	5.85 g NaCl 6.8 g KH_2PO_4 300 g Glycerol 5.6 ml 1M NaOH	Cryopreservation of *C. elegans* strains

	dH2O up to 1 l Autoclave and add 300 µl of 1 M $MgSO_4$	
Bleaching Solution	5.5 ml H_20 2.5 ml 2M NaOH 2 ml of bleach	Cleaning of the strains of *C. elegans*
LB	1.0% Tryptone 0.5% Yeast Extract 1.0% NaCl pH 7.0	Growth media for *E. coli*
S.O.C.	2% Tryptone 0.5% Yeast Extract 10mM NaCl 2.5 mM KCl 10mM $MgCl_2$ 10mM $MgSO_4$ 20mM glucose	Growth media for *E. coli.* Specially indicated for transformation.

2.2 DNA Methods

2.2.1 DNA extractions

A crude DNA extraction method was used in order to obtain *C. elegans* genomic DNA that could be used as a template for PCR reactions. For single worm extraction, an individual animal was transferred into a 0.2 ml PCR tube containing 10 µl of 1x PCR buffer with proteinase K (see below). The tubes were frozen in liquid N_2 and directly transferred to a PCR thermocycler, using the following program:

70 min at 60°C
15 min at 95°C.

DNA could then be used or stored at -20°C until needed. The same protocol could be used to extract DNA from several worms in a population by simply lysing multiple animals together in the same tube.

1X PCR buffer containing protease K:
Mix 100 µl of 10xPCR mix (100 mM Tris, 500 mM KCl, 15 mM $MgCl_2$ pH 8.3, autoclaved) with 900 µl of H_2O and 50 µl of 20 mg/ ml proteinase K.

2.2.2 Single Worm PCR

Using 1-2 µl of DNA extraction as template, a 25µl PCR reaction was set up as follows:

10.5 µl H_2O,
12.5µl Taq PCR Master mix (Quiagen)
1 µl of the required primer pair at a 10µM concentration

The annealing temperature used based on the melting temperature (Tm) of each primer pair and the extension of the elongation step was chosen assuming an extension rate of approximately 1 kbp per minute. The reaction product was checked by running 5 µl of the reaction on an agarose gel by standard electrophoresis procedures, and cleaned for sequencing using a PCR purification kit (QIAGEN) if necessary.

The following PCR program was used:

	5 min at 95˚C	
Denaturation	30 sec at 95˚C	
Annealing	30 sec at Tm	x35 cycles
Elongation	x sec at 72˚C	
	10 min at 72˚C	

2.3 RNA Methods

2.3.1 RNAi by feeding

RNA-mediated interference (RNAi) was first described in *C. elegans* (Fire et al., 1998). The introduction of double-stranded RNA (dsRNA) results in inactivation of the corresponding gene. This can be achieved by feeding worms *E. coli* expressing a dsRNA fragment of the gene you wish to deplete.

2.3.1.1 dsRNA *in vivo* expression

A fragment of the gene of interest had to be cloned into a feeding vector (L4440) between two T7 promoters in inverted orientation. This then has to be transformed into the *E. coli* strain HT115(DE3), which carries an Isopropyl β-D-1-thiogalactopyranoside (IPTG)-inducible T7 polymerase and lacks double-strand specific RNaseIII. the Gateway Technology from Invitrogen was used to clone fragments from genomic DNA.

2.3.1.2 RNAi plates

RNAi feeding plates are comprised of standard NGM plates with the addition of:

IPTG 1 mM final concentration
Ampicillin (Sigma) 25 mg/ml final concentration

Just before the seeding, the plates were supplemented with 50 ml of 1M IPTG and 50 ml of 100mg/ml ampicillin spread over the surface of the media with a sterile glass spreader.

Individual colonies of the desired clones were picked and grown overnight (ON) at 37˚C, with 200rpm shaking, in 20 ml of LB with ampicillin (100 mg/ml). The bacteria was pelleted and re-suspended in 1 ml of LB with ampicillin (100 mg/ml). From this, 100 ml per plate were used to seed the RNAi plates. The bacteria were induced ON by incubating the plates at 37˚C.

2.3.1.3 Worm handling

Five L4 worms were transferred to RNAi-seeded plates and grown at 20˚C or 25˚C. Once the first L4 progeny appeared on the plates they were transferred to fresh RNAi-seeded plates and dissected 18hrs later.

2.3.1.4 Gateway cloning for dsRNA expression

2.3.1.4.1 Insert production

Using genomic DNA from a single-worm lysis as template, a fragment 500 bp to 1 kbp in size of the gene of interest was amplified. Primers were designed by adding the attB sequence to the 5' position of normal primers. The fragment was amplified using the Expand Long Template PCR System (Roche) with the following conditions:

10X Expand Long Template Buffer 1:	5 ml
Expand Long Template Enzyme Mix:	0.75 ml
Primers (each):	300 nM (final concentration)
dNTP (each):	350 mM (final concentration)
Template:	2 ml

The PCR program used was a combination of 10 cycles with a 52°C annealing temperature, followed by 30 cycles with a 60°C annealing temperature, both with 1min extension steps at 68°C. The PCR product was purified directly from the solution or extracted from an agarose gel using QIAGEN kits, following the manufacturers' protocol.

2.3.1.4.2 BP reaction

The purified PCR-attB product was cloned into the p221 vector which contains attP sites, using the Gateway BP Clonase II Enzyme Mix (Invitrogen). The manufacturers' standard protocol was followed, with slight modifications:

250ng of insert
150ng of p221 vector

The reaction was incubated at 25°C ON and terminated by adding 1 ml of Proteinase K solution and incubating the samples at 37°C for 10 min. Recombination between the attB sites of the insert and the attP sites of the vector produces attL sites, allowing Gateway cloning into the L4440 vector.

The reaction product was used to transform chemically competent One Shot OmniMAX 2-T1 Phage-Resistant *E. coli* cells, following the manufacturer's specifications. The cells were spread on LB plates with 50mg/ml kanamycin. Plasmids were harvested with QIAprep Spin Miniprep Kit (QIAGEN).

2.3.1.4.3 LR reaction

Using the Gateway LR Clonase II Plus Enzyme Mix (Invitrogen), the fragment cloned into the p221 vector (now with attL sites) was cloned by recombination in the pL4440 gateway vector. The manufacturers' standard protocol was followed with slight modifications:

p221-insert	150ng
pL4440 vector	250ng

As before, the reaction was incubated at 25°C ON and terminated by adding 1 ml of Proteinase K solution and incubating the samples at 37°C for 10 min.

The reaction product was used to transform the chemically competent One Shot Mach1 T1, following the manufacturer's specifications. The cells were plated on LB plates with 50 mg/ml ampicillin, and plasmids harvested as above.

2.3.1.4.4 *E. coli* transformation

Plasmid DNA was added to chemically-competent *E. coli* cells, HT115(DE3) thawed on ice. The cells were then incubated on ice for 30 min, heat-shocked for 90s at 42°C, followed by 1 min of cooling on ice. A 6x-volume of S.O.C. medium (Invitrogen) was added and the cells were incubated with shaking at 37°C for 1 h before plating on LB with 100 mg/ml ampicillin and 12.5 mg/ml tetracycline for ON incubation at 37°C. This creates *E. coli* expressing an IPTG inducible dsRNA fragment, allowing for RNAi knockdown by feeding.

2.3.2 mRNA expression

A powerful tool that has been used in other model organisms is the introduction of mRNA into cells. However, until recently this technique had not been used in *C. elegans*, due to the propensity of introduction of RNA into the germline to cause suppression of the exogenous gene by RNAi. To overcome the RNAi pathway by using a kit which not only produces high yields of very pure ssRNA, but also caps the RNA at its 5' end, and a secondary kit to add a polyA tail to the 3' end, both of which mimic *in vivo* mRNA in most eukaryotes. This should prevent degradation of the mRNA within the worm.

2.3.2.1 mRNA *in vitro* transcription

2.3.2.1.1 Preparation of template DNA

Plasmids used for mRNA synthesis had a T7 promotor immediately upstream of the cDNA sequence with a fluorescent tag, followed by a unique restriction site. Plasmid DNA was purified from a 5ml ON bacterial culture using the QIAprep Spin Miniprep Kit (QIAGEN). The concentration of DNA was quantified using the Qubit Flurometric system. Then 5μg of plasmid was linearised by restriction enzyme digest as per the manufacturer's instructions. 5μl of the restriction reaction was examined on a gel to confirm that cleavage was complete, as it is important to have linearized template DNA, with very little circular DNA contamination. The restriction digest was terminated by adding the following:

1/20th volume 0.5 M EDTA
1/10th volume of 3M Na acetate
2 volumes of ethanol

This was mixed well and chilled at –20°C for 20 min and pelleted in a microcentrifuge at 14000rpm and 4°C, for 15mins. The supernatant was removed and the tube re-spun for 30secs and residual fluid removed with a fine-tipped pipette. This was resuspended in 50µl of dH_2O.

As DNA from some miniprep procedures may have residual RNase A contamination and the restriction enzymes reaction occasionally introduces RNase or other inhibitors of transcription, the template DNA was treated with proteinase K (100–200 µg/mL) and 0.5% SDS for 30 min at 50°C, and then the DNA purified by phenol/chloroform extraction and ethanol precipitation, and resuspended in 10µl of H_2O. The concentration of DNA was quantified using the Qubit Flurometric system.

2.3.2.1.2 Capped reaction

The T7 mMessage mMachine Kit (Ambion AM1344) was used for the synthesis of mRNA as per the manufacturers instructions. Briefly the following reaction was set up:

10µl 2X NTP/CAP
2µl 10X Reaction Buffer
1µg linear template DNA
2µl Enzyme Mix
up to 20µl nuclease free H_2O

This was mixed thoroughly and incubated for 2hrs at 37°C.

2.3.2.1.3 PolyA tailing reaction

The Poly(A) Tailing Kit (Ambion AM1350) was used to add a polyA tail to the mRNA product, as per the manufacturer's instructions. Briefly the following reaction was set up at room temperature:

20µl mMESSAGE mMACHINE reaction
36µl Nuclease-free Water
20µl 5X E-PAP Buffer
10µl 25 mM MnCl2
10µl 10 mM ATP

0.5µl of the reaction mixture was removed before adding the E-PAP enzyme as a minus-enzyme control. 4µl of E-PAP was added to the reaction and mixed gently, giving a final reaction volume of 100µl. This was incubated at 37°C for 1 hr.

2.3.2.1.4 RNA recovery

The mRNA was recovered by phenol:chloroform extraction and isopropanol precipitation. An equal volume of phenol/chloroform was added to the reaction and the aqueous phase recovered and transferred to new tube. The RNA was precipitated by adding 1 volume of isopropanol and mixing well. The mixture was chilled for 15mins at –20°C and then centrifuged at 4°C for 15 min at 14000rpm to pellet the RNA. The supernatant was carefully removed and the RNA resuspended in H_2O.

2.3.2.1.5 Quantification of RNA product

The quality of the product as well at the success of the tailing reaction was assessed by denaturing gel electrophoresis. The RNA content was quantified using the Qubit Flurometric system diluted to a concentration of 0.1µg/µl, alliquoted and stored at -80°C

2.3.2.2 Worm handling

To immobilize the worms for injection, the animals were transferred into 2% agarose pads. Dehydration of the worms was avoided by immersing them into a drop of Halocarbon oil 700 (Sigma-Aldrich). Animals were injected into the gonad with needles made from borosilicate glass (OD 1.0 mm, ID 0.78 mm, from Sutter Instrument) by pulling them with the Flaming/Brown Micropipette Puller (model P-97, Sutter Instrument). Injected animals were recovered from the pads by gentle washing with M9. They were pipetted on NGM plates for recovery.

2.4 Cytological Methods

2.4.1 Ethanol Fixation

Ethanol fixation followed by DAPI staining is a quick and simple way to observe *C. elegans* chromosomes cytologically. Approximately 20 worms were picked to 8 μl M9 buffer on a superfrost charged slide (VWR scientific). As much liquid as possible was wicked away using filter paper until the worms were left in only a small volume of M9. 10 μl 95% ethanol was added to the slide and air-dried. This was repeated to fully dehydrate the worms. 8 μl of 2μg/ml DAPI was added and a 22 x 22 glass cover slip was placed on the top of the worms. Animals were viewed on a Leica DMRB microscope using 20X, 40X, or 62X lenses and imaged with a Leica DFC300 FX camera.

2.4.2 Immunostaining of *C. elegans* germlines

A slightly modified protocol for immunostaining staining was carried out as described in Howe et al. (2001). Worms were synchronised by transferring L4s to a fresh NGM plate and allowing them to mature for 18hr, unless otherwise specified, yielding a population of young adults.

20 to 30 age matched adult worms were picked into 15 μl egg buffer (118 mM NaCl, 48 mM KCl_2, 2 mM $CaCl_2$, 2 mM $MgCl_2$, 5 mM HEPES, at pH 7.4) with 0.1% tween on a 22 x 22 glass cover slip. The animals were carefully dissected just

behind the pharynx using a fine needle in order to achieve optimum gonad extraction. Germlines were fixed by the addition of 15 µl 2% paraformaldehyde (PFA) in egg buffer and 0.1% tween. Pipetting gently ensured an even mix of PFA throughout and aided in extruding the gonads. 15µl of the solution was then removed and the remaining solution covered with a superfrost charged slide (VWR scientific). The dissections were fixed for a total 5 min from the addition of the PFA and then immediately immersed in liquid N_2. The cover slip was removed using a razor blade and the slide placed in -20°C methanol.

Slides could be stored in -20°C methanol for several days but as little as 3 min was sufficient for aiding adherence of the germlines to the slides. The slides were washed 3 x 5 min in PBST (1x PBS, 0.1 % Tween) in coplin jars before being blocked for 1 hr in 0.7 % BSA in PBST. 50µl of primary antibody diluted in PBST was added to each slide and covered with a parafilm cover slip. Slides were incubated in a dark humid chamber at room temperature (RT) ON.

The primary antibody was then washed off by 3 x 10 min washes in PBST in coplin jars. 50 µl of the appropriate Alexa secondary antibody (Invitrogen) in PBST was then added at a dilution of 1:300. Another parafilm cover slip was placed over the slides and they were again incubated for 2 hr RT in the dark in a humid chamber.

Finally, the secondary antibodies were washed off by 3 x 10 min washes in PBST in coplin jars. 75µl of 2µg/ml DAPI in water was added to the slides and left in the dark for 5 min. This was removed by a 5 min wash in PBST and the slides mounted by the addition of 15 µl of vectashield (Vector labs). A 22 x 40 glass cover slip was used to seal the immunostaining.
(49290002)

Table 2: Antibodies used in this study

Antibody	Host	Main Staining	Dilution	Source
SMC-1	Rat	Cohesin complex	1:300	Dr Barbara J. Meyer (UC Berkely)

SMC-3	Rabbit	Cohesin complex	1:200	Millipore (ref. AB3914)
REC-8	Mouse	Cohesin complex	1:100	Abcam, Mouse polyclonal (ab38372)
COH-3	Rabbit	Cohesin complex	1:1000	Novus Biologicals (49290002)
HTP-1	Rabbit	Axial element	1:200	SDIX
HIM-3	Rabbit	Axial element	1:200	Dr Monique Zetka (McGill University)
SYP-1	Chicken	Central element	1:300	SDIX
RAD-51	Rabbit	Recombination intermediates	1:200	Dr Adriana La Volpe (Naples University)
RAD-51	Rabbit	Recombination intermediates	1:10000	SDIX
HCP-6	Rabbit	Condensin complex	1:100	Dr Barbara J. Meyer (UC Berkely)
SCC-2	Rabbit	Cohesin loader	1:50	SDIX
HIM-8	Rabbit	Pairing centre	1:500	SDIX
GFP-488	Rabbit	Transgenic GFP proteins	1:200	InvitroGen
RFP-555	Rat	Transgenic RFP proteins	1:1000	Chromatech (5F8)

2.4.3 Microscopy

Immunostained germlines were imaged using a DeltaVision Deconvolution Microscope developed by Applied Precision (DeltaVision system core, Olympus 1X70 microscope, CoolSNAP$_{HQ}^2$ Monochrome camera). Germlines were imaged in a series of Z-stacks that required deconvolution to reverse the optical distortion. Images in different z-axis planes were analysed and processed in Softworx (version 3.7.1) and were subsequently flattened into a two-dimensional projection. The relatively large size of a *C. elegans* germline prohibited imaging of the whole structure in a single field and so several fields were required. Reconstruction of the whole image germline was achieved using Photoshop (Adobe) or ImageJ.

2.4.4 Quantification of ZHP-3 foci

Quantification of the recombination intermediate ZHP-3 was carried out on α-GFP immunostained germlines of *scc-2* RNAi treated ZHP-3:GFP worms (Bhalla et al., 2008). Images were acquired using a Delta Vision Deconvolusion Microscope (Deltavision system core, Olympus 1X70 microscope, CoolSNAP$_{HQ}^2$ Monochrome camera) as in 2.5.2. Softworx (version 3.7.1) was used to scan through the Z-stacks. Foci were therefore counted within the 3D context of the nuclear space.

2.4.5 Quantification of DAPI-stained bodies in diakinesis oocytes

Diakinesis staged *C. elegans* nuclei were quantified by dissecting germlines from required genotypes and fixing as in 2.5.2. If antibody staining was not required, DAPI was immediately after the initial washing steps and slides mounted appropriately. Images of the -1 and -2 diakinesis were acquired on a Delta Vision Deconvolusion Microscope developed by Applied Precision (Deltavision system core, Olympus 1X70 microscope, CoolSNAP$_{HQ}^2$ Monochrome camera). Deconvolved images were converted into maximum intensity projections and cropped to the size of an individual nucleus using ImageJ. These cropped images were analysed in CellProfiler to identify each DAPI stained body, calculating the number of bodies per nucleus as well as the area of each individual body. My colleague Oliver Crawley carried out this anaylsis on wild-type and mutants with known diakinesis oocytes phenotypes, in order to determine the area in pixel of different DAPI mass types. This now allows us to identify DAPI mass types according to their area, with a bivalent 500-1000 pixels, a univalent 250-500 pixels, an individual sister 120-250 pixels, and a fragment less than 120 pixels (Fig. 5).

2.4.6 Quantification of apoptotic corpses

An apoptosis quantification assay was carried out using the *ced-1::GFP* reporter strain. *ced-1* is a single-pass transmembrane protein expressed in

engulfing cells, acting on cell surfaces as a phagocytic receptor for neighboring apoptotic cells. Consequently it recognises the cell-surface features of cell corpses and can act as a marker specifically labelling corpses in the process of being engulfed (Lu et al., 2009).

Adult worms (18hrs post L4) were immunostained by standard methods with anti-GFP-488 to detect the *ced-1::GFP* transgene and anti-SMC-1 to assess the efficacy of the RNAi knockdown. A DeltaVision Deconvolusion Microscope developed by Applied Precision (Deltavision system core, Olympus 1X70 microscope) was used to view the slides and the number of nuclei surrounded by a halo of green signal counted.

Table 3: List of buffers and solutions used in the study

Name	Composition	Use
10 X PCR Lysis Buffer	100 mM Tris 500 mM KCl 15mM $MgCl_2$ pH 8.3 Add Proteinase K to 1XPCR Lysis Buffer before use to a final concentration of 1mg/ml	DNA extraction
10 X EGG Buffer	118 mM NaCl 48 mM KCl_2 2 mM $CaCl_2$ 2 mM $MgCl_2$ 5 mM HEPES pH 7.4	Immunostaining
10 X PBS	0.2 M Sodium phosphate 1.5 M NaCl pH 7.4	Immunostaining

2.5 γ-irradiation of *C. elegans*

Radiation experiments were carried out using an IBL 637 cell irradiator containing a caesium *137* source.

Irradiation was carried out using adult worms (18 hr post L4) irradiated with 10, 50 or 100Gys and dissected at 30 hr post irradiation. Animals were antibody stained using the standard protocol. Images were acquired on a Delta Vision Deconvolution System (Deltavision system core, Olympus 1X70 microscope, CoolSNAP$_{HQ}^2$ Monochrome camera) and DAPI stained bodies in diakinesis oocycytes quantified.

2.6 Transgenic Methods

Recent development of the Mos1 Single Copy Insertion (MosSCI) developed by Roberts & Bessereau (2007) and improved by the Jorgensen lab, has been used for the creation of all transgenic lines for this study. Briefly, your insert, a tagged gene for example, is cloned into a vector containing a functional copy of the unc-119 gene and ~1.5kb of sequence which has homology to a chromosomal locus with a Mos1 site. Mos1 excision is induced by expression of Mos1 transposase and gene insertions are generated by repair of the double stranded break. This occurs by homologous recombination between the break ends and the regions of homology within the vector. It is therefore necessary to use the appropriate *C. elegans* strain and vector combination. (See table below.)

2.6.1 Preparation of worms for injection

The strains injected in order to generate transgenic lines all contain a mutation in the *unc-119* gene, which acts as a positive marker as worms in which the *unc* phenotype has been recovered to wild-type by injection, are easily identifiable. These strains are naturally unhealthy and therefore are maintained at 15°C on plates seeded with HB101
E. coli, as this improves viability and brood size.

The day before injection L4 larvae are picked to a fresh plate to ensure that the worms used are young adults. This is particularly important, as older *unc-119*

worms are difficult to inject, have small brood sizes and egg laying defects, and consequently have very few transformed progeny.

Table 4: List of vectors with their corresponding strains and insertion loci

Vector	Strain	Locus	Chromosomal position
pCFJ151	EG4322	ttTi5605	Chr II:0.77
pCFJ352b	EG6701	ttTi4348	Chr I:5.32
pCFJ178	EG5003	cxTi10882	Chr IV:0.00

2.6.2 Generation of plasmids for injection

All constructs used were produced by gene synthesis and cloned into the MosSCI vectors by GeneScript.

2.6.3 Generation of transgenic strains

Worms are injected with the transgene construct directly into their germline. However, in order to be able to differentiate worms that have been correctly injected into the germline from those that have not, and those which have the insert integrated from those which are expressing from a non-inserted extrachromosomal array, a number of positive and negative selection markers are used. Positively injected worms are be identified by the presence of *non-unc* progeny, as the *unc-119* phenotype is rescued by the presence of the functional gene in the transgene vector. In addition to this three markers are co-injected with transgene vector. These have mCherry expression driven by pharyngeal, neural and muscle promoters, and as a consequence the progeny of correctly injected worms will exhibit mCherry expression. As these animals pass through successive generations the extrachromosomal arrays should be lost, resulting in *non-unc*, non-mCherry worms, which should be positive for an insertion event. This can then be checked by PCR (See below).

This method of detecting positive insertion events was initially used, however, the later strains made utilise a negative selection marker, *peel-1*. Worms are

co-injected with a plasmid containing the *peel-1* toxin driven by and heat shock promoter. *peel-1* expression causes the presence of extrachromosomal arrays to become toxic. Therefore, subsequent to heat shocking the only *non-unc* worms alive should be those with a positive insertion event and no array. To check for occasional survivors from the heat shock that are array positive, worms are checked for the absence of the mCherry markers.

2.7.3.1 Preparation of injection mix

All constructs were suspended in 20µl of H_2O and 1 µl of this was used to transform chemically competent DH115α *E. coli* cells, following the manufacturer's specifications. The cells were spread on LB plates with 50mg/ml ampicillin and harvested with QIAprep Spin Miniprep Kit (QIAGEN). The DNA content was quantified using the Qubit Flurometric system.

The following 10X injection mix was made, and 5µl aliquots stored at -20°C:

Plasmid	Description	Final concentration
pCFJ601	Peft-3::transposase	500ng/µl
pGH8	Prab-3::mCherry (Pan-neuronal)	100ng/µl
pCFJ90	Pmyo-2::mCherry (pharynx muscle)	25ng/µl
pCFJ104	Pmyo-3::mCherry (body muscle)	50ng/µl
pMA122	Phsp::peel-1	100ng/µl

On the day of injection, a 1X mix was made with the addition of the transgene vector to a final concentration of 50ng/µl and H_2O. 5µl aliquots if this were again made and stored at -20°C. It is important to have as little freeze thawing of the injection mix, as possible, for better transformation rates.

2.7.3.2 Worm handling

See section 2.4.2.2. Plates with individual injected worms are allowed to recover at 15°C ON and then are transferred to 25°C until completely straved.

2.7.3.3 Screening for full insertion events

The fully starved plates are placed in a 34°C air incubator for two hours. It takes a few hours for the *peel-1* toxin to kill the worms, so 4-6 hours after the heat-shock plates were screened for MosSCI insertions. Insertion animals are typically L1 or dauer animals that are *non-unc* and do not have any of the fluorescent co-injection markers. A few putative insertion animals are picked to individual plates. Once these worms have produced progeny the P_0 is lysed and the presence of an insert checked by PCR and by checking for fluorescence of the tagged gene, where possible. Once an insert has been confirmed the insertion is brought into homozygosity, by picking 10 individual worms to separate plates and a) ensuring that none of their progeny are *unc* and b) lysing the parent and carrying out an "insert homozygous" PCR, which has one primer over the Mos excision site and therefore will not produce any product if the transgene is in homogygosity. Once all of this has been verified the transgene carrying strain is crossed into its mutant background to check that it is functional.

Primers used:

Chromosome I insert positive	F:	CGTCAGAGAAGGAGAGGAAC
	R:	ATCGCTGTCGTCGAGTTTCT
Chromosome II insert positive	F:	TCTGGCTCTGCTTCTTCGTT
	R:	CAATTCATCCCGGTTTCTGT
Chromosome IV insert positive	F:	GGGTGCCAAATAACCAGCTA
	R:	TCCCCATTTCACCAGAGAAC
Chromosome I insert homozygous	F:	GGGGAGCGAAAAATAATTGA
	R:	TGAAAACCGAAAATCGACAA
Chromosome II insert homozygous	F:	CGCTACTTACCGGAAACCAA
	R:	CCCGGGTTTGTCTAGATATGA
Chromosome IV insert homozygous	F:	GCCTTATGCGTTGCTCAAA
	R:	GCGGAGCATGCTTGATTCT

Table 4: Transgenic plasmids used

Vector	Transgene	Regulatory sequence	Discription
pCFJ151	*rec-8::GFP*	*rec-8* 5' and 3' UTRs	rec-8 tagged with GFP
pCFJ151	*rec-8::GFP*	*fbf-2* 3' UTR	early prophase expression of *rec-8* tagged with GFP
pCFJ151	*rec-8::GFP*	*mex-5* 3' UTR	late prophase expression of *rec-8* tagged with GFP
pCFJ352b	*coh-3::mCherry*	*coh-3* 5' and 3' UTRs	*coh-3* tagged with mCherry
pCFJ178	*scc-3::GFP*	*scc-3* 5' and 3' UTRs	*coh-3* tagged with GFP
pCFJ151	*rec-8::IAA17*	*rec-8* 5' and 3' UTRs	*rec-8* tagged with IAA17 for auxin-degron system
pCFJ178	*tir1*	*rec-8* 5' and 3' UTRs	*Arabidopsis tir1* for auxin-degron system
pCFJ151	*rec-8::SNAP*	*rec-8* 5' and 3' UTRs	*rec-8* tagged with SNAP for covalent labelling
pCFJ151	*rec-8$^{SEP(3)}$::GFP*	*rec-8* 5' and 3' UTRs	putative non-cleavable *rec-8* with 3 separase sites mutated R to E, tagged with GFP
pCFJ151	*rec-8$^{SEP(5)}$::GFP*	*rec-8* 5' and 3' UTRs	putative non-cleavable *rec-8* with 5 separase sites mutated R to E, tagged with GFP
pCFJ151	*rec-8 (AIR-2^{A})::GFP*	*rec-8* 5' and 3' UTRs	putative non-phosphorylatable, non-cleavable *rec-8* with 3 AIR-2 sites mutated S/T to A, tagged with GFP
pCFJ151	*rec-8 (AIR-2^{E})::GFP*	*rec-8* 5' and 3' UTRs	putative phosphomimetic, hyper-cleavable rec-8 with 3 AIR-2 sites mutated S/T to E, tagged with GFP
pCFJ151	*Phsp-16.1::rec-8::GFP*	*hsp-16.1* promoter	heat-shock inducible rec-8 tagged with GFP

2.7 *C. elegans* strains used

Table 5: List of strains used in this study.

	Strain	Genotype
Wild Type	N2	*Wild-type (Bristol)*
Translocations	JK2663	*dpy-11(e224) mes-4(bn67) V/nT1[unc-?(n754) let-? qIs50]*
	AV106	*spo-11(ok79)/nT1[qIs50]*
	AV276	*syp-2(ok307)*
	AV307	*syp-1(me17)/nT1[qIs50]*
	EG4322	*ttTi5605; unc-119(ed9)*
	EG5003	*unc-119(ed3); cxTi10882*
	EG6701	*ttTi4348; unc-119(ed3);oxEx1580.*

CGC Strains	TY5120	*coh-3(gk112);coh-4(1857)/nT1[qls51]*
	TY5121	*rec-8(ok978);coh-3(gk112);coh-4(1857)/nT1[qls51]*
	UV7	*zhp-3::GFP(jfls2)*
	VC131	*coh-3(gk112)*
	VC666	*rec-8(ok978)/nT1[qls51]*
	WS1433	*hus-1(op241);hus-1::GFP(opls34)*
	TY5115	*coh-4(1857)*
	MD701	*ced-1::GFP*
Lab Generated	ATG47	*scc-2(fq1)/sqt-2*
	ATG76	*scc-3(ku263)/nT1[qls50]*
		scc-2(fq1);hus-1::GFP(opls34)/sqt-2
		spo-11(ok79);hus-1::GFP(opls34)/nT1[qls50]
		syp-1(me17);hus-1::GFP(opls34)/nT1[qls50]
Lab Generated for this study		*coh-3(gk112);coh-4(1857);spo-11(ok79)/nT1[qls50]*
	ATG186	*coh-3(gk112);coh-4(1857);syp-2(ok307)/nT1[qls50]*
	ATG168	***coh-3;coh-3::mCherry***
	ATG169a	***coh-3;coh-4;coh-3::mCherry***
	ATGSi104	***Phsp-16.1::rec-8::GFP***
		rec-8(ok978);coh-3(gk112)/nT1[qls50]
	ATGSi81	***rec-8(ok978);coh-3(gk112);coh-3::mCherry/nT1[qls50]***
	ATG180	*rec-8(ok978);coh-3(gk112);coh-4(1857);spo-11(ok79);wapl-1(tm1814)/nT1[qls50]*
		rec-8(ok978);coh-3(gk112);rec-8(AIR-2^{E})::GFP
		rec-8(ok978);coh-3(gk112);rec-8::GFP;coh-3::mCherry
	ATG148	*rec-8(ok978);coh-4(1857)/nT1[qls50]*
	ATGSi111	***rec-8(ok978);rec-8(AIR-2^{A})::GFP***
	ATGSi88	***rec-8(ok978);rec-8(AIR-2^{E})::GFP***
	ATGSi45	***rec-8(ok978);rec-8::GFP fbf-2 3' UTR***
		rec-8(ok978);rec-8::GFP mex-5 3' UTR
	ATGSi46	***rec-8(ok978);rec-8::IAA17***
	ATGSi80	***rec-8(ok978);rec-8::IAA17;tir1***
		rec-8(ok978);rec-8::SNAP
		rec-8(ok978);rec-8$^{SEP(3)}$::GFP
	ATG137	*rec-8(ok978);spo-11(ok79)/nT1[qls50]*
	ATGSi107	***rec-8(ok978);spo-11(ok79);coh-3(gk112);coh-3::mCherry/nT1[qls50]***
		rec-8(ok978);spo-11(ok79)wapl-1(tm1814);/nT1[qls50]
	ATGSi108	***rec-8(ok978);spo-11(ok79)wapl-1(tm1814);coh-3(gk112);coh-3::mCherry/nT1[qls50]***
	ATG183	*rec-8(ok978);syp-2(ok307)/nT1[qls50]*
		rec-8(ok978);syp-2(ok307);coh-3(gk112);coh-3::mCherry/nT1[qls50]
		rec-8(ok978);syp-2(ok307);wapl-1(tm1814)/nT1[qls50]
		rec-8(ok978);syp-2(ok307);wapl-1(tm1814);coh-3(gk112);coh-3::mCherry/nT1[qls50]
	ATG130	*rec-8(ok978);wapl-1(tm1814)/nT1[qls50]*
	ATGSi82	***rec-8(ok978);wapl-1(tm1814);coh-3(gk112);coh-3::mCherry/nT1[qls50]***
	ATGSi23	***rec-8(ok978);rec-8::GFP***
		scc-3(ku263);scc-3::GFP
		syp-2(ok307);coh-3(gk112);coh-3::mCherry/nT1[qls50]
		syp-2(ok307);wapl-1(tm1814)/nT1[qls50]
		syp-2(ok307);wapl-1(tm1814);coh-3(gk112);coh-3::mCherry/nT1[qls50]
	ATGSi79	***tir1***
	ATG98	*wapl-1(tm1814)*

N.B. Genotypes with lab generated transgenes in bold type-face

Figure 5. Calibration of DAPI area binning for CellProfiler analysis

A Diakinesis oocytes from strains with known DAPI mass number and type: N2 (6 bivalents), *coh-3;coh-4* (12 univalents), *rec-8;spo-11* (24 individual sister chromatids) and *rec-8;syp-2* (fragments and chromatid aggregates)

B Graph showing the ranges of areas in pixels for each DAPI mass type given by CellProfiler analysis

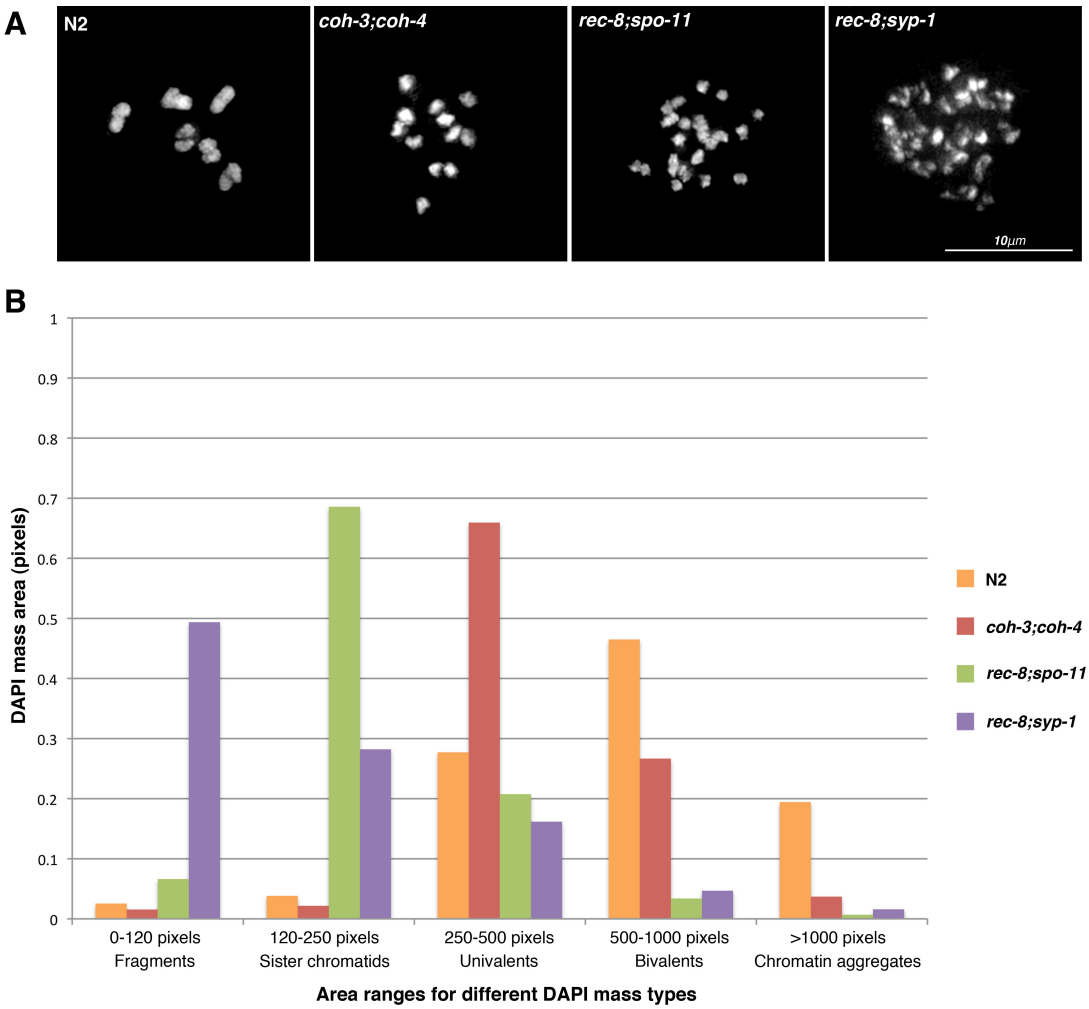
A
N2
coh-3;coh-4
rec-8;spo-11
rec-8;syp-1
10µm
B
DAPI mass area (pixels)
1
0.9
0.8
0.7
0.6
0.5
0.4
0.3
0.2
0.1
0
0-120 pixels
Fragments
120-250 pixels
Sister chromatids
250-500 pixels
Univalents
500-1000 pixels
Bivalents
>1000 pixels
Chromatin aggregates
Area ranges for different DAPI mass types
N2
coh-3;coh-4
rec-8;spo-11
rec-8;syp-1

CHAPTER 3: RESULTS

INVESTIGATING THE ROLES OF SCC-2 IN THE LOADING OF MEIOTIC COHESIN BY RNAI

3.1 Objectives

At the outset of my PhD, a number of interesting observations had been made during the characterisation of a mutant allele of the cohesin loader *scc-2*. For the first time it had been demonstrated that SCC-2 was required for cohesin loading during meiosis. However, there are limitations as to what can be discovered using the *scc-2* mutant alone. It is not possible, for example, to differentiate roles of cohesin loading at different times in meiosis. For this reason, I sought to deplete SCC-2 by RNAi thereby creating a situation in the germline in which two populations of nuclei existed: those which had cohesin loaded prior to the knockdown, and those which underwent S-phase subsequent to RNAi knockdown. This was in particular to extend the data obtained from the study of the *scc-2(fq1)* mutant regarding the apoptotic response. These experiments led to some unexpected results which hinted at a number of roles for cohesin loading during prophase I.

3.2 SCC-2 localisation

During the initial characterisation of the *scc-2(fq1)* mutants carried out in our lab, we raised an anti-SCC-2 antibody against a 100 amino acid peptide located near the N-terminus of the *C. elegans* SCC-2 protein (Fig. 7A). Using this antibody we sought to address the localisation of SCC-2 in the germlines of wild-type worms. Early immunostaining using a standard fixation protocol revealed the presence of nucleoplasmic SCC-2 throughout the whole germline. However, chromatin associated SCC-2 was difficult to detect. As this was possibly due to the high levels of soluble protein, a modified immunostaining protocol was used with a stringent triton wash, to remove this pool. Under these conditions, a chromatin-bound pool of SCC-2 was clearly seen to localise to meiotic

chromosomes in a pattern reminiscent of the SC (Fig. 6B). At the onset of late pachytene this pattern was lost and substituted by an intense nucleoplasmic signal peaking in diakinesis (Fig. 6).

(This experiment was carried out by James Lightfoot)

3.3 Phenocopying *scc-2(fq1)* by RNAi knockdown

In order to use *scc-2* RNAi to dissect out the roles of cohesin loading subsequent to the S-phase requirement for cohesion establishment, I first had to ensure that knockdown of *scc-2* was possible by RNAi using the feeding method. I expected that by using different RNAi conditions I would be able to modulate the intensity of the knockdown. To initially validate the efficacy of the RNAi, I sought to find conditions in which the knockdown phenotype would recapitulate that of the *scc-2 (fq1)* mutant.

As no clones targeting *scc-2* are present in the commercially available Ahringer RNAi library, we designed two RNAi vectors targeting different coding sequences within the gene. This was done via the gateway cloning system as described in section 2.4.1.4. The first clone was derived from a 858 bp genomic fragment including portions of exons 6 and 7, and the second was derived from *scc-2* cDNA corresponding to the first 300 amino acids of the SCC-2 protein, and encompassing exon 1 and 2, and most of exon 3 (Fig. 7A). Each RNAi vector was tested independently, using the standard protocol (Section 2.4.1). Individuals were picked at the L4 stage of worm development (this is the 4th and final larval stage, prior to adulthood) to RNAi plates and grown ON at 20°C. Adults (18-20 hours post L4) were stained with DAPI (Section2.5.1) and screened for any cytological defects similar to those seen in *scc-2(fq1)* mutants. All animals appeared completely wild type, therefore I decided to screen the worms after a longer exposure to the RNAi. To do this, L4 individuals were picked to RNAi plates and grown ON at 20°C, transferred to fresh RNAi plates and grown ON again at 20°C and then stained with DAPI and screened for defects. Again, no defects were observed. To strengthen the effect of the RNAi further, I carried

out the longer RNAi exposure but incubated the worms at 25°C rather than 20°C, as this has been shown to increase RNAi efficacy. However, still no cytological defects were observed.

In other instances where RNAi has no effect on the phenotype of the P_0 generation, possibly due to a long half-life of the target protein, it is possible to see a knockdown in the F_1 progeny. I therefore carried out the RNAi knockdown with the two individual clones as described in section 2.4.1. When adult F_1 worms (18-20 hours post L4) were screened by DAPI staining, in both clones and at both 20 and 25°C a number of adults had cytological defects, consistent with defects in cohesin loading, although none as severe as those seen in *scc-2(fq1)* mutants. The nature of these defects will be discussed in the later sections of this chapter. However, key for the optimisation of the RNAi conditions to exact full SCC-2 knockdown, were the observations that the RNAi clone targeting the cDNA sequence gave more robust knockdown, both in terms of the portion of affected individuals and the severity of the defect. In addition to this, by both these measures, carrying out the RNAi at 25°C also increased the efficacy of the knockdown , as has been previously reported.

With this in mind, I decided to combine cultures of bacteria containing both RNAi vectors in a 1:1 ratio and use this to seed the RNAi plates. I reasoned that this would produce a stronger RNAi phenotype as a greater proportion of the *scc-2* gene would be directly targeted. In addition to this, the worms where incubated at 25°C to further boost the effectiveness of the RNAi. When adult F_1s were stained with DAPI and screened after exposure to these stringent RNAi conditions, the most severe phenotypes were observed, including individuals with phenotypes indistinguishable from the *scc-2(fq1)* mutant.

3.3.1 Chromatin phenotype

With the conditions now established for optimum knockdown of *scc-2*, I carried out a more detailed cytological analysis of the phenotypes observed after RNAi. By dissecting and staining the treated worms with DAPI and imaging these

germlines with the DeltaVision, I could see the degree of similarity between the *scc-2* mutant and the *scc-2* RNAi worms. In both cases chromosome staining in whole mount germlines revealed nuclei with abnormal chromatin structure throughout meiotic prophase I. After *scc-2* RNAi, meiotic nuclei displayed chromatin which appeared disorganized with only extremely thin tracks visible, rather than having the highly organised thick tracks of chromatin indicative of paired homologous chromosomes that are seen in the wild-type (Fig. 7B and C and 8A and B). In addition these germlines contained nuclei of varying sizes indicating aneuploidy, presumably as a result of undergoing divisions in the mitotic tip in the absence of cohesin (Fig. 8A). Analysis of the diakinesis oocytes showed a variable number of DAPI-stained bodies. In many instances the number of DAPI masses was close to 24, indicating complete loss of cohesion in diakinesis oocytes (Worms carry six pairs of homologous chromosomes, and therefore a total of 24 chromatids are presents in meiotic prophase nuclei). Also, diakinesis nuclei with small DAPI masses that are likely to constitute chromosome fragments were present (Fig. 9D). These three phenotypes are identical to those observed in *scc-2(fq1)* mutants (Fig. 8C and 9C) and strongly suggest a defect SCC throughout meiotic prophase.

3.3.2 Cohesin localisation

Analysis of the *scc-2(fq1)* mutant has shown that SCC-2 is required for cohesin loading during meiosis. When germlines from these worms were immunostained with antibodies against the cohesin subunits SMC-1, SMC-3 and the meiosis-specific kleisin subunit REC-8, it was seen that they were expressed in the mitotic region of the germline at comparable levels to those in wild-type worms, but upon meiotic entry the signal became undetectable and remained so throughout the rest of the germline, apart from a nucleoplasmic re-expression in late pachytene (Fig. 7C). This is in contrast to the situation in wild-type germlines, in which the cohesin subunits can be seen decorating the axial element of meiotic chromosomes throughout meiotic prophase (Fig. 7B).

After knockdown of *scc-2* by RNAi, we would expect to see a pattern of cohesin staining the same as that seen in the *scc-2(fq1)* mutant. Indeed this was the case.

SMC-1 and 3 and REC-8 all showed expression in the mitotic tip, which disappeared at the onset of meiosis (Fig. 8A). Chromatin-associated cohesin could not be detected by immunofluorescence anywhere in prophase nuclei of these germlines. Taken together with the similarity in chromatin structure between the *scc-2(fq1)* mutant and the *scc-2* RNAi treated worms, this demonstrates that it is possible to knockdown SCC-2 to the extent that the phenotypes in meiosis are identical between the RNAi treated worms and the null mutant. In both cases there is no SCC, resulting in disorganised chromatin structure and micro- and meganuclei, individualised sisters and fragments at diakinesis, and a complete lack of cohesin present on the chromatin of meiotic nuclei.

3.4 Partial knockdown of *scc-2*

As mentioned earlier one of the key advantages of using RNAi to knockdown gene expression is that you are able to create phenotypes intermediate between the wild type and the null mutant situations. In order to create this partial knockdown of *scc-2,* animals were treated only with the RNAi clone targeting the cDNA and were incubated at 20°C. Germlines of F1 progeny were then dissected and stained by the standard protocol with α-SMC-1, α-SMC-3 or α-REC-8 antibodies. In this way, effects on chromatin structure as well as the pattern of chromatin-associated cohesin could be assessed.

3.4.1 Rational

We have seen already that *scc-2* RNAi can decrease protein levels to the extent that we could call a knockdown complete. That is, the phenotype produced is identical to that of the null mutant. However, with exposure to the *scc-2* RNAi for a shorter period of time, or by using less stringent conditions for the RNAi, it might be possible to create a partial knockdown of *scc-2.* The aim in this instance was to create a subset of nuclei within the germline which had already undergone meiotic S-phase prior to *scc-2* RNAi treatment. The expectation being that these would have SCC intact but any requirement for cohesin loading

elsewhere in prophase would be abolished. An alternative outcome would be that the knockdown of *scc-2* would impair but not completely eliminate cohesin loading. In this case we would expect to see lower levels of cohesin decorating the axis than in wild type germlines.

However, in the first scenario, the expression pattern of the cohesin complex would be as follows: in the mitotic tip cohesin would be expressed in high levels, as is the case in the wild-type and *scc-2(fq1)* mutant, this would be followed by the disappearance of cohesin as soon as entry into meiosis occurs, where in wild-type germlines one would see cohesin loaded to the axial element. These cohesin-free nuclei from transition zone and early pachytene represent those which underwent meiotic S-phase in the absence of SCC-2, and therefore were not competent to have cohesin loaded. However, proximal to this band of nuclei a pool of late pachytene nuclei would exist in which cohesin would have been loaded onto meiotic chromosomes. These represent nuclei that had gone through S-phase before the effect of the RNAi was sufficient to prevent cohesin loading (Fig. 10A). Any defects in these late pachytene nuclei or those later in prophase would be due to a role of SCC-2 in cohesin loading after S-phase.

3.4.2 SMC-1 and 3 localisation

In order to determine the extent of the SCC-2 knockdown, as well as to discover if either of the two predicted outcomes described above occurred, I stained germlines of F1 animals treated with the less rigorous *scc-2* RNAi knockdown protocol with either α-SMC-1 or α-SMC-3 antibodies. The staining pattern observed in these germlines was of a region of nuclei in transition zone and earlier pachytene with very little or no detectable SMC-1 or SMC-3, followed by a region of later pachytene nuclei with these subunits loaded onto chromosomes. This was the preferred outcome as it provided the possibility of separating the different requirements of cohesin loading at different stages of meiosis.

A number of striking observations were immediately apparent in germlines in which partial *scc-2* knockdown had been achieved and I will discuss these later in the chapter. However, as stated earlier a particular aim of creating this situation was to extend the data obtained from studying *scc-2(fq1)* mutants regarding the apoptotic response. I will briefly describe the data derived from the analysis of *scc-2(fq1)* null mutant that was carried out by James Lightfoot previously in the lab, and then go on to discuss the data from my own RNAi experiments.

3.5 Apoptotic response

3.5.1 Apoptotic response in *scc-2(fq1)*

In wild-type worms a basal level of apoptosis occurs as some nuclei undergo physiological germcell apoptosis (Gumienny et al., 1999). This type of cell death usually occurs in the germline bend. James Lightfoot undertook an apoptosis assay utilising the SYTO12 green fluorescent nucleic acid dye, which allows nuclei containing intensely condensed chromatin characteristic of apoptosis to be visualised. In wild-type animals low levels of apoptosis occurred with the number of corpses showing a mean value of 6.5 ± 3.0 corpses per germline. In the *spo-11(ok79)* mutant, in which no DSBs are made, the levels of apoptosis were slightly lower, with a mean of 6.2 ± 2.4 corpses per germline. The *syp-1(me17)* mutant, which is deficient in SC assembly, was used as a positive control, as it is known that failure in SC assembly causes activation of the pachytene checkpoint due to accumulation of recombination intermediates. The SYTO12 assay detected high levels of apoptosis in *syp-1* mutants, as previously shown (MacQueen et al., 2002), with an average of 18.5 ± 7.0 apoptotic corpses observed per germline.

As *scc-2(fq1)* mutants, as well as other cohesin mutants also accumulate large numbers of recombination intermediates, it was expected that they too would have high levels of apoptosis. However this was not the case. In *scc-2(fq1)* mutants only few a apoptotic corpses were observed per germline, with an

average of 4.8 ± 2.4 corpses, and treating these worms with γ-irradiation (γ-IR) to induce even higher levels of DNA damage failed to significantly increase the quantity of apoptotic corpses (5.8 ± 3.0 per germline). This was in contrast to γ-IR treated wild-type worms which when exposed to the same dose showed a clear increase in the number of corpses (13.9 ± 4.6 per germline). SYTO12 assay in *scc-3(ku263)* mutants revealed similarly low levels of apoptosis to *scc-2(fq1)* (2.6 ± 2.2 corpses per germline), suggesting that the apoptotic response of the pachytene checkpoint cannot occur in the absnce of cohesin (Fig. 10A).

James Lightfoot went on to examine the cause for this lack of apoptotic response by monitoring loading of the DNA damage sensor 9-1-1 complex (Navadgi-Patil and Burgers, 2009). This was done using a strain expressing the 9-1-1 complex component *hus-1* fused to GFP (*hus-1::GFP (opls34))* (Hofmann et al., 2002) as a control, and comparing the levels of HUS-1::GFP of this strain with those seen in *scc-2(fq1);hus-1::GFP* and *syp-1(me17);hus-1::GFP* as a positive control. This revealed that in pachytene nuclei of *scc-2(fq1)* mutants very little HUS-1 is loaded (0-3 HUS-1 foci per nucleus) despite the extensive accumulation of RAD-51, unlike in *syp-1(me17)* mutants, which had 7-16 HUS-1 foci per nucleus. It is therefore clear that the 9-1-1 complex fails to localise to unrepaired DSBs in *scc-2(fq1)* mutants, and as a consequence the level of apoptosis is very low in spite of the high levels of DNA damage.

3.5.2 Monitoring apoptosis by CED-1::GFP after *scc-2* RNAi

Carrying on from this, we wanted to know whether germlines in which cohesin was loaded onto chromatin, but in which no additional cohesin loading could occur, could still trigger the apoptotic response. In this way we could determine whether cohesin bound to chromatin itself was part of the signalling cascade involved in the pachytene checkpoint. To do this, *scc-2* RNAi was carried out in worms expressing CED-1::GFP. As previously described, CED-1 is expressed in engulfing cells and can act as a marker labelling corpses in the process of being engulfed (Lu et al., 2009). This was used rather than SYTO12, so that both apoptosis and cohesin loading could be assessed in the same germline.

scc-2 RNAi was performed in worms expressing CED-1::GFP. These were then immunostained by the standard protocol with α-GFP antibodies to mark the nuclei undergoing apoptosis, and α-SMC-1 to monitor the success of the knockdown (Fig. 11B). In order to achieve a strong knockdown, worms were treated with the cDNA RNAi clone and incubated at 25°C, whereas for a milder knockdown, the RNAi was carried out at 20°C. This provided us with two classes of germlines after RNAi, those in which no visible SMC-1 staining could be detected and those with only reduced levels of SMC-1. Control RNAi experiments using CED-1::GFP worms treated with the empty vector were carried out at both 20 and 25°C.

The RNAi controls at both temperatures displayed similar levels of apoptosis to those previously seen in wild-type worms stained with SYTO 12, with a mean of ~7 corpses per germline in the 20°C controls and ~8 in the 25°C controls. The milder *scc-2* RNAi germlines in which SMC-1 staining was reduced, but with very high levels of accumulated DNA damage, showed a marked increase of apoptosis, with almost double the number of apoptotic corpses (~14 corpses per germline on average). In contrast, germlines with no SMC-1 staining displayed levels of apoptosis similar to the controls at ~ 6 apoptotic corpses per germline (Fig 11C). This reinforces the idea that chromatin-associated cohesin might be required for the functionality of the pachytene DNA damage checkpoint.

3.6 Impairment of chiasmata formation or maintenance by *scc-2* RNAi

3.6.1 Gradient of diakinesis phenotypes

One of the initial and most striking phenotypes revealed when examining the chromatin structure upon partial knockdown of *scc-2* by RNAi, was the presence of more than 6 DAPI masses in diakinesis oocytes. The number of these masses was most frequently 11 or 12, which together with the shape and size of these

DAPI massed led to the conclusion that they were univalents (Fig. 12). This might be because cohesin loading is required for the formation of COs and therefore chiasmata, or it may be that COs are formed but then chiasmata fall apart due to a later loss of cohesin. It is noticeable that the levels of REC-8 loaded onto chromatin of pachytene nuclei correlate well with the number of DAPI masses seen in diakinesis oocytes. Germlines with detectable levels of REC-8 typically display diakinesis oocytes with up to 12 DAPI masses, while germlines in which the REC-8 signal fell below detectable levels showed 12 to 24 DAPI masses (Fig. 11). This provides further evidence that the DAPI masses seen in diakinesis oocytes after partial *scc-2* RNAi are univalents. In order to try to determine the cause of this phenotype, I first examined an initial step of meiotic recombination: the generation of DSBs, to see whether a lack of breaks could be responsible for the absence of chiasmata.

3.6.2 DSB formation

In order to analyse the effect of *scc-2* RNAi in DSB formation, whole mounted germlines were stained with antibodies against the recombinase RAD-51, which serves as a proxy, as break formation *per se* cannot be directly assessed. These germlines were costained with α-REC-8 or α-SMC-3 antibodies to monitor the extent of *scc-2* knockdown. In wild-type germlines the number of RAD-51 foci peaks in early pachytene at approximately 9 foci per nucleus, and then decreases towards late pachytene as the breaks are repaired (Alpi et al., 2003). In the RNAi empty vector control, similar levels and dynamics of RAD-51 are observed. In *scc-2(fq1)* the RAD-51 profile is very different to that of wild type, with exceptionally high numbers of SPO-11-dependant RAD-51 foci that persist late into pachytene. In addition to this, RAD-51 signals were often detected as "stretches" covering several μm rather than distinct single foci. Both of these observations are strongly indicative of impaired DSB repair (Lightfoot et al., 2011). It was therefore our expectation that in germlines severely affected by *scc-2* RNAi, we would observe a similar phenotype, and indeed this was the case (Fig. 13). Levels of RAD-51 in germlines in which cohesin is undetectable on chromosomes by immunofluorescence are astonishingly high, with levels

probably greater than that of *scc-2(fq1)* mutants, and numerous stretches of RAD-51 can be seen decorating chromatin.

What then is the effect of partial *scc-2* knockdown on RAD-51 levels, bearing in mind that these germlines have impaired chiasma formation? In germlines in which cohesin is detectable on chromatin, albeit at lower than wild-type levels, numbers of RAD-51 foci are significantly higher than those of the RNAi control, with some stretches also present. It is noticeable that most of these foci do not colocalize with REC-8, perhaps demonstrating that regions of chromatin with cohesin still present are more competent to repair DSBs than their cohesin-negative counterparts. It is clear, from the presence of high numbers of RAD-51 recombination intermediates, that the absence of chiasmata in partially depleted *scc-2* RNAi germlines is not due to a defect in the generation of DSBs, but rather there is an impairment of DSB repair in a situation similar to the *scc-2(fq1)* null. I therefore decided to examine a later marker of recombination, ZHP-3, to see if the absence of chiasmata was due to a defect later on in the processing recombination intermediates.

3.6.3 Formation of ZHP-3 recombination intermediates

zhp-3 is the homologue of the budding yeast Zip3 protein, which is a member of the ZMM class of proteins (Section 1.2.7.5 of the Introduction) and is required for the commitment to crossover formation (Borner et al., 2004). ZHP-3 has been implicated as an important player in these events in *C. elegans*, where it localises along the SC in early pachytene, before contracting asymmetrically on the SC in late pachytene to form characteristic "commas", and finally forming foci in late pachytene/diplotene. As the number of foci per nucleus in wild-type hermaphrodites is 6, it is believed that that ZHP-3 foci correspond to sites of crossing over. Worms carrying a ZHP-3::GFP fusion protein expressed from a low-copy-number transgene that has been stably integrated into the genome can therefore be used to monitor recombination intermediates fated to become COs. In *spo-11* and *msh-5* mutants, which fail to make DSBs and COs respectively, ZHP-3 localises to SC in early pachytene, as in wild-type, but fails

to undergo any reorganisation and therefore does not form foci (Bhalla et al., 2008).

In order to interrogate whether the DSBs formed in *scc-2* RNAi depleted germlines continue to be fated to become COs, or whether this step is impaired and this is responsible for the lack of chiasmata in these worms, I carried out *scc-2* RNAi on the ZHP-3::GFP strain. I then immunostained these germlines with α-GFP antibodies to quantify the number of ZHP-3 foci per nucleus, as well as α-SMC-1 antibodies to monitor the extent of *scc-2* knockdown. Subsequent to *scc-2* RNAi, when 12 univalents are present, one might expect, that as in the case of mutants that completely fail to make COs, ZHP-3 would not become restricted to foci but rather remain as tracts throughout pachytene. Whereas in germlines with a milder depletion, which have a mixture of univalents and bivalents at diakinesis, fewer than 6 foci would be observed. However, in both instances, mild and severe *scc-2* knockdown, nuclei with both greater and fewer than 6 foci are detected (Fig. 13). An interpretation of this observation is that very early CO-fated events for which ZHP-3 is a marker (Bhalla et al., 2008), can be formed, to an extent, in the absence of normal levels of cohesin loading, but that the completion of CO recombination requires cohesin loaded to chromatin or perhaps cohesin reloading.

3.7 Differing patterns of cohesin localisation

3.7.1 REC-8 localisation

As described earlier, in germlines in which *scc-2* was partially depleted by RNAi, the pattern of cohesin staining, as visualised using α-SMC-1 or α-SMC-3 antibodies, showed cohesin present on chromatin in mid to late pachytene nuclei, but absent from transition zone to early pachytene (Fig. 9B and C). Unexpectedly, immunostaining using an α-REC-8 antibody revealed that its loading in the germline followed a quite different pattern to that of the SMC subunits. In the context of a partial *scc-2* RNAi phenotype, REC-8 is absent from nuclei in early meiotic prophase as are SMC-1 and 3, however REC-8 is also

absent in late pachytene nuclei, which are SMC positive (Fig. 15). It is unclear whether the remaining SMC protein represents complexes in which the REC-8 has been unloaded or whether entire REC-8 containing complexes are removed and what is left are complexes which contain the alternative meiotic α-kleisins, COH-3 and COH-4 (Severson et al., 2009). In order to assess whether the nuclei in late pachytene with little or no REC-8 loaded to chromatin are present as a consequence of the loss/removal of protein that had previously been loaded, I co-stained *scc-2* RNAi treated germlines with α-REC-8 and α-SYP-1 antibodies.

3.7.2 REC-8 is lost or removed from meiotic chromosomes in late pachytene

It has been demonstrated that loading of meiotic cohesin to the axial element is required for the loading of HTP-1/2, HIM-3 and HTP-3 (Martinez-Perez et al., 2008; Pasierbek et al., 2003; Severson et al., 2009), and therefore promotes formation of a mature SC. In wild-type germlines, SYP-1 forms tracks along the entire lengths of paired homologues. Immunostaining with α-SYP-1 antibodies in the *scc-2(fq1)* mutant reveals that SYP-1 is sequestered into extrachromosomal aggregates, with no signal detectable on chromosomes. Therefore, by co-staining *scc-2* RNAi germlines with α-SYP-1 and α-REC-8 antibodies we should be able to tell whether late pachytene nuclei are lacking in REC-8 staining because either, REC-8 was not loaded in the first place, in which case, nuclei without REC-8 should be similarly lacking in chromosome-associated SYP-1 staining, or REC-8 was initially loaded but subsequently lost/removed, in which case it would be possible to have nuclei with little or no REC-8, but with staining by SYP-1 forming wild-type looking tracks. It is this second scenario which appears to be the case, since in germlines in which the *scc-2* depletion has led to late pachytene nuclei with some REC-8 loaded, there is extensive SYP-1 staining similar to the levels observed in wild type germlines. In germlines in which the *scc-2* RNAi is more severe and no REC-8 can be detected by immunofluorescence, SYP-1 can still been seen to form chromatin-associated tracks (Fig. 16). It therefore seems likely that in late pachytene REC-8 is passively lost or actively removed from chromatin. Stemming from the fact

that the decrease in REC-8 on chromatin occurs in late pachytene, it was tempting to speculate that this was triggered by an event in the recombination repair pathway. In order to investigate whether this might be the case, I carried out *scc-2* RNAi in *spo-11(ok79)* null mutants, in which no DSBs are made.

3.7.3 REC-8 is not lost in response to DSBs

If the loss or removal of REC-8 from late pachytene nuclei is in response to the formation of DSBs or a downstream process involved in the repair of these breaks, we would expect to see that the late pachytene nuclei from *spo-11(ok79)* mutants with partial *scc-2* depletion by RNAi would retain REC-8 loaded to chromatin. Therefore, we would anticipate that when stained with α-SMC-1 and α-REC-8 antibodies these germlines will display an expression pattern in which both proteins co-localise throughout meiosis, even in late pachytene. This is not the case, with both REC-8 and SMC-1 in *spo-11(ok79) scc-2* RNAi treated worms exhibiting patterns of expression very similar to their wild-type *scc-2* RNAi treated counterparts. Therefore DSBs are not the trigger for the loss or removal of REC-8 in late meiotic prophase.

3.7.4 *scc-2* RNAi by injection

A limitation of the RNAi experiments described so far is that all observations were made in F_1 worms coming from P_0 treated mothers, and these trans-generation experiments make it difficult to follow the levels of *scc-2* knockdown. That is because the *C. elegans* germline provides a snapshot of meiosis in time. After RNAi depletion it is impossible to know the history of a nucleus' cohesin status. Also RNAi will deplete SCC-2 protein levels at different rates depending on the worm and variations in its environment and this cannot be controlled for. In order to get an idea of the time scale in which REC-8 is lost subsequent to *scc-2* RNAi, a swifter destruction of SCC-2 was required. To do this, I depleted *scc-2* by carrying out RNAi by injection and then immunostaining the injected worms with α-REC-8 antibodies. This is technically very challenging to do, however, in the few instances in which the injected worms survived and the knockdown was successful, I observed a pattern of REC-8 staining similar to that seen the in the

partial knockdown by *scc-2* RNAi by feeding, 24 hours after injecting (Fig. 17). Since nuclei take about 35-40 hours to move from transition zone to late pachytene (Jaramillo-Lambert et al., 2007), the presence of late pachytene nuclei with reduced levels of REC-8 staining is consistent with an SCC-2-dependent reloading of cohesin during pachytene. Interestingly, diakinesis oocytes of these germlines had 6 bivalents, suggesting at the time of *scc-2* depletion chiasmata had been successfully formed and remained intact throughout the *scc-2* knockdown.

3.8 Summary of results

The previous identification of an *scc-2* null allele has enabled us to elucidate some of the functions of SCC-2 during meiosis, but it has not been possible to separate the roles of S-phase cohesin loading from specific prophase requirements. I sought to further investigate SCC-2's function in meiosis by depleting SCC-2 in the germlines of wild-type worms by RNAi. In doing so, and thereby impairing cohesin loading in meiosis, we have gained some tantalizing insights into the role that SCC-2 plays after meiotic S-phase. The results presented in this chapter demonstrate that RNAi can deplete *scc-2* in such a way that we can have two populations of nuclei within one germline: those in which cohesin loading was impaired at S-phase and therefore have no chromatin-associated cohesin, and those which had already undergone S-phase at the time of *scc-2* knockdown and therefore have cohesin associated with their chromosomes but cannot reload it. In studying these germlines, I have demonstrated that normal cohesin levels, and perhaps cohesin reloading by SCC-2, are required for chiasma formation and/or maintenance, and timely repair of meiotic DSBs. In addition to this, my observations of apoptotic induction in response to DNA damage suggest that chromosome-associated cohesin is required for signalling in the DNA damage checkpoint. In addition to this, REC-8 is lost or removed from late pachytene nuclei where both SMC-1 and SMC-3 are retained, and that this loss of REC-8 is not in response to DSBs and occurs within 24 hours of *scc-2* knockdown. These observations strongly suggest that in the absence of SCC-2 REC-8-containing cohesin complexes are

not preserved on chromatin, which by extension makes it tempting to speculate that *de novo* cohesin loading occurs after meiotic S-phase and that it is perhaps the perturbation of this cohesin homeostasis on chromosomes in pachytene that results in the impairment of chiasma formation.

Figure 6. SCC-2 localisation in wild-type germlines

A Whole mount wild-type germline stained with DAPI and anti-SCC-2 antibodies after triton fixation, which enhances the chromatin bound anti-SCC-2 signal.

B Magnification of pachytene nuclei showing SCC-2 staining reminiscent of the SC.

A
B
DNA
SCC-2
Merge
50μm
10μm
DNA + SCC-2

Figure 7. Localisation of cohesin in wild-type and *scc-2(fq1)* germlines

A Diagram of the predicted structure of the *C. elegans* scc-2 gene with exons indicated by blue boxes and introns as thin black lines. The position of the early STOP codon caused by the *fq1* mutation is indicated by a red line above the diagram. Regions used to create the two RNAi vectors and the region against which an antibody was raised, are indicated by green lines below the diagram.

B Whole mount wild-type germline stained with DAPI and α-REC-8. Magnification inset show mid pachytene nuclei.

C Whole mount *scc-2(fq1)* germline stained with DAPI and α-REC-8. Magnification inset show mid pachytene nuclei.

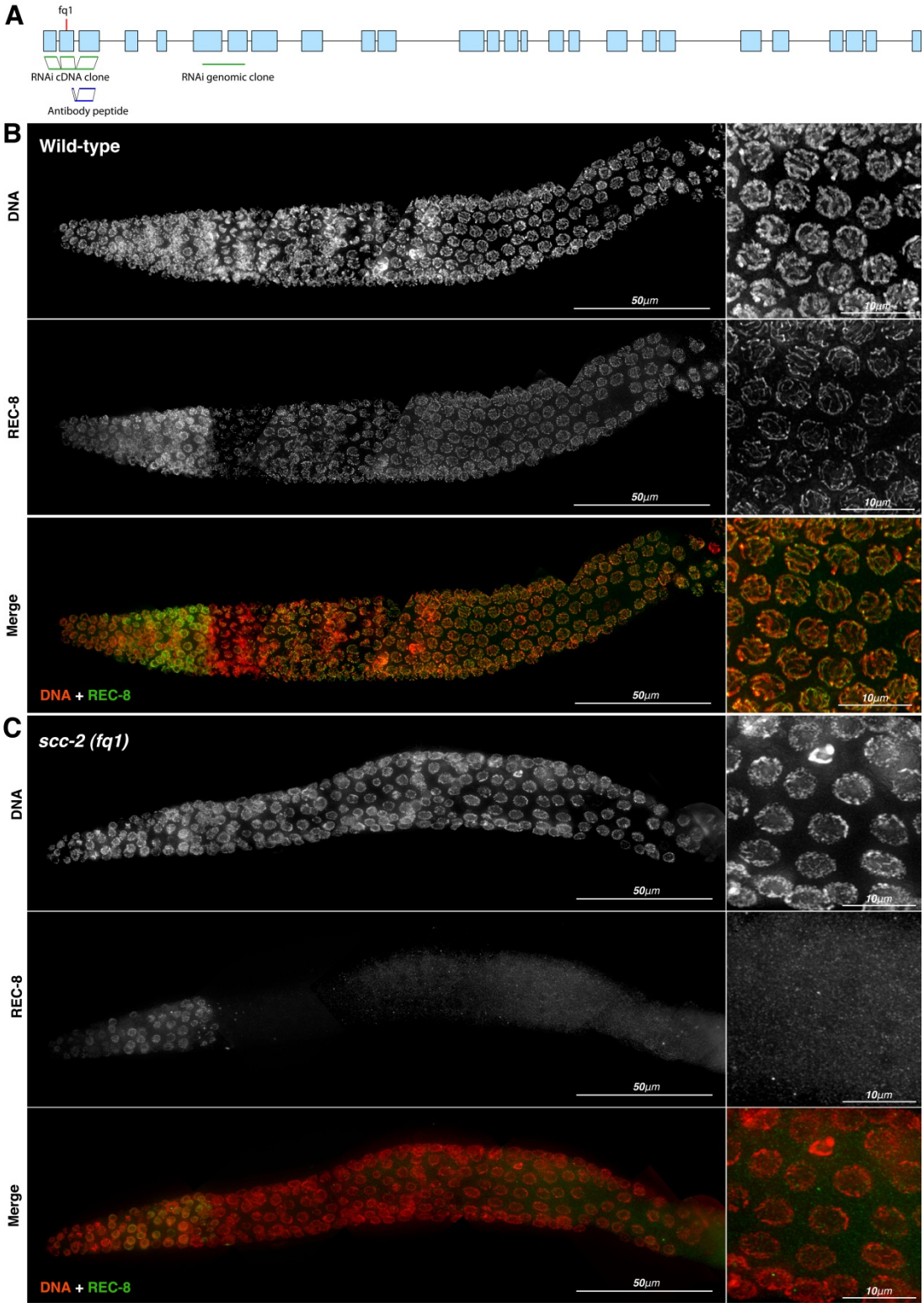
A
fq1
RNAi cDNA clone
RNAi genomic clone
Antibody peptide
B
Wild-type
DNA
REC-8
Merge
DNA + REC-8
50µm
10µm
C
scc-2 (fq1)
DNA
REC-8
Merge
DNA + REC-8
50µm
10µm

Figure 8. *scc-2* RNAi can phenocopy *scc-2(fq1)* mutant

A Whole mount of N2 germline following *scc-2* complete RNAi knockdown stained with DAPI and α-REC-8. Green arrowheads show enlarged polyploidy nuclei, red arrowheads show aneuploid micronuclei

B Magnification showing mid pachytene nuclei with thin disorganised chromatin.

C Diakinesis oocyte from *scc-2(fq1)* mutant showing individualised sisters

D Diakinesis oocyte from N2 following *scc-2* complete RNAi knockdown mutant showing individualised sisters

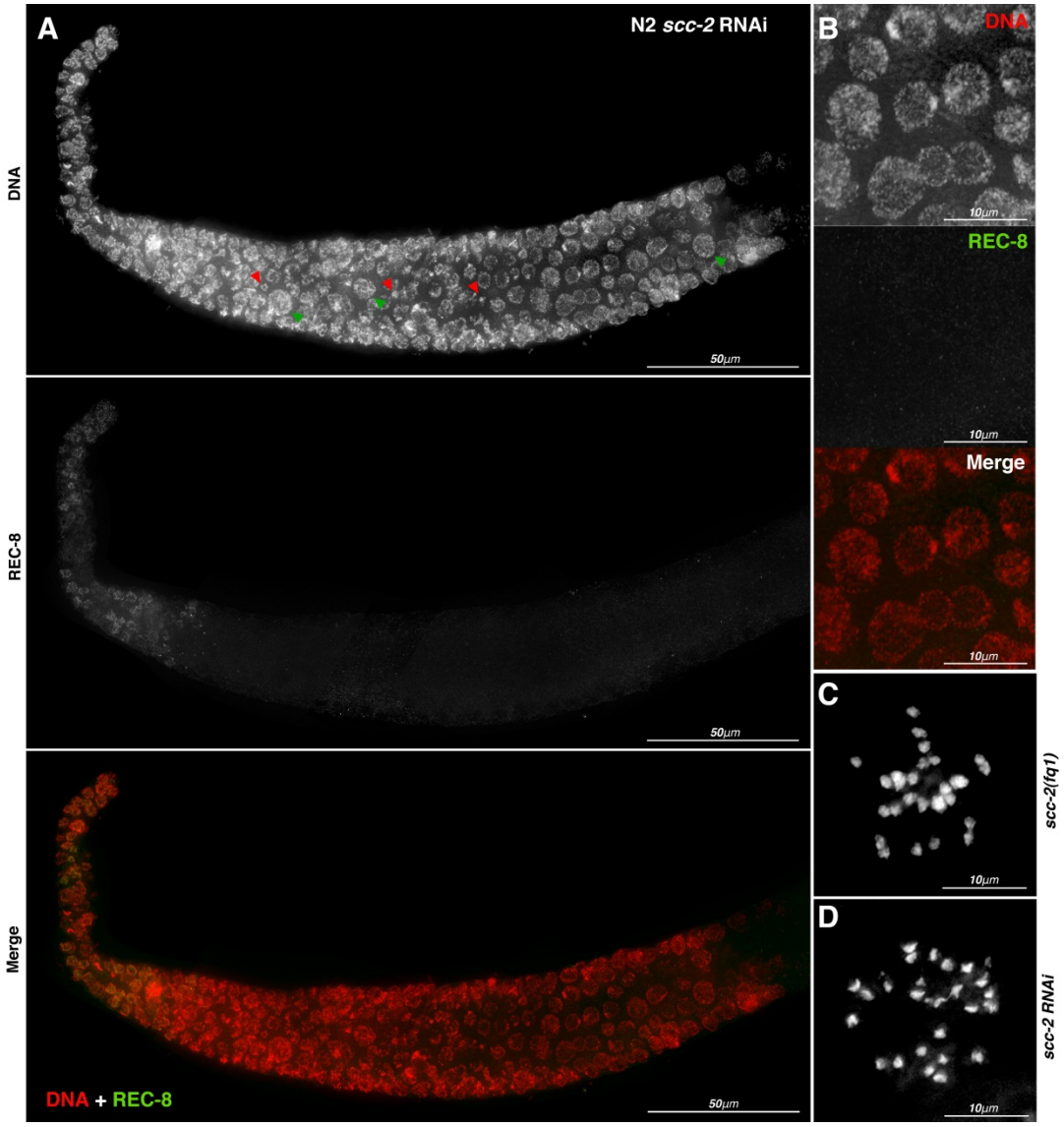
A
N2 scc-2 RNAi
DNA
REC-8
Merge
50μm
DNA + REC-8
B
DNA
10μm
REC-8
Merge
C
scc-2(lq1)
D
scc-2 RNAi

Figure 9. N2 following partial *scc-2* RNAi knockdown

A Diagram illustrating rational for partial *scc-2* RNAi knockdown showing two populations of nuclei; those which had undergone S-phase after RNAi knockdown, are cohesin negative, those which had undergone S-phase before RNAi knockdown, are cohesin positive.

B Whole mount of N2 germline following *scc-2* partial RNAi knockdown stained with DAPI and α-SMC-1.

C Whole mount of N2 germline following *scc-2* partial RNAi knockdown stained with DAPI and α-SMC-3.

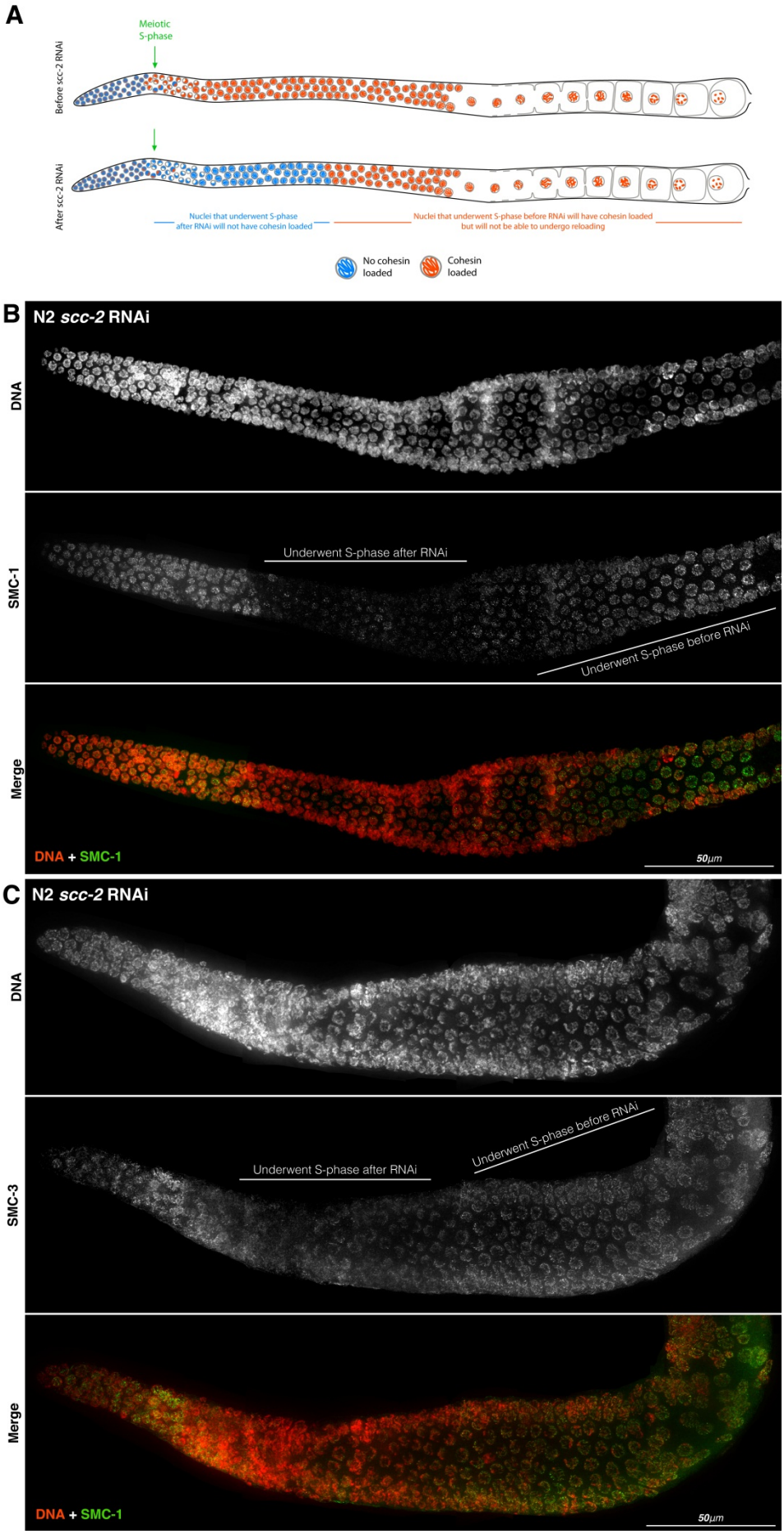
A
Meiotic
S-phase
Before scc-2 RNAi
After scc-2 RNAi
Nuclei that underwent S-phase
after RNAi will not have cohesin loaded
Nuclei that underwent S-phase before RNAi will have cohesin loaded
but will not be able to undergo reloading
No cohesin
loaded
Cohesin
loaded
B
N2 scc-2 RNAi
DNA
SMC-1
Underwent S-phase after RNAi
Underwent S-phase before RNAi
Merge
DNA + SMC-1
50μm
C
N2 scc-2 RNAi
DNA
SMC-3
Underwent S-phase after RNAi
Underwent S-phase before RNAi
Merge
DNA + SMC-1
50μm

Figure 10. Meiotic Cohesin Is Required for the Apoptotic Response of the DNA Damage Checkpoint

A Quantification of apoptotic corpses by SYTO12 staining in the indicated genotypes. Error bars indicate standard error of the mean (SEM). The numbers of germlines scored per genotype were: WT (120), *scc-2(fq1)* (95), *syp-1(me17)* (69), *scc-3(ku263)* (73), irradiated WT (53), irradiated *scc-2(fq1)* (88), and irradiated *scc-3(ku263)* (69). Scoring of apoptotic corpses following γ irradiation was performed 20 hr after treatment of young adult worms (18 hr post L4) with 75 Gy. Experiments carried out by James Lightfoot.

B-C The green circles seen in the bend of these germlines are nuclei undergoing apoptosis and being engulfed.

B Un-deconvolved germline bend of ced-1::GFP worms treated with *scc-2* RNAi to give partial knockdown stained with α-SMC-1 and α-GFP

C Un-deconvolved germline bend of ced-1:GFP worms treated with *scc-2* RNAi to give complete knockdown stained with α-SMC-1 and α-GFP

D Quantification of ced-1:GFP-labeled apoptotic corpses following *scc-2* or control RNAi at 20°C and 25°C in germlines that were also costained with α-SMC-1 antibodies to determine the amount of chromosomal cohesin present in each germline. Statistical analysis demonstrates that although apoptosis levels are significantly different between control RNAi at 20°C and scc-2 RNAi at 20°C with reduced SMC-1 levels (P value ** = 2 × 10−7), apoptosis levels are not different between control RNAi at 25°C and scc-2 RNAi at 25°C with no visible SMC-1 staining (P value * = 0.29). Twenty germlines were scored per genotype. Error bars indicate SEM.

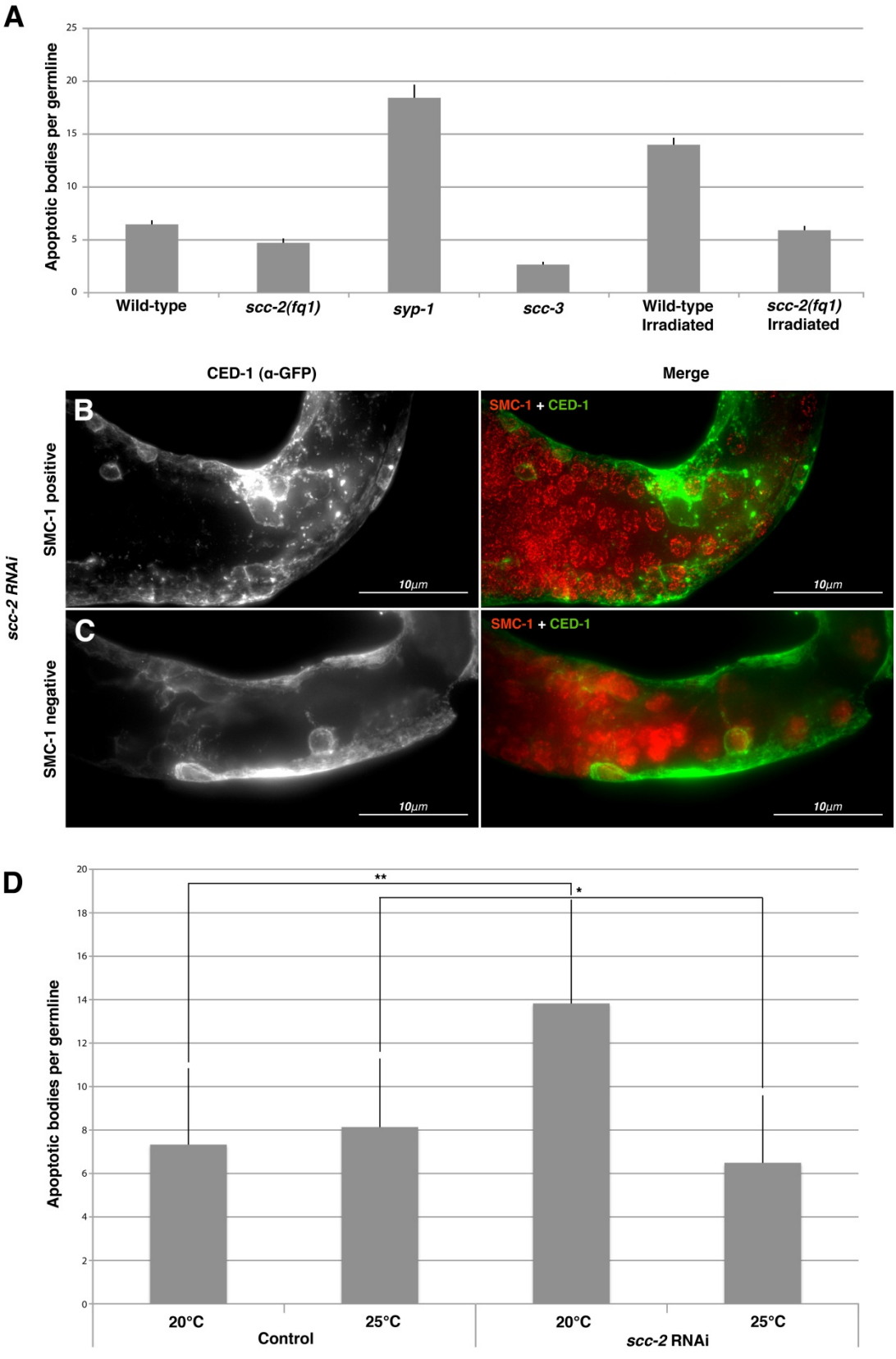
A
Apoptotic bodies per germline
25
20
15
10
5
0
Wild-type
scc-2(fq1)
syp-1
scc-3
Wild-type Irradiated
scc-2(fq1) Irradiated
CED-1 (α-GFP)
Merge
scc-2 RNAi
B
SMC-1 positive
SMC-1 + CED-1
10μm
C
SMC-1 negative
SMC-1 + CED-1
10μm
D
Apoptotic bodies per germline
20
18
16
14
12
10
8
6
4
2
0
**
*
20°C
25°C
20°C
25°C
Control
scc-2 RNAi

Figure 11. *scc-2* RNAi impairs chiasmata formation

A N2 treated with empty vector RNAi control showing pachytene nuclei chromatin morphology stained with DAPI and α-REC-8 and diakinesis oocyte with 6 bivalents

B N2 treated with *scc-2* RNAi causing mild and severe knockdown showing pachytene nuclei chromatin morphology stained with DAPI and α-REC-8, with low levels of REC-8 loading and no REC-8 loading, respectively and diakinesis oocyte with 12 univalents and 24 individualised sister chromatids respectively.

C *scc-2(fq1)* showing pachytene nuclei chromatin morphology stained with DAPI and α-REC-8 and diakinesis oocyte with individualised sister chromatids

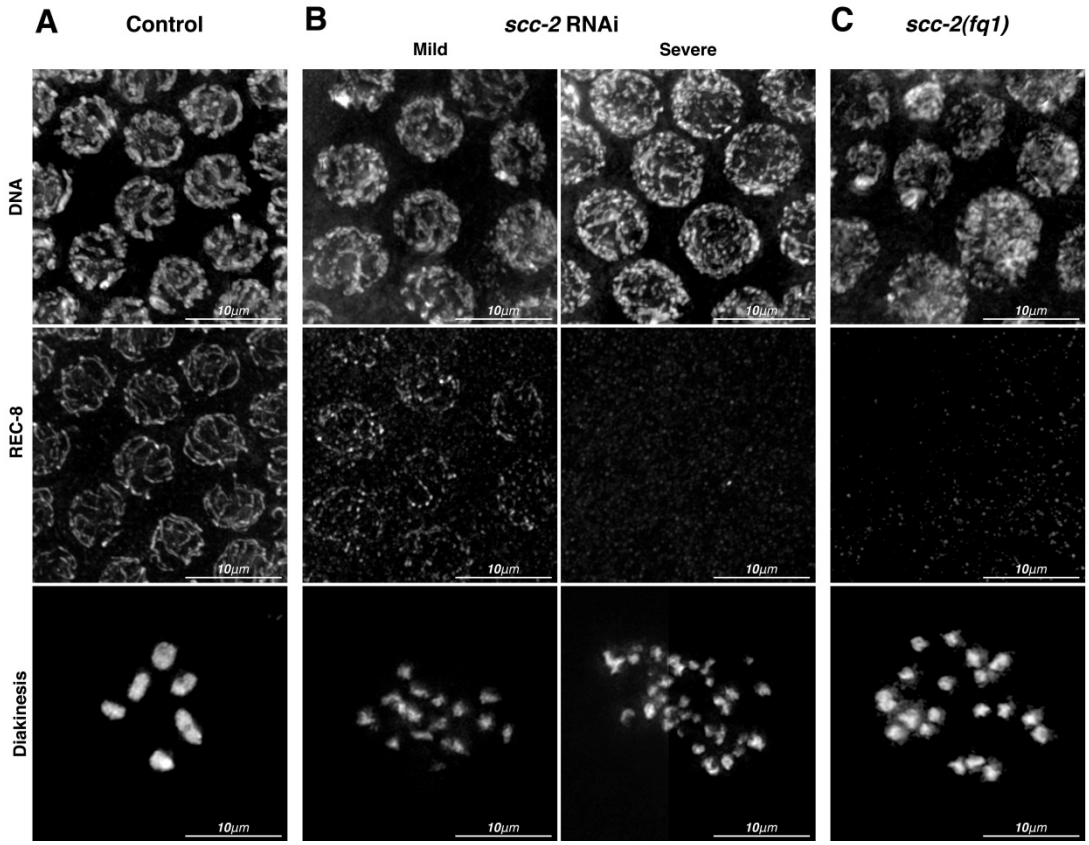
A
Control
B
scc-2 RNAi
Mild
Severe
C
scc-2(fq1)
DNA
REC-8
Diakinesis
10μm

Figure 12. *scc-2* RNAi impairs DSB repair

A N2 treated with empty vector RNAi control showing pachytene nuclei stained with DAPI, α-REC-8 and α-RAD-51.

B N2 treated with *scc-2* RNAi at 20°C causing mild knockdown showing pachytene nuclei stained with DAPI, α-REC-8 and α-RAD-51.

C N2 treated with *scc-2* RNAi at 25°C causing severe knockdown showing pachytene nuclei stained with DAPI, α-REC-8 and α-RAD-51.

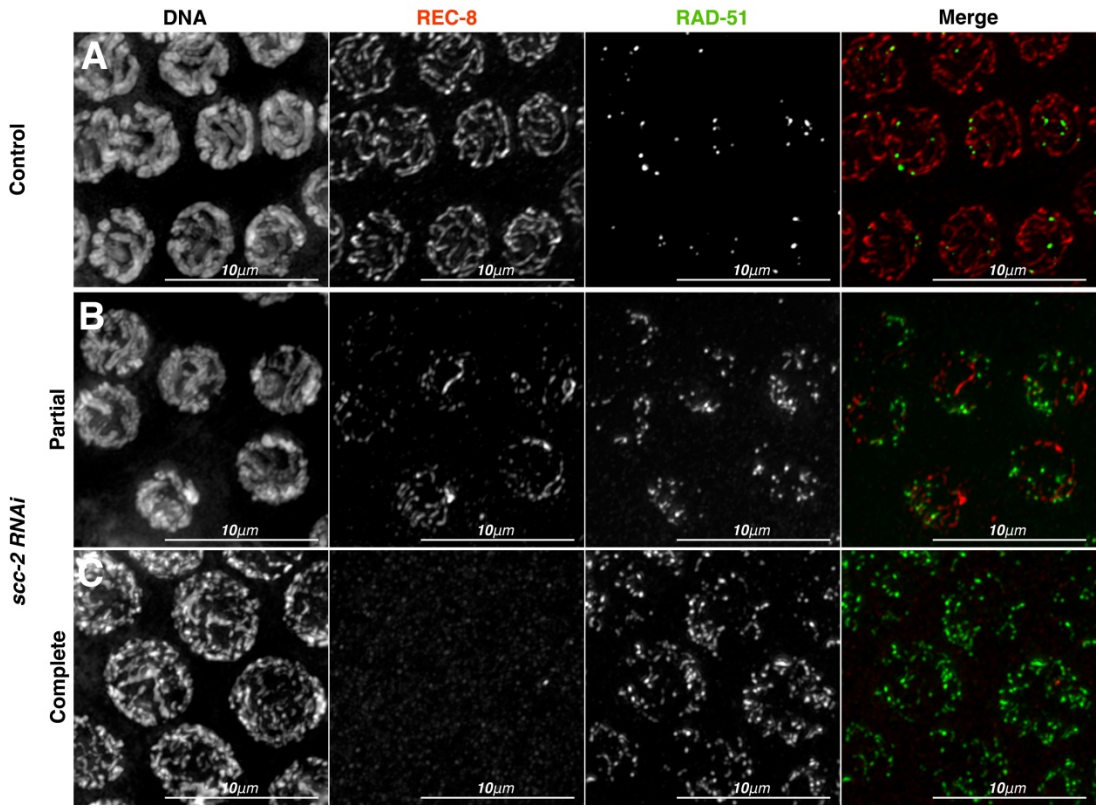
DNA
REC-8
RAD-51
Merge
Control
scc-2 RNAi
Partial
Complete
A
B
C
10μm

Figure 13. *scc-2* RNAi causes dysregulation of CO formation

A ZHP-3:GFP treated with empty vector RNAi control and *scc-2* RNAi at 20°C and 25°C causing mild and severe knockdowns respectively, showing pachytene nuclei stained with DAPI, α-SMC-1 and α-GFP. Dashed circles indicate nuclei with 6 foci in controls and variable numbers of foci in RNAi treated worms. Diakinesis insets show bivalent oocyte in control and univalents indicating lack of chiasmata in RNAi treated worms.

B Quantification of ZHP-3:GFP foci following scc-2 or control RNAi stained with α-SMC-1 to determine the amount of chromosomal cohesin present in each germline. The numbers of nuclei scored were: Control (85); *scc-2* RNAi SMC-1 positive (78); *scc-2* RNAi SMC-1 negative (72).

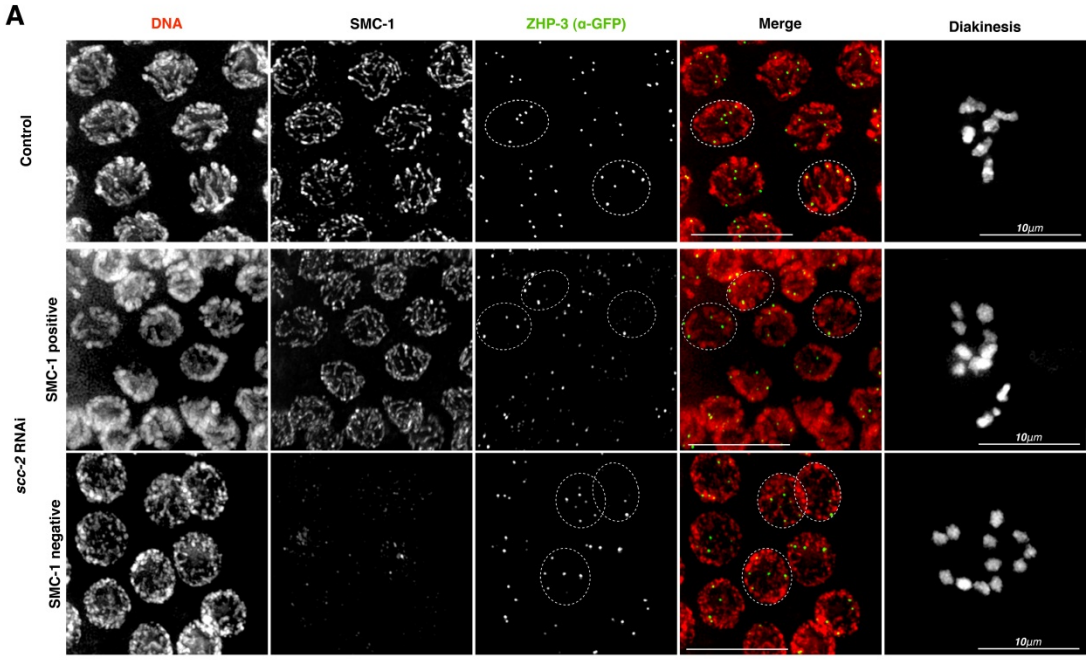
A
DNA
SMC-1
ZHP-3 (α-GFP)
Merge
Diakinesis
Control
scc-2 RNAi
SMC-1 positive
SMC-1 negative
10μm

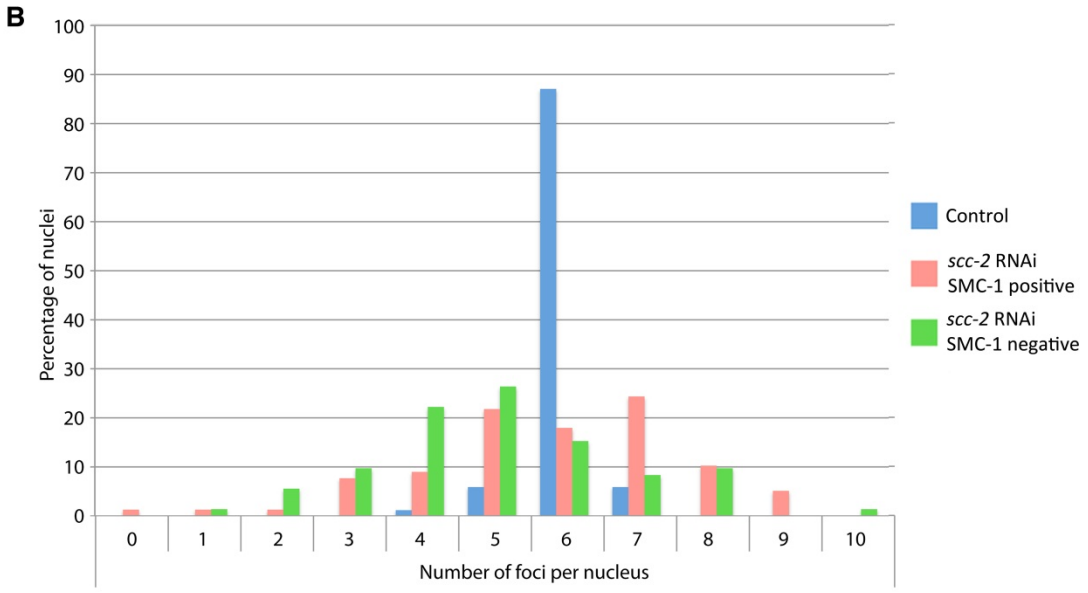
B
Percentage of nuclei
100
90
80
70
60
50
40
30
20
10
0
0
1
2
3
4
5
6
7
8
9
10
Number of foci per nucleus
Control
scc-2 RNAi
SMC-1 positive
scc-2 RNAi
SMC-1 negative

Figure 14. Differing patterns of cohesin subunit localisation following partial *scc-2* RNAi knockdown

A Whole mount of N2 germline following *scc-2* partial RNAi knockdown stained with DAPI, α-SMC-3 and α-REC-8.

B Enlarged details comparing REC-8 and SMC-3 staining patterns in early and late pachytene, showing faster loss of REC-8 that SMC-3 in late pachytene nuclei.

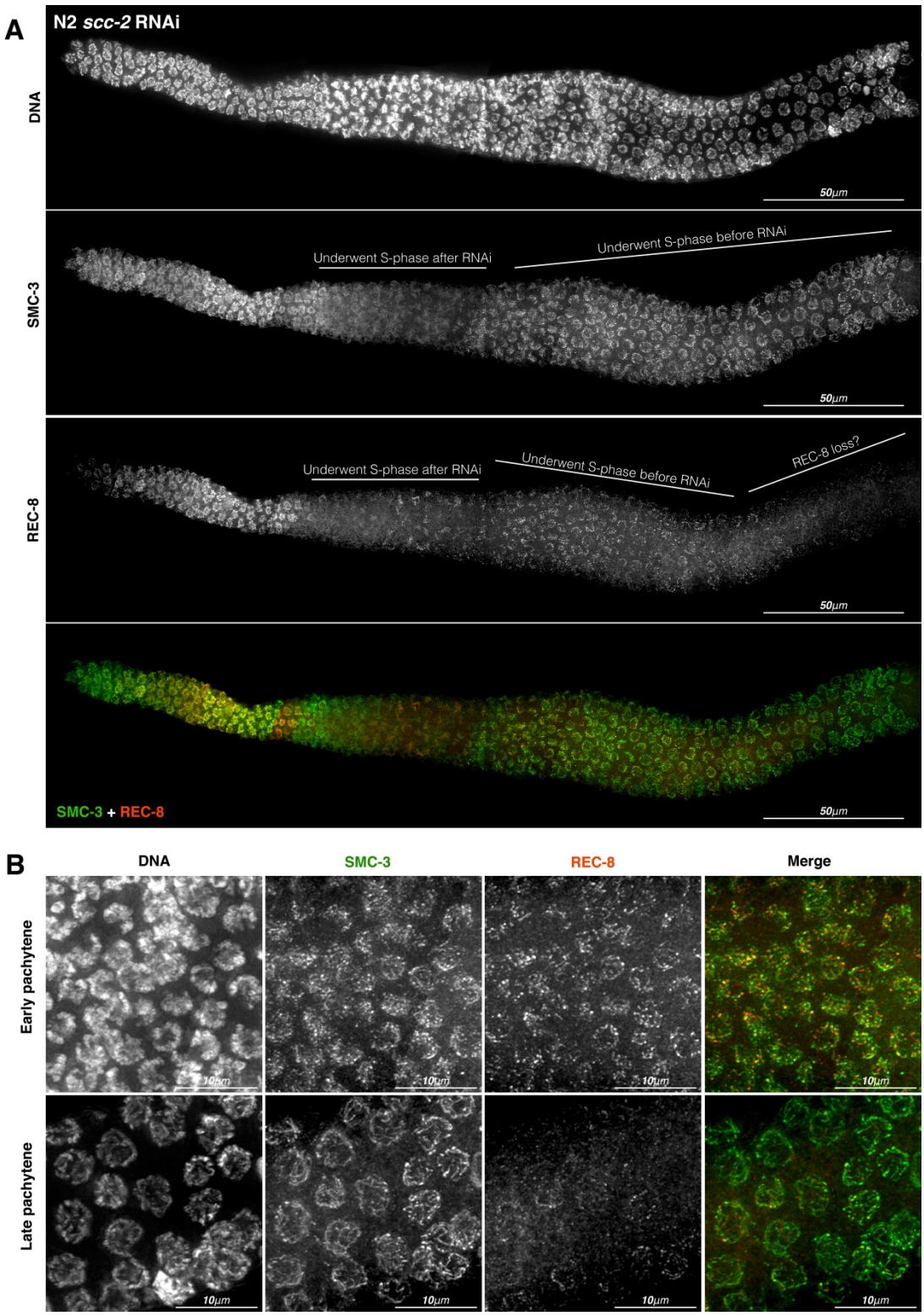
A
N2 scc-2 RNAi
DNA
SMC-3
REC-8
Underwent S-phase after RNAi
Underwent S-phase before RNAi
REC-8 loss?
SMC-3 + REC-8
50μm
B
DNA
SMC-3
REC-8
Merge
Early pachytene
Late pachytene
10μm

Figure 15. REC-8 is lost from chromatin following *scc-2* RNAi

A Pachytene nuclei following empty vector control RNAi stained with α-REC-8 and α-SYP-1 showing colocalisation of cohesin and CE, counterstained with DAPI.

B *scc-2(fq1)* pachytene nuclei stained with α-REC-8 and α-SYP-1 showing failure of CE to form in the absence of cohesin loading, and therefore without any cohesin on the axis, counterstained with DAPI.

C Pachytene nuclei following *scc-2* RNAi causing mild or severe knockdown, in which cohesin loading is impaired and therefore any removed cohesin cannot be replenished, stained with α-REC-8 and α-SYP-1 showing CE formation with impaired REC-8 staining and no REC-8 staining, respectively, counterstained with DAPI

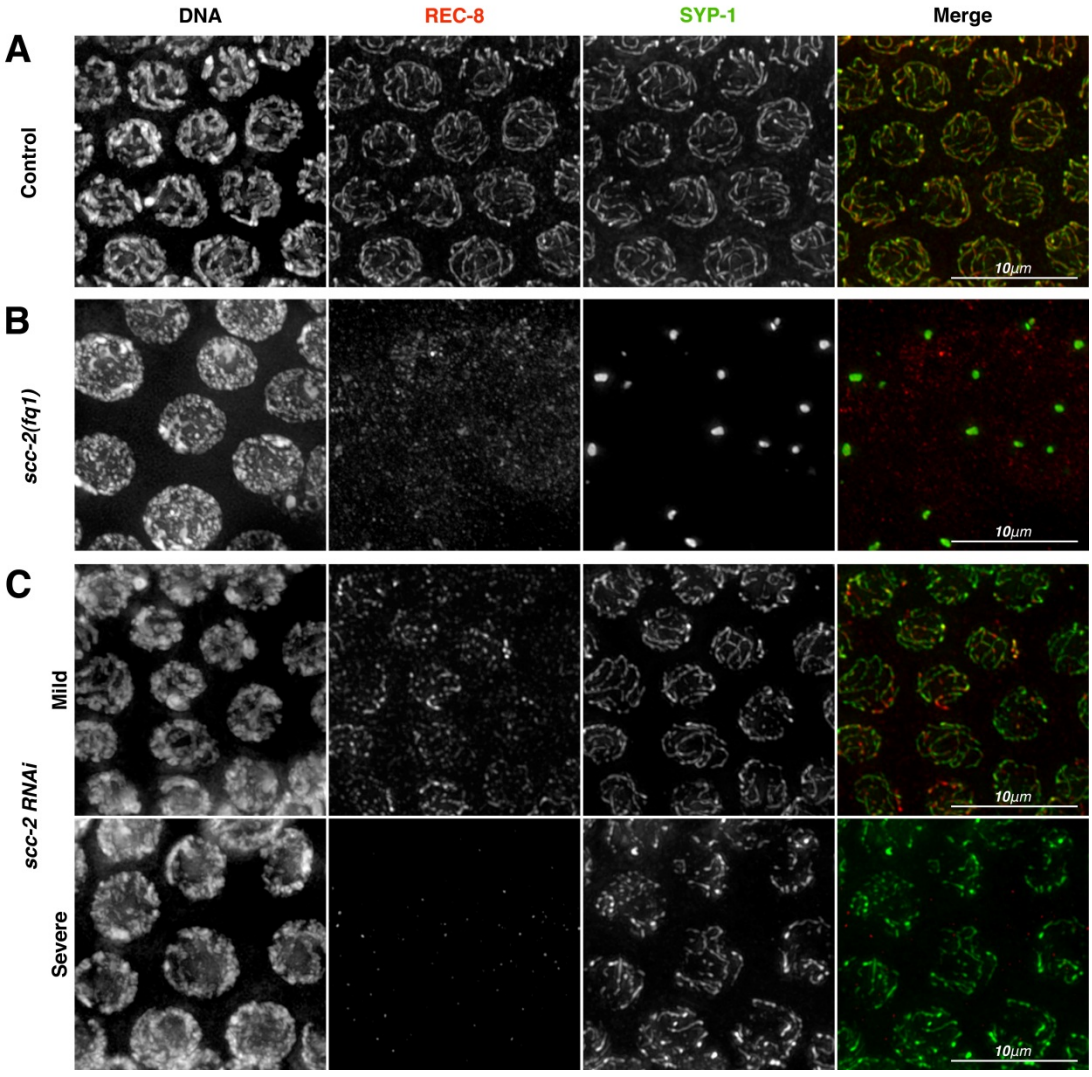
DNA
REC-8
SYP-1
Merge
A
Control
B
scc-2(fq1)
C
scc-2 RNAi
Mild
Severe
10μm

Figure 16. DSB formation does not cause REC-8 loss from late pachytene nuclei.

Whole mount of *spo-11(ok79)* germline following *scc-2* partial RNAi knockdown stained with DAPI, α-SMC-3 and α-REC-8.

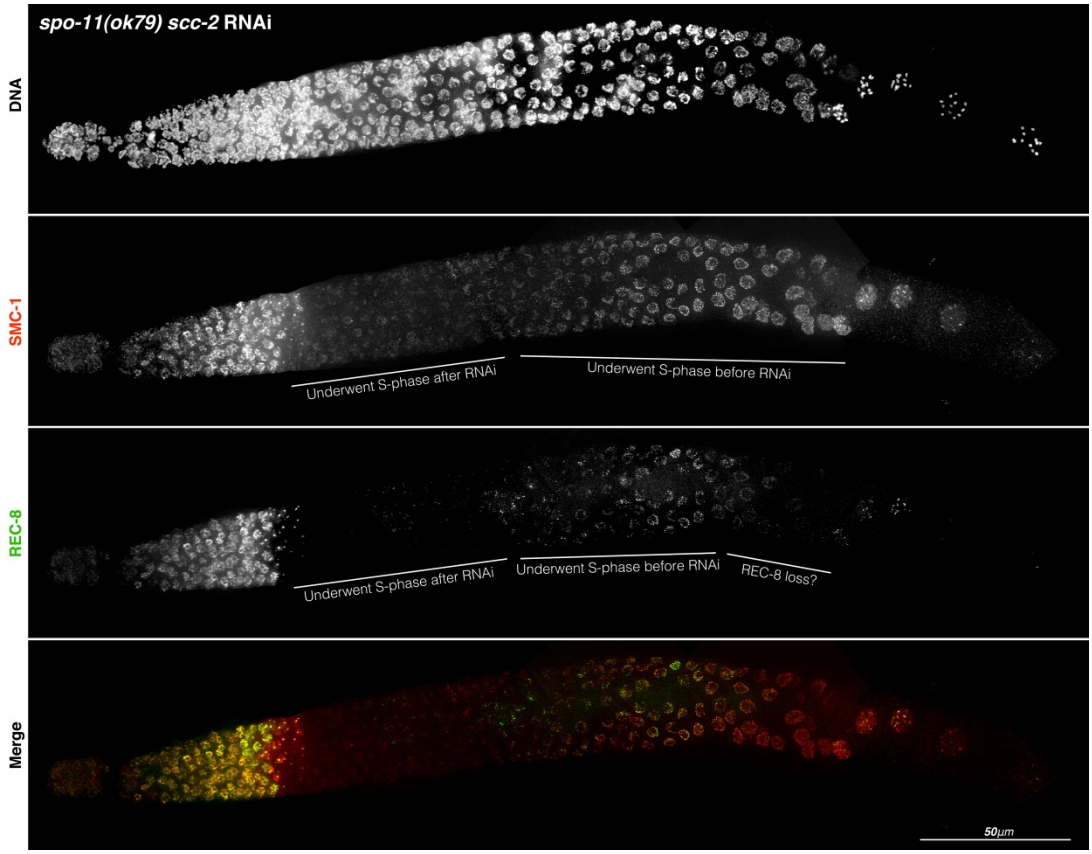
spo-11(ok79) scc-2 RNAi
DNA
SMC-1
Underwent S-phase after RNAi
Underwent S-phase before RNAi
REC-8
Underwent S-phase after RNAi
Underwent S-phase before RNAi
REC-8 loss?
Merge
50μm

Figure 17. *scc-2* RNAi by injection

A Whole mount of N2 germline 24 hrs following *scc-2* RNAi injection stained with DAPI and α-REC-8.

B Enlarged details comparing REC-8 staining in early and late pachytene and -1 diakinesis oocyte.

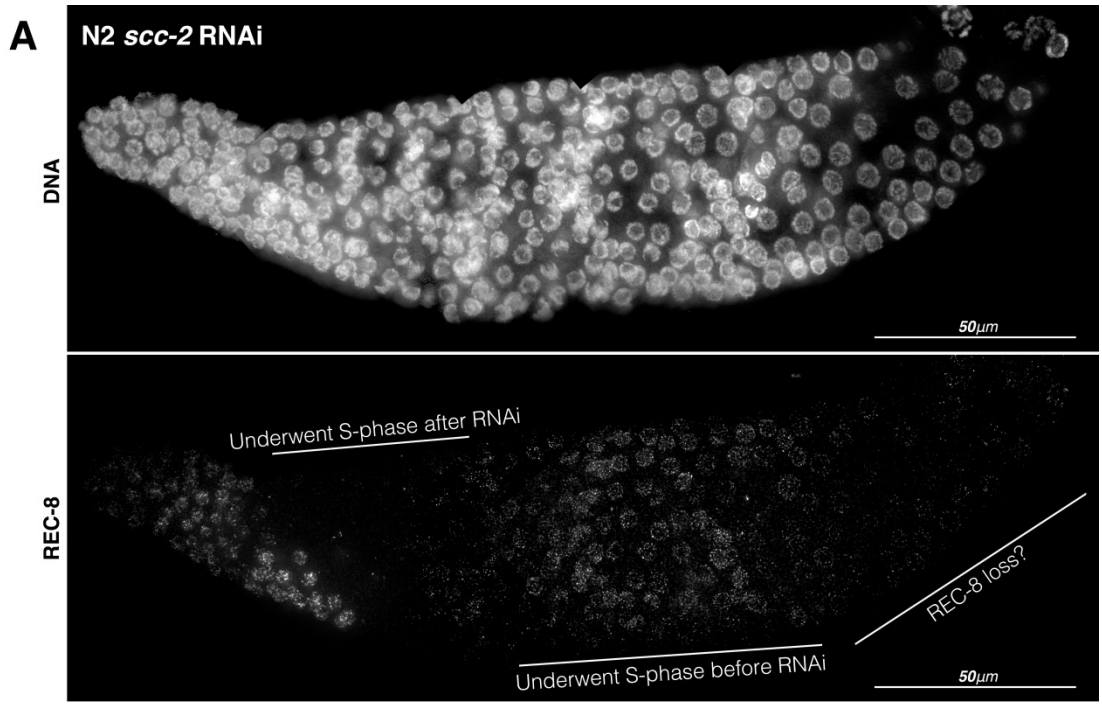
A
N2 scc-2 RNAi
DNA
50μm
REC-8
Underwent S-phase after RNAi
REC-8 loss?
Underwent S-phase before RNAi
50μm

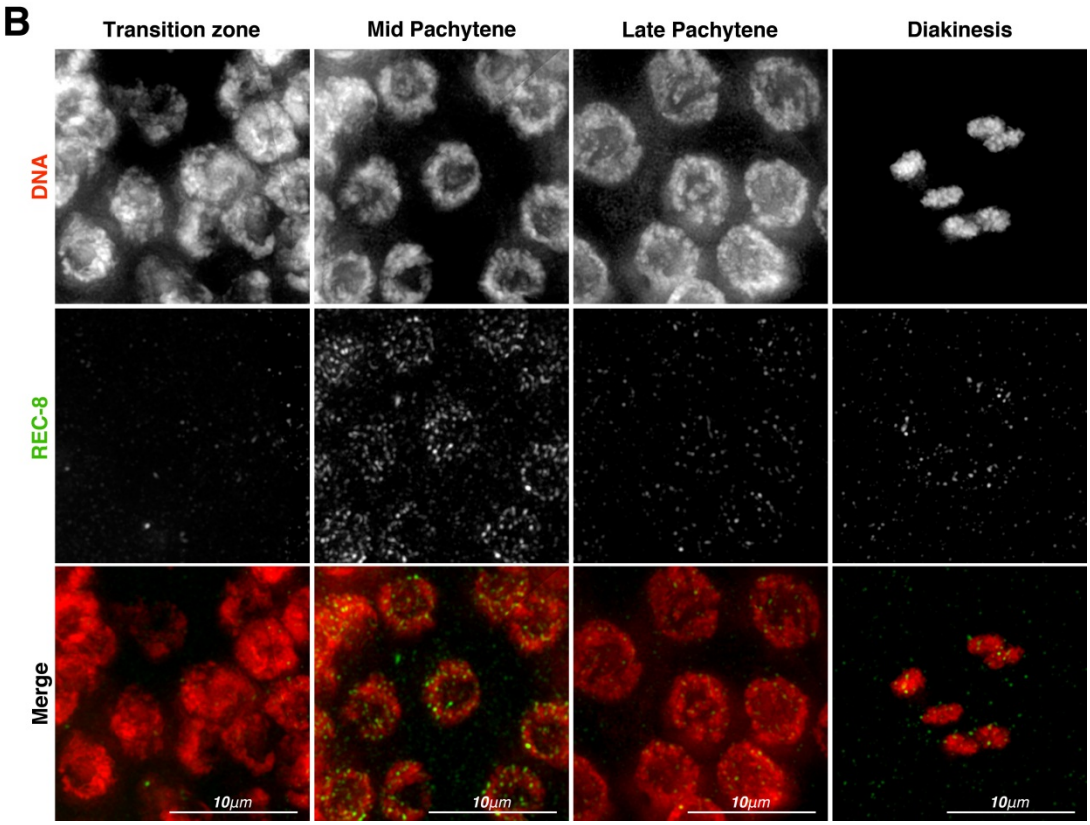
B
Transition zone
Mid Pachytene
Late Pachytene
Diakinesis
DNA
REC-8
Merge
10μm
10μm
10μm
10μm

CHAPTER 4: RESULTS
NOVEL APPROACHES TO INVESTIGATE COHESIN LOADING DURING MEIOTIC PROPHASE

4.1 Objectives

The *scc-2* RNAi data presented in the previous chapter strongly suggests that cohesin removal and reloading both take place during meiotic prophase in the *C. elegans* germline. However, the time scale over which the events of meiotic prophase take place are significantly shorter than the period over which the RNAi treatment is administered. Therefore, I sought to engineer a system that would allow investigation of cohesin loading with greater temporal resolution, thus allowing me to elucidate the exact timing of cohesin loading dynamics. To this end, I used the recent advances in generating single-copy insertion transgenes to control cohesin expression in the germline. In addition to this, I combined this transgenic technology with molecular tools that have previously not been used in worms, looked at the possibly of using mRNA to express proteins in the germline, and aimed to map AIR-2 phosphorylation and separase cleavage sites on the kleisin subunit REC-8. This was an ambitious undertaking, and was met with variable success, but the experiments performed in this chapter illustrate the potential for using these novel technologies in the future.

4.2 Altering cohesin expression patterns

To investigate if cohesin removal and/or reloading occurs during meiotic prophase, I sought to engineer a system in which cohesin expression was restricted to nuclei in the mitotic tip of the germline and those in the early stages of meiotic prophase. The rational behind this is that if there is no cohesin expression in pachytene, any cohesin reloading occurring in pachytene dependent on *de novo* synthesis of that subunit would be impaired. As a consequence of this, one would expect to see a progressive decline in the levels of cohesin loaded to chromatin as nuclei progress into late prophase. This

should mimic the results seen in the *scc-2* RNAi experiments and therefore might lead to loss of chiasmata. This result would demonstrate that cohesin loss does occur in pachytene and further support the idea that cohesin reloading parts place in meiotic prophase.

To demonstrate that cohesin loading occurs in meiotic prophase, I sought to engineer the reverse system, with cohesin only being expressing in late pachytene. In this case, if cohesin loading does occur one would expect to see this late expressing cohesin being loaded onto chromatin.

4.2.1 Generating transgenic worms with fluorescently tagged cohesin subunits

To visualise early and late expressing cohesin complexes, the initial step was to generate transgenic strains in which fluorescently tagged cohesin subunits could be stably expressed in the germline and to ensure that these were functional. To this end, three single-copy insertion transgenic lines were generated, in which REC-8, COH-3 and SCC-3 were tagged with a fluorescent protein.

A detailed protocol for creating single copy insertion transgenics using the MosSCI system is presented in the Materials and Methods (section 2.6). Briefly, a plasmid with your insert sequence is flanked by ~1.5kb of sequence with homology to a chromosomal locus with a Mos1 transposon site. This plasmid, along with a vector coding for expression of the Mos1 transposase and some selection marker plasmids are injected directly into the *C. elegans* germline. Mos1 excision is induced by expression of Mos1 transposase and gene insertions are generated by repair of this double stranded break with the regions of homology within the insert vector. In this way one can insert a single copy of a sequence of interest at a particular genetic locus.

4.2.1.1 REC-8::GFP

The EG4322 *unc-119* strain, containing the ttTi5605 chromosome II Mos locus was injected with pCFJ151 containing the wild-type *rec-8* gene with a GFP sequence in place of its stop codon and with its endogenous 3' and 5' UTRs. Putative insert positive lines were checked for GFP expression in the germline, by visualising live worms using the Leica DMRB microscope. From this it was possible to see GFP in all germline nuclei, with clear chromatin-associated GFP tracks being visible in pachytene nuclei visible using a 62X lens. In order to check the functionality of this *rec-8::GFP* transgene, the strain was crossed with the *rec-8(ok978)* null allele to create a strain with both the *rec-8* deletion and the transgene in homozygosity. This *rec-8; rec-8::GFP* strain has wild-type fertility and DAPI staining of whole worms reveals a wild type germline with 6 bivalents at diakinesis (Fig. 18D and H). This demonstrates that this GFP tagged version of *rec-8* can carry out all the functions of the endogenous gene. Whole mount germlines were stained with α-GFP antibodies, revealing an identical pattern to that seen in wild-type germlines stained with α-REC-8 antibodies (Fig. 18). With the knowledge that this REC-8::GFP is functional and has wild-type localisation, I could continue to try to engineer a system in which REC-8::GFP expression was restricted to either the early or late stages of meiotic prophase. I will discuss this in section 4.2.2.

4.2.1.2 SCC-3::GFP

An *scc-3::GFP* transgene was engineered as with the *rec-8::GFP* strain, but this time using the EG5003 *unc-119* strain, containing the cxTi10882 insertion site on chromosome IV, EG5003 worms were injected with pCFJ178 containing the wild-type *scc-3* gene with a GFP sequence in place of its stop codon and carrying the *scc-3* endogenous 3' and 5' UTRs. Checking putative insert positive strains using the Leica DMRB microscope it was possible to see very bright GFP signal from all somatic and germline nuclei, with this signal visible using a 20X lens. As with the *rec-8::GFP* transgene, when using the 62X lens, chromatin-associated GFP tracks could clearly be seen in pachytene nuclei. In order to test the functionality of this transgene, the strain was crossed to the *scc-3(ku263)*

mutant to obtain a strain which was homozygous for both the *scc-3::GFP* transgene and the *scc-3* deletion. However, the outcome of these crosses was surprising. The first isolated *scc-3; scc-3::GFP* worms, had very high embryonic lethality, producing fewer than 10 viable offspring, suggesting that the transgene did not complement the mutation. However, whilst these worms were homozygous from the insert it was no longer possible to see a GFP signal in the live worms. Furthermore, DAPI staining of whole worms revealed a phenotype that was distinct from *scc-3* mutants, displaying univalents in diakinesis, rather than the individualised sister chromatids and chromosome fragments that are normally present in the oocytes of *scc-3* mutants. This suggested that perhaps the transgene was being silenced to some extent, a phenomenon that has been reported before. The few surviving *scc-3; scc-3::GFP* individuals were left to self-fertilize and after a few generations the plates were completely starved of bacteria, something impossible to achieve if these worms were maintaining their high levels of infertitily. Further investigation of these worms revealed that the GFP expression had returned, that the embryonic lethality was disappearing, and that their oocytes appeared normal with 6 DAPI masses at diakinesis. At this point the strain was completely stable and the *scc-3::GFP* transgene fully rescued the meiotic and mitotic defects seen in *scc-3* mutants, providing a useful tool for live imaging of cohesin as the levels of GFP expression are extremely high.

4.2.1.3 COH-3::mCherry

Since I had successfully created a *rec-8::GFP* transgene but less is known about the α-kleisins COH-3 and COH-4, and at the time of making these transgenic strains there were not effective α-COH-3 or α-COH-4 antibodies, engineering a fluorescently tagged COH-3 would prove invaluable for further investigation of its function. An COH-3::mCherry strain was engineered as with the REC-8::GFP and SCC-3::GFP strains, this time using the EG6701 *unc-119* strain, containing the *ttTi4348* insertion site on chromosome. This strain was injected with pCFJ352b containing the wild-type *coh-3* gene with a mCherry sequence in place of its stop codon and with its endogenous 3' and 5' UTRs. Similarly to the

previous stains, mCherry signal could be seen in putative insert positive lines using Leica DMRB microscope with a 62X lens, however the signal was less bright than that of the REC-8::GFP. As before, it was important to test the functionality of COH-3::mCherry. However, the *coh-3(gk112)* single mutant does not have a phenotype since COH-3 and COH-4 appear to be redundant (Severson et al., 2009), so creating a strain homozygous for this deletion and the transgene would not be informative. The *coh-3;coh-4* double mutant has 12 univalents at diakinesis and consequently a high level of embryonic lethality (Severson et al., 2009). Therefore, crossing the *coh-3:mCherry* transgene into the *coh-3;coh-4* double mutant background was required to check the functionality of the transgene. This revealed that COH-3:mCherry was functional, since the embryonic survival was restored to wild-type levels in the *coh-3::mCherry*; *coh-3; coh-4* strain, and 6 DAPI bodies were visible in diakinesis oocytes. In addition, the mCherry signal was clearly visible throughout the meiotic prophase region of the germline, forming tracks in pachytene nuclei visible in live worms.

4.2.2 Generating REC-8::GFP transgenic lines with 3' UTRs to alter expression patterns

In the *C. elegans* germline the 3' UTRs of mRNAs have been shown to determine the temporal expression of proteins, and 3'UTRs that induce protein expression in specific regions of the germline have been identified (Merritt et al., 2008). By combining these regulatory sequences with the functional *rec-8::GFP* gene, I sought to manipulate the stage of meiosis at which this cohesin subunit could be expressed.

4.2.2.1 *fbf-2* 3' UTR

The *fbf-2* 3' UTR has been shown to limit gene expression to the mitotic tip, transition zone and early pachytene stages of the germline (Merritt et al., 2008). One would predict the *rec-8::GFP* driven by its endogenous promoter and this 3' UTR would restrict REC-8::GFP from the later stages of meiotic prophase, which could create an effect similar to that following *scc-2* RNAi if REC-8 loading at late prophase required synthesis of REC-8 during pachytene. I therefore inserted

this transgene into the chromosome II Mos site by the methods previously described, and I crossed this strain to the *rec-8* mutant background to check whether the transgene complements the mutation. Unfortunately *rec-8; rec-8::GFP fbf-2 3'UTR* worms did not display any meiotic defects, showing both wild-type levels of viability (99.50% compared with controls) and wild type levels of males (0.22% compared with controls) (Fig. 19E). In addition to this, staining of these germlines with α-GFP antibodies revealed REC-8::GFP localisation that was almost identical to that of controls, with no decrease in the levels of chromatin-associated REC-8 in late pachytene nuclei (Fig. 19A-D and 18E-H). The only difference observed was the absence of nucleoplasmic localisation of REC-8::GFP in late pachytene/diplotene nuclei in germlines of the *rec-8; rec-8::GFP fbf-2 3'UTR* compared with controls (Fig. 19C and 18G), suggesting that REC-8 re-expression in oocytes is impaired by the *fbf-2* 3'UTR. It is possible that the *fbf-2* 3'UTR does not restrict REC-8::GFP expression to a sufficiently early stage of meiosis for any removal to have an impact. Alternatively, it may be that removed REC-8-cohesin molecules can themselves be reloaded, and consequently early REC-8 expression is sufficient to carry out all the events of meiosis, that only low levels of removal that do not result in a phenotype occur, or that REC-8 is not being removed.

4.2.2.2 mex-5 3' UTR

The *mex-5* 3' UTR has been shown to restrict GFP expression to mid/late pachytene nuclei onwards. Therefore, by placing *rec-8::GFP* under the control of the *mex-5* 3' UTR we would hope to restrict its expression from the mitotic tip, transition zone and early pachytene nuclei. I inserted a *rec-8::GFP mex-5 3'UTR* transgene into the chromosome II Mos site, by the methods previously described. Unfortunately, in this strain REC-8::GFP could only be seen in very late pachytene nuclei onwards (a later stage than expected) and demonstrated a nucleoplasmic localisation (Data not shown). As one would expect, this transgene did no complement the *rec-8* mutation. By expressing *rec-8* at this very late stage of meiosis it is not possible to detect cohesin reloading, however, this is later that the mid/late pachytene stage in which cohesin reloading is

predicted to happen by the *scc-2* RNAi experiments. Further work is required to address whether cohesin reloading occurs in meiotic prophase.

4.3 Expressing cohesin from mRNA vectors

A powerful tool that has been used in other model organisms is the introduction of mRNA into cells. This allows tight temporal control of gene expression and allows the expression of tagged or modified genes without the necessity of generating transgenics, which can be time-consuming and expensive. However, until recently this technique had not been used in *C. elegans*, due to the propensity of introduction of RNA into the germline to cause suppression of the exogenous gene by RNAi, perhaps due to contamination of the RNA preparations with dsRNA. We sought to overcome the RNAi pathway by using a kit which not only produces high yields of very pure ssRNA, but also caps the RNA at its 5' end, and a secondary kit to add a polyA tail to the 3' end, both of which mimic *in vivo* mRNA in most eukaryotes. This should prevent degradation of the mRNA within the worm. In fact, while these experiments were being performed, a similar approach was shown to succeed in expressing protein in the C elegans germline from mRNA expression (Wood et al., 2011).

4.3.1 Histone H2B mRNA

To initially test whether it was possible to see expression of a gene driven by injected mRNA molecules, we decided to use an mRNA expression vector that has been preciously shown to be effective. To this end, Dr. Nobu Kudo from Imperial College kindly gave us a histone H2B::mCherry vector that has been used for live imaging in mouse oocytes (Kudo et al., 2009). This contains the murine cDNA sequence of histone H2B, tagged with mCherry and flanked by *Xenopus* regulatory sequences, with a T7 promoter upstream. Capped mRNA was synthesised using the T7 mMessage mMachine Kit (Ambion AM1344) and diluted to a concentration of 0.1μg/μl. This was injected directly into the body cavity or germline of N2 worms. Only 1 hour post injection it was possible to see mCherry signal in the somatic nuclei of gut, and in the bivalents in diakinesis

oocytes (Fig. 20A and B). Six hours after injection into the gonad, mCherry could be seen in all the nuclei of the germline (Fig. 20C). This illustrates that it is possible to drive expression of a tagged protein from exogenous mRNA injected into the germline of *C. elegans.* Furthermore, it demonstrates that the rate of histone turnover in diakinesis oocytes is very rapid, possibly due to the extensive DNA compaction that is occurring at this stage.

4.3.2 SCC-3::GFP mRNA

To test whether cohesin reloading is occurring, we designed an mRNA expression vector containing *scc-3* tagged with GFP, an SL1 splice leader as 5'UTR and the endogenous scc-3 3' UTR, and this cassette was preceded by a T7 promoter. Capped mRNA was synthesised using the T7 mMessage mMachine Kit (Ambion AM1344) and poly(A) tailed with the Poly(A) Tailing Kit (Ambion AM1350) as described in Materials and Methods (section2.4.2). However, running the synthesis product on a RNA denaturing gel revealed that the mRNA transcript was not of the appropriate length. Therefore, the expression of SCC-3::GFP protein from this vector was never tested in worms and further work will be required to develop this system.

4.4 Developing a degron system in *C. elegans*

The ability to conditionally control gene expression is one of the most powerful tools in the study of a protein's function. Often this manipulation takes place at the level of DNA or mRNA, however more recently a system has been developed which allows rapid protein degradation. The auxin degron exploits a unique system that exists in plants to regulate protein expression. Briefly, when transgenic cells containing the *Arabidopsis* gene *TIR1*, and a gene of interest tagged with the IAA17 peptide are exposed to auxin, this induces the formation of a complex between the tagged protein and the TIR-1 protein that promotes an E2 ubiquitin conjugating enzyme to induce polyubiquitination and rapid degradation of the tagged protein by the proteasome (Fig. 21A) (Nishimura et al., 2009). This system has been used in *S. cerevisiae* and in mammalian cells

resulting in almost complete protein destruction in less than 1 hour (Nishimura et al., 2009). However, it has not yet been utilized in the context of a multicellular organism.

In order to develop this system in *C. elegans* two transgenic stains must be created: one in which TIR1 is expressed in the germline, and a second expressing a functional IAA17-tagged cohesin subunit. Then the method for introducing auxin or its analogue NAA can be tested to optimise the conditions that provide the most robust protein degradation. Hopefully it will be possible to induce cohesin degradation within a matter of hours of auxin treatment. This gives it a huge advantage over RNAi, where it takes a generation to see knockdown. Therefore, this approach will hopefully allow investigation of the specific stages of meiosis at which cohesin is required, and perhaps allow us to differentiate the different roles of cohesin within prophase.

4.4.1 Generating a REC-8::IAA17 transgenic strain

The EG4322 *unc-119* strain, containing the ttTi5605 chromosome II Mos locus was injected with pCFJ151 containing the wild-type *rec-8* gene with a IAA17-tag sequence in place of its stop codon and with its endogenous 3' and 5' UTRs. These worms were crossed to the *rec-8(ok978)* mutants to create a *rec-8::IAA17 ;rec-8 strain*. These worms had a wild-type brood size and DAPI staining of whole worms reveals a wild type germline with 6 bivalents at diakinesis, demonstrating that the tagged protein is functional and fully complements the absence of the endogenous REC-8 protein.

4.4.2 Generating a TIR1 transgenic strain

A TIR1 strain was engineered using the EG5003 *unc-119* strain, containing the cxTi10882chromosome IV Mos locus, which was injected with pCFJ178 containing the *Arabidopsis* TIR1 sequence, in which 3 artificial introns were introduced, and carrying the 5' and 3' UTR sequences from *rec-8*, which are expected to allow expression throughout the germline. TIR1 homozygous worms were then crossed to the strain containing the *rec-8::IAA17*;*rec-8*

transgene to finally produce worms homozygous for both transgenes. This strain offers an easy method by which to test the potential of the degron system in worms, as protein degradation of REC-8 should cause an obvious phenotype in the diakinesis oocytes of treated worms. An initial test to degrade REC-8::IAA17 by adding NAA to the plate media was unsuccessful. The reason for this failure is not clear, it may be that in order to quickly deliver NAA to the germline, it must be injected, or it could be that the TIR1 protein is not efficiently expressed in the germline or imported into the nucleus, or that higher quality auxin must be used. In any case, establishing the auxin degron system in worms will require further work, and this is an important aim for future studies.

4.5 Developing a SNAP-tag system in worms

A technique that has been used in organisms such as yeast and Zebrafish (Campos et al., 2011; Regoes and Hehl, 2005), and in cell culture (Maurel et al., 2008), but not in *C. elegans*, is the SNAP-tag system of covalently labelling proteins. The SNAP-tag is a 20 kDa mutant form of the DNA repair protein O^6-alkylguanine-DNA alkyltransferase. It reacts specifically and rapidly with benzylguanine derivatives, leading to irreversible covalent labelling of the SNAP-tag with a synthetic probe (Fig. 21B) (Regoes and Hehl, 2005). The SNAP-tag technology has been used in fluorescent pulse-chase and quench-chase-pulse experiments to determine the rate of protein turnover (Bodor et al., 2012). In order to carry out similar experiments in worms, and use the system to assess cohesin turnover in the germline, it will be necessary to create a transgenic strain carrying a functional SNAP-tagged cohesin subunit. Then a SNAP ligand would have to be introduced to the germline where it would covalently bind to all the cohesin::SNAP protein. Then, after a period of time a second, differently coloured, SNAP ligand would be introduced to the germline of the same worm. This would label all newly synthesised cohesin::SNAP. If this second ligand were seen on chromatin that had undergone meiotic S-phase before the second labelling step it would demonstrate that cohesin reloading occurs in meiotic prophase.

4.5.1 Generating a REC-8::SNAP transgenic strain

The EG4322 *unc-119* strain, containing the ttTi5605 chromosome II Mos locus was injected with pCFJ151 containing the wild-type *rec-8* gene with a SNAP sequence in place of its stop codon and containing the endogenous 3' and 5' UTRs from *rec-8*. These worms were crossed to the *rec-8(ok978)* mutant strain to obtain a *rec-8*; *rec-8::SNAP* strain. From this we could see that the REC-8::SNAP protein fully complemented the *rec-8* mutation and therefore would be suitable for further experiments.

4.5.2 Methods of introducing SNAP ligands

There are a number of possible methods by which the SNAP ligands might be introduced into the *C. elegans* germline. Attempts to administer the ligands by adding them to the plate media or to grow worms in liquid culture containing the ligands were unsuccessful. The only remaining option was to inject the ligands directly into germlines of the transgenic worms. SNAP-Cell® TMR-Star (NEB S9105S), a red fluorescent ligand was injected at a concentration of 12μM in DMSO. 3 hours post injection red fluorescence could be seen in burst live worms in which the germline had been extruded, using Leica DMRB microscope with a 62X lens. This signal could be seen to form tracks with pachytene nuclei. This demonstrates that the SNAP-tag system can be used in worms (Fig. 21C). However, further optimization will be required before it can be used to answer questions about cohesin turnover in meiotic prophase, as injecting the same germline two times, so that two pools of cohesion can be labelled, is a difficult procedure.

4.6 Inducing non-cleavable REC-8 expression using a heat shock promoter

In many organisms transcription of a gene can be controlled using inducible promoters, with expression under the control of either heat shock (Allard et al., 2013) or chemically inducible promoters (Beard et al., 2013). In *C. elegans* chemically inducible promoters have not yet been developed, however, the *hsp*-

16.1 promoter has been shown to induce expression in response to a heat shock (Lee, 2013). By creating a transgenic strain in which *rec-8::GFP* expression is controlled by the *hsp-16.1* promoter, I hoped to gain temporal control of cohesin loading and thereby assess whether cohesin reloading is taking place. Ideally, worms would be treated with the 34°C heat shock for 2 hours to induce REC-8::GFP expression. These worms would be allowed to recover and their germlines stained with α-GFP antibodies 12-24 hours after the heat shock. As it takes 35-40 hours for nuclei to progress from the transition zone to late pachytene (Jaramillo-Lambert et al., 2007), any chromatin associated GFP signal in late pachytene would have to originate from *de novo* cohesin loading after S-phase.

In addition to this, I sought to create a non-cleavable form of REC-8::GFP. By coupling the *hsp-16.1* promoter with a non-cleavable form of REC-8::GFP it should be possible to determine whether reloaded cohesin becomes cohesive. The rational is that one would begin to see segregation defects in heat shocked worms in under 60 hours (the time it takes from S-phase to ovulation (Jaramillo-Lambert et al., 2007)) as the loaded and cohesive uncleavable REC-8 would interfere with the metaphase to anaphase transitions in MI and MII. If the reloaded cohesin does not become cohesive it should not have any effect on chromosome segregation.

4.6.1 Generating *Phsp-16.1::rec-8:GFP*

Phsp-16.1::rec-8:GFP was inserted into the Chromosome II Mos site using the method outlined above. To test that in this strain REC-8::GFP expression could be induced, these worms were heat-shocked 34°C for 2 hours and then dissected and stained with α-GFP antibodies 3 hours later, as this is the time at which expression has been shown to peak (Zeiser et al., 2011). Imaging these germlines with the DeltaVision revealed that the level of REC-8::GFP expression is exceptionally low, with the highest levels of signal coming from the distal tip cell and a tiny amount of signal coming from nuclei in the mitotic tip (Fig. 23A). Carrying out antibody staining on worms 12 hours post heat shock revealed

that there was no detectable signal anywhere in the germline. In addition to this, the heat shock itself almost kills the worms, making this a inappropriate method to induce REC-8::GFP expression. Expression of a transgene can be greatly improved by codon optimization (Slimko and Lester, 2003) and perhaps this could be utilised to improve the system.

4.6.2 Creating a non-cleavable form of REC-8

In *C. elegans*, for meiotic cohesin to disassociate from chromosomes at the metaphase to anaphase transitions, REC-8 must be cleaved by separase (Siomos et al., 2001). It has been suggested that phosphorylation of REC-8 by AIR-2 promotes this cleavage in *C. elegans*, however this has never been formally demonstrated (Rogers et al., 2002). In yeast a non-cleavable form of REC-8, created by mutating two of its separase cutting sites, blocks chiasma resolution (Buonomo et al., 2000). The phosphorylated sites of REC-8 have been identified in yeast by mass spectrometry, and mutation of these sites to make them non-phosphorylatable renders REC-8 resistant to separase and consequently blocks chiasma resolution (Katis et al., 2010). I therefore, undertook to identify the predicted separase cleavage sites and putative AIR-2 phosphorylation sites of *C. elegans* REC-8 in order to be able to create a non-cleavable form of REC-8.

4.6.3.1 *In silico* analysis

The consensus recognition sequence of separase is (D/E)XX(R) (Mito et al., 2003; Sullivan et al., 2004). AIR-2/Aurora-B have been shown to recognise (R/K)X(S/T) consensus sequences (Resnick et al., 2006; Wang et al., 2011). By scrutinising the amino acid sequence of REC-8 we can see that it has 14 possible separase cleavage sites and 10 putative AIR-2 phosphorylation sites (Fig. 22). Three of these putative AIR-2 phosphorylation sites overlap or are adjacent to a separase site, making them attractive residues for mutation to create a non-cleavable form of REC-8.

4.6.3.2 Generating REC-8 transgenic strains with mutated separase sites

I created a transgenic line in which *rec-8::GFP* amino acid residues 63, 400 and 631, which correspond to the three separase sites that are flanked by AIR-2 phosphorylation sites (Fig. 22), were mutated from R to E, which should prevent cleavage by separase (Kitajima et al., 2003). I will refer to this transgene as *rec-8$^{SEP(3)}$::GFP* from here on. Although the expression of *rec-8$^{SEP(3)}$::GFP* was expected to block chiasma resolution, unfortunately, the introduction of this transgene onto the *rec-8* background revealed that this transgene complements the mutant, indicating that it has little or no effect on chromosome segregation. To further test this, the viability of *rec-8;rec-8$^{SEP(3)}$::GFP* was compared to that of *rec-8; rec-8::GFP* controls. The embryonic lethality of *rec-8; rec-8 $^{SEP(3)}$::GFP* is 1.05% compared with 0.34% in controls and the incidence of males is 0.77% compared with 0.27%, neither of these differences are significant (P=0.17 and P=0.11, respectively), further demonstrating that abolishing these separase sites has a negligible impact on chromosome separation at the metaphase to anaphase transition. Unsurprisingly, DAPI staining on whole worms revealed no defects in prophase, and visualising the GFP in live worms showed the protein to have wild type localisation.

It may be that the mutated residues in *rec-8; rec-8$^{SEP(3)}$::GFP* are not the primary targets for separase, or it may be that abolishing some sites promotes usage of others. To test this, I attempted to create a transgenic strain with amino acid residues 364, 400, 570, 631 and 666 mutated from R to E. After numerous injections I was unable to derive any viable transgenic lines with a complete insertion from these injections. This may have been bad luck, however, it is also possible that this is due to the fact that mutating these sites has had the desired effect and prevented cohesin disassociation. One would expect mutations that severely hinder cohesin cleavage to have a dominant effect, as a small amount of this protein would be sufficient to prevent chromosome segregation.

4.6.3.3 Generating a REC-8: GFP transgenic strain with mutated AIR-2 sites

In order to determine if mutating putative AIR-2 phosphorylation sites that occur next to separase sites would impact on chromosome segregation, I

generated a transgenic line in which *rec-8::GFP* amino acid residues 65, 404 and 634 were mutated from S/T to A, which could prevent separase from cutting at the sites described in the first part of section 4.6.3.2. I will refer to this transgene as *rec-8(AIR-2^{A})::GFP* from here on. The change of S/T to A should render these three putative AIR-2 sites unphosphorylatable and thereby hinder separase cleavage of this mutant protein, blocking chiasmata resolution. As before, I introduced this transgene into the *rec-8* background to determine whether the transgene complements the mutation. Initial screening of these *rec-8;rec-8(AIR-2^{A})::GFP* worms on the plate suggested that the transgene does complement and this was confirmed by comparing the viability of this strain with that of *rec-8;rec-8::GFP* (Fig. 23B). As with *rec-8;rec-8$^{SEP(3)}$::GFP* it may be that these are not the primary targets for AIR-2 phosphorylation or it may be that other site become targets, when these site are made unavailable. Therefore, mutating further sites might be necessary to prevent cleavage of REC-8.

To test whether these three sites are targets of AIR-2 phosphorylation, I created a transgenic line in which the amino acid residues were mutated from S/T to E rather that A. I will refer to this as *rec-8(AIR-2^{E})::GFP* from here on. If these sites are phosphorylated by AIR-2, this mutated REC-8::GFP protein should be prematurely lost from chromosomes, since the negative charge of E mimics the effect of phosphorylation on S or T. Unlike the previous strains in which mutating the putative sites might cause other to be used, if these sites are phosphorylated to promote cleavage, one would expect to see a phenotype. I crossed this transgene onto the *rec-8* mutant background to create *rec-8; rec-8(AIR-2^{E})::GFP* and compared its viability to that of *rec-8::GFP* to assess whether there might be any meiotic defects. This revealed a significant increase in embryonic lethality with 31.86% compared with 0.34% (P=0.0001), and a higher incidence of males with 2.26% in *rec-8;rec-8(AIR-2^{E})::GFP* compared with just 0.27% in controls (P=0.0025) (Fig. 23B). I also crossed this stain to the *coh-3* mutant background to create *rec-8;coh-3;rec-8(AIR-2^{E})::GFP*, to determine whether this has a further detrimental effect on viability. Indeed this proved to be the case, with embryonic lethality increasing to 44.58% (P=1.75x10^{-7}

compared with *rec-8;rec-8::GFP* controls) and the percentage of males increasing to 2.76% (P=0.0043 compared with controls).

The expectation is that this phosphomimetic REC-8::GFP causes premature loss of cohesin from chromosomes. To confirm this I had to rule out the possibility that these mutations affected REC-8 protein function in meiotic prophase, for example by interfering with crossover formation. In order to do this, I stained whole mount germlines with α-GFP antibodies and DAPI to check chromatin morphology and REC-8 localisation. This revealed that meiotic prophase in these worms appeared normal, with germlines having no defects in meiotic progression, chromatin structure and 6 DAPI masses in diakinesis oocytes. In addition to this, the localisation of REC-8::GFP appears identical to that of wild-type and *rec-8; rec-8::GFP* controls (Fig. 18 and 23C-E). This suggests that the defects responsible for the decreased viability in these worms does not originate in prophase and is therefore likely to be due to problems at a latter stage of meiosis such as the metaphase to anaphase transition in MI. I have built a strain in which *rec-8;rec-8(AIR-2^{E})::GFP* carries a H2B::mCherry marker and will use this to carry out live imaging to further investigate the cause of these defects. Finally, the data from the *rec-8; coh-3; rec-8(AIR-2^{E})::GFP* suggests that COH-3/4 play a role in orchestrating proper chromosome segregation during the meiotic divisions.

4.7 Summary of results

In the chapter I have described the initial steps in engineering novel systems by which to address whether cohesin reloading is occurring in meiotic prophase. I have created three transgenic lines expressing functional copies of fluorescently tagged cohesin subunits. By placing *rec-8::GFP* under the control of the *fbf-2* 3'UTR, I hoped to restrict expression to the early stages of meiotic prophase. However, antibody staining has revealed that REC-8::GFP remains localised to chromatin throughout the germline and no meiotic defects are observed when this transgene is expressed in the place of endogenous *REC-8*. I placed *rec-8::GFP* under the control of the *mex-5* 3'UTR allow expression in mid/late pachytene,

however, the protein was expressed at a later stage than expected forming a nucleoplasmic localisation in very late pachytene/diplotene nuclei onwards, with no *REC-8::GFP* present on chromatin. Furthermore, when this transgene was introduced in the background of the *rec-8* mutation it did not improve the mutant phenotype. I have demonstrated that injected mRNA can induce expression in the *C. elegans* germline, however, I encountered problems in synthesising a full length transcript of *scc-3::GFP.* In addition to this, I have generated a strain with which to test the possibility of using the auxin-mediated degron system to degrade REC-8, and shown that the SNAP-tag technology can be used to covalently label proteins in the *C. elegans* germline. While I have shown that the heat shock promoter, *hsp-16.1* does not drive sufficient expression of *rec-8::GFP*, my attempts to map the key REC-8 sites for phosphorylation by AIR-2 have met with more success. I have identified three residues of REC-8 that when mutated to a phosphomimetic amino acid result in high embryonic lethality that likely originates from errors in chromosome segregation during the meiotic divisions. I have also identified 5 separase sites that may be require for REC-8 cleavage. A great deal of further work will be required to demonstrate cohesin reloading, however some of these techniques show great promise for the future.

Figure 18. GFP localisation in *rec-8;rec-8::GFP* germlines

A Whole mount of N2 germline stained with DAPI and α-REC-8 showing REC-8 localisation in meiotic nuclei forming tracks decorating the axial element in pachytene.

B Magnification showing mid pachytene nuclei

C Late diplotene nuclei for N2 showing nucleoplasmic REC-8 localisation.

D Diakinesis oocyte from N2 showing 6 bivalents with REC-8 displaying a cruciform localisation between homologues and sister chromatids.

E Whole mount of *rec-8;rec-8::GFP* germline stained with DAPI and α-GFP showing REC-8::GFP localisation in meiotic nuclei forming tracks decorating the axial element in pachytene identical to REC-8 localisation in wild type germlines.

F Magnification showing mid pachytene nuclei

G Late diplotene nuclei for *rec-8;rec-8::GFP* showing nucleoplasmic REC-8::GFP localisation.

H Diakinesis oocyte from *rec-8;rec-8::GFP* showing REC-8::GFP localisation identical REC-8 in wild type controls.

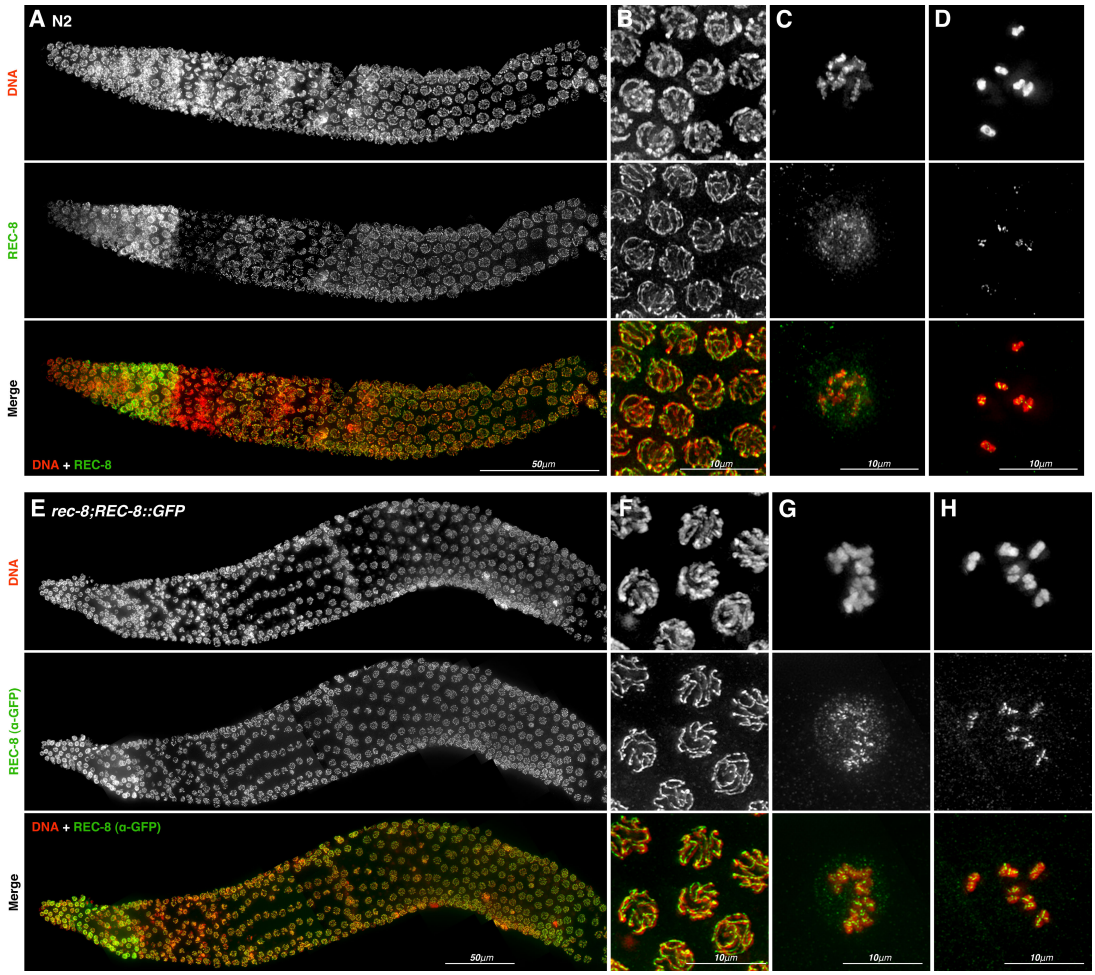
A N2
B
C
D
DNA
REC-8
Merge
DNA + REC-8
50μm
10μm
10μm
10μm
E rec-8;REC-8::GFP
F
G
H
DNA
REC-8 (α-GFP)
Merge
DNA + REC-8 (α-GFP)
50μm
10μm
10μm
10μm

Figure 19. Characterisation of *rec-8;rec-8::GFP fbf-2* 3'UTR

A Whole mount of *rec-8;rec-8::GFP fbf-2* 3' UTR germline stained with DAPI and α-GFP showing REC-8::GFP localisation throughout the germline identical to that seen in *rec-8;rec-8::GFP* controls, rather than restricted to early prophase.

B Magnification showing mid pachytene nuclei

C Late diplotene nuclei from *rec-8;rec-8::GFP fbf-2* 3' UTR showing no nucleoplasmic REC-8::GFP localisation unlike *rec-8;rec-8::GFP* controls.

D Diakinesis oocyte from *rec-8;rec-8::GFP fbf-2* 3' UTR

E Viability of *rec-8;rec-8::GFP fbf-2* 3' UTR compared with *rec-8;rec-8::GFP* and N2 controls showing no decrease in viability.

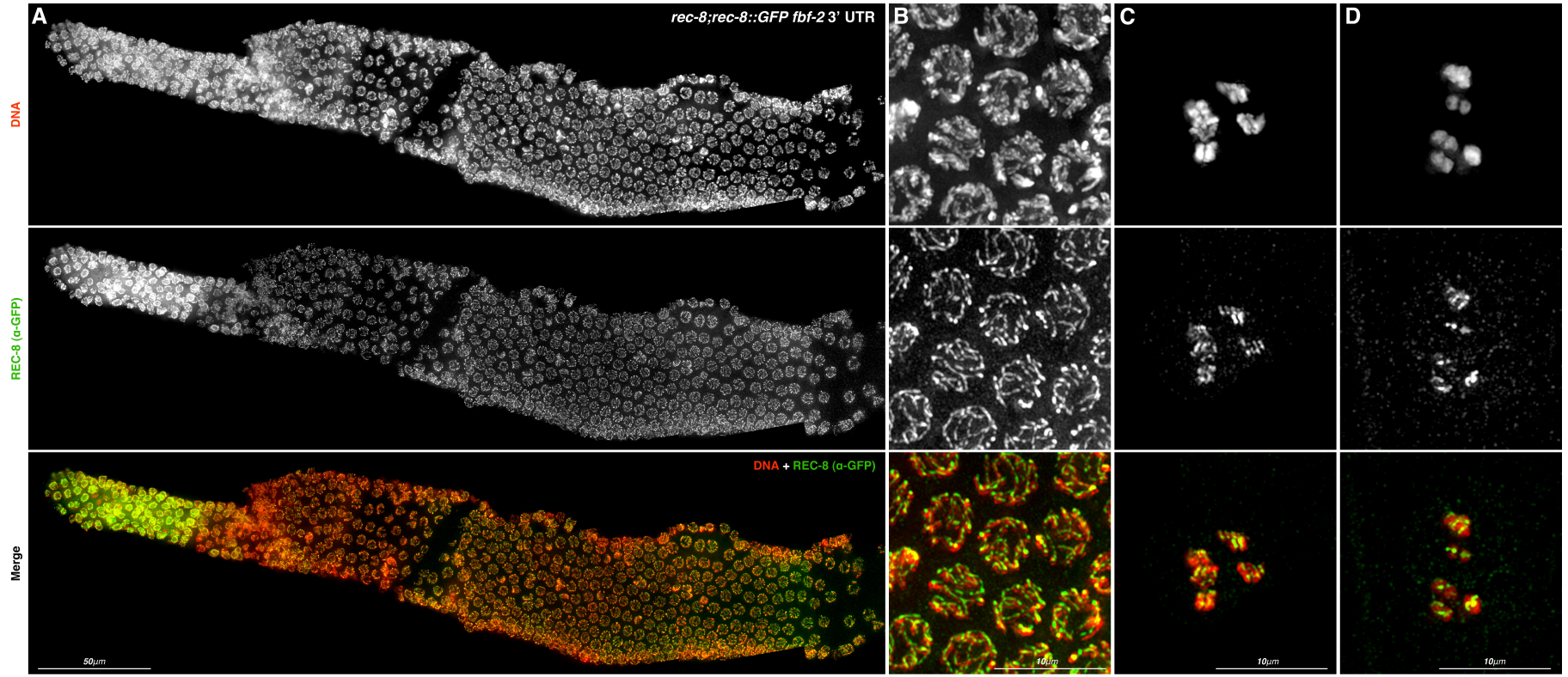

E

	N2	*rec-8;rec-8::GFP*	*rec-8;rec-8::GFP* fbf-2 3'UTR
percentage viability	99.86	99.82	99.50
percentage males	0.00	0.18	0.22

Figure 20. mRNA driven *H2B::mCherry* expression

A H2B::mCherry expression in gut nuclei 1 hour after mRNA injection

B H2B::mCherry expression in diakinesis oocyte 1 hour after mRNA injection

C H2B::mCherry expression in pachytene nuclei 6 hour after mRNA injection

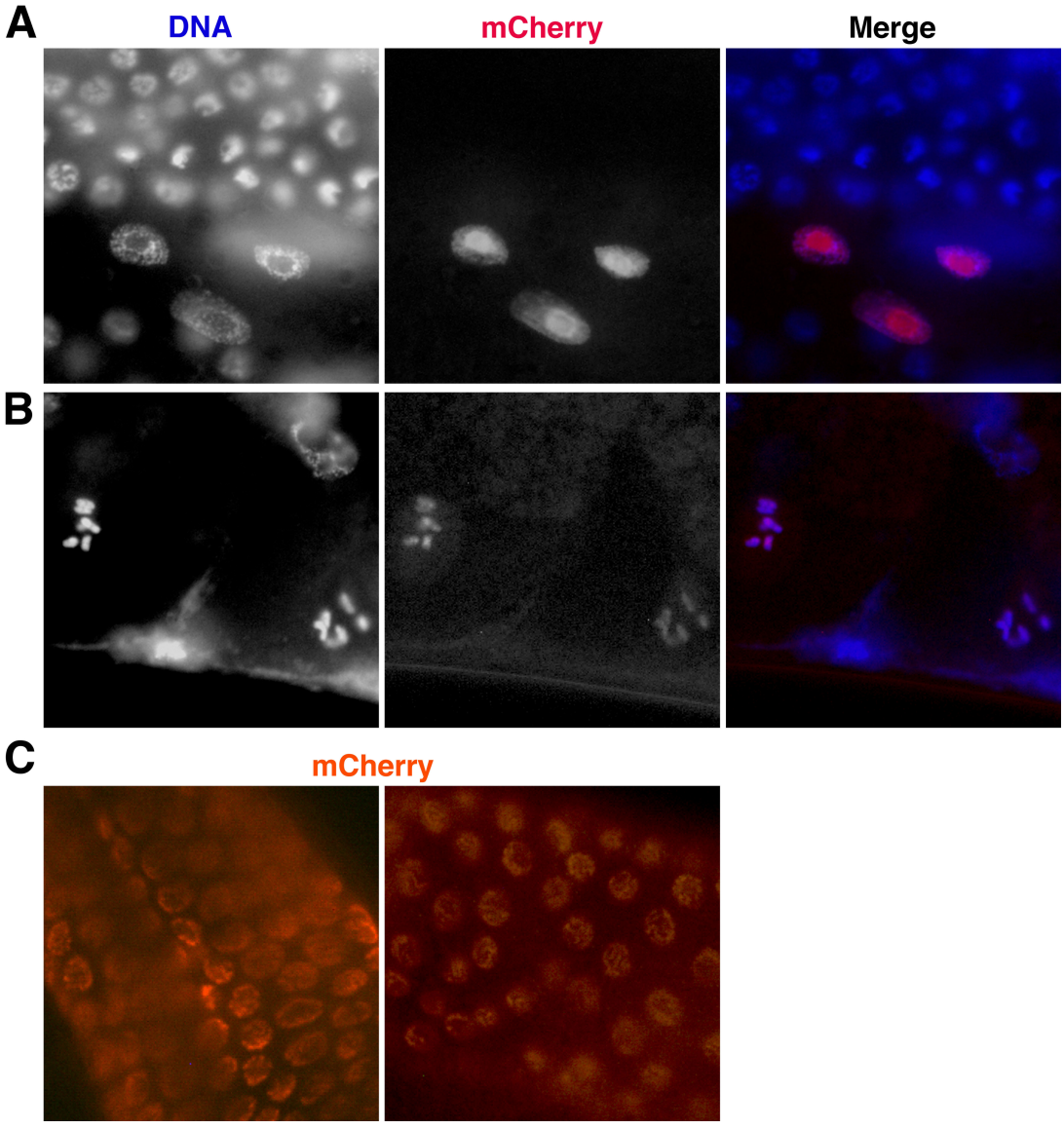
A
DNA
mCherry
Merge
B
C
mCherry

Figure 21. Auxin-mediated degron and SNAP-tag

A Schematic of auxin-mediated degron system

B Schematic of SNAP-tag system for covalently labelling proteins

C Germline extruded from a live *rec-8;rec-8::SNAP* worm 3 hours after injection with the TMR-Star ligand imaged with Leica DMRB microscope using 62X lens and imaged with a Leica DFC300 FX camera showing red fluorescence in all nuclei in the germline.

D Enlargement of pachytene nuclei. Arrows indicate red fluorescence forming tracks in a manner similar to REC-8 localisation in wild type worms.

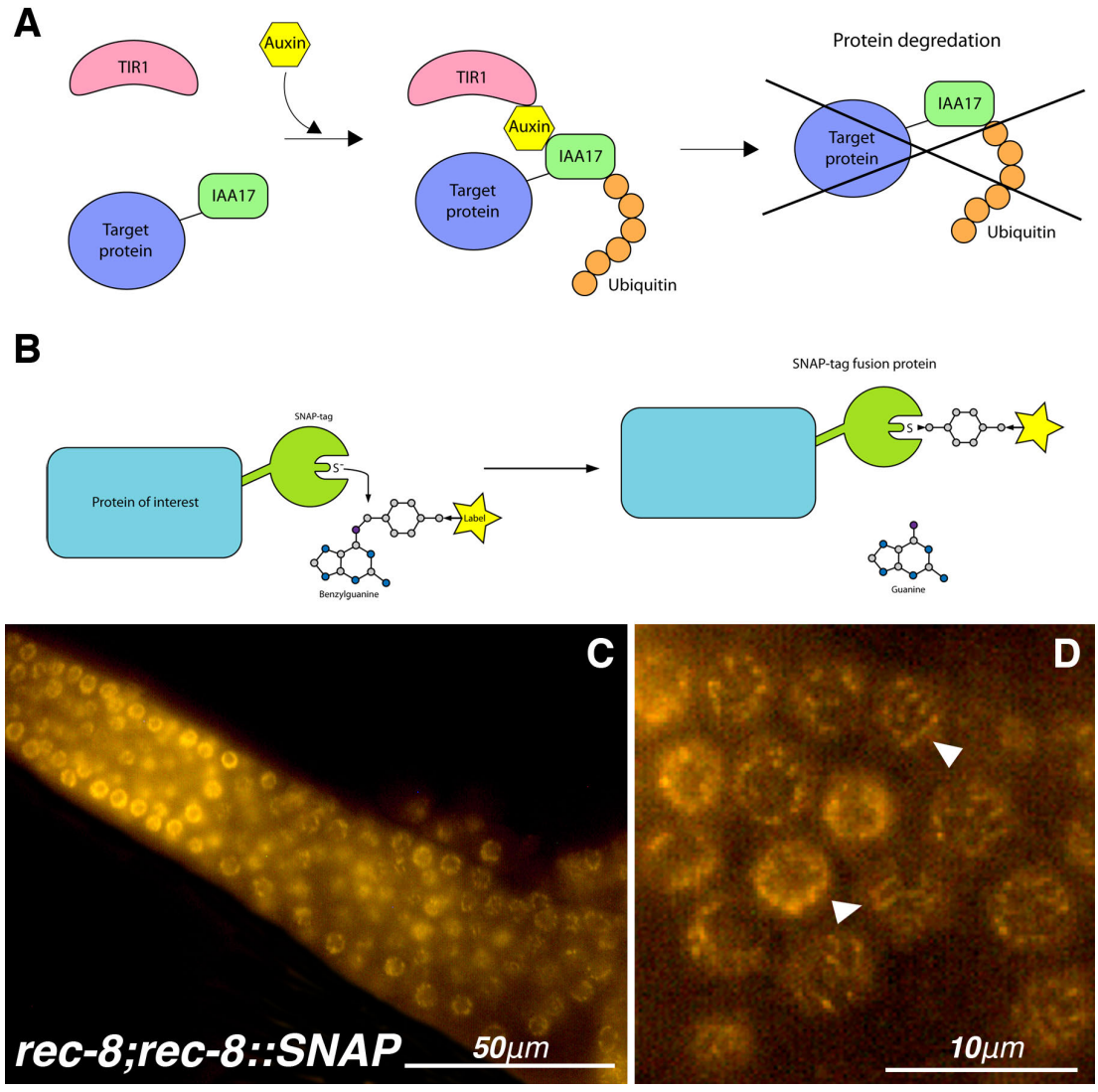
A
TIR1
Auxin
IAA17
Target protein
Ubiquitin
Protein degredation
B
SNAP-tag
Protein of interest
Label
Benzylguanine
SNAP-tag fusion protein
Guanine
C
rec-8;rec-8::SNAP
50µm
D
10µm

Figure 22. Mapping of separase and putative AIR-2 phosphorylation sites in REC-8

REC-8 amino-acid sequence with putative separase and AIR-2/Aurora B phosphorylation sites indicated, as well as mutated residues harboured in *rec-8;rec-8$^{SEP(3)}$::GFP, rec-8;rec-8(AIR-2^{A})::GFP* and *rec-8;rec-8(AIR-2^{E}) ::GFP* as well as in the *rec-8$^{SEP(5)}$::GFP* construct with which I was unable to generate a transgenic strain


10 20 30 40 50
MVVSAEVIRK DAVFHVAWIL GTGDSKKLSR REILDQNLPE LCHSIIEMVP
60 70 80 90 100
ERHRGSATKT GLYLLSLLTY GTVLIHQVQV DFLKRDVEKL KELMKKKSFI
110 120 130 140 150
LLMAERFDRN QELQRKEDKF ARLRSKPIMC VEELDRVDLA HLQAIGDELG
160 170 180 190 200
INGNPGDFIM MDALPNMNQW IDNNSELNAI YGCVEPYLRE KEITMHSTFV
210 220 230 240 250
EGNGSNEHNK ERRNDAVIAD FSQLLFPEIP EITLGEKFPI DVDSRKRSAI
260 270 280 290 300
LQEEQEEALQ LPKEASEIVQ EEPTKFVSIA LLPSETVEQP APQEPIQEPI
310 320 330 340 350
QPIIEEPAPQ LELPQPELPP QLDAIDLVTI PASQQDMVVE YLQLINDLPD
360 370 380 390 400
DENSRLPPLP KDLELFEDVI LPPPAKKSKV EEEEDALERA RRRPSSRPVT
410 420 430 440 450
PINQTDLTDL HSTVRPEDPS FAIDSQIHDV LPQRKKSKRN LPIIHSDDLE
460 470 480 490 500
IDEAVQKVLQ ADYSSLVRKK EDVIAKIPPK TDAVAVLMNL PEPVFSIGYR
510 520 530 540 550
LPPEVRDMFK ACYNQAVGSP VSDDEEDEDE EEEEEYKYAK VCLLSPNRIV
560 570 580 590 600
EDTLLLEEQP RQPEEFPSTD NINPPRQLQE NPVFENLEYE APPHPIRTAR
610 620 630 640 650
TPTPIKDLKY SVISLFPTPE KRRETSIIAE LNLDPIPVEE IDPLLTMRTE
660 670 680 690 700
EELENVRRRQ KSSLGVQFMR TDDLEEDTRR NRLFEDEERT RDAREDELFF
710 720 730 740 750
YSSGSLLPNN RLNIHKELLN EAEARYPEWV NFNEFTADHD RKKAATAFEG
760 770 780
LLLSLKNMKV EAKQEDPYFP ILVRHISHEE M
Predicted separase sites
((E)XX(R))
((D)XX(R))
Predicted AIR-2/AuroraB sites
AIR-2 = ((R)X(T/S))
AuroraB = ((R/K)X(T/S))-I/L/V
AuroraB = ((K)X(S))
Mutated sites
AIR-2 non-phosphorylatable (T/S)→(A)
AIR-2 phosphomimetic (T/S)→(E)
Non-cleavable separase 1 (R)→(E)
Non-cleavable separase 2 (R)→(E)

Figure 23. Heat-shock promoter and characterisation of *rec-8;rec-8::GFP(AIR-2^{E})*

A Tip of whole mount of *Phsp-16.1::rec-8::GFP* stained with DAPI and α-GFP showing very low levels of REC-8::GFP localisation in nuclei of the mitotic tip and slightly higher levels in the distal tip cell

B Viability counts of *rec-8;rec-8$^{SEP(3)}$::GFP, rec-8;rec-8(AIR-2^{A})::GFP, rec-8;rec-8(AIR-2^{E})::GFP, rec-8;coh-3;rec-8(AIR-2^{E})::GFP,* and *rec-8;rec-8::GFP* controls

C Whole mount of *rec-8;rec-8(AIR-2^{E})::GFP* germline stained with DAPI and α-GFP showing REC-8(AIR-2^{E})::GFP localisation throughout the nuclei of the germline identical to that seen in *rec-8;rec-8::GFP* controls indicating no impairment of cohesin loading

D Magnification showing mid pachytene nuclei

E Diakinesis oocyte from *rec-8;rec-8(AIR-2^{E})::GFP* with 6 bivalents, demonstrating that chiasmata formation is not impaired due to the mutation of AIR-2 sites harboured in this strain.

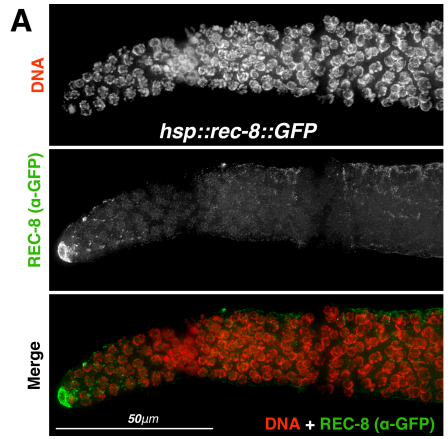

B

		Brood size	Unhatched eggs	Adults	Males
rec-8:GFP;rec-8	Average	302.20	0.80	300.60	0.80
	Percentage		0.26	99.47	0.26
rec-8:GFP (AIR-2^{A}); rec-8	Average	295.80	0.20	295.40	0.20
	Percentage		0.07	99.86	0.07
rec-8:GFP$^{(\Delta EP3)}$; rec-8	Average	278.25	3.00	272.75	2.50
	Percentage		1.08	98.02	0.90
rec-8:GFP (AIR-2^{E}); rec-8	Average	221.00	70.40	145.60	5.00
	Percentage		31.86	65.88	2.26
rec-8:GFP (AIR-2^{E}); rec-8;coh-3	Average	195.60	87.20	103.00	5.40
	Percentage		44.58	52.66	2.76

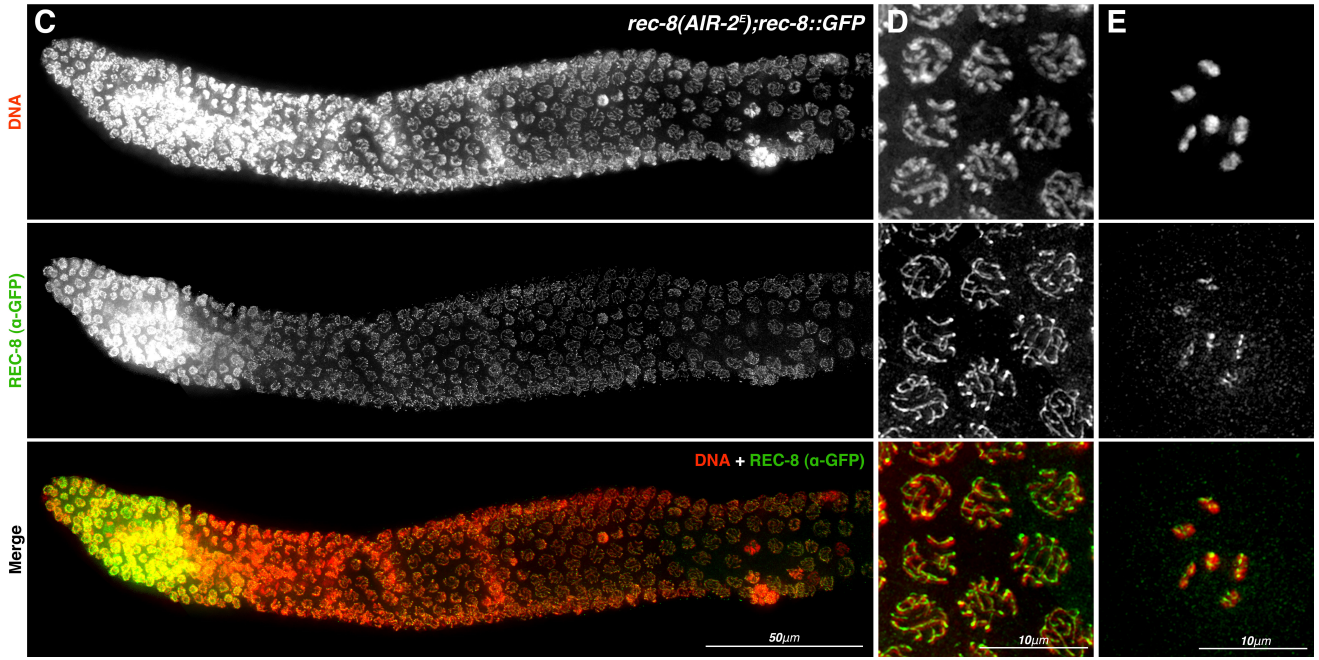

CHAPTER 5: RESULTS
THE DIFFERENT ROLES OF THE MEIOTIC KLEISINS

5.1 Objectives

The previous results chapters have mainly focused on the cohesin complexes comprised of SMC-1, SMC-3, SCC-3 and the meiotic α-kleisin REC-8. However, as mentioned in the introduction, other meiotic α-kleisins are known to be present in worms: COH-3, COH-4, COH-1 and SCC-1. COH-3 or COH-4 have been shown to play a key role in meiosis. They are functionally redundant but when both are absent SC assembly is severely impaired and, perhaps because of this, *coh-3/4* double mutants fail to form chiasmata (de Carvalho et al., 2008; Severson et al., 2009). COH-1 has been implicated in both meiosis and mitosis, though little is known of its function (Mito et al., 2003; Pasierbek et al., 2001). In addition, the mitotic kleisin SCC-1 is also expressed in the germline and the *scc-1* mutant shows meiotic defects, indicating that it too plays a role in meiosis (Mito et al., 2003). Unfortunately, in the *scc-2* RNAi experiments we did not have antibodies with which to monitor the localization of these other kleisins and therefore were unable to investigate the effect of *scc-2* knockdown on their loading. Following on from the *scc-2* RNAi experiments my attempts to investigate cohesin reloading focused on creating transgenic strains with tagged versions of REC-8. To address whether the different kleisins play different roles in meiotic prophase, I have utilized the *rec-8*; *rec-8::GFP* and *coh-3*; *coh-3::mCherry* transgenic strains that have been generated, to examine the localisation of REC-8 and COH-3. In addition to this, I have undertaken a cytological examination of the kleisin null mutants singularly and in combination with one another, as well as in combination with other mutants that are defective in the CO formation pathway. With these two approaches I hoped to be able to dissect apart the roles of the different kleisins.

5.2 Kleisin localization

In order to determine the localization of REC-8 and COH-3 in wild-type worms , I generated a strain containing both REC-8::GFP and COH-3::mCherry in the background of both the *rec-8* and *coh-3* mutations. Germlines from these worms were co-stained with α-GFP and α-RFP antibodies.

5.2.1 REC-8 localisation

Analysis of REC-8 localisation in dissected germlines stained with α-GFP antibodies reveals that REC-8 is highly expressed in the mitotic tip of the germline, however, it is unclear due to the less ordered chromatin structure in this region as to whether REC-8 is interacting with DNA in these nuclei. Upon entry into meiosis, REC-8 can be seen decorating the axial element of meiotic chromosomes and this pattern persists throughout prophase (Fig. 24A and B). In diakinesis oocytes REC-8 can clearly be seen on both the long and short arms (inter-chromatid and inter-homologue) of bivalents and this pattern is present until the final oocytes, closest to the spermatheca, known as the -1 oocyte (Fig. 24C and D). In addition to this, from very late pachytene to diakinesis we can also observe a diffuse nuclear staining, suggesting perhaps that REC-8 is being re-expressed in these late stages, or potentially being released from chromatin into a soluble nucleoplasmic pool (Fig. 17C).

5.2.2 COH-3 localization

Analysis of COH-3 localisation in dissected germlines stained with α-RFP antibodies reveals that COH-3, like REC-8, is expressed in the mitotic tip. However, the level of expression is considerably lower than that of REC-8 and appears to start slightly more distally from the tip of the germline (Fig. 24A). As with REC-8, at the onset of meiosis, COH-3 can be seen decorating the axial element of meiotic chromosomes throughout prophase. In nuclei which have been co-stained with α-RFP and α-GFP we can see that both REC-8 and COH-3 almost perfectly colocalize with one another from the transition zone through to diplotene (Fig. 24A and B). In early diakinesis oocytes we can see that COH-3 and REC-8 colocalize with both being present on the long and short arms of

bivalents (Fig. 24C). Interestingly, in bivalents in which the chiasmata is oriented so that we can clearly see its cruciform shape, it is noticeable that REC-8 is absent from the region around the CO site, unlike COH-3, which makes a "full" cross shape. In the -1 diakinesis oocyte we can also see a difference in the localisation of COH-3 and REC-8. Whereas REC-8 is retained on both the long and short arms of the bivalent, COH-3 is only present on what is likely to be the short arm (Fig. 24C and D). Finally, we do not see the diffuse COH-3 staining pattern in the nucleoplasm of late pachytene to diakinesis nuclei that we see with REC-8 (Fig. 24C), suggesting that COH-3 is not re-expressed at these stages.

5.3 Meiotic kleisin mutants

In order to help to determine the different roles of the three meiotic kleisins, I undertook a basic cytological analysis of their mutants, checking the basic chromatin phenotype, SC loading, cohesin loading and the formation of DSBs and their repair.

5.3.1 *rec-8* mutant

The *ok978* allele of *rec-8* that has been used in these experiments was produced by the *C. elegans* Knockout Consortium and contains a 1577bp deletion, which removes almost the entire portion of exon 3. It has been previously shown that REC-8 plays a key role providing SCC in meiosis and that in addition to this it is required for normal pairing and for the timely repair of DSBs (Loidl et al., 1994).

5.3.1.1 Chromatin phenotype

DAPI staining of dissected germlines reveals that the *rec-8* mutant has an extended region of the germline with nuclei exhibiting the characteristic conformation of transition zone, which is normally indicative of a defect in SC assembly. The nuclei in pachytene have highly ordered tracts, similar to those seen in wild type germlines (Fig. 26A and B). The diakinesis phenotype is very variable. Oocytes typically have univalents with a characteristic bi-lobed shape, but in addition to this, one can also see separated sister chromatids, as well as

fragments (Fig. 26C). These observations suggest that although sister chromatids are not fully separated, *rec-8* mutants have severe cohesion defects.

5.3.1.2 SC loading

In wild-type worms loading of SC components starts during transition zone (Fig. 25A). The loading of HIM-3 and HTP-3 to the axial elements are required to promote the formation of a mature SC (Severson et al., 2009; Zetka et al., 1999), which occurs when CE components "zip" together the axial elements (Colaiacovo et al., 2003; MacQueen et al., 2002). In order to determine whether SC loading occurs normally in *rec-8* mutants, germlines were dissected and stained with α-SYP-1 antibodies, a component of the CE. This revealed that SC assembly was delayed with respect to wild type (Fig. 25), with tracts starting to appear upon entry into meiosis but synapsis only reaching completion by mid pachytene. At this stage SYP-1 forms continuous tracts colocalising to tracts of chromatin (Fig. 26A and B). Delayed SC loading is often associated with a defect in pairing (Couteau and Zetka, 2005), and it is possible that this is the cause of the delay in SC assembly in this mutant background, as REC-8 has been shown to be required for proper pairing (Loidl et al., 1994). Alternatively there may be some requirement for loaded REC-8 in normal SC formation.

5.3.1.3 DSB formation and repair

To analyse the effect of the absence of REC-8 on meiotic recombination and DSB repair, whole mounted germlines were stained with α-RAD-51 antibodies. This revealed that the number of RAD-51 foci is far higher than that seen in wild-type germlines (Fig. 26A and B). In addition to this, these foci persist into diplotene, unlike in wild type germlines, where all DSBs have been repaired by the end of pachytene. This indicates that REC-8 is required for the timely repair of meiotic DSBs.

5.3.1.4 Cohesin loading

In order to assess whether the absence of REC-8 impairs the loading of cohesin complexes containing other α-kleisins, α-RFP antibodies were used to stain whole mount germlines of *rec-8; coh-3; coh-3::mCherry* worms. This showed that the loading of COH-3 appears unaffected in *rec-8* mutants, with COH-3 decorating the axial element of meiotic chromosomes throughout prophase, in a manner almost identical to that seen in *rec-8; coh-3*; *rec-8::GFP; coh-3::mCherry* germlines (Fig. 24A and B, 27A and B). In diakinesis one might expect to see cohesin staining in between the two lobes (each presumed to be a sister chromatid) of the bi-lobed univalents, in a manner indicating that it is this cohesin providing the cohesive force holding them together. While this can sometimes be observed, the pattern or staining is certainly not present in all univalents, with the majority of COH-3 staining appearing on the lobes themselves (Fig. 27C). It might be that COH-1 and/or SCC-1 are providing the cohesive force holding the lobes together. Another possibility is that the quantity of COH-3-containing cohesin complexes required to provide cohesion is below the levels that can be detected by immunofluorescence. Indeed it has been shown in yeast that cohesin can be depleted to 10% of wild-type levels without an impact on SCC (Heidinger-Pauli et al., 2010).

5.3.2 *coh-3;coh-4* mutant

The *gk112* allele of *coh-3* used in these experiments contains a 969bp deletion, which removes exons 2 to 6. The *tm1857* allele of *coh-4* used in these experiments contains a 8bp insertion and a 828bp deletion, which removes most of exon 2 and exons 3 and 4. Both strains were produced by the *C. elegans* Knockout Consortium. Both individual mutants appear to have a wild-type phenotype, however, the *coh-3;coh-4* double mutant has numerous meiotic defects, with impaired SC formation, DSB repair and univalents in diakinesis oocytes indicating a failure to form chiasmata (Severson et al., 2009).

5.3.2.1 Chromatin phenotype

Gross morphological defects in the germline were assessed by DAPI staining of whole-mount germlines. This revealed that *coh-3; coh-4* double mutants have no region of the germline with the characteristic crescent moon shaped conformation of transition zone nuclei. The chromatin structure throughout prophase is abnormal with extremely thin DNA tracks visible, rather than the highly organised, thick tracks of chromatin that are seen in the wild type and *rec-8* germlines (Fig. 25A and 28A and B). The diakinesis phenotype is also distinct from that of *rec-8*, with oocytes containing 12 regularly shaped univalents, without individualised sister chromatids or fragments (Fig. 28C), demonstrating that SCC is not severely compromised in *coh-3;coh-4* double mutants, but is required for CO formation.

5.3.2.2 SC loading

Monitoring SC formation by immunostaining of whole-mount germlines with α-SYP-1 antibodies revealed that SC assembly is greatly impaired with no tracts of SC staining visible at any stage of meiosis but rather a punctate pattern evident (Fig. 28A and B). This is distinct from the *rec-8* mutant in with SC loading is delayed but tracks are formed on chromatin (Fig. 25B and 26A and B) and from the *scc-2* mutant in which SC loading is entirely abolished (Fig. 15B), this is consistent with COH-3/4 playing a key role in SC assembly.

5.3.2.3 DSB formation and repair

Immunostaining of whole mount germlines with α-RAD-51 antibodies to monitor the formation and repair of DSBs shows that *coh-3;coh-4,* similarly to *rec-8*, accumulate large numbers of RAD-51 foci (Fig. 28A and B and 32). However, unlike *rec-8* the majority of these breaks do not persist past late pachytene, into diplotene (Fig. 26A and B). This suggests, as is the case with REC-8, COH3 and COH-4 are required for the timely repair of meiotic DSBs.

5.3.2.4 Cohesin loading

Cohesin loading in *coh-3; coh-4* was gauged by co-staining whole mount germlines with α-REC-8 and α-SMC-1 antibodies. Here too, the phenotype was different from that of *rec-8*. The staining pattern of REC-8 showed a punctate pattern throughout prophase I, likely indicating reduced REC-8 loading onto chromatin (Fig. 29A and B). In diakinesis a clear line of REC-8 staining can be seen across the middle of each univalent (Fig. 29C). However, staining with α-SMC-1 antibodies reveals a different pattern. SMC-1 expression can be seen in the mitotic tip, but is undetectable on chromatin throughout prophase I (Fig.29A and B). The characteristic nucleoplasmic staining in late pachytene to diakinesis nuclei seen in wild type meiosis is present, however, no SMC-1 staining can been seen on the univalents themselves (Fig. 29C). It may be that the nucleoplasmic SMC-1 signal is masking the chromatin-associated signal. Alternatively, SMC-1 may truly not be bound to the univalents in *coh-3;coh-4* double mutants begging the question, what kind of cohesin complex is providing cohesion between the sister chromatids in these diakinesis oocytes?

5.3.3 *rec-8;coh-3;coh-4* mutant

5.3.3.1 Chromatin phenotype

Similarly to the *coh-3;coh-4* double mutant, *rec-8;coh-3;coh-4* has no transition zone and all nuclei have disorganized thin tracks of chromatin (Fig. 30A and B). Diakinesis oocytes have approximately 24 DAPI-stained bodies indicating full separation of sister chromatids (Fig 30C).

5.3.3.2 SC loading

Immunostaining of *rec-8;coh-3;coh-4* with α-SYP-1 antibodies reveals a similar staining pattern to that in the *scc-2(fq1)* mutant, with SYP-1 undetectable in chromosomes and instead sequestered into extrachromosomal aggregates (Fig 30A and B, Fig. 15B). This is consistent with the observation that cohesin loading is required for SC assembly (Lightfoot et al., 2011), and suggests that COH-1 and SCC-1 cohesin complexes alone cannot support SC assembly.

5.3.3.3 DSB formation and repair

Immunostaining of whole mount germlines with α-RAD-51 antibodies shows that almost no RAD-51 foci are present throughout meiotic prophase, and that the few foci that appear in late pachytene are often uncharacteristically large or form a short track, suggesting that this damage is mitotic in origin (Fig. 30A and B). In all the other situations studied, in which cohesin is compromised, DSBs accumulate (*scc-2* (Lightfoot et al., 2011)*, rec-8* (Loidl et al., 1994)*, coh-3;coh-4* (Fig. 32)) and it is therefore surprising that the *rec-8;coh-3;coh-4* triple mutant have almost no DNA damage. This suggests that REC-8, COH-3 and COH-4 are cooperatively required for DSB formation, but that in the *scc-2* mutants in which no cohesin subunits are loaded this level of control is not exercised.

5.3.4. *rec-8;coh-3* and *rec-8;coh-4* mutants

5.3.4.1 Chromatin phenotype

DAPI staining of whole mount *rec-8;coh-3* and *rec-8;coh-4* germlines reveals them to have very similar phenotypes to one another. The phenotypes seen are similar but more severe than those of the *rec-8* single mutant: germlines have a highly extended transition zone and chromatin in pachytene nuclei is organised into ordered tracts (Fig. 31A and B). The phenotype in diakinesis oocytes is, like *rec-8* quite variable, with a mixture of bi-lobed univalents, some sister chromatids and large numbers of fragments (Fig. 31C), demonstrating compromised SCC.

5.3.4.2 SC loading

As with the gross morphological phenotypes observed in *rec-8; coh-3/4* germlines, staining with α-SYP-1 antibodies reveals a staining pattern very similar to *rec-8*, with SC loading delayed but synapsis eventually achieved by mid pachytene (Fig. 31A and B).

5.4 Response of meiotic kleisins to disruptions in the CO repair pathway

In mitosis DSBs have a profound affect on cohesin. In budding yeast breaks trigger reloading of cohesin around the site of damage as well as globally across the genome, and this reloaded cohesin have been show to provide cohesion (Strom et al., 2004; Unal et al., 2007). In addition to this, it has been demonstrated that the formation of a DSB also promotes the dissociation of S-phase loaded cohesin from the break site (McAleenan et al., 2013). This may indeed be one of the most important roles of cohesin as it has been shown that cells can undergo mitosis without segregation defects, with less than 30% of the wild type levels of cohesin, but that this is not sufficient to enable them to carry out successful DNA damage repair (Heidinger-Pauli et al., 2010).

In meiosis, programmed DSBs are required to initiate the formation of COs, however, it is unknown as to whether these breaks have any effect on meiotic cohesin. As I have shown in the previous sections, it is clear that deleting one or more kleisin genes has a profound effect on the efficacy of DSB repair. Both *rec-8* and *coh-3;coh-4* mutants accumulate large numbers of RAD-51 foci. Surprisingly, *rec-8;coh-3;coh-4* display exceptionally low levels of RAD-51 foci, indicating that there is a complex relationship between the presence of particular kleisin containing cohesin complexes and DSB formation and repair. Furthermore, the presence of fragments in the diakinesis oocytes of *rec-8* and *rec-8;coh-3/4* mutants indicates that substantial amounts of DNA damage are left entirely unrepaired. This is in contrast to the *coh-3;coh-4* double mutant in which fragments are rarely, if ever, seen (Fig 32).

In order to examine the relationship between DSB formation and processing on *rec-8* and *coh-3;coh-4,* I have combined these mutations with a mutation in *spo-11*, the gene responsible for creating meiotic DSBs and a mutation in *syp-2*, a component of the CE of the SC, which when absent prevents inter-homologue recombination (Colaiacovo et al., 2003). Finally, to perturb the DNA damage

response further, I have exposed these mutants to γ-IR to create levels of DSBs even above endogenous levels.

5.4.1 DSB formation can modulate cohesion

In order to explore the effect of DSB formation on cohesin complexes containing *rec-8* or *coh-3/4*, I created the following strains: *rec-8;spo-11* to examine whether the absence of DSBs affects complexes containing COH-3 and COH-4, and *coh-3;coh-4;spo-11*, to determine whether DSB formation has an effect on cohesin complexes containing REC-8.

5.4.1.1 *rec-8;spo-11*

An initial analysis of the gross morphological phenotype of *rec-8;spo-11* by DAPI staining revealed a striking phenotype. Unlike the *rec-8* single mutant, *rec-8;spo-11* has approximately 24 individualised sister chromatids in diakinesis oocytes, as has been previously reported (Severson et al., 2009) (Fig. 33C and 37). Therefore the phenotype at diakinesis is most similar to that of *rec-8;coh-3;coh-4* in which there is presumably no cohesin loaded. However, the phenotype earlier in prophase I is very similar to that of *rec-8,* with an extended transition zone and pachytene nuclei with ordered chromatin tracks. The most obvious explanation for this would be that DSBs are required for the loading of COH-3 and COH-4 containing-cohesin complexes. In order to test this, I immunostained *rec-8;spo-11;coh-3;coh-3::mCherry* with α-RFP antibodies to determine whether cohesin was being loaded to chromatin. Surprisingly, COH-3 decorates the axial element of nuclei throughout prophase I in these germlines (Fig. 33A and B) as is the case in controls (Fig. 24A and B). In fact, when we look in diakinesis oocytes, COH-3 staining can clearly be seen on the individual sister chromatids (Fig. 33C and 37). This was an unexpected result and so to further investigate this, I immunostained *rec-8;spo-11;coh-3;coh-3::mCherry* germlines with α-SMC-1 antibodies. For the majority of prophase I the staining pattern of SMC-1 was identical to that of COH-3 (Fig 34A and B). However, in diakinesis oocytes the pattern of SMC-1 staining showed high levels of nucleoplasmic staining but there was no SMC-1 signal visible on any of the individualised sister chromatids

(Fig. 34C). This then, may be the reason we see separated sisters in *rec-8;spo-11* diakinesis oocytes, and suggests that in the absence of DSBs and REC-8, SMC-1 might be removed from chromosomes at late prophase.

5.4.1.2 *coh-3;coh-4;spo-11*

The *coh-3;coh-4;spo-11* mutant strain was analysed by DAPI staining in order to determine the loading of cohesin complexes containing REC-8 or if their cohesiveness was affected in a similar manner to COH-3/4. This revealed that the *coh-3;coh-4;spo-11* phenotype is identical to that of *coh-3;coh-4*, both in terms of the chromatin phenotype in pachytene, which has thin disordered track, and the diakinesis oocyte phenotype, in which 12 univalents can be seen (Fig. 38). This demonstrates that REC-8 can provide SCC in the absence of DSBs.

5.4.2 Preventing inter-homologue DSB repair

We have seen that the absence of DSBs has different effects on cohesin complexes contain REC-8, versus those containing COH-3/4. Also the difference in the diakinesis phenotypes of *rec-8,* which has chromosome fragments, and *coh-3;coh-4*, which does not, might be indicative of different responses to accumulated DSBs. In order to test this, I combined the *rec-8* and *coh-3;coh-4* mutants with a null allele of *syp-2*. As previously mentioned, *syp-2* is a component of the CE of the SC that is required to promote inter-homologue recombination, and for this reason *syp-2* mutants accumulate recombination intermediates as DSBs cannot be repaired by the usual pathway involving the homologous chromosome (Martinez-Perez and Villeneuve, 2005). Therefore, in these two mutant combinations the remaining cohesin complexes will be challenged to deal with abundant unrepaired breaks.

5.4.2.1 *rec-8;syp-2*

The preliminary analysis of the chromatin morphology showed that the chromatin structure of nuclei in pachytene was distinct from that of the *rec*-8 single mutant with thin disorganised chromatin rather than thick ordered

tracts. Interestingly, the mitotic accumulation of COH-3 appears to be absence in these germlines (Fig. 35A and B). Also, a striking phenotype could be observed in diakinesis oocytes, with numerous small irregular DAPI masses as well as fragments. The presence of fragments itself could be an indication of loss of cohesin or cohesion, as a break alone should not be sufficient to detach a piece of chromatin from the rest of a chromosome. Therefore, I immunostained *rec-8;syp-2;coh-3;coh-3::mCherry* whole-mounted germlines with α-RFP antibodies. This showed that COH-3 is loaded onto chromatin from the transition zone until diakinesis (Fig. 35A,B and 37). In the -1 diakinesis oocyte very little COH-3 staining is visible, however, in the -2 oocyte COH-3 can be seen to colocalize with chromatin. This loss of COH-3 staining between the -1 and -2 diakinesis oocyte has been observed both in *rec-8* and *rec-8;spo-11,* but this will be discussed in the following chapter.

Following this, I co-stained *rec-8;syp-2* with α-SMC-1 and α-RAD-51 antibodies to check that the SMC-1 localisation was the same as that of COH-3 and to monitor the repair of DSBs. As with the COH-3 staining pattern, SMC-1 appears to be absent in the mitotic tip, but then does load to chromatin in the transition zone, persisting until diakinesis (Fig. 36A and B). Also as with the COH-3 staining pattern, SMC-1 is absent for the chromatin in -1 diakinesis oocytes. Staining with RAD-51 shows, as one would expect, exceptional high levels of RAD-51 foci, in greater abundance than in any of the mutants analysed previously (Fig. 36A and B) and these foci persist until the transition between diplotene and diakinesis. This might suggest that cohesin complexes containing COH-3/4 are insufficient to carry out intersister repair.

5.4.2.2. *coh-3;coh-4;syp-2*

The chromatin morphology of the *coh-3;coh-4;syp-2* mutant strain was analysed by DAPI staining in order to determine whether REC-8 is similarly affected by numerous unrepaired DSBs. The diakinesis phenotype of this mutant revealed a phenotype identical to that of *coh-3;coh-4*, with 12 univalents and no fragments (Fig.38), demonstrating that SCC is not impaired in this genetic background.

5.4.3 Treatment with γ-IR

The experiments above indicate that REC-8 and COH-3/4 containing cohesin complexes respond differently when challenged with the accumulation of DSBs due to the prevention of interhomologue repair. However, this might be due to a requirement of interactions between SYP-2 itself and cohesin complexes in order to repair DNA damage. Whilst this seems unlikely, I decided to test the ability of *rec-8* and *coh-3;coh-4* mutants to respond to DSBs in the presence of an intact SC. To this end, I treated these mutants with a high dose (100Gy) of γ-IR to induced DSBs.

5.4.3.1 *rec-8* versus *coh-3;coh-4*

Young adult worm (18 hrs post L4) were irradiated and the germlines dissected and stained with DAPI 30 hrs post irradiation. Diakinesis oocytes were imaged using the DeltaVision and following this, the z-stacks were cropped to the size of an individual nucleus and maximum intensity projections were made using Fiji ImageJ. These cropped images were analysed in CellProfiler, which identifies individual DAPI masses, counts the number of masses per cropped image and the area of each DAPI mass (Fig. 39D). In this way the number of DAPI bodies per nucleus can be quickly counted for a given phenotype or treatment. In addition to this, the percentage frequency of bivalents, univalents, sisters, fragments, or large aggregates can be determined by binning masses of certain size ranges together. This is not a perfect method for quantifying the number and types of bodies in diakinesis as it tends to over-represent larger bodies and under-represent small bodies, which is due to individual masses overlapping one another in the projected images. However, it has the advantage of being able to count large numbers of fragments in a nucleus, which is virtually impossible by hand.

Initial staining of diakinesis oocytes shows that un-irradiated *coh-3;coh-4* diakinesis oocytes look identical to those treated with 100Gy of γ-IR. However, *rec-8* irradiated diakinesis oocytes have more small irregular DAPI masses as

well as fragments than their un-irradiated counterparts (Fig. 39A). This observation is borne out when the number of DAPI masses per nucleus is analysed, with both treated and un-treated *coh-3;coh-4* mutants having close to 12 DAPI bodies per nucleus. This is distinct from the comparison between non-irradiated *rec-8* worms, which have on average 15 DAPI bodies per nucleus, and irradiated *rec-8* worms, which have approximately 25 DAPI masses on average per nucleus (Fig. 39B).

When we look at the more detailed analysis of the sizes of the DAPI masses we can see even more clearly the difference between the response to DNA damage of *rec-8* and *coh-3;coh-4*. For both irradiated and non-irradiated *coh-3;coh-4* diakinesis oocytes the most frequent type of DAPI mass is univalents, followed by bivalents, which probably reflect univalents lying over one another in the projection, with very few fragments, (or sisters, or large chromatin aggregates). Untreated *rec-8* diakinesis oocytes have sisters as their more common DAPI mass type. This is because the link between the two lobes of the *rec-8* univalents is very tenuous and as a consequence the software often calls a bi-lobed univalent as 2 sisters. In the treated *rec-8* diakinesis oocytes the difference is stark. By far the most abundant type of DAPI body is fragments, with a percentage frequency of almost 0.6, three times higher than that seen in the untreated *rec-8* diakinesis oocytes (Fig. 39C). This suggests that REC-8, but not COH-3/4, are required for repair of accumulated DSBs.

5.4.3.2 *rec-8;spo-11*

This ability to induce DSBs by γ-IR and then analyse the effect this has on the diakinesis phenotype, allows us to investigate whether it is the absence of DSBs in *rec-8;spo-11* mutants that prevents cohesion from being established or causes it to be lost. If DSBs are required to make COH-3/4 cohesin containing complexes cohesive, then treatment of *rec-8;spo-11* worms with γ-IR to induce DSBs should change the diakinesis phenotype from individualised sister chromatids to one that is more similar to *rec-8.* In order to test this *rec-8;spo-11* worms were treated with varying doses of γ-IR. The germlines were then

dissected and diakinesis oocytes imaged and analysed as in the previous section.

The phenotypes observed with higher doses of γ-IR (100 and 50Gy) was similar to that observed in *rec-8* diakinesis oocytes treated with 100Gy of γ-IR, as would be expected (Fig. 40A). When we analyse the number of DAPI masses per nucleus we can see that the number rises from approximately 20 per nucleus in untreated oocytes, to approximately 33 in those treated with 100Gy. The number of bodies per nucleus falls as the dose of γ-IR decreases, with approximately 26 per nucleus in diakinesis oocytes treated with 50Gy, and then falling to the same number as seen in untreated worms at 10Gy (Fig. 40B). This is consistent with the theory that the number of fragments in diakinesis oocytes correlates to the amount of unrepaired DNA damage.

By carrying out the thorough analysis of the sizes of the DAPI masses we can get a more informative picture. In untreated *rec-8;spo-11* diakinesis oocytes the most frequent class of DAPI mass is individual sister chromatids, as we would expect. The percentage frequency of sister chromatids falls as the dose of γ-IR increases. Conversely, the percentage frequency of fragments increases with increasing dose. For all three doses (100, 50 and 10Gy) the number of univalents does not significantly increase. However, the time it takes for a nucleus to travel from S-phase to diakinesis is about 60hrs (Jaramillo-Lambert et al., 2007), while the analysis of these oocytes was carried out 30 hours post irradiation and so, the DSBs induced by the γ-IR may not have occurred sufficiently early in prophase. Therefore diakinesis oocytes were also analysed 60 hrs post irradiation. When we compare the non-irradiated, 10Gy (30hrs) irradiated and the 10 (60hrs) irradiated *rec-8;spo-11* diakinesis oocytes for DAPI bodies in the sister and univalent classes we can see the following: the percentage frequency of sister chromatids is slightly lower in the 10Gy (30hrs) versus untreated, but the percentage frequency of sister in the 10Gy (60hrs) drops to less than half that of the untreated oocytes; at the same time the percentage frequency of univalents almost triples between the non-irradiated and the 10Gy (60hrs) irradiated, and almost doubles between the non-

irradiated and the 10Gy (30hrs) irradiated worms (Fig. 40C). This indicates that at least some sister chromatids become linked as univalents, and from the images of diakinesis, it can be seen that they are phenotypically similar to the univalents of *rec-8* (Fig. 40A and C). This demonstrates that DSBs are sufficient to partially restore cohesion in the diakinesis oocytes of *rec-8;spo-11* mutants.

5.5 Summary

The presence of multiple meiotic kleisins and therefore different forms of cohesin complexes, suggests the possibly that they may carry out different roles in meiosis. In this chapter I sought to address whether this might be the case. By examining the localisation of COH-3 and REC-8 in wild-type germlines we can see subtle differences, in particular in the mitotic tip and in -1 diakinesis oocytes, in which REC-8 remains present of both arms of the bivalent, whereas COH-3 becomes restricted to one (presumably the short) arm.

Examination of meiotic kleisin mutants also suggests differences in function. *coh-3* and *coh-4* are functionally redundant with one another, whereas *rec-8* has a strong phenotype on its own. When we compare *rec-8* to *coh-3;coh-4*, we can see that in diakinesis the cohesion defect is severe in *rec-8*, with the univalents adopting a tenuous bi-lobed structure. Whereas in the diakinesis of *coh-3;coh-4* mutants cohesion appears unaffected. The diakinesis phenotype of *rec-8;coh-3/4* is slightly more acute than that of *rec-8,* with more fragments. This is in contrast to the chromatin phenotype of pachytene nuclei which appear far more similar to that of wild-type in the *rec-8* mutants than in *coh-3;coh-4.* The formation of the SC is also affected differently by loss of *rec-8*, which has delayed SC loading, as opposed to *coh-3;coh-4*, in which SC loading is almost completely impaired. Both *rec-8* and *coh-3;coh-4* accumulate RAD-51 foci. Interestingly, in the *rec-8;coh-3;coh-4* triple mutants it appears that no meiotic breaks are made.

Finally, by comparing *rec-8* and *coh-3;coh-4* coupled with mutations affecting the CO repair pathway, and by treating them with γ-IR we can see that cohesin

complexes containing different meiotic kleisins respond differently to DNA damage. *rec-8;spo-11* has individualised sister chromatids in diakinesis oocytes. However, COH-3 appears to be loaded normally throughout prophase I and is even present on individual sister chromatids (Fig. 33B and 37). This suggests that COH-3/4 require DSBs to become cohesive, whereas this is not the case for REC-8. In addition to this, in diakinesis oocytes of *rec-8;syp-2* worms, we see large numbers of small fragments, which are not seen in *coh-3;coh-4;syp-2* diakinesis oocytes (Fig. 27A and 32). This suggests that REC-8 but not COH-3/4 are required for repair of DSBs, and this is supported by the irradiation data.

For a table summarising the phenotypes observed in the diferent mutant backgrounds, analysed in this chapter, see Table 6 on pages 194-195.

Table 6: Summary of phenotypes of mutants analysed

Genotype	Pachytene Structure	Diakinesis	SC assembly	Cohesin loading	DSB repair
N2 (wild-type)	Thick organised tracks comprised of synapsed homologous chromosomes	Six DAPI masses, comprised of homologues held together with a CO and by SCC	SC assembly assembled between pairs homologues, forming tracks at the onset of meiosis	All cohesin subunits loaded at meiotic S-phase, colocalizing with the SC	RAD-51 foci peak at 11 per nucleus in mid pachytene and are lost by the end of pachytene
coh-3/4	As wild-type	As wild-type	As wild-type	As wild-type	As wild-type
rec-8	Organised tracks, similar to wild-type	Bi-lobed univalents, indicating that sister chromatids are tenuously attached. Average number of DAPI masses 18	SC assembly is delayed, but reaches completion in mid pachytene.	COH-3 and SMC-1 are loaded normally, decorating the axial element	High numbers of RAD-51 foci, persisting until diplotene
coh-3;coh-4	Extremely thin disorganised DNA tracks	12 univalents	Very low levels of SC assembly.	Reduced REC-8 loading. No visible SMC-1 loaded.	Very high numbers of RAD-51 foci, persisting until diplotene
rec-8;coh-3/4	Organised tracks, similar to wild-type	A mixture of bi-lobed univalents, some sister chromatids and large numbers of fragments	SC assembly is delayed, but reaches completion in mid pachytene.	Expected: COH-3/4 and SMC-1 are loaded normally, decorating the axial element	Very high numbers of RAD-51 foci, persisting until diplotene
rec-8;coh-3;coh-4	Extremely thin disorganised DNA tracks	24 individual sister chromatids	No SC	No cohesin loading	No DSBs
rec-8;spo-11	Organised tracks, similar to wild-type	24 individual sister chromatids	SC assembly is delayed, but reaches completion in mid pachytene.	COH-3 and SMC-1 are loaded normally, decorating the axial element. However, SMC-1 is lost from chromosomes in diakinesis, whereas COH-3 can be seen on DNA	No DSBs
rec-8;syp-2	Extremely thin disorganised DNA tracks	A mixture of sister chromatids and large numbers of fragments, and chromatin aggregates	No SC	COH-3 is loaded thoughout meiotic prophase	Very high numbers of RAD-51 foci, persisting until diplotene
coh-3;coh-4;spo-11	Identical to coh-3;coh-4	12 univalents	Expected: Identical to *coh-3;coh-4*	Expected: Identical to *coh-3;coh-4*	No DSBs
coh-3;coh-4;syp-2	Identical to coh-3;coh-4	12 univalents	Expected: Identical to *coh-3;coh-4*	Expected: Identical to *coh-3;coh-4*	Expected: Identical to *coh-3;coh-4*
rec-8;wapl-1	Compact defined chromatin tracks	Mainly univalents. Average number of DAPI masses 15	Expected: Identical to *rec-8*	COH-3 is loaded thoughout meiotic prophase forming thick tracks	Expected: High numbers of RAD-51 foci, persisting until diplotene

rec-8;spo-11;wapl-	Compact defined chromatin tracks	Mainly univalents. Average number of DAPI masses 14	Expected: Identical to *rec-8*	COH-3 is loaded thoughout meiotic prophase forming thick tracks	No DSBs
rec-8;syp-2;wapl-1	Compact defined chromatin tracks	Mainly univalents. Average number of DAPI masses 14	No SC	COH-3 is loaded thoughout meiotic prophase forming thick tracks	A reduction in the number of RAD-51 foci compared with *rec-8;syp-2*, but also persisting until diplotene

Figure 24. Localisation of REC-8::GFP and COH-3::mCherry in *rec-8;coh-3;rec-8::GFP;coh-3::mCherry* germlines

A Whole mount of *rec-8;coh-3;rec-8::GFP;coh-3::mCherry* germline stained with α-GFP and α-RFP antibodies and counterstained the with DAPI, showing REC-8::GFP and COH-3::mCherry colocalising, loaded to chromatin, decorating the axial element from transition zone onwards.

B Magnification showing mid pachytene nuclei

C Diplotene nucleus showing nucleoplasmic localisation of REC-8::GFP only, with both REC-8::GFP and COH-3::mCherry colocalising to form a cruciform pattern on chromatin

D Diakinesis oocyte showing REC-8::GFP forming a cruciform pattern on both the long and short arms of bivalents localising between sister chromatids and homologue pairs, with COH-3::mCherry localising only on the short arm of bivalents, between homologous chromosomes

A rec-8;rec-8::GFPcoh-3;coh-3::mCherry
B
C
D
DNA
REC-8 (α-GFP)
COH-3 (α-RFP)
Merge
REC-8 (α-GFP) + COH-3 (α-RFP)
50μm
10μm
10μm
10μm

Figure 25. Localisation of SYP-1 in N2 germlines

A Whole mount of N2 germline stained with α-SYP-1 antibodies and counterstained the with DAPI, showing the central element (of which SYP-1 is a component) assembled between pairs of tightly juxtaposed homologues, forming characteristic tracks. RAD-51 foci mark recombination intermediates

B Comparison of SYP-1 loading in early and late pachytene nuclei of N2 and *rec-8* worms, showing a delay in assembly of the central element in *rec-8* germlines

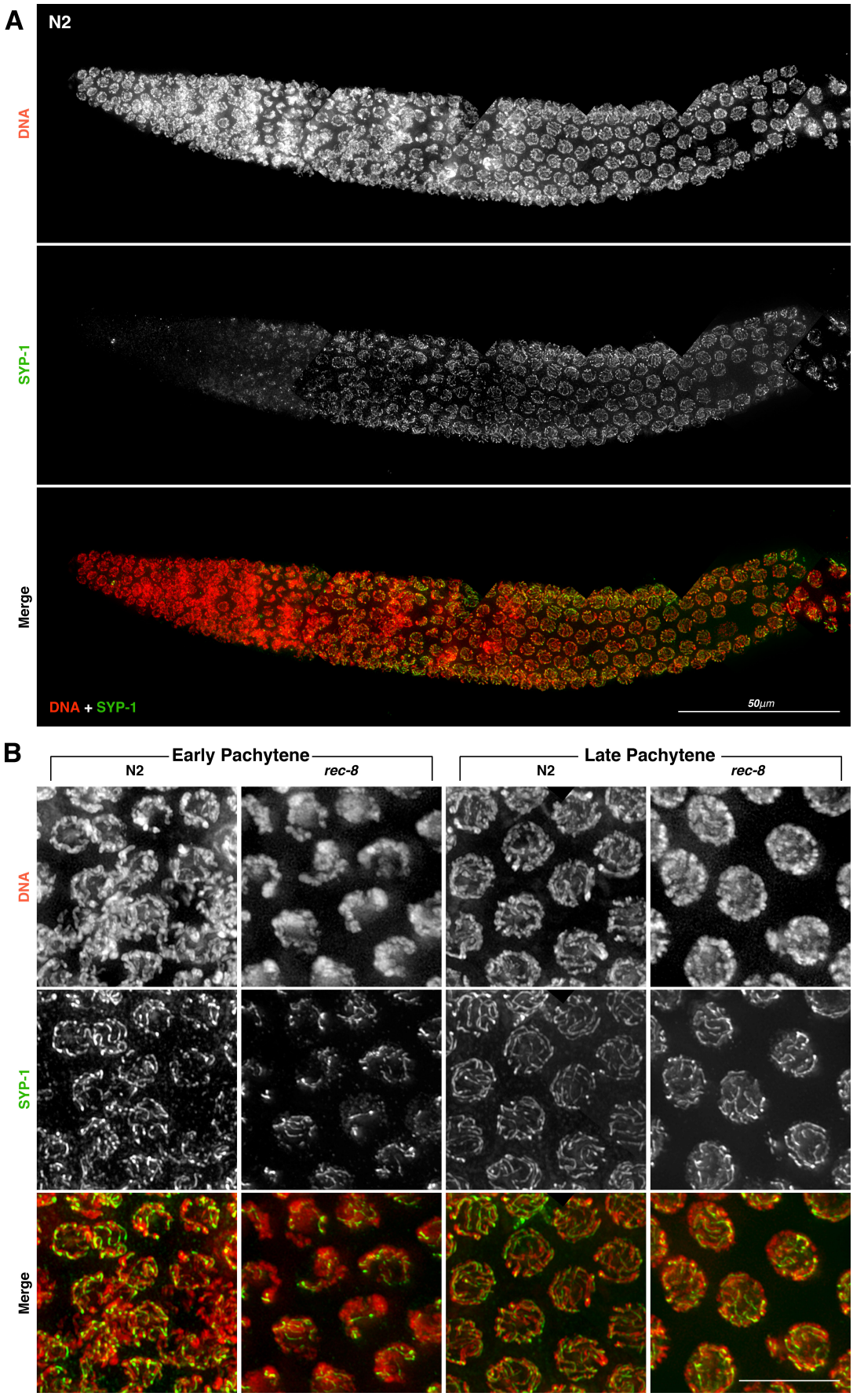
A
N2
DNA
SYP-1
Merge
DNA + SYP-1
50µm
B
Early Pachytene
Late Pachytene
N2
rec-8
N2
rec-8
DNA
SYP-1
Merge

Figure 26. Localisation of SYP-1 and RAD-51 in *rec-8* mutant germlines

A Whole mount of *rec-8* germline stained with α-SYP-1 and α-RAD-51 antibodies counterstained with DAPI, showing a delay in assembly of the central element of the SC, with full synapsis only achieved in mid pachytene nuclei, as well as accumulation of recombination intermediates extending beyond the end of pachytene, indicating impairment of DSB repair.

B Magnification showing mid pachytene nuclei

C Diakinesis oocyte from *rec-8* showing bi-lobed univalents

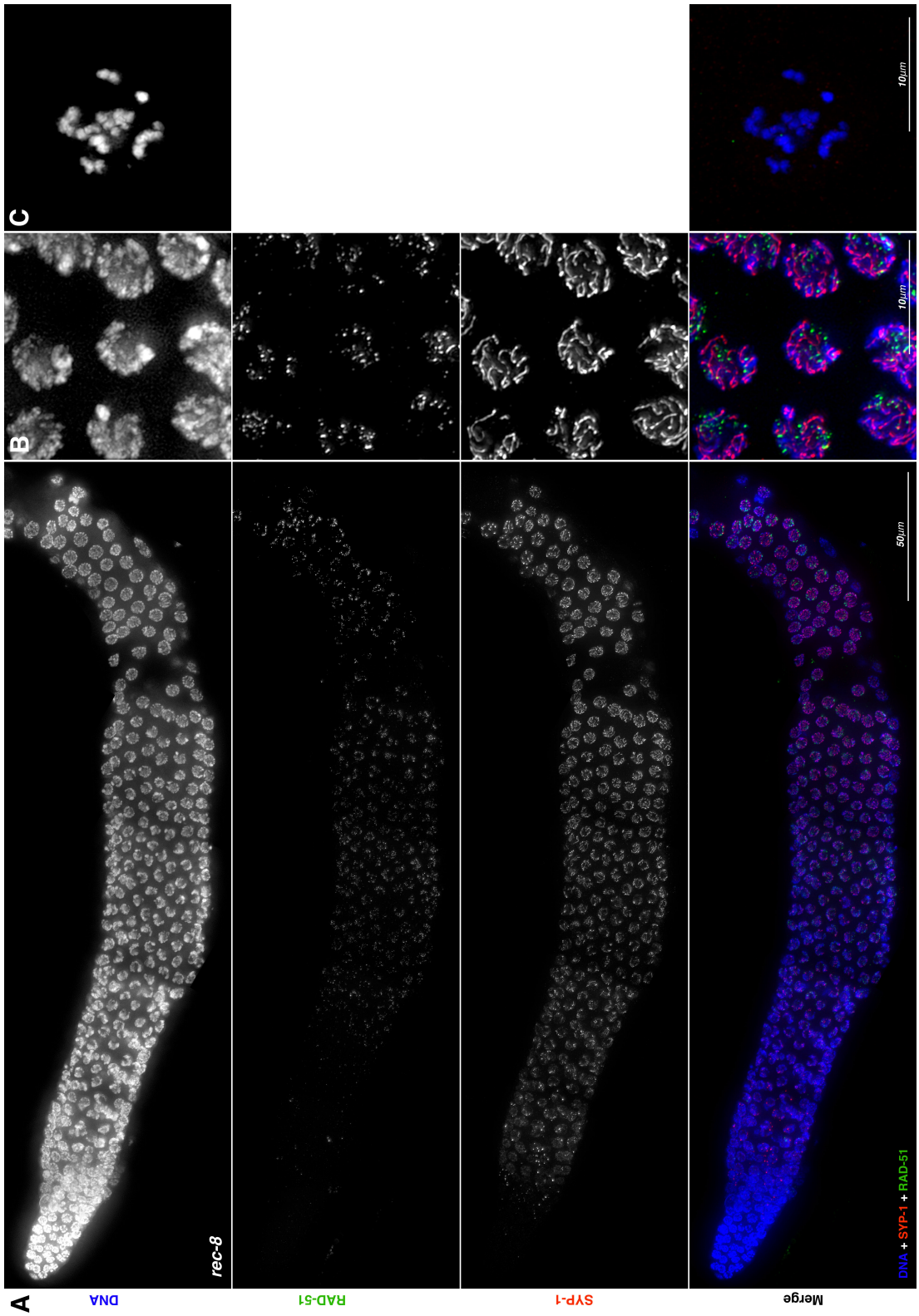
A
B
C
DNA
RAD-51
SYP-1
Merge
rec-8
50μm
10μm
10μm
DNA + SYP-1 + RAD-51

Figure 27. Localisation of COH-3::mCherry in *rec-8;coh-3;coh-3::mCherry* germlines

A Whole mount of *rec-8;coh-3;coh-3::mCherry* germline stained with α-RFP antibodies counterstained the DAPI, showing COH-3::mCherry loaded to chromatin, decorating the axial element from transition zone onwards

B Magnification showing mid pachytene nuclei

C Diakinesis oocyte from *rec-8* showing bi-lobed univalents, demonstrating the tenuous link between sister chromatids in this mutant. Notice the lack of COH-3::mCherry staining between the lobes of many univalent (arrow). Inset: Magnification of a univalent with COH-3 seemingly linking the two sister chromatids (Scale bar 1μm).

A rec-8;coh-3;coh-3::mCherry
B
C
50µm
10µm
10µm
DNA
COH-3 (α-RFP)
Merge
DNA + COH-3 (α-RFP)

Figure 28. Localisation of SYP-1 and RAD-51 in *coh-3;coh-4* mutant germlines

A Whole mount of *coh-3;coh-4* germline stained with α-SYP-1 and α-RAD-51 antibodies counterstained with DAPI, showing a severe impairment in loading of the central element of the SC, with full synapsis never achieved, as well as accumulation of recombination intermediates extending beyond the end of pachytene, indicating impairment of DSB repair.

B Magnification showing mid pachytene nuclei

C Diakinesis oocyte from *coh-3;coh-4*, showing regular shaped univalents indicating impairment of chiasmata formation

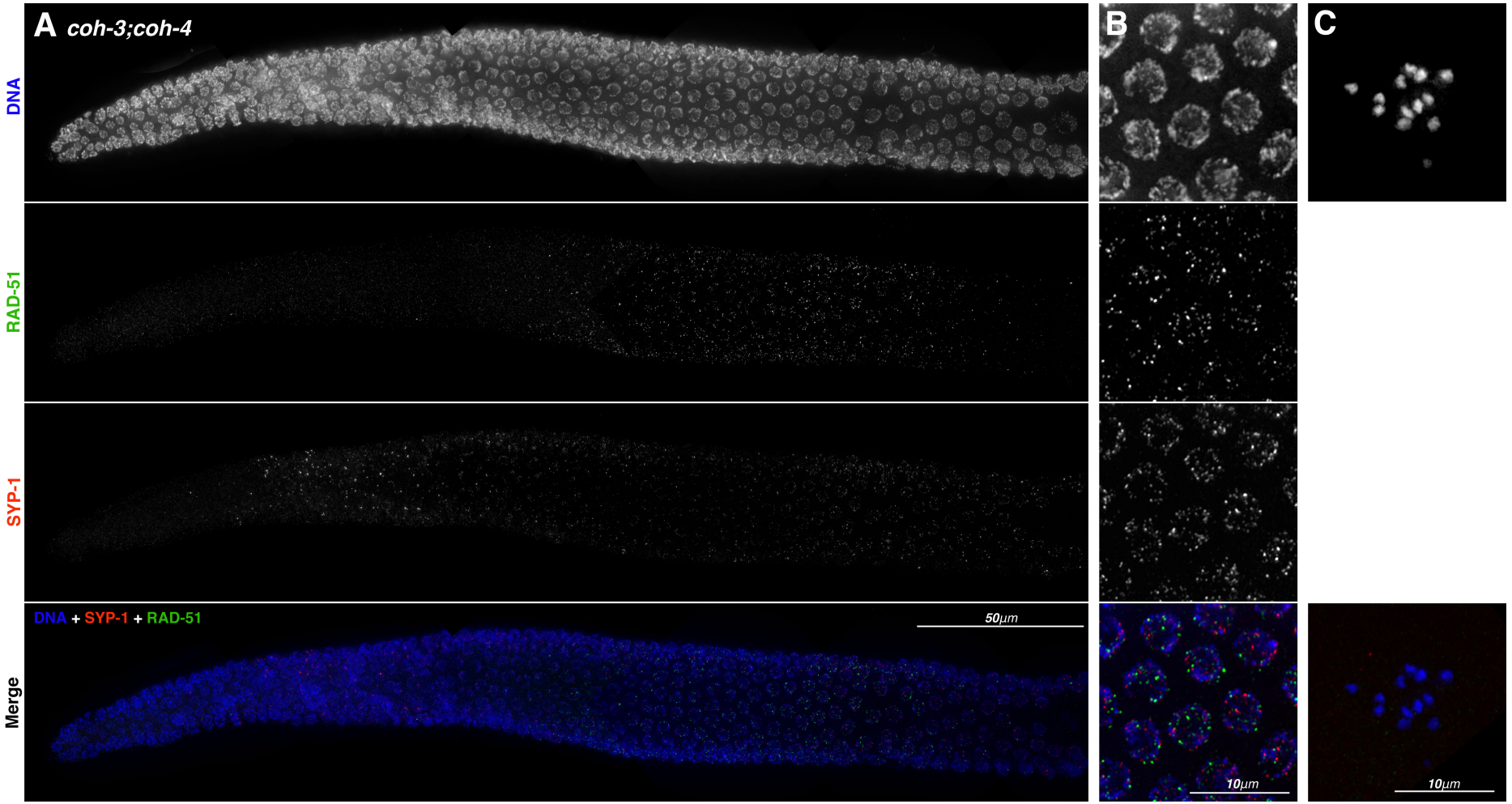
A coh-3;coh-4
B
C
DNA
RAD-51
SYP-1
Merge
DNA + SYP-1 + RAD-51
50μm
10μm
10μm

Figure 29. Localisation of SMC-1 and REC-8 in *coh-3;coh-4* mutant germlines

A Whole mount of *coh-3;coh-4* germline stained with α-SMC-1 and α-REC-8 antibodies counterstained with DAPI, showing impairment of REC-8 loading with a punctate staining pattern rather than organised tracks, and no detectable SMC-1. This is noticeable as one would always expect to see REC-8 colocalising with SMC-1 as part of a cohesin ring.

B Magnification showing mid pachytene nuclei

C Diakinesis oocyte from *coh-3;coh-4* showing regular shaped univalents indicating impairment of chiasmata formation, but no loss of SCC. Notice REC-8 decorating the interface between the sister chromatids in each univalent. SMC-1 is not visible on chromatin, but rather displays a nucleoplasmic localisation.

A
B
C
coh-3;coh-4
DNA
SMC-1
REC-8
Merge
SMC-1 + REC-8
DNA + SMC-1 + REC-8
50μm
10μm
10μm

Figure 30. Localisation of SYP-1 and RAD-51 in *rec-8;coh-3;coh-4* mutant germlines

A Whole mount of *rec-8;coh-3;coh-4* germline stained with α-SYP-1 and α-RAD-51 antibodies counterstained the DAPI, showing complete loss of SC loading and surprisingly, very low levels of RAD-51 foci.

B Magnification showing mid pachytene nuclei

C Diakinesis oocyte from *rec-8;coh-3;coh-4* showing individualised sister chromatids, indicating complete absence of SCC.

A rec-8;coh-3;coh-4
B
C
DNA
RAD-51
SYP-1
Merge
DNA + SYP-1 + RAD-51
50μm
10μm
10μm

Figure 31. Localisation of SYP-1 in *rec-8;coh-3* mutant germlines

A Whole mount of *rec-8;coh-3* germline stained with α-SYP-1 antibodies and counterstained with DAPI, showing a delay in assembly of the central element of the SC, with full synapsis only achieved in mid pachytene nuclei. This phenotype is similar to that of *rec-8* single mutants

B Magnification showing mid pachytene nuclei.

C Diakinesis oocyte from *rec-8;coh-3* showing chromatin aggregates and fragments indicating accumulation of unrepaired DNA damage.

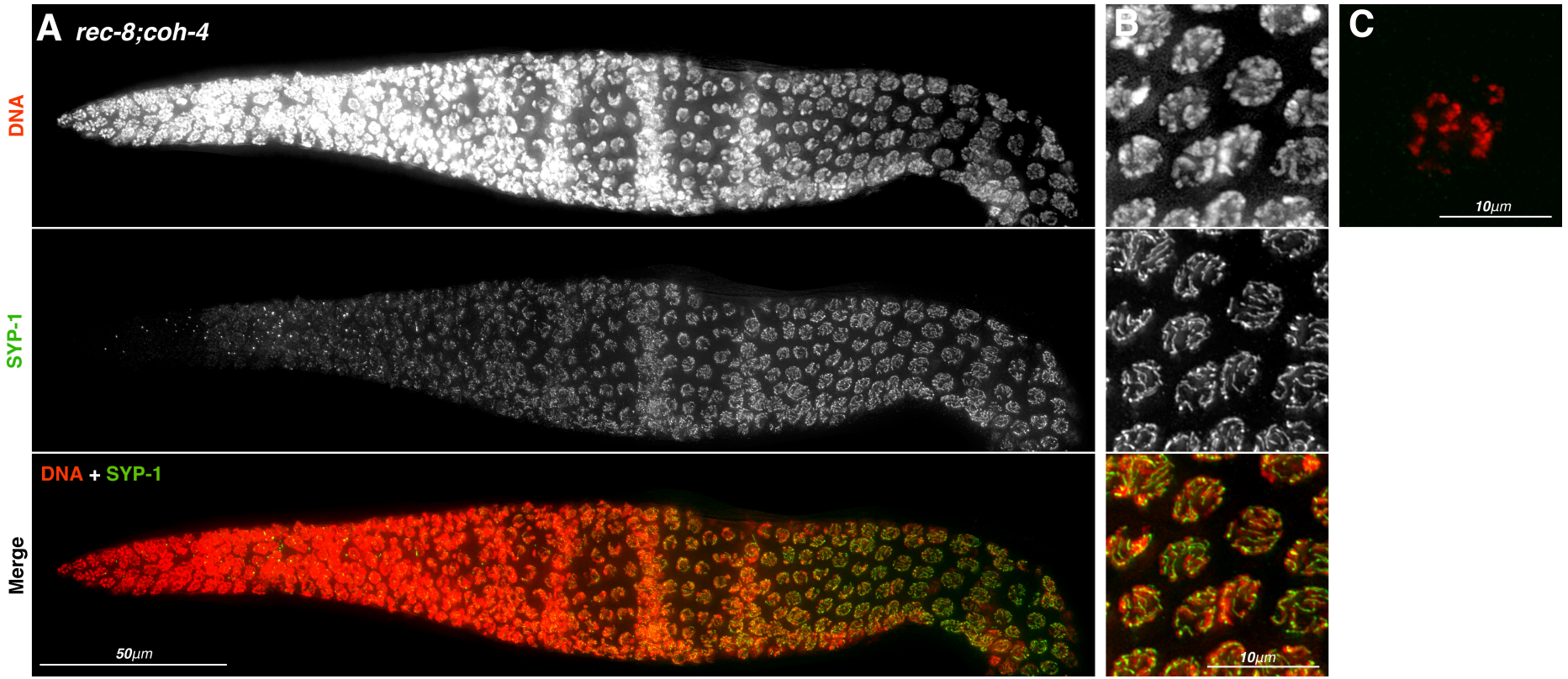
A rec-8;coh-4
B
C
DNA
SYP-1
Merge
DNA + SYP-1
50μm
10μm
10μm

Figure 32. SC loading and DNA damage in α-kleisin mutants

A comparison of *rec-8* single, *coh-3;coh-4* double and *rec-8;coh-3;coh-4* triple mutants. A relatively high degree of synapsis is achieved in *rec-8* mutants, whereas in *coh-3;coh-4* mutants extremely little SC loading occurs, and in *rec-8;coh-3;coh-4* loading of the SC is completely abolished with SYP-1 forming large aggregates. Both *rec-8* and *coh-3;coh-4* have extensive accumulation of recombination intermediates, whereas in *rec-8;coh-3;coh-4* almost none are detectable indicating that DSB formation is impaired.

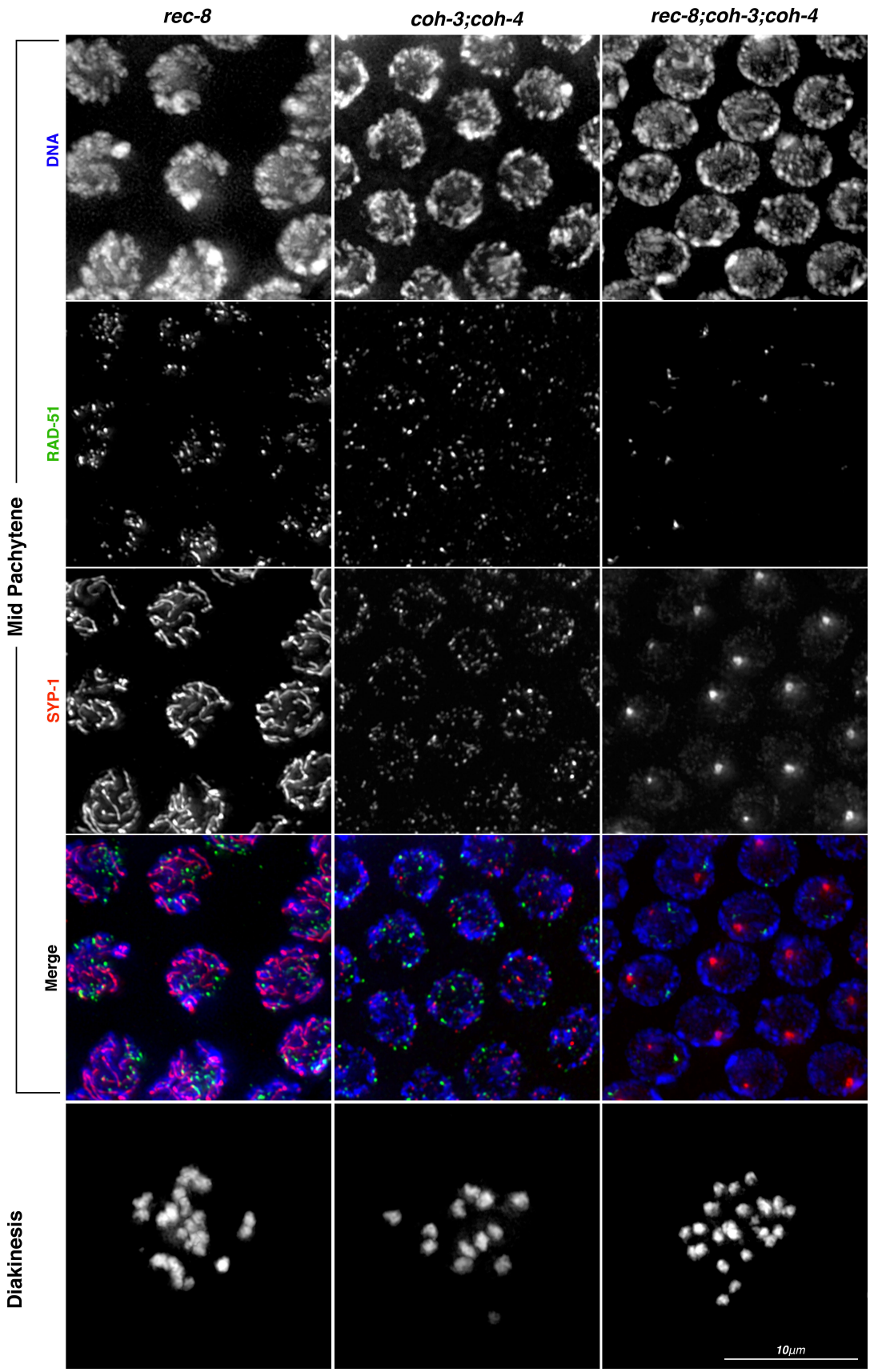
rec-8
coh-3;coh-4
rec-8;coh-3;coh-4
Mid Pachytene
DNA
RAD-51
SYP-1
Merge
Diakinesis
10μm

Figure 33. Localisation of COH-3::mCherry in *rec-8;spo-11;coh-3;coh-3::mCherry* germlines

A Whole mount of *rec-8;spo-11;coh-3;coh-3::mCherry* germline stained with α-RFP antibodies counterstained with DAPI, showing COH-3::mCherry loaded to chromatin, decorating the axial element from transition zone onwards

B Magnification showing mid pachytene nuclei

C Diakinesis oocyte from *rec-8;spo-11* showing individualised sister chromatids, indicating complete absence of SCC. Notice chromatin-associated COH-3::mCherry on some sister chromatids. Inset: Magnification of an individual sister chromatid clearly showing COH-3::mCherry loaded to chromatin (Scale bar 1μm).

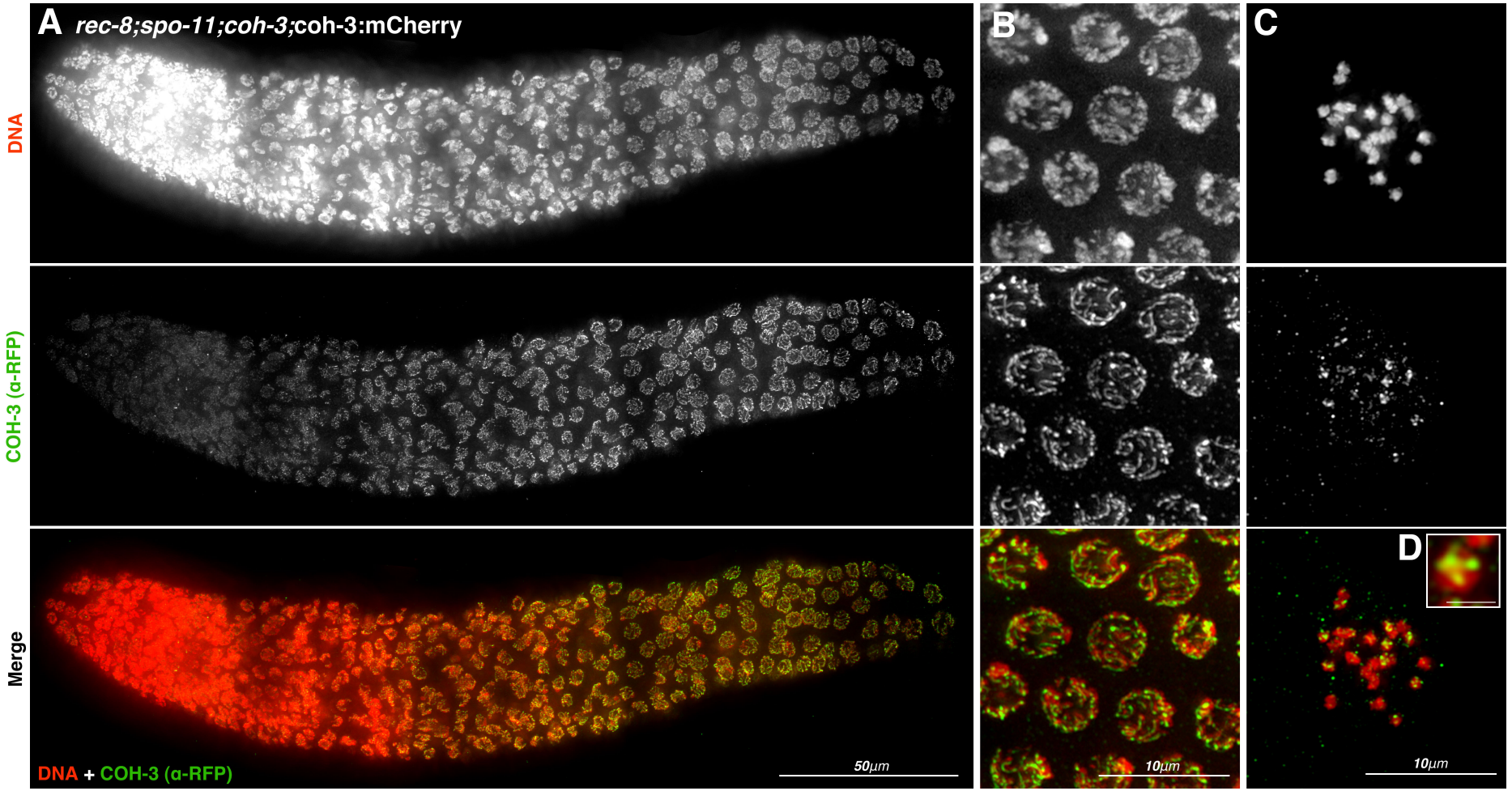
A rec-8;spo-11;coh-3;coh-3:mCherry
B
C
D
DNA
COH-3 (α-RFP)
Merge
DNA + COH-3 (α-RFP)
50μm
10μm
10μm

Figure 34. Localisation of SMC-1 in *rec-8;spo-11;coh-3;coh-3::mCherry* germlines

A Whole mount of *rec-8;spo-11;coh-3;coh-3::mCherry* germline stained with α-SMC-1 antibodies counterstained with DAPI, showing SMC-1 loaded to chromatin, decorating the axial element from transition zone onwards

B Magnification showing mid pachytene nuclei

C Diplotene nucleus showing nucleoplasmic localisation of SMC-1, with no chromatin-associated signal

D Diakinesis oocyte from *rec-8;spo-11* showing no chromatin-associated SMC-1, but nucleoplasmic localisation only

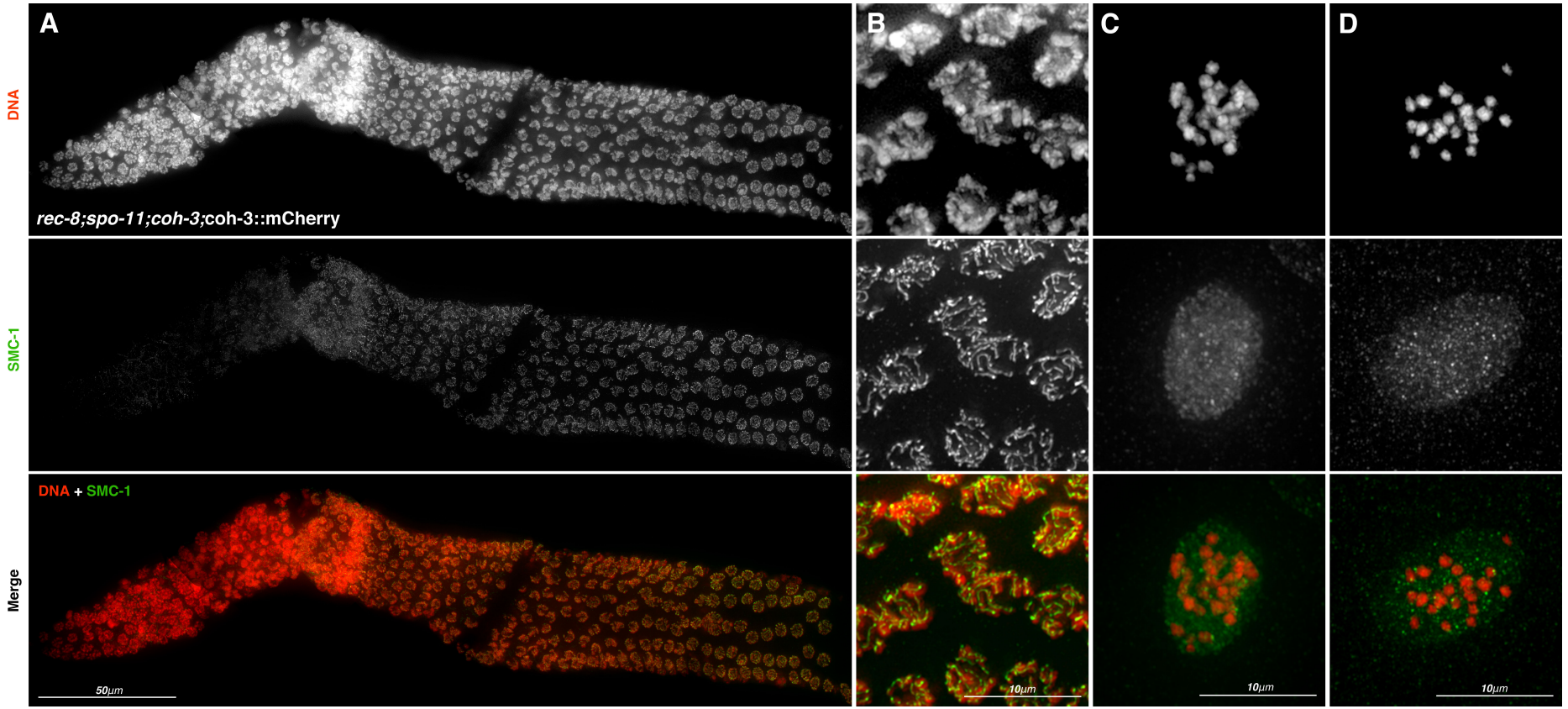
A
B
C
D
DNA
SMC-1
Merge
rec-8;spo-11;coh-3;coh-3::mCherry
DNA + SMC-1
50μm
10μm
10μm
10μm

Figure 35. Localisation of COH-3::mCherry in *rec-8;syp-2;coh-3;coh-3::mCherry* germlines

A Whole mount of *rec-8;syp-2;coh-3;coh-3::mCherry* germline stained with α-RFP antibodies counterstained with DAPI, showing COH-3::mCherry loaded to chromatin, forming thin discontinuous tracks.

B Magnification showing mid pachytene nuclei

C Diakinesis oocyte from *rec-8;syp-2* showing small irregular sister chromatid-sized DAPI bodies as well as high levels of fragmentation, indicating complete absence of SCC and accumulation of persistent DNA damage.

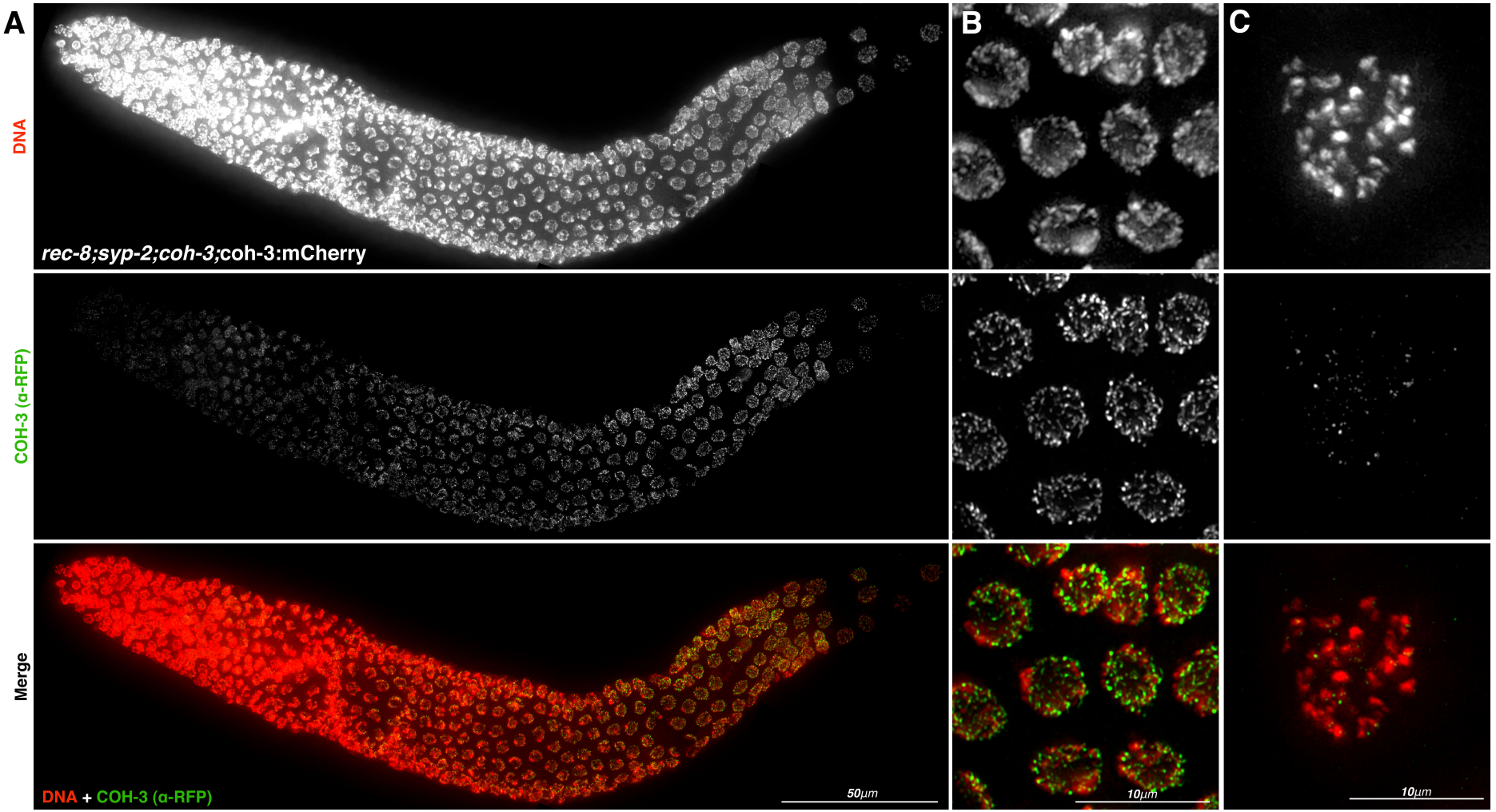
A
B
C
DNA
COH-3 (α-RFP)
Merge
rec-8;syp-2;coh-3;coh-3:mCherry
DNA + COH-3 (α-RFP)
50μm
10μm
10μm

Figure 36. Localisation of SMC-1 and RAD-51 in *rec-8;syp-2;coh-3;coh-3::mCherry* germlines

A Whole mount of *rec-8;syp-2;coh-3;coh-3::mCherry* germline stained with α-SMC-1 and α-RAD-51 antibodies, counterstained with DAPI, showing SMC-1 loaded to chromatin, forming thin discontinuous tracks and massive accumulation of recombination intermediates extending beyond the end of pachytene, indicating a severe impairment of DSB repair.

B Magnification showing mid pachytene nuclei

C Diakinesis oocyte from *rec-8;syp-2* showing small irregular sister chromatid-sized DAPI bodies as well as high levels of fragmentation, indicating complete absence of SCC and accumulation of persistent DNA damage.

A rec-8;syp-2
B
C
DNA
SMC-1
RAD-51
Merge
DNA + SMC-1 + RAD-51
50μm
10μm
10μm

Figure 37. Comparison of SCC deficient mutants

Panel comparing COH-3::mCherry loading and diakinesis phenotype in *rec-8;coh-3;coh-3::mCherry, rec-8;spo-11;coh-3;coh-3::mCherry* and *rec-8;syp-2;coh-3;coh-3::mCherry* germlines, showing a clearing impairment in SCC in all diakinesis oocytes, despite significant levels of COH-3::mCherry loading earlier in meiotic prophase, suggesting that either COH-3 containing cohesin complexes never establish cohesion, or that cohesion is lost at some point in prophase before the diakinesis stage is reached.

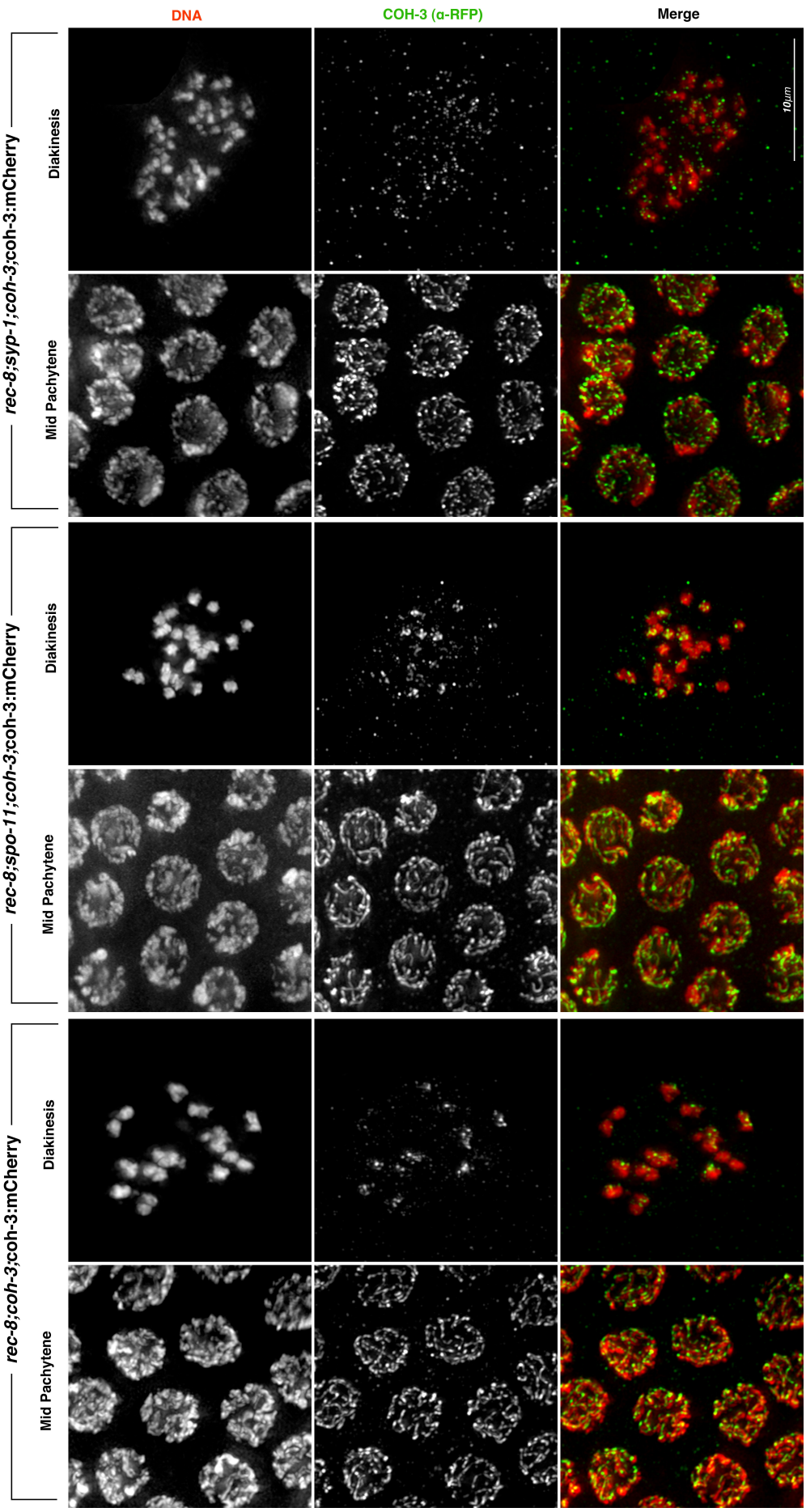
DNA
COH-3 (α-RFP)
Merge
10μm
rec-8;syp-1;coh-3;coh-3:mCherry
Diakinesis
Mid Pachytene
rec-8;spo-11;coh-3;coh-3:mCherry
Diakinesis
Mid Pachytene
rec-8;coh-3;coh-3:mCherry
Diakinesis
Mid Pachytene

Figure 38. *rec-8* and *coh-3;coh-4* mutants respond differently to perturbations in CO repair

Comparison of *rec-8;spo-11* and *coh-3;coh-4;spo-11* diakinesis phenotypes, showing individualised sisters indicating loss of SCC, and univalents indicating intact SCC, respectively.

Comparison of *rec-8;syp-2* and *coh-3;coh-4;syp-2* diakinesis phenotypes, showing small irregular sister chromatid-sized DAPI bodies as well as high levels of fragmentation indicating loss of SCC and persist DNA damage, and univalents indicating intact SCC and completion of DSB repair, respectively.

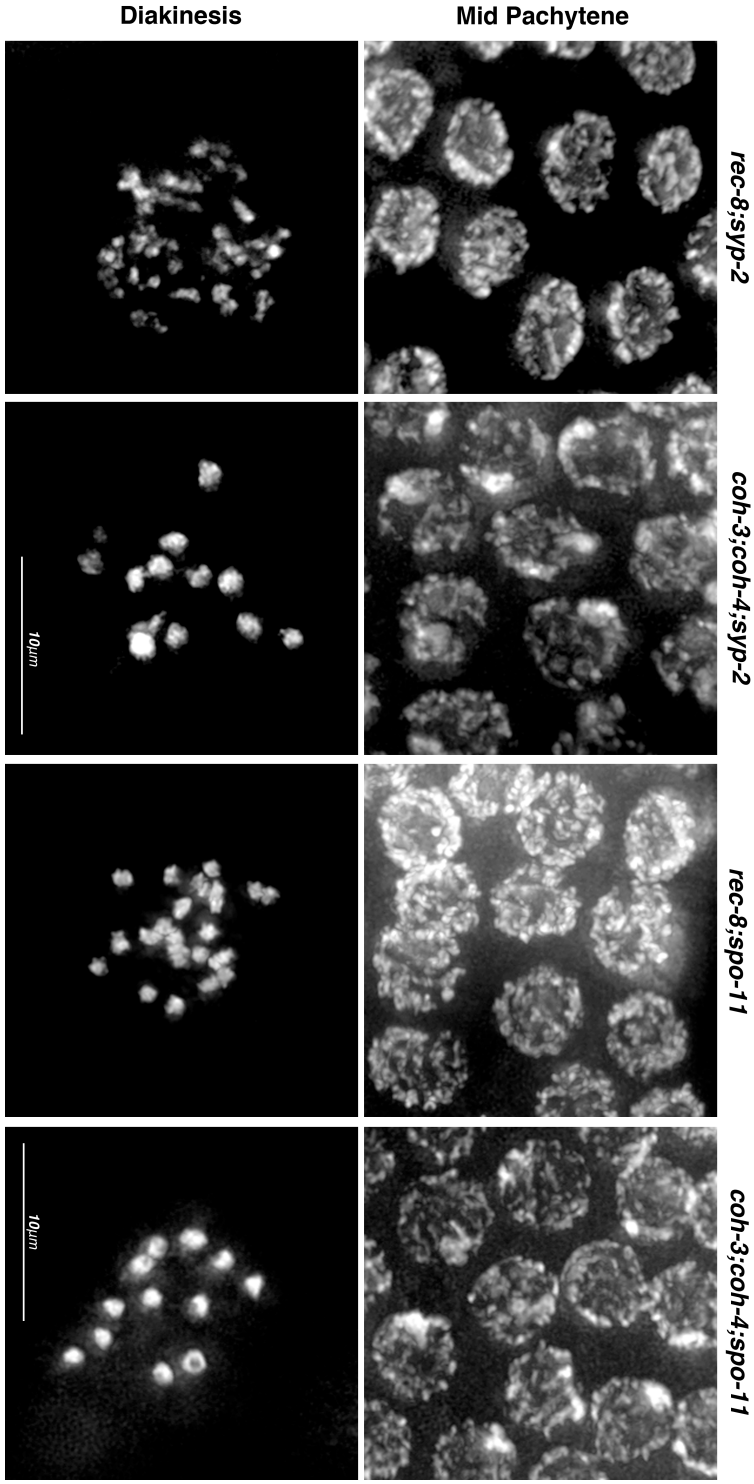
Diakinesis
Mid Pachytene
rec-8;syp-2
coh-3;coh-4;syp-2
rec-8;spo-11
coh-3;coh-4;spo-11
10μm
10μm

Figure 39. *rec-8* and *coh-3;coh-4* mutants respond differently to γ-IR

A Diakinesis oocytes of irradiated (100Gy) and non-irradiated *rec-8* and *coh-3;coh-4* mutants, showing extensive fragmentation in *rec-8* only indicating that DSB repair cannot efficiently occur, whereas in *coh-3;coh-4* mutants DNA repair is less affected, or not affected at all.

B-C For control data see Fig. **5.**

B Graph showing the average number of DAPI masses in diakinesis oocytes of irradiated (100Gy) and non-irradiated *rec-8* and *coh-3;coh-4* mutants, showing no significant difference in the number of masses between treated and untreated *coh-3;coh-4* mutants (P-value **=0.30), but a significant increase in the number of DAPI masses in irradiated (100Gy) *rec-8* diakinesis oocytes compared with there non-irradiated counterparts (P-value *=$6.24x10^{-6}$)

C Graph showing CellProfiler analysis of DAPI mass area in diakinesis oocytes of irradiated (100Gy) and non-irradiated *rec-8* and *coh-3;coh-4* mutants, showing the highest percentage frequency category of both treated and untreated *coh-3;coh-4* worms is univalents (0.59% and 0.53%, respectively, whereas the highest percentage frequency category of irradiated *rec-8* was fragments (0.60%) versus sister chromatids in un-irradiated *rec-8* diakinesis oocytes (0.36%).
Number of worms used for each genotype and treatment given in brackets: *rec-8* irradiated(35), *coh-3;coh-4* irradiated(39), *rec-8* non-irradiated(34), and *coh-3;coh-4* non-irradiated(31).

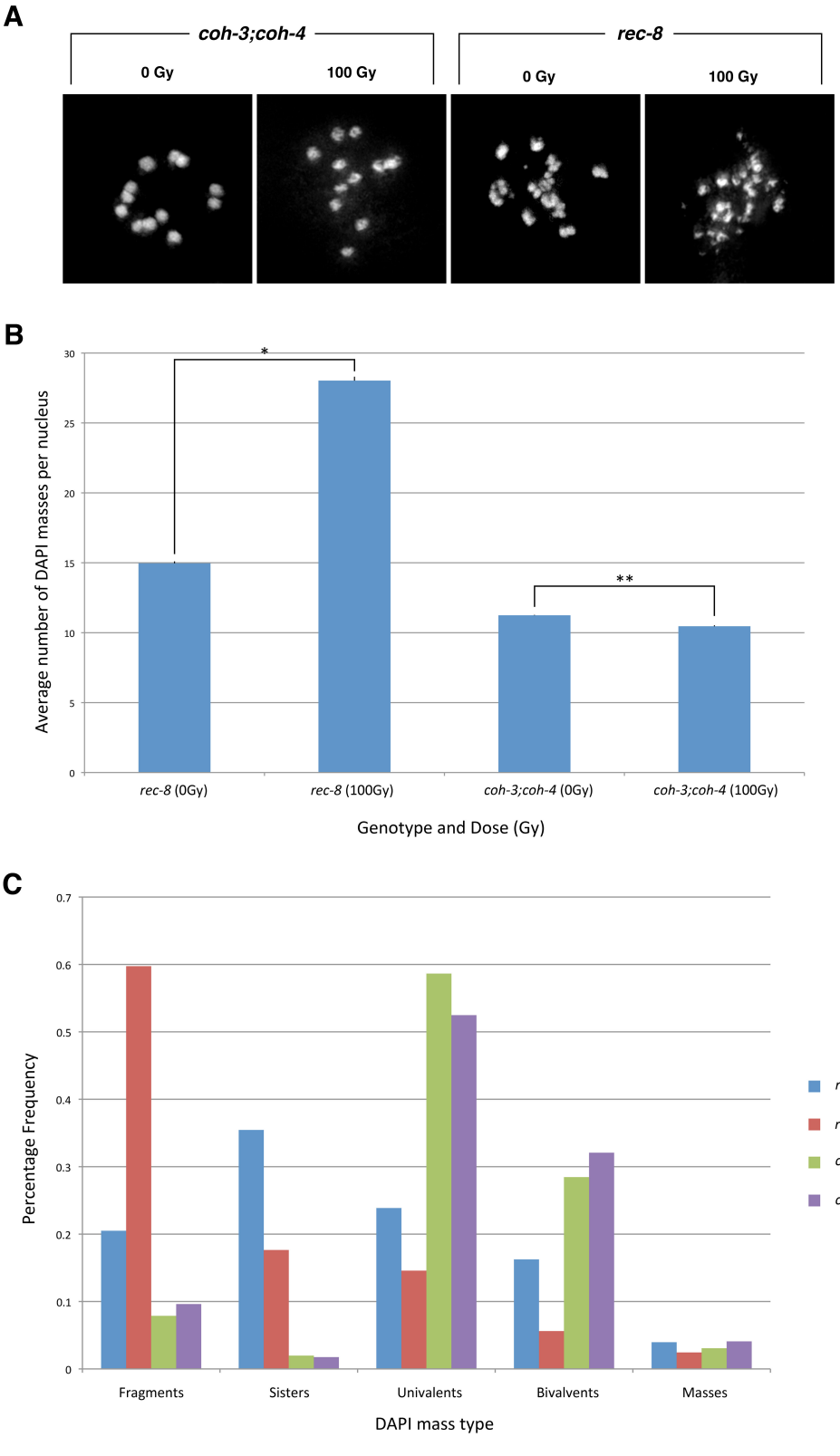
A
coh-3;coh-4
rec-8
0 Gy
100 Gy
0 Gy
100 Gy
B
Average number of DAPI masses per nucleus
30
25
20
15
10
5
0
*
**
rec-8 (0Gy)
rec-8 (100Gy)
coh-3;coh-4 (0Gy)
coh-3;coh-4 (100Gy)
Genotype and Dose (Gy)
C
Percentage Frequency
0.7
0.6
0.5
0.4
0.3
0.2
0.1
0
Fragments
Sisters
Univalents
Bivalents
Masses
DAPI mass type
rec-8 (0Gy)
rec-8 (100Gy)
coh-3;coh-4 (0Gy)
coh-3;coh-4 (100Gy)

Figure 40. DSBs can improve cohesion defects in rec-8;spo-11 diakinesis oocytes

A Diakinesis oocytes of *rec-8;spo-11* with different doses of γ-IR showing a gradient in the amount of fragmentation correlating with dose of treatment. Diakinesis oocytes of *rec-8* for comparison.

B Graph showing the average number of DAPI masses in diakinesis oocytes of *rec-8;spo-11* with different doses of γ-IR showing an increasing average number of DAPI bodies with increasing dose of irradiation.

C Graph showing CellProfiler analysis of DAPI mass area in diakinesis oocytes of *rec-8;spo-11* treated with different doses of γ-IR, showing that at both 100Gy and 50Gy the highest percentage frequency category was fragments (0.62% and 0.45%, respectively), compared with untreated *rec-8;spo-11* diakinesis oocytes in which the highest percentage frequency category sister chromatids (0.63%). In *rec-8;spo-11* treated with 10Gy and analysed 60hrs post-γ-IR, the highest percentage frequency category was univalents (0.38%), suggesting that formation of some chiasmata in these diakinesis oocytes has occurred.
Number of worms used for each genotype and treatment given in brackets: *rec-8;spo-11* 0Gy 30hrs(30), *rec-8;spo-11* 10Gy 30hrs(32), *rec-8;spo-11* 50Gy 30hrs(30), *rec-8;spo-11* 100Gy 30hrs(27), and *rec-8;spo-11* 10Gy 60hrs(32).

D Examples of the CellProfiler analysis process: individual bodies are identified based on threshold intensities and the number and area of area body calculated per nucleus.

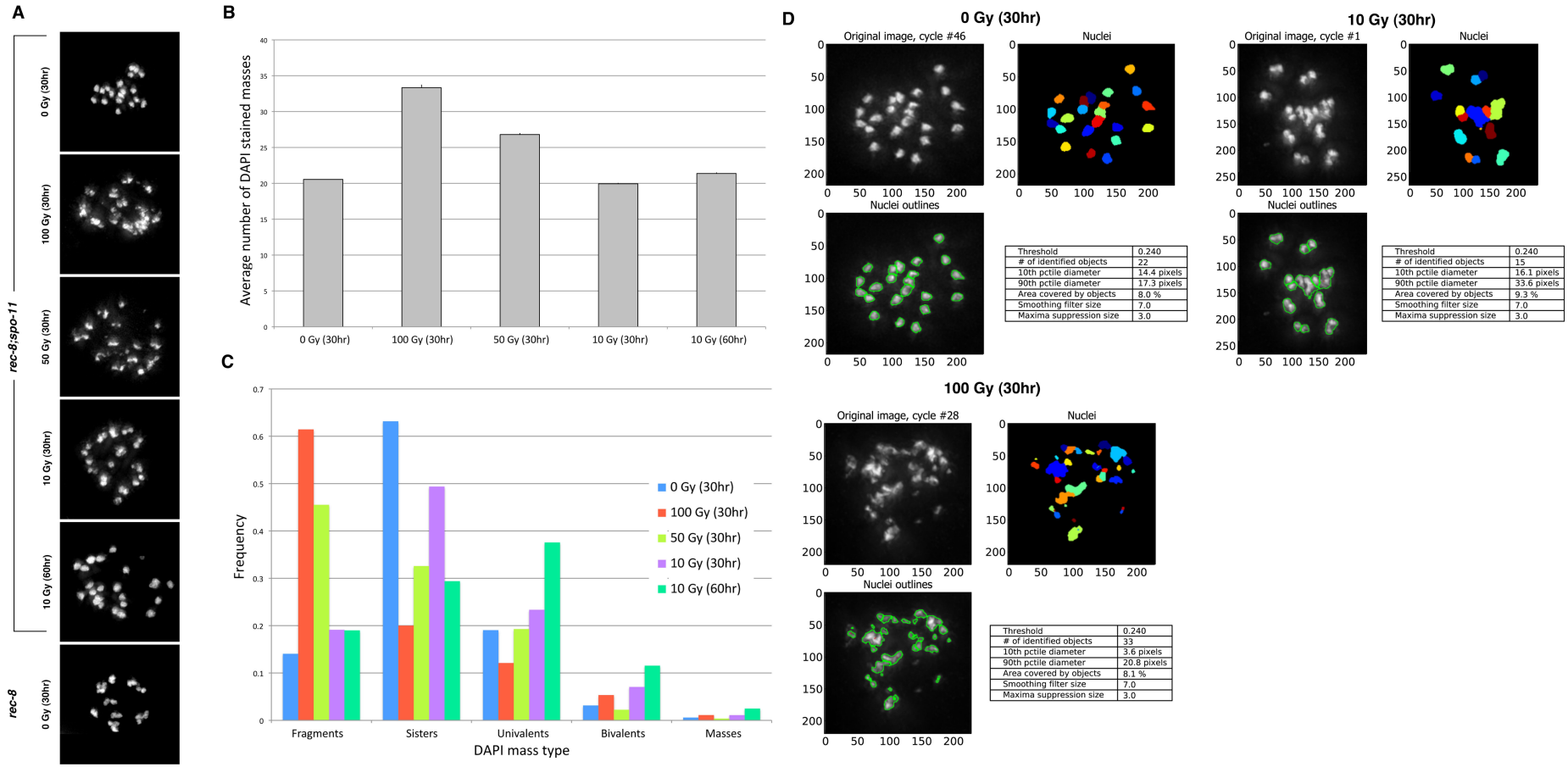
A
rec-8;spo-11
0 Gy (30hr)
100 Gy (30hr)
50 Gy (30hr)
10 Gy (30hr)
10 Gy (60hr)
rec-8
0 Gy (30hr)
B
Average number of DAPI stained masses
0 Gy (30hr)
100 Gy (30hr)
50 Gy (30hr)
10 Gy (30hr)
10 Gy (60hr)
C
Frequency
Fragments
Sisters
Univalents
Bivalents
Masses
DAPI mass type
0 Gy (30hr)
100 Gy (30hr)
50 Gy (30hr)
10 Gy (30hr)
10 Gy (60hr)
D
0 Gy (30hr)
Original image, cycle #46
Nuclei
Nuclei outlines
Threshold 0.240
# of identified objects 22
10th pctile diameter 14.4 pixels
90th pctile diameter 17.3 pixels
Area covered by objects 8.0 %
Smoothing filter size 7.0
Maxima suppression size 3.0
10 Gy (30hr)
Original image, cycle #1
Nuclei
Nuclei outlines
Threshold 0.240
# of identified objects 15
10th pctile diameter 16.1 pixels
90th pctile diameter 33.6 pixels
Area covered by objects 9.3 %
Smoothing filter size 7.0
Maxima suppression size 3.0
100 Gy (30hr)
Original image, cycle #28
Nuclei
Nuclei outlines
Threshold 0.240
# of identified objects 33
10th pctile diameter 3.6 pixels
90th pctile diameter 20.8 pixels
Area covered by objects 8.1 %
Smoothing filter size 7.0
Maxima suppression size 3.0

CHAPTER 6: RESULTS

THE ROLE OF WAPL-1 IN MEIOSIS

6.1 Objectives

Data from the *scc-2* RNAi experiments strongly suggests that without reloading, cohesin complexes are lost from chromatin during late meiotic prophase. In the previous chapter I have shown that cohesiveness can be modulated by altering DSB formation and repair in *rec-8* mutants, suggesting that that COH-3/4 complexes may require DSBs in order to provide cohesion. In addition to this, I have also shown that COH-3/4 are not sufficient to promote DNA damage repair. As mentioned in the introduction, Wapl has been implicated in promoting cohesin removal in mitosis, in what is known as the prophase I pathway (Gandhi et al., 2006). It has been suggested that it does so by acting as an antagonist to factors involved in maintaining cohesion, such as Pds5 (Liu et al., 2013; Nishiyama et al., 2010). However, very little is known about the role of WAPL-1 in meiosis, and whilst a *wapl-1* homologue has been identified in *C. elegans* by sequence homology, its function remains unknown. However, generation of a *wapl-1*::GFP strain in our lab by my colleague Oliver Crawley shows that WAPL-1 is expressed in the nucleoplasm of all nuclei in the germline, suggesting that it may play a role in meiotic prophase. In this chapter I sought to examine whether *wapl-1* plays a role the meiotic prophase of *C. elegans*, and in particular to see whether it could be responsible for the cohesin loss we observe in the *scc-2* RNAi experiments. In order to do this, I have combined the *wapl-1* mutation with other mutations in which SCC is highly impaired, reasoning that these phenotypes should be ameliorated if WAPL-1 plays a role as a cohesion anti-establishment/maintenance factor.

6.2 Basic characterisation of *wapl-1* mutants

The *tm1814* allele of *wapl-1* has a 600bp deletion at the start of the gene that removes the ATG start codon and it therefore expected to be a null allele. *wapl-1*

mutants display phenotypes that are consistent with *wapl-1* playing a role in *C. elegans* development. Whilst the larval stages and very young adults appear normal on the plate, as the worms age they become increasingly less healthy. Older worms have a vulva defect, which prevents them from laying eggs causing accumulation of eggs and larval worms inside the hermaphrodites. They also exhibit slight morphological and locomotion defects, with some worms displaying uncoordinated *(unc*) and dumpy *(dpy)* phenotypes. This maybe because the vulva defect causes them to fill up with eggs, or it may be a genuine result of the *wapl-1* mutation. Importantly, there is some indication that *wapl-1* mutants may have meiotic defects based on their plate phenotype. They have a very small brood size and reduced viability, with 55.6 eggs laid compared with 300 in wild-type controls, and 3.9% embryonic lethality compared with 0.5%, as well as a larval lethality of 10.5% versus 0% in controls. Brief DAPI staining of *wapl-1* adult worms reveals that in terms of gross chromatin morphology, the germline appears normal, with a normal length transition zone, pachytene nuclei with chromatin forming thick organised tracts and diakinesis oocytes with 6 regular looking bivalents. Therefore the decrease in viability in *wapl-1* worms does not originate from defects in CO formation and may instead be due to segregation errors occurring in either the first or second meiotic division. One noticeable difference between wild type and *wapl-1* germlines is that they tend to be much shorter in length and have a very abrupt transition from late pachytene to diakinesis. In addition to this, *wapl-1* germlines occasionally have meiotic progression defects whereby distal to the diakinesis oocytes there are a population of nuclei with characteristic pachytene morphology. In other organisms *wapl-1* has been shown to affect gene expression and this may also be the cause of the phenotypes observed in the *C. elegans* germlines (Verni et al., 2000).

6.3 Removal of WAPL-1 improves cohesin defects in *rec-8* mutants

In the previous chapter, we saw that SCC is severely affected in *rec-8* mutants, that in *rec-8;spo-11* double mutants SCC is abolished and that in *rec-8;syp-2*

double mutants both SCC and DSB repair are highly compromised. This is distinct from mutant combinations containing *coh-3;coh-4*, in which cohesion remains intact, suggesting that REC-8 containing cohesin complexes are more efficient in providing cohesion and have a more crucial role in DSB repair than those containing COH-3/4. In order to assess whether WAPL-1 has any role in cohesin removal, or acts as a cohesin anti-establishment factor during meiotic prophase, I combined the *tm1814* allele of *wapl-1* with these three SCC deficient mutants (*rec-8, rec-8;spo-11, rec-8;syp-2)*, to determine whether they show any signs of improved cohesion in the absence of WAPL-1.

6.3.1 *rec-8;spo-11;wapl-1*

I began by looking at *rec-8;spo-11;wapl-1* triple mutants as its WAPL-1 containing counterpart (*rec-8;spo-11)* shows the most complete loss of SCC and because DSBs are not present to confound the analysis. Initial examination of the gross morphological phenotype of *rec-8;spo-11;wapl-1* by DAPI staining revealed a striking improvement in the diakinesis phenotype, with the number of DAPI bodies reducing from approximately 24 individual sister chromatids in *rec-8;spo-11* to approximately 12 univalents in *rec-8;spo-11;wapl-1* (Fig. 41D-E). In addition to this, and unlike *rec-8;spo-11*, *rec-8;spo-11;wapl-1* has no extended transition zone (Fig. 41A, 33A and 47A). The phenotype in pachytene is also improved with the chromatin tracts appearing more compact and defined (Fig. 41A, 33A and 47A).

Immunostaining *rec-8;spo-11;wapl-1;coh-3* quadruple mutants carrying the *coh-3::mCherry* transgene with α-RFP antibodies showed COH-3 decorating the axial element of nuclei throughout prophase I, in a manner almost identical to that seen in *rec-8;spo-11* double mutants (Fig. 41A). In diakinesis oocytes COH-3 can be seen on univalents, however, it demonstrates a different pattern from REC-8 staining seen in *coh-3;coh-4* univalents. COH-3 covers the chromatin in a somewhat diffuse manner in *rec-8;spo-11;wapl-1* diakinesis oocytes, rather than only localising to the interface between the two sisters as REC-8 is presumed to do in *coh-3;coh-4* double mutant oocytes (Fig. 41C). Perhaps in the absence of

WAPL-1, COH-3/4 are loaded precociously or not properly removed from chromosomes in diakinesis oocytes, or it is possible that COH-3/4 containing cohesin complexes bind to different regions of chromatin than those containing REC-8.

As shown in the previous chapter, in *rec-8;spo-11* double mutants SMC-1 is lost from chromatin during late pachytene/diplotene, rather displaying only nucleoplasmic localisation, unlike COH-3 which remains loaded to chromosomes throughout prophase (Fig. 33 and 34). This suggests a possible explanation for the presence of individualised sisters in *rec-8;spo-11* double mutants. In *rec-8;spo-11;wapl-1*, in which the diakinesis oocytes have univalents, one would expect to see SMC-1 loaded to chromatin to provide the cohesion required to hold the structure of univalents together. To test this, whole mount *rec-8;spo-11;wapl-1* germlines were stained with α-SMC-1 antibodies. From this we can see that SMC-1 is retained on chromosomes throughout diplotene and diakinesis in a pattern that seems identical to that of COH-3, with a more dispersed staining over the DAPI masses and a loss of localisation to chromosomes between final and penultimate diakinesis oocytes (known as the -1 and -2 oocytes, respectively), as will be discussed later (Fig. 42). This data suggests that a cohesin complex containing SMC-1 and COH-3/4 is providing the cohesion that is holding the univalents in *rec-8;spo-11;wapl-1* diakinesis oocytes together, and furthermore that it is the *wapl-1* mutation that is enabling this to happen.

6.3.2 *rec-8;wapl-1*

I have shown that removing WAPL-1 can ameliorate the SCC defects seen in *rec-8;spo-11* mutants. One would expect then that this would also improve the phenotype of *rec-8* mutants. I therefore generated a *rec-8;wapl-1;coh-3* triple mutant carrying the *coh-3::mCherry* transgene in order to determine whether there is an improvement in chromatin morphology throughout prophase but particularly in diakinesis, and to assess COH-3 loading to chromatin. Whole mount staining of these germlines with DAPI and α-RFP does show an

improvement between the phenotype of *rec-8;wapl-1* (Fig. 43, 48A) compared with *rec-8* (Fig. 27), however it is less marked than the difference between *rec-8;spo-11* and *rec-8;spo-11;wapl-1.* In *rec-8;wapl-1* germlines there is no extended transition zone, as is the case in *rec-8* (Fig. 43A and 27A) and pachytene nuclei have very compact chromatin tracts, more so even than those of wild type (Fig. 43B and 27B), perhaps suggesting that *wapl-1* also plays a role in chromosome compaction. This can be even more clearly seen when looking at the COH-3 expression pattern in pachytene nuclei in this mutant (Fig. 43B) versus controls (Fig. 24A). The tracks appear very short by comparison and perhaps thicker too. However, in diakinesis the situation is not so clear. *rec-8;wapl-1* diakinesis oocytes have only a modest reduction in the number of DAPI masses, decreasing from almost 19 in *rec-8* to approximately 14 in *rec-8;wapl* double mutants (Fig. 43D). Analysis of the types of DAPI masses seen reveals that the percentage frequency of sister chromatids drops from 0.43 in *rec-8* to 0.23 in *rec-8;wapl*, whereas the percentage frequency of univalents increases from 0.18 to 0.36. As mentioned in Section 5.4.3.1, because the link between adjacent sister chromatids in the *rec-8* bi-lobed univalents is very tenuous, cell CellProfiler identifies them as two sisters, rather than as a univalent. Therefore the reduction in percentage frequency of sister chromatids and increase in percentage frequency of univalents in *rec-8;wapl* indicates that the structure of its univalents are more rounded and less bi-lobed than those of it's *rec-8* counterpart (Fig. 43E). Since I have shown that *rec-8* is required for DSB repair, it may be that the presence of persistent DSBs in *rec-8;wapl* mutants will compromise the chromosome structure, despite the increased cohesiveness of the COH-3/4 cohesin complexes on chromosomes.

6.3.3 *rec-8;syp-2;wapl-1*

In the previous two sections we have seen that removing WAPL-1 in cohesion-deficient mutants can improve their phenotype. To further test this, I constructed a *rec-8;syp-2;wapl-1;coh-3* quadruple mutant carrying the *coh-3::mCherry* transgene to assess chromatin morphology and COH-3 loading. As mentioned, the *rec-8;syp-2* mutant has a very severe phenotype with an

extended transition zone, pachytene nuclei with highly disorganised chromatin, and diakinesis oocytes with large numbers of small irregular DAPI masses and a high degree of fragmentation (Fig. 35). Removal of WAPL-1 from *rec-8;syp-2* double mutants improves all of these phenotypes to a great degree (Fig 44 and 47A). Nuclei in pachytene have short, dense, ordered tracts of chromatin and α-RFP staining to show COH-3 loading highlights the extent of the difference. Whereas in *rec-8;syp-2* pachytene nuclei COH-3 staining shows a tangle of extremely thin and highly discontinuous tracks, in *rec-8;syp-2;wapl-1* nuclei COH-3 staining is highly ordered, with short, thick and more continuous tracks loaded to chromatin (Fig. 44B).

Whilst an improvement in the phenotype in pachytene is perhaps to be expected, given the previous data, the sheer degree of this improvement is somewhat surprising. In *syp-2* mutants, in which no synapsis occurs, one can see organised tracts in pachytene nuclei, however these are much longer and thinner than those of wild type, as homologue pairs are not tightly juxtaposed to one another. This pachytene phenotype is more severe than that seen in *rec-8* mutants. One would expect that any improvement in the phenotype of *rec-8;syp-2;wapl-1* triple mutants would push it to appear more like the *syp-2* single mutant, as it would affect SCC and not synapsis. This is clearly not the case, with *rec-8;syp-2;wapl-1* pachytene nuclei bearing far more in common with wild-type chromosome morphology. A possible explanation for this is that COH-3 is capable of acting in an SC-like manner and that without a component of the CE, and without WAPL-1 to counteract its loading, it provides precocious cohesion between homologues, as well as presumably between sister chromatids. Finally, in the diakinesis oocytes of *rec-8;syp-2;wapl-1* worms we see univalents rather than a mixture of small DAPI masses and fragments (Fig. 44C-E), likely demonstrating SCC improvement brought about by the absence of WAPL-1. Given this, it is perhaps surprising that in *rec-8;wapl-1* mutant diakinesis oocytes there is not a greater improvement with respect to *rec-8*, as DSB repair should also be impaired in *rec-8;syp-2* double mutants. It may be that loading COH-3 inappropriately, which may occur to a greater degree in the absence of

SYP-2, enables maintenance of better chromosome structure, perhaps by conferring a greater ability to repair DSBs (See Section 6.6).

In all three of these experiments I have assumed that removing WAPL-1 is increasing the cohesive properties of COH-3/4 containing cohesin complexes. However, as previously mentioned SCC-1 and COH-1 have both been suggested to play a role during meiotic prophase (Mito et al., 2003; Pasierbek et al., 2001), and so it is possible that WAPL-1 acts through them as well. In order to test this, I checked the diakinesis phenotype of *rec-8;coh-3;coh-4;spo-11;wapl-1* quintuple mutants. If WAPL-1 acts through SCC-1 and COH-1 one would expect to see univalents, in a phenotype similar to *rec-8;spo-11;wapl-1*, however if it acts through COH-3/4 the phenotype should be that of individualised sister chromatids, as is the case in *rec-8;spo-11*. The latter scenario is observed, suggesting that WAPL-1 mediates the cohesiveness of COH-3/4 containing cohesin complexes. It is important to note that none of this data excludes the possibly that WAPL-1 could operate on REC-8 containing cohesin complexes as well.

6.4 Removal of WAPL-1 improves defects in *syp-2* mutants

The observations in the section above indicated that COH-3 might be able to load where the SC would normally be assembled in the absence of SYP-2. If this is the case, then we would expect the phenotype of *syp-2;wapl-1* to be better than that of *syp-2* alone. To test this, I built *syp-2;coh-3* double mutants and *syp-2;wapl-1;coh-3;* triple mutants each carrying the *coh-3::mCherry* transgene and stained whole mounted germlines with DAPI and α-RFP antibodies and counterstained them with α-HIM-3 antibodies to visualise the AE of the SC. From this we can see that, as expected in the *syp-2* single strain HIM-3 and COH-3 colocalize on the axis of unsynapsed homologues, forming very thin tracks that correspond to individualised axial elements (Fig. 45A and 45B). The difference between this and the *syp-2;wapl-1* strain is clear. HIM-3 and COH-3 also colocalize in these germlines, however the tracks themselves are much

shorter and thicker, indistinguishable from wild type, suggesting that they represent two juxtaposed axial elements (Fig. 46A-B and 48B). In diakinesis oocytes univalents are present in both *syp-2* and *syp-2;wapl-1* mutants (Fig. 45C, 46C and 48B). It therefore appears that without WAPL-1 to restrain it and in the absence of a CE component, COH-3 can act to apparently bind homologues together, but that this structure is not capable of promoting COs at least in the absence of CE components.

6.5 WAPL-1 independent cohesin removal

In the previous section we have seen data that strongly suggests that WAPL-1 acts in preventing the establishment of, or counteracting the maintenance of cohesion provided by complexes containing COH-3 and COH-4. However, antibody staining from this and the previous chapter, as well as the *scc-2* RNAi experiments, have indicated that cohesin complexes are lost or removed from chromatin during meiotic prophase.

6.5.1 COH-3/4 loss at diakinesis

Whilst analysing the SCC deficient strains and their *wapl-1* mutant background counterparts discussed previously, two observations became apparent: that the phenotypes of the final and penultimate diakinesis oocytes (known as -1 and -2, respectively) are not the same, with the -1 oocytes appearing worse, and that the levels of COH-3 decreases concurrently with this. I undertook to compare the -1 and -2 phenotypes using the analysis pipeline discussed earlier to quantify the change in the areas of DAPI stained bodies in diakinesis oocytes (Section 5.4.3.1). Additionally, I stained these germlines with α-COH-3 antibodies in order that I could compare the COH-3 loss in adjacent -1 and -2 diakinesis oocytes from the same germline. From the staining of these diakinesis oocytes one can see a clear reduction in the amount of COH-3 on chromatin between -1 and -2 in all strains (Fig. 47). It is plausible that this loss of COH-3 in the -1 diakinesis oocyte is in preparation for the first meiotic division. In wild-type worms COH-3 is lost from the long arm of bivalents (Fig.

24D) and it has been suggested that all COH-3 is cleaved during MI enabling homologues to separate (Severson et al., 2009). In the mutants tested, where there is no bivalent structure it may be that COH-3 removal becomes dysregulated. This would explain why in *rec-8;spo-11* -1 diakinesis oocytes one clearly sees some sister chromatids with significant COH-3 staining and others with none visible (Fig. 33C). Irrespective of this, the fact that there is a reduction in both *wapl-1* positive and negative strains suggests that a WAPL-1-independent pathway removes COH-3 containing cohesin complexes before metaphase I.

6.5.2 COH-3/4 loss in response to DSBs

In the subsequent section I will discuss the impact of WAPL-1 on DSB repair. Briefly, the ability of strains, in the presence and absence of WAPL-1, to respond to DNA damage was tested by analysing their diakinesis phenotype subsequent to γ-IR. However during this analysis, in addition to DAPI staining, germlines were also stained with α-RFP antibodies to detect COH-3 loading. When compared with their unirradiated equivalents one can observe a difference in the staining. Whereas in the *rec-8* single mutant*, rec-8;wapl-1, rec-8;spo-11* double mutant and *rec-8 spo-ll;wapl-1* triple mutant unirradiated strains COH-3 forms clear continuous tracks, after a dose of 100Gy γ-IR these tracks become discontinuous, forming a punctate pattern (Fig. 49). It is possible that this indicates COH-3 removal in response to DNA damage and that this removal is independent of WAPL-1, however further investigation is required to clarify this point.

6.6 DSB repair in *wapl-1* mutants

Cohesin has been shown to play an important role in the repair of DSBs in mitosis (Sjogren and Nasmyth, 2001) (Strom et al., 2004; Unal et al., 2007) (McAleenan et al., 2013). The irradiation data in chapter 5 suggests that in *C. elegans* REC-8 but not COH-3/4 act in the repair of meiotic DSBs. However, in the absence of WAPL-1 it appears that cohesin complexes containing COH-3/4

can provide a greater cohesive force. In this section I sought to address the hypothesis that in making COH-3/4 more cohesive by removing WAPL-1, they might gain some function in undertaking DSB repair.

6.6.1 DSBs in *rec-8;syp-2* versus *rec-8;syp-2;wapl-1*

The data in the sections above demonstrates that in the absence of WAPL-1 the diakinesis phenotype of cohesion-deficient mutants is improved, suggesting that removing WAPL-1 improves SCC. In particular the difference between *rec-8;syp-2* and *rec-8;syp-2;wapl-1* diakinesis oocytes shows a vast improvement with regards to the number of fragments, which is significantly reduced in *rec-8;syp-2;wapl-1* triple mutants. This could indicate that fewer DSBs are made, or their repair can occur more efficiently, in the absence of WAPL-1.

In order to assess whether the absence of fragments in *rec-8;syp-2;wapl-1* diakinesis oocytes might be due to a reduction in the number of repaired DSBs, whole mount *rec-8;syp-2;wapl-1* germlines were immunostained with α-RAD-51 antibodies to monitor the number of recombination intermediates, and counterstained with α-SMC-1 antibodies. From this we can see that the RAD-51 foci appear much later in prophase in *rec-8;syp-2;wapl-1* than in *rec-8;syp-2* mutants (Fig. 50A and 36A). In addition to this the number of foci is greatly reduced in the *rec-8;syp-2;wapl-1* mutant (Fig. 51), although in both mutants the foci persist until diplotene. This suggests that in the absence of WAPL-1 either fewer DSBs are made, and/or that breaks are repaired more efficiently and therefore do not accumulate to the same extent. Interestingly, the SMC-1 staining shows that in *rec-8;syp-2;wapl-1* mutants there is a delay in SMC-1 loading, compared with *rec-8;syp-2*, with tracks becoming visible in early pachytene and transition zone, respectively (Fig. 50A and 36A). This is particularly surprising as COH-3 is clearly expressed in transition zone nuclei in *rec-8;syp-2;wapl-1* germlines. This indicates that COH-3 may not always act in a complex with SMC-1 and also that SMC-1 loading might be impaired in the absence of WAPL-1.

6.6.2 γ-IR

We have seen in the previous chapter that irradiation of strains carrying the *rec-8* mutation causes high levels of fragmentation in diakinesis oocytes. If the removal of WAPL-1 enables COH-3/4 to take part in DSB repair, one would expect that *rec-8* mutant strains combined with the *wapl-1* mutation would have an improved diakinesis phenotype after irradiation than those with a wild type copy of *wapl-1*. In order to test this, *rec-8*, *rec-8;wapl-1*, *rec-8;spo-11* and *rec-8;spo-11;wapl-1* young adults were irradiated with 100Gy of γ-IR. These worms were dissected at 30 hours post irradiation, stained with DAPI and imaged on the DeltaVision. These images were analysed as in the previous chapter, with the z-stacks cropped to the size of an individual nucleus and maximum intensity projections made using Fiji ImageJ, and these cropped images analysed with CellProfiler to determine the number and type of DAPI mass per nucleus. The DAPI staining alone reveals a difference in diakinesis phenotype (Fig. 52E) and from the image analysis we can see that the number of DAPI masses per nucleus decreases in both *wapl-1* mutants compared with their *wapl-1*-positive counterparts (Fig. 52A). The more detailed analysis of DAPI-mass type reveals that in the absence of WAPL-1 the percentage frequency of fragments lessens slightly, likely indicating that the amount of persistent DNA damage is reduced (Fig. 52B-D). For this analysis -1 and -2 diakinesis oocytes were grouped together, however I also carried out the analysis only comparing -2 oocytes, to mitigate any possible effect of COH-3 loss between these two stages. In this case the improvement in diakinesis phenotype was even greater than in the joint analysis, with the percentage frequency of fragments falling by approximately a quarter and a third between *rec-8* and *rec-8;wapl-1*, and *rec-8;spo-11* and *rec-8;spo-11;wapl-1* respectively (Fig. 53B and C). This indicates that without WAPL-1, DSB repair can occur more efficiently, perhaps mediated by improved SCC provided by COH-3/4 cohesin complexes.

6.7 Summary of results

WAPL-1 has been shown to be responsible for cohesin removal in mitotic prophase (Nishiyama et al., 2010) and also to act a cohesion anti-establishment

factor (Lopez-Serra et al., 2013). The data in this chapter also implicates WAPL-1 as playing a similar role in meiosis. The absence of WAPL-1 in *rec-8, rec-8;spo-11* and *rec-8;syp-2* mutants causes an improvement in their chromatin morphology. In *wapl-1* mutant background the chromatin of pachytene nuclei appears more compacted, forming short thick tracts than when WAPL-1 is present. Furthermore, whilst these mutants display a severe defect in SCC in diakinesis oocytes, in their *wapl-1* mutant equivalents this appears to be greatly ameliorated, with a reduction in the number of fragments and a shift from individualised sister chromatids to univalents. These two results strongly suggest that in the absence of WAPL-1 SCC is improved. As this does not occur when COH-3/4 are removed, we assume that WAPL-1 is acting on cohesin complexes containing these two α-kleisins. COH-3 loading occurs in all the analysed mutants lacking *rec-8*, suggesting that WAPL-1 plays a role in preventing cohesion maintenance of COH-3/4 containing complexes. This is supported by the observation that without WAPL-1 these strains appear to display less unrepaired DNA damage after irradiation, which one might expect following an improvement of SCC. It also appears that in the absence of both WAPL-1 and SYP-1, COH-3 can act in a manner that seems to provide synapsis as well as cohesion between chromosomes. Finally, we have shown COH-3 removal occurs between -2 and -1 diakinesis oocytes and possibly in response to DSBs. This further demonstrates the complex regulation of cohesin dynamics in meiotic prophase.

For a table comparing a summary of the phenotypes observed in *wapl-1* rescue strains and those mutants analysed in the previous chapter, see Table 6 on pages 194-195.

Figure 41. Characterisation of *rec-8;spo-11;wapl-1* triple mutants carrying *coh-3::mCherry* transgene

A Whole mount of *rec-8;spo-11;wapl-1;coh-3;coh-3::mCherry* germline stained with α-RFP antibodies counterstained the DAPI, showing COH-3::mCherry loaded to chromatin, decorating the axial element from transition zone onwards, forming short thick tracts.

B Magnification showing mid pachytene nuclei

C Diakinesis oocyte from *rec-8;spo-11;wapl-1* showing regular shaped univalents (unlike separated sisters seen in *rec-8;spo-11* mutants), with COH-3::mCherry localising to chromatin.

D Graph showing the average number of DAPI masses in diakinesis oocytes of *rec-8;spo-11;wapl-1* versus *rec-8;spo-11* mutants, showing a decrease in the average number of DAPI masses in *rec-8;spo-11;wapl-1*, indicating that in absence of WAPL-1 SCC is improved.

E Graph showing CellProfiler analysis of DAPI mass area in diakinesis oocytes of *rec-8;spo-11;wapl-1* versus *rec-8;spo-11* mutants a decrease in the percentage frequency of separated sister chromatids and an increase in the percentage frequency of univalents in *rec-8;spo-11;wapl-1* compared with *rec-8;spo-11*, supporting the theory that in absence of WAPL-1 SCC is improved.

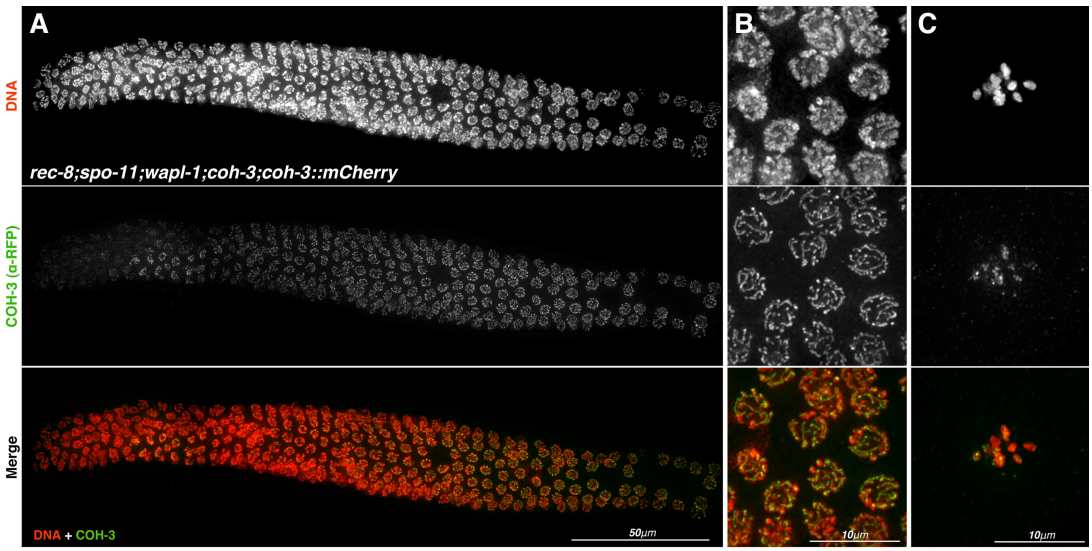
A
B
C
DNA
COH-3 (α-RFP)
Merge
rec-8;spo-11;wapl-1;coh-3;coh-3::mCherry
DNA + COH-3
50μm
10μm
10μm

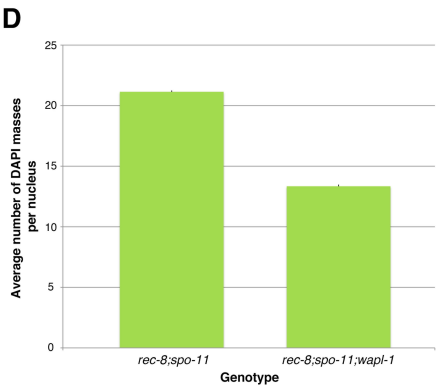
D
Average number of DAPI masses per nucleus
25
20
15
10
5
0
rec-8;spo-11
rec-8;spo-11;wapl-1
Genotype

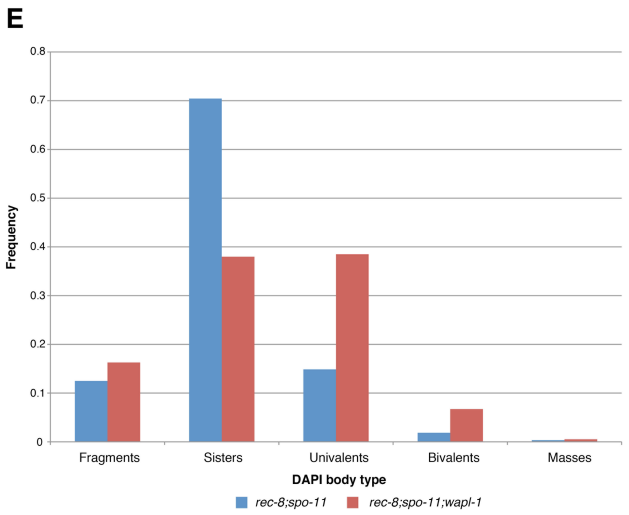
E
Frequency
0.8
0.7
0.6
0.5
0.4
0.3
0.2
0.1
0
Fragments
Sisters
Univalents
Bivalents
Masses
DAPI body type
rec-8;spo-11
rec-8;spo-11;wapl-1

Figure 42. Localisation of SMC-1 in *rec-8;spo-11;wapl-1;coh-3;coh-3::mCherry* germlines

A Whole mount of *rec-8;spo-11;wapl-1;coh-3;coh-3::mCherry* germline stained with α-SMC-1 antibodies counterstained with DAPI, showing SMC-1 loaded to chromatin, decorating the axial element from transition zone onwards

B Magnification showing mid pachytene nuclei

C Diplotene nucleus showing SMC-1 localising to all chromosomes.

D Diakinesis oocyte showing some chromatin-associated SMC-1.

A
B
C
D
rec-8;spo-11;wapl;coh-3;coh-3::mCherry
DNA + SMC-1
50μm
10μm
10μm
10μm
DNA
SMC-1
Merge

Figure 43. Characterisation of *rec-8;wapl-1* double mutants carrying *coh-3::mCherry* transgene

A Whole mount of *rec-8; wapl-1;coh-3;coh-3::mCherry* germline stained with α-RFP antibodies counterstained the DAPI, showing COH-3::mCherry loaded to chromatin, decorating the axial element from transition zone onwards, forming short thick tracts.

B Magnification showing mid pachytene nuclei

C Diakinesis oocyte from *rec-8;spo-11;wapl-1* showing more regular shaped univalents (unlike the bi-lobed univalents seen in *rec-8* mutants), with COH-3::mCherry localising to chromatin.

D Graph showing the average number of DAPI masses in diakinesis oocytes of *rec-8;wapl-1* versus *rec-8* mutants, showing a decrease in the average number of DAPI masses in *rec-8;spo-11;wapl-1*, indicating that in absence of WAPL-1 SCC is improved.

E Graph showing CellProfiler analysis of DAPI mass area in diakinesis oocytes of *rec-8;spo-11;wapl-1* versus *rec-8;spo-11* mutants a decrease in the number of separated sister chromatids and an increase in the number of univalents in *rec-8;wapl-1* compared with *rec-8* mutants, supporting the theory that in absence of WAPL-1 SCC is improved.

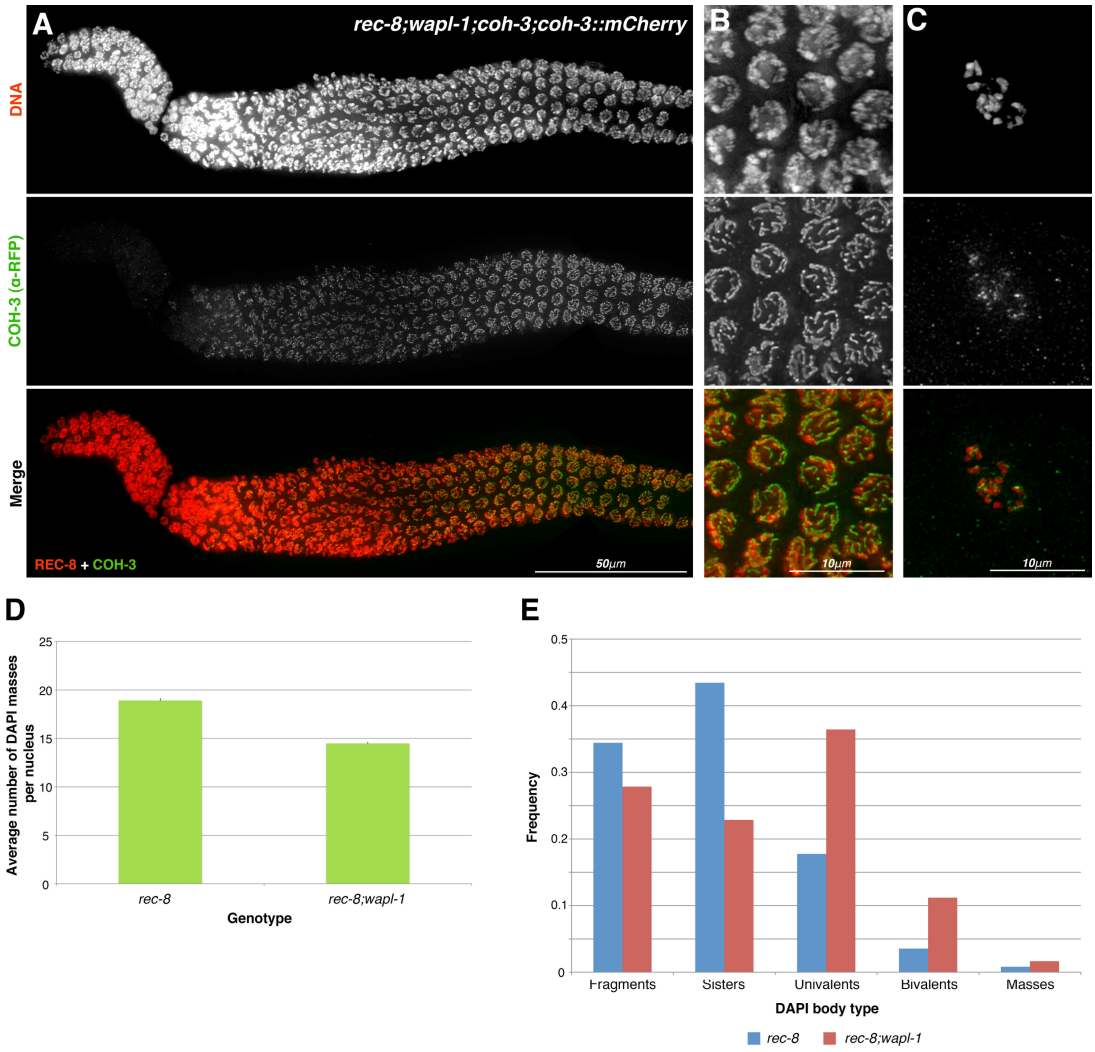
A
rec-8;wapl-1;coh-3;coh-3::mCherry
B
C
DNA
COH-3 (α-RFP)
Merge
REC-8 + COH-3
50μm
10μm
10μm
D
Average number of DAPI masses per nucleus
25
20
15
10
5
0
rec-8
rec-8;wapl-1
Genotype
E
Frequency
0.5
0.4
0.3
0.2
0.1
0
Fragments
Sisters
Univalents
Bivalents
Masses
DAPI body type
rec-8
rec-8;wapl-1

Figure 44. Characterisation of *rec-8;syp-2;wapl-1* triple mutants carrying *coh-3::mCherry* transgene

A Whole mount of *rec-8;syp-2;wapl-1;coh-3;coh-3::mCherry* germline stained with α-RFP antibodies counterstained the DAPI, showing COH-3::mCherry loaded to chromatin, decorating the axial element from transition zone onwards, forming short thick tracts.

B Magnification showing mid pachytene nuclei

C Diakinesis oocyte from *rec-8;syp-2;wapl-1* showing regular shaped univalents (unlike small irregular sister-sized masses and fragmentation seen in *rec-8;syp-2* mutants), with COH-3::mCherry localising to chromatin.

D Graph showing the average number of DAPI masses in diakinesis oocytes of *rec-8;syp-2;wapl-1* versus *rec-8;syp-2* mutants, showing a decrease in the average number of DAPI masses in *rec-8;syp-2;wapl-1*, indicating that in absence of WAPL-1 SCC is improved.

E Graph showing CellProfiler analysis of DAPI mass area in diakinesis oocytes of *rec-8;spo-11;wapl-1* versus *rec-8;spo-11* mutants a decrease in the number of fragments and separated sister chromatids, and an increase in the number of univalents in *rec-8;syp-2;wapl-1* compared with *rec-8;syp-2* mutants, supporting the theory that in absence of WAPL-1 SCC is improved.

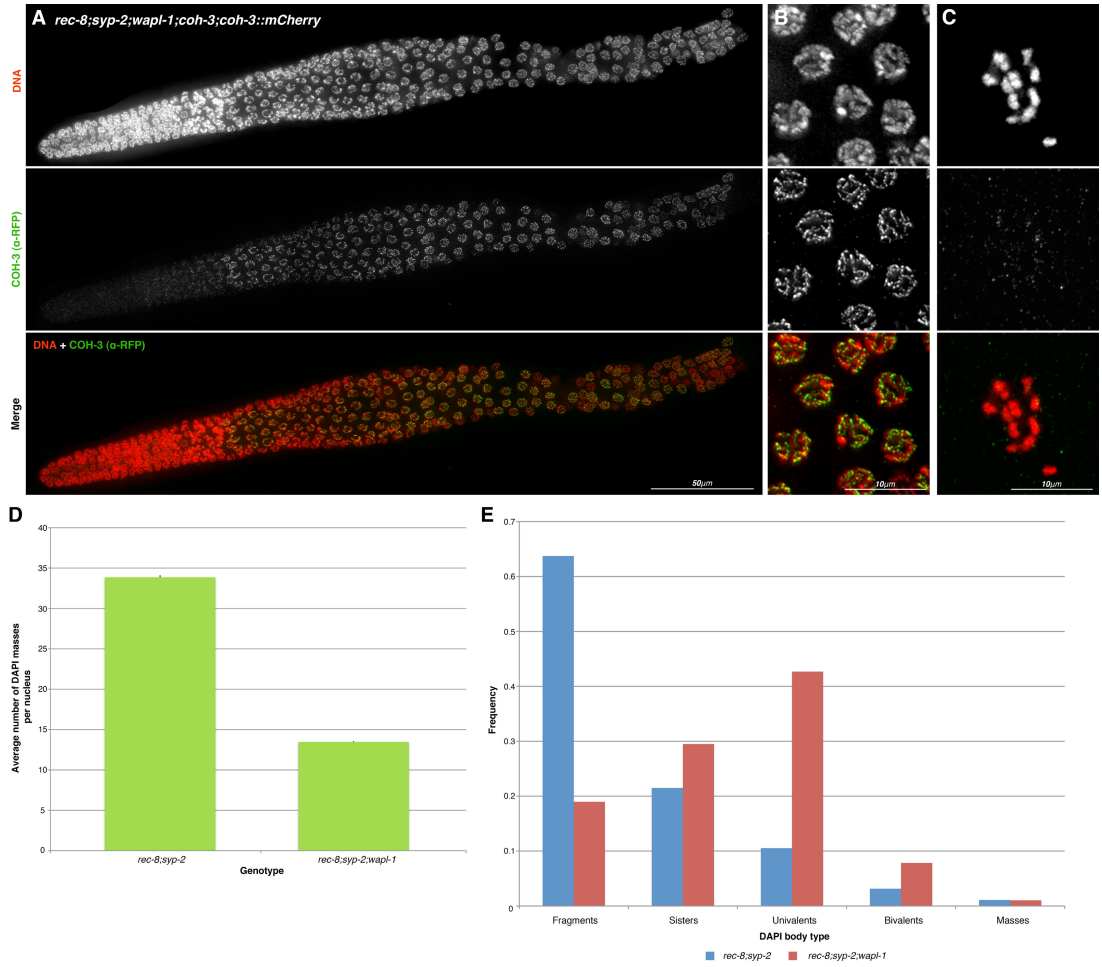
A rec-8;syp-2;wapl-1;coh-3;coh-3::mCherry
B
C
DNA
COH-3 (α-RFP)
DNA + COH-3 (α-RFP)
Merge
50μm
10μm
10μm
D
Average number of DAPI masses per nucleus
40
35
30
25
20
15
10
5
0
rec-8;syp-2
rec-8;syp-2;wapl-1
Genotype
E
Frequency
0.7
0.6
0.5
0.4
0.3
0.2
0.1
0
Fragments
Sisters
Univalents
Bivalents
Masses
DAPI body type
rec-8;syp-2
rec-8;syp-2;wapl-1

Figure 45. Localisation of COH-3::mCherry and HIM-3 in *syp-2;coh-3;coh-3::mCherry* germlines

A Whole mount of *syp-2;coh-3;coh-3::mCherry* germline stained with α-RFP and α-HIM-3 antibodies counterstained with DAPI, showing HIM-3 and COH-3::mCherry colocalising, loaded to chromatin, forming thin tracks.

B Magnification showing mid pachytene nuclei

C Diakinesis oocyte from *syp-2;coh-3;coh-3::mCherry* showing univalents.

A
B
C
syp-2;coh-3;coh-3::mCherry
DNA
COH-3 (α-RFP)
HIM-3
Merge
COH-3 (α-RFP) + HIM-3
50μm
10μm
10μm

Figure 46. Localisation of COH-3::mCherry in *syp-2;wapl-1;coh-3;coh-3::mCherry* germlines

A Whole mount of *syp-2;wapl-1;coh-3;coh-3::mCherry* germline stained with α-RFP and α-HIM-3 antibodies counterstained with DAPI, showing HIM-3 and COH-3::mCherry colocalising, loaded to chromatin, forming thick tracks, usually indicative of synapsis.

B Magnification showing mid pachytene nuclei

C Diakinesis oocyte from *syp-2;coh-3;coh-3::mCherry* showing univalents.

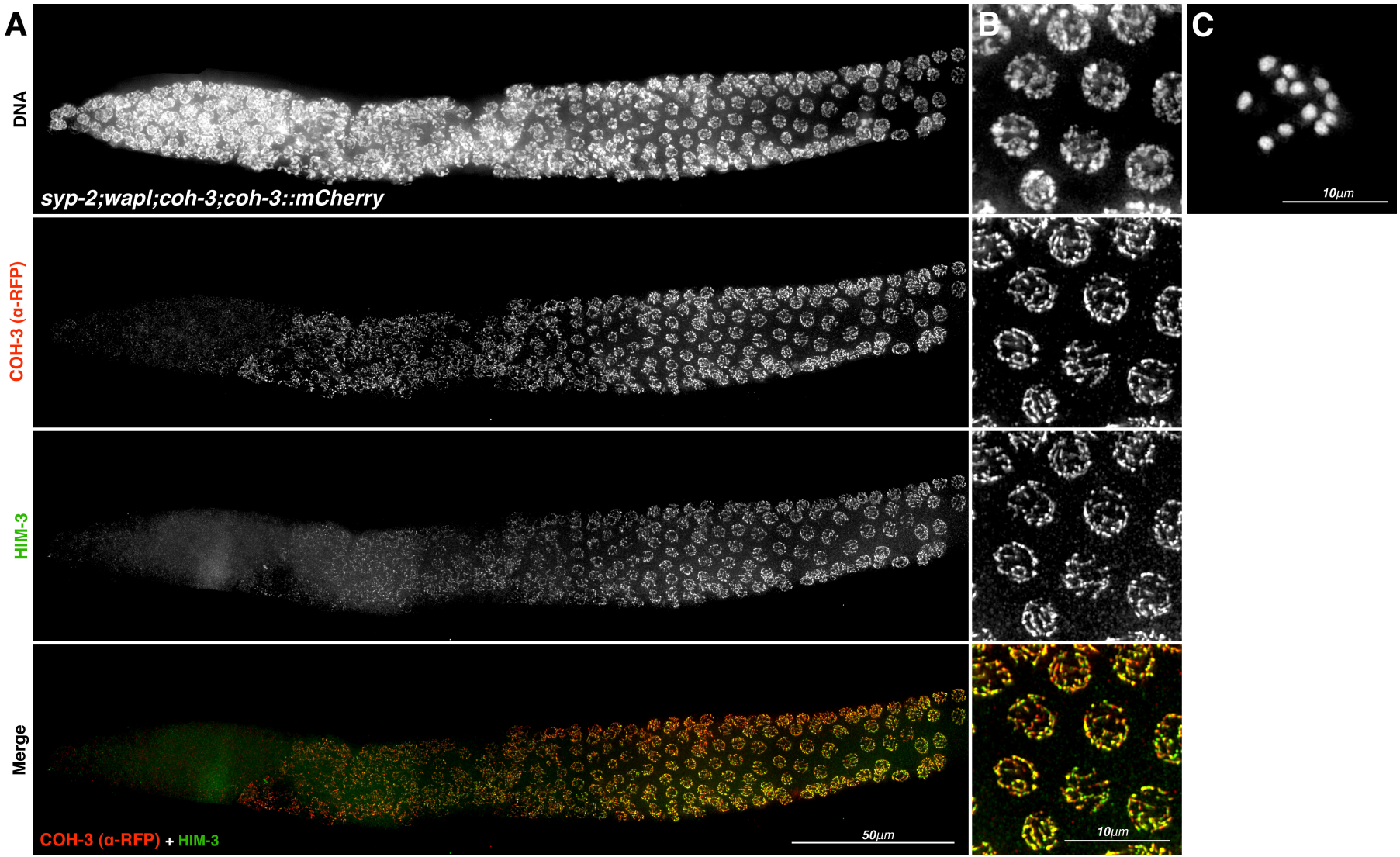
A
B
C
DNA
syp-2;wapl;coh-3;coh-3::mCherry
COH-3 (α-RFP)
HIM-3
Merge
COH-3 (α-RFP) + HIM-3
50μm
10μm
10μm

Figure 47. Removal of WAPL-1 improves phenotypes in SCC and SC deficient mutants

A Absence of WAPL-1 results in a decrease in the number of DAPI bodies seen in diakinesis oocytes of the SCC deficient mutants: *rec-8; rec-8;spo-11* and *rec-8;syp-2*, as well as a greater degree of compaction of chromatin in pachytene nuclei.

B Absence of WAPL-1 results in axial element and COH-3 staining suggestive of synapsis in the SC deficient mutant *syp-2*.

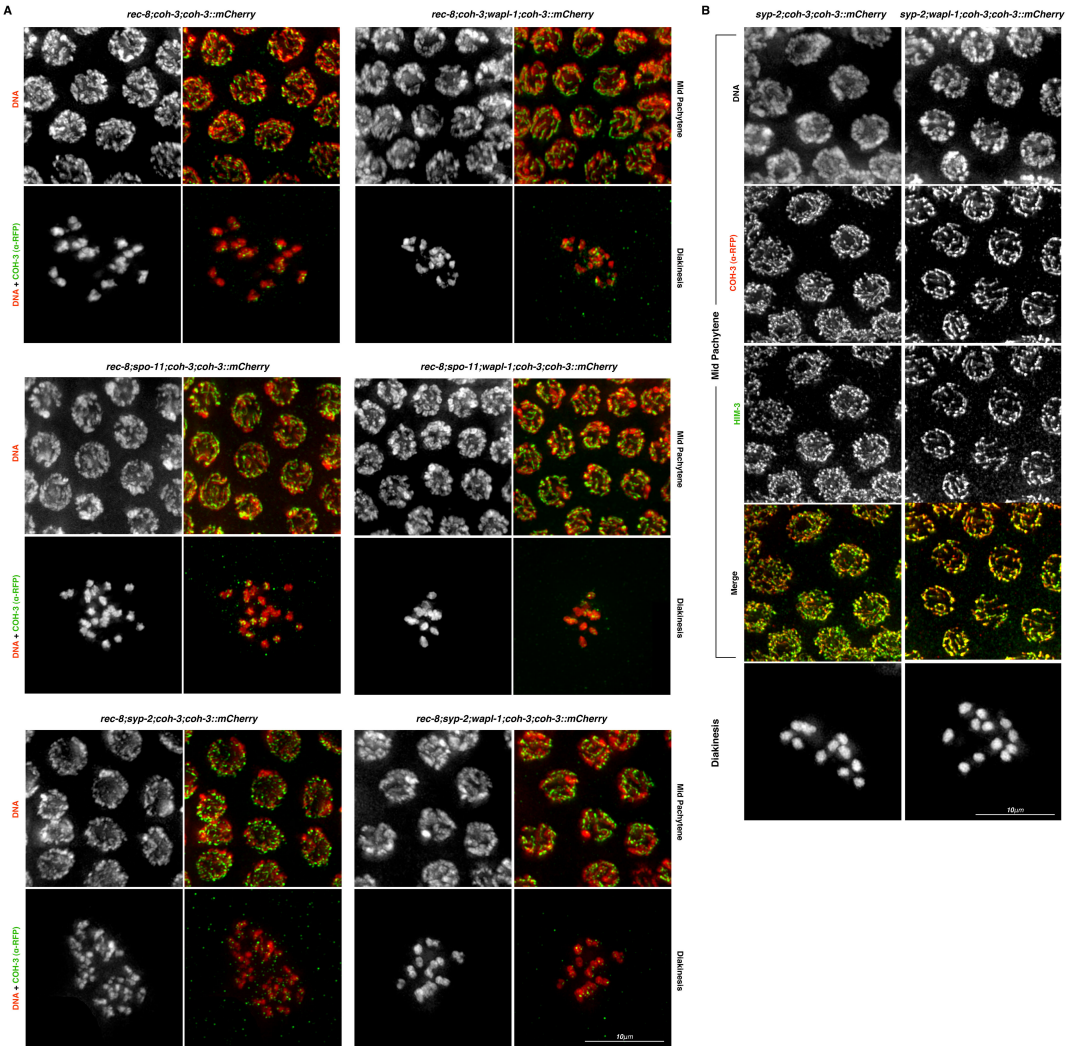
A
rec-8;coh-3;coh-3::mCherry
rec-8;coh-3;wapl-1;coh-3::mCherry
rec-8;spo-11;coh-3;coh-3::mCherry
rec-8;spo-11;wapl-1;coh-3;coh-3::mCherry
rec-8;syp-2;coh-3;coh-3::mCherry
rec-8;syp-2;wapl-1;coh-3;coh-3::mCherry
DNA
DNA + COH-3 (α-RFP)
Mid Pachytene
Diakinesis
10μm
B
syp-2;coh-3;coh-3::mCherry
syp-2;wapl-1;coh-3;coh-3::mCherry
Mid Pachytene
DNA
COH-3 (α-RFP)
HIM-3
Merge
Diakinesis
10μm

Figure 48. Loss of COH-3::mCherry localisation between -1 and -2 diakinesis oocytes

A -1 and -2 diakinesis oocytes from the same germline of *rec-8;coh-3;rec-8::GFP;coh-3::mCherry* controls showing a loss in COH-3 staining between the -2 and -1 stages

B -1 and -2 diakinesis oocytes from the same germline of SCC deficient mutants *rec-8, rec-8;spo-11* and *rec-8;syp-2,* showing a loss in COH-3 staining between the -2 and -1 stages, indicating that COH-3 has been lost from chromatin.

C -1 and -2 diakinesis oocytes from the same germline of SCC deficient mutants *rec-8, rec-8;spo-11* and *rec-8;syp-2,* in the absence of WAPL-1 showing a loss in COH-3 staining between the -2 and -1 stages, indicating that COH-3 has been lost from chromatin and that this occurs in a WAPL-1 independent manner.

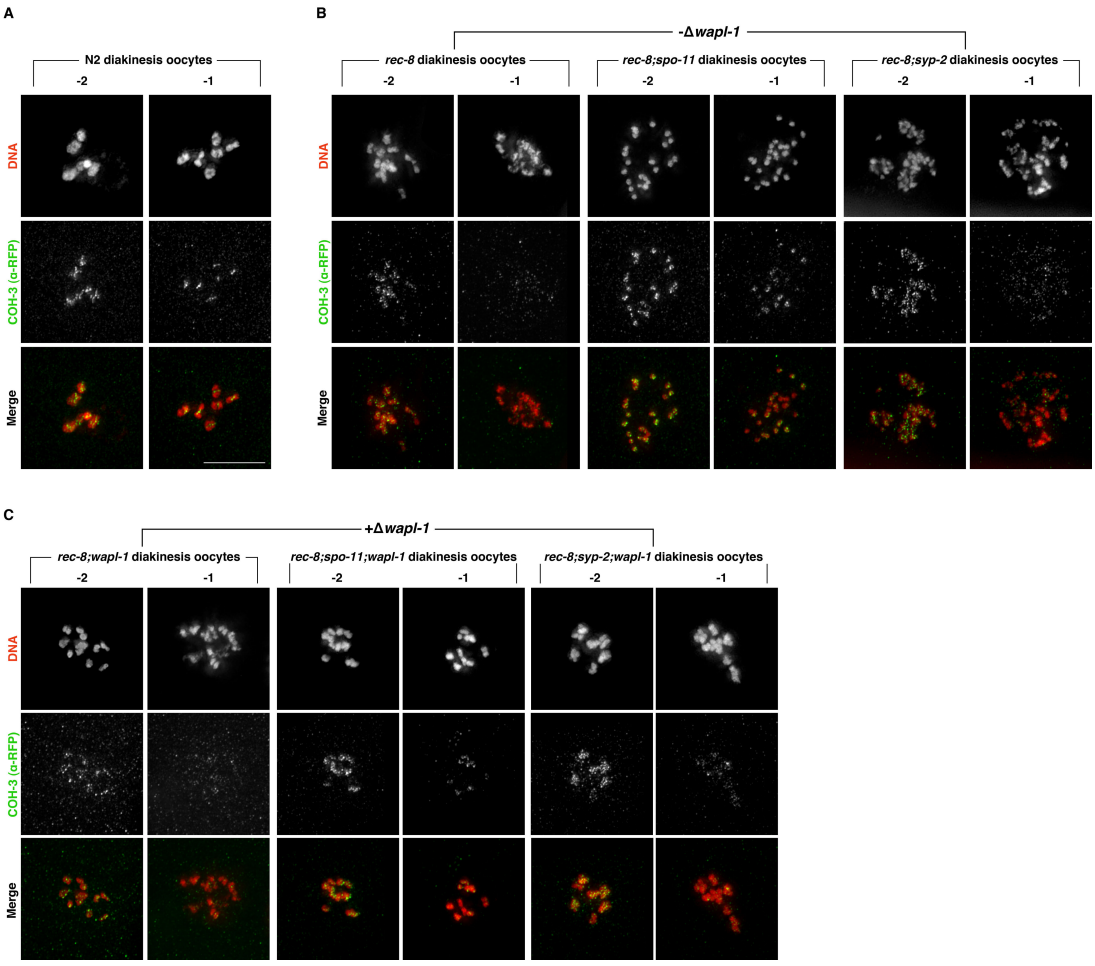
A
N2 diakinesis oocytes
-2
-1
DNA
COH-3 (α-RFP)
Merge
B
-Δwapl-1
rec-8 diakinesis oocytes
rec-8;spo-11 diakinesis oocytes
rec-8;syp-2 diakinesis oocytes
C
+Δwapl-1
rec-8;wapl-1 diakinesis oocytes
rec-8;spo-11;wapl-1 diakinesis oocytes
rec-8;syp-2;wapl-1 diakinesis oocytes

Figure 49. COH-3 loss in response to DSBs

γ-IR and non-irradiated pachytene nuclei in SCC deficient mutants, in the presence and absence of WAPL-1, stained with α-RFP and counterstained with DAPI, showing continuous tracks in non-irradiated nuclei, but punctate staining in all irradiated nuclei, suggesting that COH-3 may be

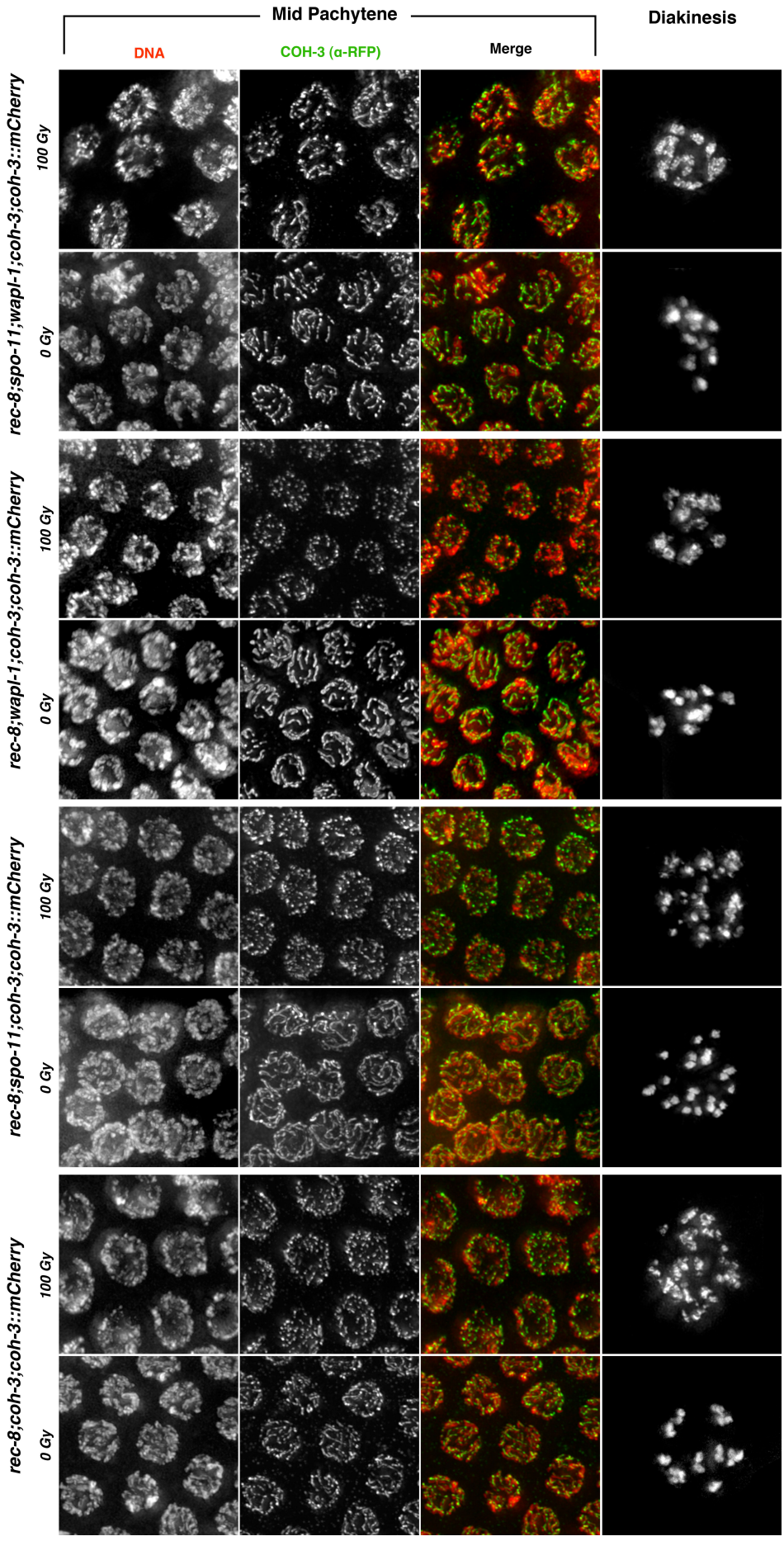

removed in response to DSBs.

Figure 50. Localisation of SMC-1 and RAD-51 in *rec-8;syp-2;wapl-1;coh-3;coh-3::mCherry* germlines

A Whole mount of *rec-8;syp-2;wapl-1;coh-3;coh-3::mCherry* germline stained with α-SMC-1 and α-RAD-51 antibodies, counterstained with DAPI, showing SMC-1 loaded to chromatin, forming tracks and some accumulation of recombination intermediates in pachytene nuclei, indicating an impairment of DSB repair.

B Magnification showing mid pachytene nuclei

C Diakinesis oocyte from *rec-8;syp-2;wapl-1* showing regular shaped univalents (unlike small irregular sister-sized masses and fragmentation seen in *rec-8;syp-2* mutants), suggesting that DSB repair is occurring.

A
rec-8;syp-2;wapl-1;coh-3;coh-3::mCherry
B
C
DNA
SMC-1
RAD-51
Merge
DNA + SMC-1 + RAD-51
50μm
10μm
10μm

Figure 51. Removal of WAPL-1 improves DSB repair in *rec-8;syp-2* mutants

Comparison of levels of RAD-51 foci in rec-8;syp-2 and rec-8;syp-2;wapl-1 pachytene nuclei, revealing significantly fewer foci in rec-8;syp-2;wapl-1 suggesting that DSB repair occurs more efficiently in the absence of WAPL-1.

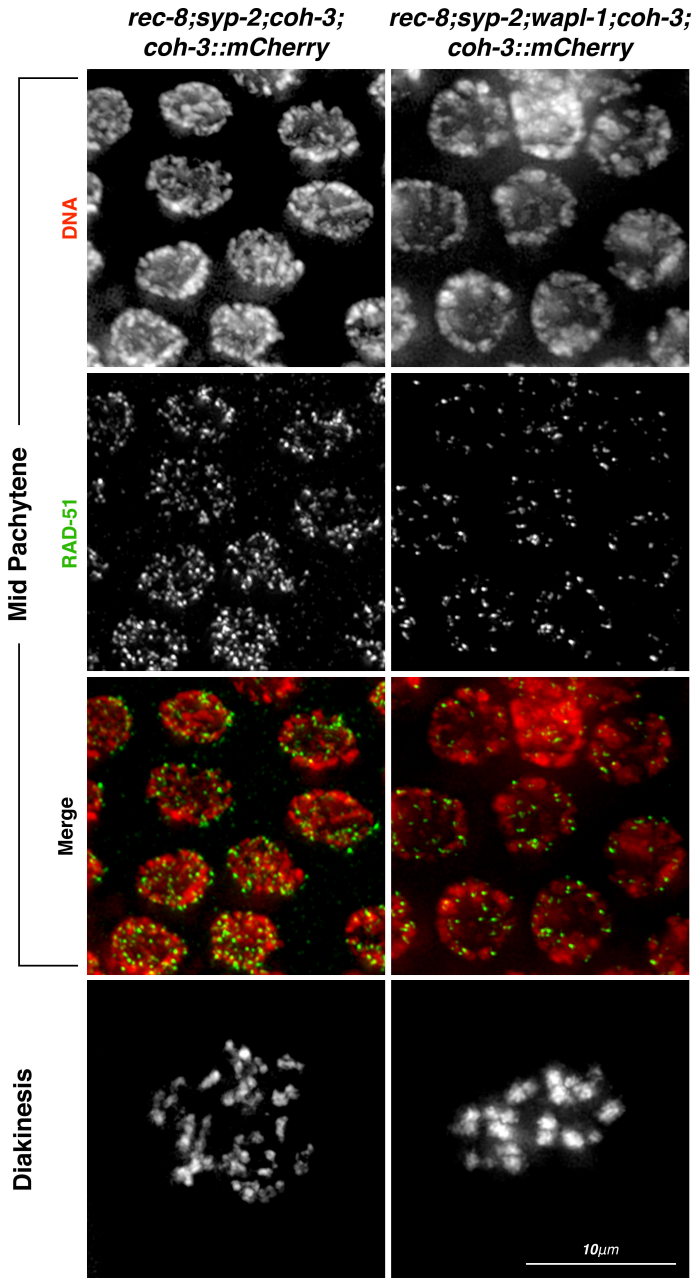
rec-8;syp-2;coh-3;
coh-3::mCherry
rec-8;syp-2;wapl-1;coh-3;
coh-3::mCherry
Mid Pachytene
DNA
RAD-51
Merge
Diakinesis
10μm

Figure 52. Removal of WAPL-1 improves phenotype in diakinesis in γ-irradiated SCC deficient mutants

Diakinesis oocytes of the SCC deficient mutants *rec-8* and *rec-8;spo-11* and their *wapl-1* deletion counterpart treated with 100Gy γ-IR and analysed with CellProfiler. Analysis was carried out on -1 and -2 (total) diakinesis oocytes and on -2 only.

A Graph showing the average number of DAPI masses in diakinesis oocytes of all irradiated mutants with their unirradiated controls. As expected the number of DAPI masses is higher in all mutants after irradiation. The increase between treated and untreated is greater in the absence of WAPL-1 and the overall number of DAPI bodies amongst the treated worms is also higher in the absence of WAPL-1

B Graph showing CellProfiler analysis of DAPI mass area in diakinesis oocytes comparing *rec-8* +/- 100Gy γ-IR and *rec-8;wapl-1* +/- 100Gy γ-IR.

C Graph showing CellProfiler analysis of DAPI mass area in diakinesis oocytes comparing *rec-8;spo-11* +/- 100Gy γ-IR and *rec-8;spo-11;wapl-1* +/- 100Gy γ-IR.

D Graph showing CellProfiler analysis of DAPI mass area in diakinesis oocytes of all treated and untreated SCC deficient mutants.

E DAPI stained diakinesis oocytes of irradiated *rec-8* and *rec-8;spo-11* and there *wapl-1* harbouring counterparts, showing that in the absence of WAPL-1 less chromosome fragmentation occurs, suggesting that the *wapl-1* mutation results in more efficient DSB repair.

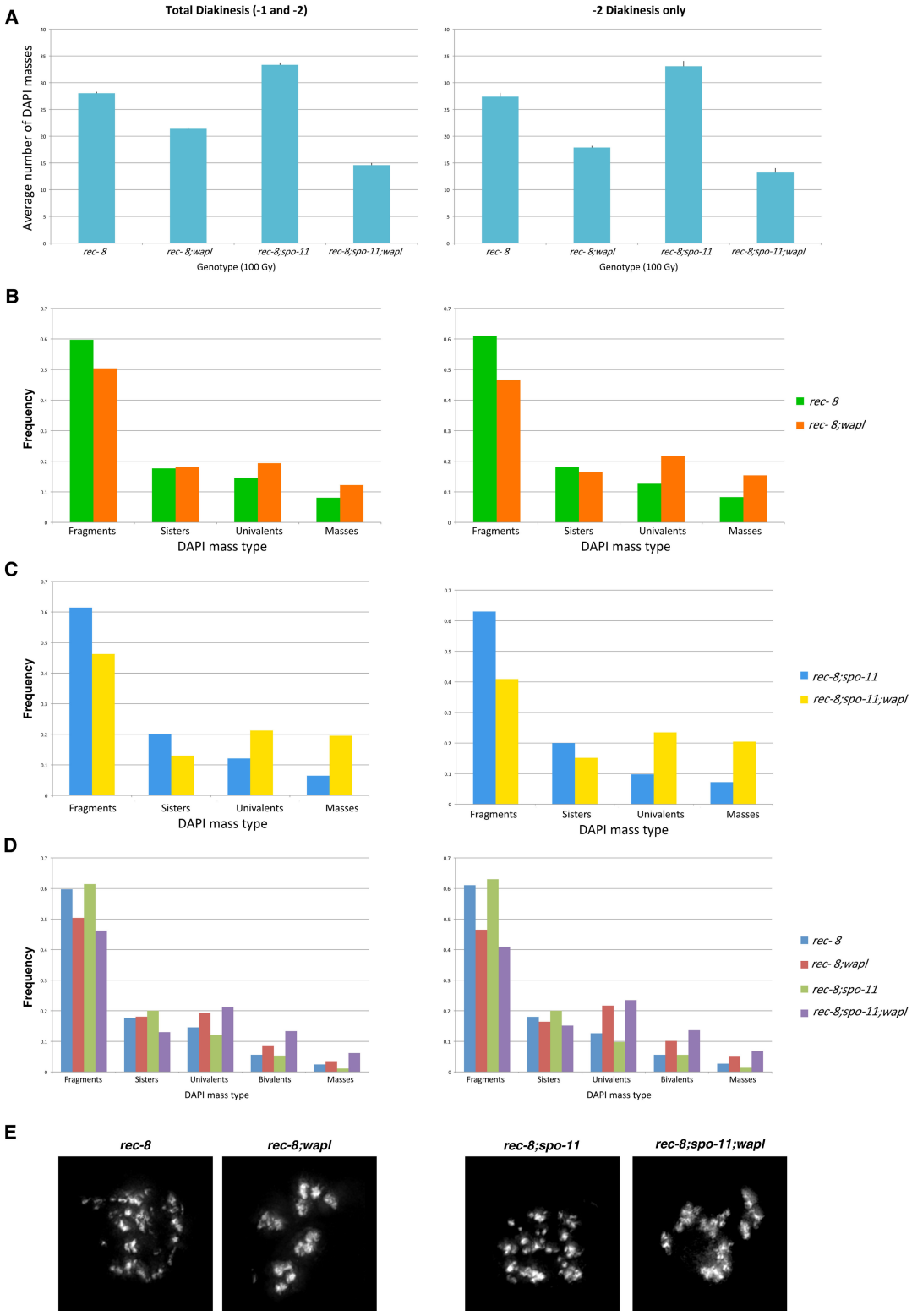
A
Total Diakinesis (-1 and -2)
-2 Diakinesis only
Average number of DAPI masses
rec- 8
rec- 8;wapl
rec-8;spo-11
rec-8;spo-11;wapl
Genotype (100 Gy)
B
Frequency
Fragments
Sisters
Univalents
Masses
DAPI mass type
rec- 8
rec- 8;wapl
C
rec-8;spo-11
rec-8;spo-11;wapl
D
Bivalents
E
rec-8
rec-8;wapl
rec-8;spo-11
rec-8;spo-11;wapl

CHAPTER 7: DISCUSSION

7.1 Summary of findings

The goal of my PhD project was to investigate the regulation of cohesin dynamics in meiosis and to understand the roles of meiotic cohesin in orchestrating the events of meiotic prophase. At the outset of my PhD, previous work by my colleague James Lightfoot characterising the *scc-2(fq1)* mutant, had demonstrated for the first time that SCC-2 is responsible for cohesin loading in meiosis. The localisation of SCC-2 to the axial element through meiotic prophase suggested that cohesin loading might be of importance at stages of meiosis other than S-phase. To address this, I depleted *scc-2* in the germline by RNAi. The first and most striking phenotype following *scc-2* RNAi was the appearance of univalents in diakinesis oocytes. This finding, together with the axial element localization of SCC-2, suggested that cohesin reloading may be required for crossover formation or for maintenance of chiasmata following crossover formation. I also saw that in the absence of SCC-2, REC-8-containing cohesin complexes are lost from chromatin in late pachytene nuclei, while SMC-1 and SMC-3 remain, suggesting that cohesin complexes with different kleisins may display different dynamics.

These data suggest that cohesin turnover might be happening in meiosis. To investigate to what extent this might be occurring, I therefore sought to engineer a system that would allow greater temporal control of cohesin expression than could be achieved by *scc-2* RNAi. I attempted this ambitious goal in several ways: first, by placing the control of *rec-8::GFP* expression under the 3' UTRs of genes that are known to restrict protein expression to specific regions in the germline, second, by inducing *rec-8::GFP* expression from a heat shock promoter, and third to induce *scc-3::GFP* expression by injection of capped, poly(A) tailed mRNA directly into the germline. I could not however use these methods to determine whether cohesin turnover occurs in meiosis. A more radical approach was to attempt to pioneer the auxin-mediated degron system in worms, the first time it would have been used in a multicellular

organism, as well as demonstrate that the SNAP-tag system of covalently labelling proteins is effective in *C. elegans.*

I also wanted to examine the roles that cohesin complexes containing different α-kleisin subunits might play in meiosis. I examined the localisation of REC-8 and COH-3 and found them to be subtly different. Cytological analysis of the different kleisin mutants revealed that REC-8 provides almost all the SCC in meiosis and therefore is the main mediator of DSB repair, whereas COH-3/4 are more important for the assembly of the SC and chiasma formation. Also, I have presented data that for the first time implicates WAPL-1 as having a role in modulating cohesin in meiosis. I demonstrate that the phenotypes of SCC-deficient mutants can be ameliorated by removal of WAPL-1, which seems to act by counteracting the cohesion of COH-3/4-containing cohesin complexes, perhaps explaining why they appear to provide so little SCC. Finally, I have demonstrated that phosphorylation of REC-8 at key residues, presumably by AIR-2, is involved in the regulation of chromosome segregation, likely by promoting its cleavage by separase.

All of this paints a complex picture in which cohesin loading, establishment and disassociation are tightly controlled throughout meiosis by multiple means, with this in turn regulating key events in the life of a meiotic nuclei. I will discuss the implications of some of these findings below.

7.2 Cohesin reloading during meiotic prophase

In mammalian oogenesis, meiosis is initiated during foetal development, but is subsequently arrested for a prolonged period at the diplotene stage of the first meiotic prophase. This prophase arrest is maintained until hormonal signals during the menstrual cycle promote the first meiotic division to take place and ovulation to occur (Maller and Krebs, 1980; Zhang and Xia, 2012). This interval could last for several decades in humans. It has been proposed that during this extended prophase arrest, oocytes age in a way that greatly increases the frequency of chromosome missegregation at both meiotic divisions and that this

is largely responsible for age-related infertility and trisomy (Hassold and Hunt, 2001; Hassold et al., 2001).

In meiosis, bivalents are thought to be held together from birth until ovulation by sister chromatid cohesion mediated by cohesin complexes. Cohesion is established during DNA replication in the embryo (Uhlmann and Nasmyth, 1998), thus cohesin rings must persist on DNA and provide cohesion for an exceptionally long period of time. It may therefore be that the gradual loss of cohesin, which will eventually lead to the degradation of cohesion over time, leads to the increasing levels of aneuploidy that are seen with increasing maternal age. This idea has been given credence by the evidence that SMC1β-deficient oocytes are sterile due to massive levels of aneuploidy, and that this worsens with the age of the female mice (Hodges et al., 2005). In addition to this, it has been demonstrated that an age-related reduction of Rec8 occurs in mice and humans (Chiang et al., 2010; Garcia-Cruz et al., 2010; Lister et al., 2010). The dynamics of cohesin during meiosis therefore has great clinical significance.

In mitosis, a great deal of work has been carried out to address the roles of cohesin loading. It has been demonstrated that cohesin's association with chromosomes requires the Scc2 protein along with other key factors (Ciosk et al., 2000; Watrin et al., 2006).
Previous work by my colleague James Lightfoot studying an *scc-2* null allele in worms demonstrated that, in meiosis too, SCC-2 was responsible for cohesin loading. However, it was not possible to assess whether cohesin reloading occurs in meiotic prophase by analysing the mutant alone.

Whilst cohesin turnover in meiosis has been implicated as key factor in age-related aneuploidy, and is therefore an area of extensive research, this has not yet been demonstrated. Indeed, two papers investigating cohesin turnover in mice have failed to find evidence that it occurs. In the first report, a conditional knockout mice in which SMC1β protein is produced only during foetal development causes no impact on fertility, leading to the suggestion that

meiotic cohesin is sufficiently robust to provide cohesion throughout the life of foetal oocytes, and that little or no turnover of meiotic cohesin occurs until fertilization (Revenkova et al., 2010). In a second paper, mature GV oocytes of mice harbouring TEV-cleavable Rec8 were injected with wild-type Rec8, followed by injection with TEV protease. The wild-type Rec8 did not prevent bivalent breakdown, indicating that Rec8 expressed after S-phase was not loaded to chromosomes or did not become cohesive (Tachibana-Konwalski et al., 2010). However, in both these cases turnover was assessed in oocytes already in meiotic arrest, and as such these findings do not preclude a role for cohesin turnover in early prophase. Indeed, we have observed that SCC-2 is localised to the axial element throughout meiotic prophase, suggesting that cohesin reloading might be occurring at this stage, and data from the *scc-2* RNAi experiments indicates that this does in fact occur and that this may play a role in orchestrating some key events in meiosis.

Following knockdown of *scc-2,* we see loss of REC-8 localisation to chromatin in late pachytene nuclei, indicating that in the absence of SCC-2, REC-8 is lost or removed from chromosomes at this stage of meiosis. However, these germlines do not exhibit loss of SMC-1 or SMC-3 at the same stage. In order to check that the absence of REC-8 on chromatin of pachytene nuclei was due to loss or removal, I monitored SC assembly following *scc-2* RNAi. As cohesin loading is required for SC formation (Colaiacovo et al., 2003; Goodyer et al., 2008; Klein et al., 1999; Martinez-Perez and Villeneuve, 2005; Pasierbek et al., 2001), the presence of SYP-1 in nuclei with little or no REC-8 demonstrates REC-8 is being lost subsequent to its loading in S-phase. As the levels of REC-8 are constant throughout the germline in wild-type worms, this indicates that *de novo* cohesin loading is occurring to counteract the REC-8 loss that we see following *scc-2* RNAi. This is the first evidence that cohesin reloading might be occurring during meiotic prophase and if proved to be true, would constitute a major breakthrough in our understanding of the role of cohesin in meiotic prophase.

It is notable that *scc-2* RNAi germlines in which we see REC-8 loss also exhibit univalents in their diakinesis oocytes, but no obvious separation of sister

chromatids. This observation could be explained in two ways: a) following *scc-2* depletion cohesin levels drop to such an extent that chiasmata breakdown; b) for CO formation to occur, sufficiently high levels of cohesin, or cohesin reloading are required, and so following *scc-2* RNAi COs cannot be formed. The first explanation seems less likely. If bivalents were falling apart one would expect this to occur randomly resulting in any number of DAPI bodies, from 6 bivalents to 24 individual sisters, in the diakinesis oocytes of *scc-2* RNAi treated worms. In fact we do not see this. In *scc-2* partial depletion germlines the number of bodies in diakinesis oocytes ranges from 6 to 12 and all the bodies are the size and shape of a bivalent or univalent, with none as small as a sister. Secondly it has been shown that very low levels of cohesin are required to provide cohesion in yeast (Heidinger-Pauli et al., 2010), and as such almost all cohesin molecules would have to be lost in order for the chiasmata to break down. This suggested that the second hypothesis is true and that wild-type levels of cohesin are required to promote CO formation or that cohesin reloading itself is required.

Cohesin has been shown to play a key role in DNA repair in mitosis. In response to DSBs, cohesin becomes reloaded at break sites, forming expanded cohesin domains spanning 50-100kb, as well undergoing a genome-wide enrichment (Kim et al., 2010a; Strom et al., 2004; Unal et al., 2007). This damage-induced cohesin is loaded by Scc2 (Unal et al., 2004) and becomes cohesive (Unal et al., 2007). It is thought that DSB repair is facilitated by cohesin by keeping sister chromatids in close proximity, which promotes the correct sequence to be used as a donor template for repair. It has been shown that in tetraploid yeast, when the levels of cohesin were reduced to that of a single copy, a significant increase in homologous chromosome directed HR, rather than sister chromosome recombination was detected (Covo et al., 2010). These observations clearly indicate that cohesin promotes inter-sister repair, but during meiosis this must be avoided in order to favour the formation of inter-homologue COs. Thus, could cohesin reloading play a role in CO formation during meiosis? One would have thought the reverse to be true, with cohesin reinforcement promoting inter sister, rather than inter-homologue recombination. Indeed, in yeast it has been

shown that Rec8 promotes a sister bias and that axial element proteins Red1 and Mek1 antagonise this effect, making a homologue bias possible (Kim et al., 2010b). The authors also suggest that Rec8 removal and maintenance is differentially regulated on either side of a DSB. On one side, the break-end must have cohesion loosened to allow for strand invasion into the homologue, whilst at the other end cohesion must be maintained to ensure that it remains quiescent. Subsequent to this, the quiescent end must be released from its sister to allow the conversion from a single-end invasion to a double Holliday junction, involving a second stage of cohesin loss.

I have seen that REC-8 is lost from chromatin in late pachytene nuclei subsequent to *scc-2* RNAi. I sought to address whether this loss was in response to DSBs or for the resolution of intermediates downstream in the CO repair pathway. This is an appealing hypothesis as visualisation of REC-8 on chiasmata reveals an absence of proteins at the CO site. In addition, in silver stained locust chromosomes one can clearly see separation of sister axes at the points of DNA exchange (Jones and Franklin, 2006), suggesting a weakening of cohesion, possibly resulting from cohesin loss. Furthermore, in mitotically dividing yeast, DSBs promote dissociation of S-phase-loaded cohesin, and this is required for the effective resection of breaks, which in turn is need for DNA repair by homologous recombination (McAleenan et al., 2013). Finally, as previously mentioned, cohesin loss has been implicated in SEI and dHJ formation in yeast meiosis (Kim et al., 2010b). However, carrying out *scc-2* RNAi on *spo-11* mutants reveals that DSBs are not the primary trigger for REC-8 loss. It is possible that the rate of REC-8-cohesin turnover is higher in late pachytene to facilitate crossing over, but that this is regulated by some other means. Indeed, Kim *et al.* have suggested that Rec8 might respond to global regulatory signals derived from the cell cycle, licensing major transitions nucleus-wide and thereby link recombination progression to overall cell status to periodically reinforce nucleus-wide synchrony (Kim et al., 2010b), and perhaps it is this phenomenon that we are observing. Finally, our data does not preclude REC-8 removal in response to DSBs, as it may occur only immediately around CO sites and therefore at levels lower than can be detected by immunofluorescence.

It is clear that cohesin is required for CO formation. Rec8 mutants in yeast, mouse and *C. elegans* fail to make crossovers (Klein et al., 1999; Llano et al., 2012; Pasierbek et al., 2001), and as with the *scc-2* RNAi data presented here, this cannot be explained by failure to form DSBs. What role could cohesin be playing in the promotion of CO formation? As discussed above, it has been suggested that one end of meiotic DSBs must remain quiescent (Kim et al., 2010b), so perhaps cohesin reloading is required at this stage. Meiotic chromosomes exist in the context of an axis with DNA forming co-oriented linear arrays (Fig. 53A) (Blat et al., 2002). At the base of these loops are AT-rich axis association sites and it is here that cohesin has been suggested to bind (Kleckner, 2006). DSBs are thought to occur in the DNA loops and are brought into the axis where they bind to recombinosomes as part of tethered-loop axis complexes (Fig. 53B) (Blat et al., 2002). In this model cohesin molecules are not close to the DSB site, so perhaps some degree of cohesion reinforcement would be required to maintain the quiescent end. However, it is difficult to imagine how in the absence of an "ends-apart" configuration at the break site, CO formation would be completely abolished.

I would like to propose a model in which cohesin plays a role at the late stages of CO formation by ensuring that dHJs are correctly repaired. One mechanism by which dHjs are resolved involves convergent branch migration, mediated by BLM/TOPOIIIα complexes, which promote topological decatenation of dHJ structures, thereby causing dissolution of dHJs without crossover formation (Wu and Hickson, 2003). Cohesin could be required to stabilise dHJs to ensure that they can be processed to form COs or NCO events. Perhaps cohesin is loaded onto the double stranded inter-homologue DNA molecules that are formed in dHJs to act as a spacer, preventing convergent branch migration, thus enabling dHJ resolvases to cleave DNA in a manner that can lead to CO events. This would cast cohesin's function in CO formation as mediating inter chromosomal interactions in a manner similar to its role in regulating gene expression (Degner et al., 2009; Hadjur et al., 2009). If this hypothesis were true, one would expect *rec-8* mutants to have elevated numbers of gene

conversion events, which would arise by the BLM/TOPOIIIα-dependent dissolution of dHJs (Fig. 53C). Another possibility would be to cross *rec-8* to the background of the *C. elegans* Blm orthologue, *him-6,* and assess whether COs are able to form. In either case, clarifying the molecular role of cohesin in inter-homologue CO formation is an interesting area for further research.

7.2.1 Developing tools to visualize cohesin reloading during meiotic prophase

As previously mentioned, there are limitations to the conclusions that can be drawn from the *scc-2* RNAi experiments described in this thesis. The phenotypes seen in these experiments are transgenerational, making it impossible to unequivocally say what the cohesin status of a nucleus was in the past. In order to strengthen the analysis presented above, I sought to develop a system that provides greater temporal resolution. This new experimental procedure would ideally be shorter in time than the events of meiotic prophase. RNAi can be used to more swiftly knockdown gene expression when injected directly into the germline. My attempts to carry out RNAi by this means revealed a pattern of REC-8 staining similar to that seen the in the partial knockdown by *scc-2* RNAi by feeding, 24 hours after injecting. As nuclei take about 35-40 hours to move from transition zone to late pachytene (Jaramillo-Lambert et al., 2007), the presence of late pachytene nuclei with reduced levels of REC-8 staining is consistent with the conclusion that REC-8 is lost from chromatin subsequent to loading at S-phase, and supports the hypothesis that SCC-2-dependent reloading of cohesin occurs during pachytene. Interestingly, diakinesis oocytes of these germlines had 6 bivalents, suggesting that at the time of *scc-2* depletion chiasmata had been successfully formed and remained intact throughout the *scc-2* knockdown. This also counters the interpretation that chiasmata fall apart due to the loss of REC-8 and supports the idea that it is impairment of CO formation that results in presence of univalents in the *scc-2* RNAi feeding experiments. However, we have seen that the SCC-2 protein is exceptionally stable, both from the RNAi by feeding experiments, and also from the fact that *scc-2* null worms develop to adulthood, presumably surviving on

scc-2 mRNA or protein inherited from their heterozygous mothers. Therefore, it is possible that an amount of SCC-2 protein remained in the oocytes of *scc-2* RNAi injected worms and that this was sufficient to prevent these bivalents from breaking apart.

Carrying out *scc-2* RNAi by injection is technically very challenging, with a large proportion of injected worms dying before any analysis can take place. I therefore, sought to create a situation analogous to the RNAi depletion by genetic means, to eliminate the variation that cannot be controlled for, which derive from the different rates of knockdown in individual worms following RNAi even by injection. To this end, I created a transgenic line in which *rec-8::GFP* was placed under the control of the *fbf-2* 3' UTR, which restricts expression to the mitotic tip and early stages of meiotic prophase. The hope was that this would cause a similar outcome to the RNAi experiments in which REC-8 is lost from late pachytene. Unfortunately, analysis of *rec-8;rec-8::GFP fbf-2* 3' UTR worms revealed no decrease in *REC-8::GFP* localisation at the later stages of meiosis and consequently had no effect on CO formation. It may be that the *fbf-2* 3' UTR does not adequately restrict *REC-8::GFP* expression, or that removed molecules of REC-8-cohesin can themselves be reloaded onto chromatin.

I therefore undertook to develop a number of novel techniques that I might use to assess whether cohesin turnover occurs during meiotic prophase. I will discuss these in a later section of the discussion. I would however, like to briefly mention some preliminary data from my colleague Oliver Crawley that I have not referred to earlier in this thesis. In order to monitor cohesin localisation, I generated three transgenic lines in which cohesin subunits were tagged with a fluorescent protein: *rec-8;rec-8::GFP, coh-3;coh-3::mCherry* and *scc-3;scc-3::GFP*, in all of which the tagged proteins are functional. This provides the possibility of carrying out FRAP experiments in the *C. elegans* germlines, something which has not been attempted before, to my knowledge.

Pilot FRAP experiments show that *COH-3::mCherry* recovers its axial element localisation only a few seconds after photobleaching, *SCC-3::GFP* also recovers but takes slightly longer to do so, and *REC-8::GFP* recovers with slower kinetics still. This suggests that REC-8 turnover is occurring during meiotic prophase but that the rate of turnover is not as rapid as that of COH-3. Unfortunately, at the time of carrying out the *scc-2* RNAi experiments it was not possible to assess COH-3/4 levels. This makes repetition of the *scc-2* RNAi experiments in the *rec-8;coh-3;rec-8::GFP;coh-3::mCherry* a key experiment, as one would expect to see COH-3 loss occurring more rapidly than that of REC-8. These observations also provide another explanation for the presence of univalents following *scc-2* RNAi: that COH-3/4 cohesin complexes are rapidly lost when SCC-2 is depleted, resulting in an effective phenocopy of the *coh-3;coh-4* double mutant in which CO formation is impaired while sister chromatids remain attached. As SMC-1 and SMC-3 are retained on chromatin in late pachytene following *scc-2* RNAi partial depletion, this raises the possibility that these remaining SMC-1/3 molecules are in complexes with either COH-1 or SCC-1 following *scc-2* RNAi. Another possibility is that they are retained on chromatin but not in the form of the canonical cohesin complex. The idea that cohesin subunits may sometimes act independently from one another is supported by the fact that in *coh-3;coh-4* double mutants REC-8 can be seen localising to chromatin throughout prophase, and that COH-3 can be seen to localise to the individual sisters in *rec-8;spo-11* diakinesis oocytes, but in both of these cases SMC-1 appears to be absent. These observations suggest that perhaps cohesin subunits can interact with DNA but not as part of the cohesin ring.

7.3 Cohesin removal in meiosis

7.3.1 Phosphorylation of REC-8 by AIR-2

The maintenance and timely release of SCC is crucial for proper chromosome segregation in meiosis. One of the key features that differentiates meiosis from mitosis is that in meiosis cohesin is disassociated from chromosomes in two steps: firstly allowing homologue segregation at meiosis I, and then sister

chromatid segregation in meiosis II. This has been shown to be mediated by cleavage of Rec8 by separase (Buonomo et al., 2000). In yeast, mutation of two separase sites renders Rec8 non-cleavable (Buonomo et al., 2000; Kitajima et al., 2003). In mouse, separase cleaves Rec8 at three positions in vitro and mutation of these three residues has been shown to prevent the production of haploid spermatids and to delay chiasma resolution in oocytes (Kudo et al., 2009). In *C. elegans,* REC-8 has 14 possible separase cleavage sites, three of which are adjacent or overlapping with putative AIR-2 phosphorylation sites. Mutating these three residues to abolish the separase sites does not have any affect on chromosome segregation, however it has been shown in vitro that mouse Rec8 is cleaved at secondary separase sites when its primary sites are mutated (Kudo et al., 2009), and this may be happening in this mutant. It was not possible to generate a transgenic worm strain in which five separase sites were mutated at residues 364, 400, 570, 631 and 666. This may be indicative of these sites being essential for cleavage of REC-8 and therefore having a dominant effect, blocking chiasma resolution at metaphase I and/or II, thereby making the transgenic worms carrying this mutant form of REC-8 sterile.

The cleavage of Rec8 by separase has been shown to be mediated by its phosphorylation. In yeast, this phosphorylation is carried out by the CK1 and Cdc7 kinases (Ishiguro et al., 2010; Katis et al., 2010; Rumpf et al., 2010). It is less clear in other organisms which kinase is responsible for the phosphorylation of Rec8. In yeast, mitotic dissociation of cohesin is dependent on the activity polo-like kinase (Plk1) (Alexandru et al., 2001; Diaz-Martinez et al., 2007; Losada et al., 2002; Sumara et al., 2002) In *C. elegans,* the Aurora B homologue AIR-2 is thought to function similarly to CK1, since depletion of AIR-2 by RNAi has been shown to prevent chromosome separation at both anaphase I and II, and AIR-2 has the capacity to phosphorylate REC-8 at a major amino acid in vitro (Rogers et al., 2002). This has lead to the hypothesis that phosphorylation of REC-8 by AIR-2 is responsible for rendering REC-8 cleavable by separase in worms. This leads to the prediction that mutation of key residues within the putative AIR-2 sites of REC-8 to a non-phosphorylatable amino acid should render the protein uncleavable. Creation of a transgenic strain

expressing a mutant form of REC-8 with three mutated residues in putative AIR-2 sites adjacent to predicted separase sites, had no effect on chromosome segregation. However in yeast, mutation of the 12 phosphorylation sites of Rec8 identified by mass spectroscopy had no effect on chromosome segregation, since, in a manner similar to mutation of Rec8's separase sites, mutation of the primary CK1 sites in Rec8 results in the phosphorylation of secondary sites (Katis et al., 2010). Therefore, it may be that these sites are responsible for REC-8 cleavage but that their mutation prompts the use of other sites.

If these putative AIR-2 sites are involved in REC-8 cleavage, one would predict that mutating key residues to phosphomimetic residues would lead to premature release of SCC and therefore affect chromosomes segregation. I have seen that worms expressing a REC-8 mutant protein that mimics constitutive phosphorylation of the three AIR-2 sites show a great increase in embryonic lethality and a higher incidence of males, indicating chromosome mis-segregation. As no obvious defects in meiotic prophase could be observed in these mutants, we conclude that the segregation defects originate from errors derived in MI or MII. This strongly suggests that REC-8 phosphorylation promotes its cleavage by separase and subsequent cohesin disassociation, in support of the previous evidence. Worms harbouring both the hyperphosphorylated REC-8::GFP and a mutation in *coh-3* have even lower viability, supporting the idea that COH-3/4 must also disassociate from chromosomes at MI or MII. To test at precisely which stage these segregation defects stem from I will carry out live imaging of the meiotic divisions using a H2B::mCherry marker.

7.3.2 Role of WAPL-1 during meiotic prophase

In mitosis, the majority of cohesin is lost before the metaphase to anaphase transition in the prophase pathway, with only a small, but essential, complement of cohesin being retained at the centromeres. A key player in this separase-independent cohesin removal pathway is Wapl, which depletion in mammalian cells causes most cohesin to remain on chromosome arms (Gandhi

et al., 2006; Kueng et al., 2006; Rowland et al., 2009). A recent study in *S. cerevisiae*, has demonstrated that Wapl is the only factor preventing G2-expressed cohesin from establishing SCC, showing that it's role is not restricted to anti-establishment activity during DNA replication, but extends to cohesion maintenance outside of S phase (Lopez-Serra et al., 2013). In mammalian cells, two other proteins that show complex interactions with Wapl, Pds5 and Sororin, have been shown to modify the association of cohesion with chromatin after S-phase. Phosphorylation of sororin by the mitotic kinase CDK1 triggers Wapl-dependent removal of cohesin, by disrupting the interaction of Sororin and Pds5, allowing Wapl to bind to Pds5 and causing cohesin disassociation from chromosome arms (Nishiyama et al., 2010). It is unknown whether Wapl is responsible for any cohesin removal in meiosis. In yeast, it has been shown that spore viability is not compromised by lack of Wapl indicating that Wapl's function in meiosis is not essential for chromosome segregation (Lopez-Serra et al., 2013), though it may have a role in other aspects of chromosome behaviour. In mouse oocytes Wapl has been shown to co-localise with the SC in pachytene nuclei, suggesting that it may play a role in meiotic prophase (Zhang et al., 2008a).

The data presented in this thesis represents the only evidence so far of a WAPL-1-mediated pathway regulating cohesin establishment and maintenance in meiosis. I have shown that in SCC deficient mutants cohesion is markedly improved after removal of WAPL-1. More specifically, I have demonstrated that WAPL-1 plays a role in preventing cohesion maintenance of COH-3/4-containing complexes. Interestingly in the absence of both WAPL-1 and the SC component SYP-1, COH-3 can act in a manner that seems to provide synapsis as well as cohesion between chromosomes. It is important to note that none of this data excludes the possibly that WAPL-1 could also operate on REC-8-containing cohesin complexes, however further work is required to demonstrate this. In addition to this, my colleague Oliver Crawley has seen that the levels of COH-3 on chromatin, as assessed by immunofluorescence, are higher in *wapl-1* mutants compared with wild type. This suggests that WAPL-1 may act in meiotic prophase in a similar fashion to mitosis. Demonstration of WAPL-1's

interaction with cohesin as well as the identification of other factors or modifications evolved in regulating these processes are areas of further research being undertaken in the lab.

Finally, I have observed two instances of a WAPL-1-independent pathway of cohesin removal during meiotic prophase. I have demonstrated that there is a decrease in the levels of chromosome-associated COH-3 between the penultimate and final diakinesis oocyte. In wild-type diakinesis oocytes COH-3 becomes restricted to the short arm of the bivalent. This loss probably occurs in preparation for the first meiotic division and occurs independently of WAPL-1. In addition to this, in SCC mutant γ-IR caused a change in the pattern of COH-3 staining in pachytene nuclei changing from continuous tracks decorating the axial element to a punctate pattern. This is suggestive of COH-3 removal in response to DSBs. As this effect can be seen even in the presence of WAPL-1 we conclude that this too is part of a WAPL-1-independent pathway of cohesin removal. In yeast mitosis cohesin has been shown to disassociate from chromatin in response to DSBs and that this requires separase (McAleenan et al., 2013). My observations provide the first evidence that something similar might occur in meiosis, although whether this removal of cohesin is separase dependent remains to be seen.

7.4 Different roles of the meiotic kleisins

In mice an SMC1 paralogue, SMC1β (Revenkova et al., 2001), and an additional α-kleisin, Rad21L (Ishiguro et al., 2011; Lee and Hirano, 2011) are all present during meiosis. Similarly, in *C. elegans,* cohesin complexes with multiple α-kleisins have been implicated as having roles in meiosis. This could provide a flexibility that allows different meiosis specific functions to be carried out by different cohesin complexes.

In *C. elegans*, REC-8, COH-3 and COH-4 have all been implicated as having a role in providing SCC (Severson et al., 2009). However, to me this appears to be an incomplete analysis. Whilst in *rec-8* mutants we see sister chromatids tenuously

connected, indicating a impairment of SSC, in *coh-3;coh-4* double mutants sisters are tightly juxtaposed in diakinesis oocytes, indicating that SCC is intact. It has previously been assumed that the bi-lobed univalents of *rec-8* mutants are held together by cohesin complexes containing COH-3/4. As a consequence, full separation of sister chromatids only occurs in the *rec-8;coh-3;coh-4*. However, I have seen that COH-3 cannot be detected by immunofluorescence between the two sister chromatids in the majority of bi-lobed univalents seen in *rec-8* diakinesis oocytes, suggesting that something other than cohesion is holding them together. In addition to this, *rec-8;spo-11* mutants have full separation of sisters in diakinesis oocytes. This might suggest that COH-3/4 cohesin complexes only become cohesive in response to DSBs, something supported by the fact that we start to see bi-lobed univalents in γ-IR *rec-8;spo-11* diakinesis oocytes. However, it is also possible that *rec-8* univalents are held together by the formation of crossover events between sister chromatids, and thus by abolishing DSB formation the link between sisters cannot be established. Interestingly, it has been suggested that in mice *rec-8* mutants the SC is formed between sister chromatids (Xu et al., 2005), and I have observed that the diakinesis oocytes of *rec-8; syp-2* double mutants, in which the SC can not be formed, display extensive separation of sisters and the presence of chromosome fragments. This could be explained because in this situation inter-sister crossovers cannot be formed due to the absence of the SC, leading to loss of SCC and chromosome fragmentation. This possibility is also consistent with the phenotype seen in *rec-8; coh-3; coh-4* triple mutants, almost complete separation of sister chromatids in diakinesis oocytes (Severson et al., 2009), as I have shown that no DSBs are made in the absence of all three meiotic kleisins. If this hypothesis is correct, *rec-8; msh-4/5* or *rec-8; cosa1* double mutants, in which crossover formation is impaired by the lack of one of these pro-crossover factors (Yokoo et al., 2012; Zalevsky et al., 1999), would display full sister separation in diakinesis oocytes, phenocopying the *rec-8;spo-11* double mutant. This is something I intend to investigate immediately.

A further piece of evidence supporting the hypothesis that COH-3/4 provide very little SCC is the fact that we see extensive accumulation of chromosome

fragments in *rec-8* mutant oocytes following γ-IR, while chromosomes appear intact in the diakinesis oocytes of irradiated *coh-3;coh-4* double mutants, suggesting that only REC-8-containing cohesin complexes are capable of supporting efficient DSB repair. SCC has been shown to play a vital role in the repair of DSBs in mitosis, therefore one might expect cohesin complexes that do not provide SCC to have little effect on the repair of accumulated DNA damage in meiosis. I would therefore suggest that the primary role of COH-3/4 in meiosis is in promoting assembly of the SC and promoting chiasma formation, as well as maintaining chromatin structure.

This is not to say, however, that COH-3/4-containing cohesin complexes cannot provide cohesion. As I have mentioned earlier in the discussion, removal of WAPL-1 from SCC-deficient mutants, *rec-8, rec-8;spo-11* and *rec-8;syp-2* results in phenotypes suggestive of an reduction in cohesion defects. Furthermore, there appears to be less persistent DSBs in γ-IR harbouring the *wapl-1* mutation. In addition, localization of COH-3 in the univalents of *rec-8;spo-11;wapl-1* and *rec-8;syp-2;wapl-1* diakinesis oocytes has a different localisation than that of REC-8 in *coh-3;coh-4* or *spo-11* univalents. Whereas REC-8 forms a thick bar in these univalents delineating the interface between sister chromatids, COH-3 is more diffusely distributed across chromatin in diakinesis. This could be indicative of the fact that COH-3 does not have a primary role in providing SCC and therefore mislocalises in *wapl-1* mutants, in which their cohesiveness is not restricted. Finally, as mentioned earlier, preliminary FRAP data suggest that COH-3 is very rapidly turned over in pachytene nuclei. It is difficult to believe that a cohesin complex with only a few second residency on chromatin could provide a great deal of cohesion. It would be invaluable to know whether COH-3 turnover is reduced in *wapl-1* mutants and this is currently being investigated in the lab.

7.5 Novel techniques

Following the *scc-2* RNAi experiments, it became apparent that the development of a novel technique would be necessary to establish emphatically that cohesin

reloading occurs. These were met with varying success and in this section I discuss their potential and future work, which I intend to undertake in order to develop them.

In other organisms the introduction of mRNA into cells has been used to achieve tight temporal control of protein expression. However, at the time of carrying out these experiments this technique had not been extensively employed in *C. elegans*. I have demonstrated that mRNA can be used to drive expression of H2B::mCherry in the *C. elegans* germline. However, I was unable to obtain full length *scc-3::GFP* transcript and therefore, could not used this method to determine whether cohesin reloading was occurring during meiotic prophase. However, subsequent to carrying out these experiments, mRNA has been used to successfully induce expression of ZFNs in the *C. elegans* germline (Wood et al., 2011). In this paper the same Ambion kits are used for synthesis, but an SP6 in vitro transcription plasmid backbone derived from pJK370 containing 5' and 3' UTR sequences that support germ-line translation was used. This plasmid was a gift from Tom Evans who has kindly provided us with the sequence, vector, and a detailed protocol for mRNA synthesis and expression in the *C. elegans* germline. Hopefully with this information it will be possible to generate mRNA that can be used to induce expression of tagged cohesin molecules, thereby enabling us to answer some remaining questions about the dynamics of cohesin in meiotic prophase. In particular, one could use this method to synthesise putative non-cleavable *rec-8* mRNA do determine whether reloaded cohesin becomes cohesive.

The auxin degron has been used in *S. cerevisiae* and in mammalian cells to allow the rapid degradation of proteins (Nishimura et al., 2009). However, it has not yet been utilized in the context of a multicellular organism. It could provide us with an excellent method of investigating molecular events that occur over a short time frame such as cohesin reloading in meiosis, giving us the temporal resolution that is lacking in the *scc-2* RNAi experiments. I have begun work to assess the feasibility of using this system in worms. I have generated a *rec-8;rec-8::IAA17* strain also expressing *tir1*. As protein degradation should cause an

obvious phenotype in the diakinesis oocytes of treated worms, this is an ideal strain with which to test the potential of the degron system in worms. I will undertake to determine the best method for auxin delivery and to optimize the conditions for degradation in the germline, and hopefully find that this technique can be as effective in worms as it is in other organisms. If established, it would not only be invaluable research into meiosis, but also for the study of any gene, in any organ of the worm. There is currently no system that can achieve total protein degradation in such a tightly-controlled temporal and tissue-specific way. Study of genes that cause embryonic lethality would be made possible by engineering worms with tissue specific *tir1* expression, creating a situation analogous to a tissue specific knockout. In addition to this, there are genes which are currently difficult to investigate by RNAi knockdown, either because they have paralogues with similar sequences which are simultaneously depleted, or because the protein is highly stable and therefore persists well after the mRNA has gone, as is the case for SCC-2. In these situations too, a degron system would provide a solution.

The SNAP-tag system of covalently labelling proteins has been used in organisms such as yeast and Zebrafish (Campos et al., 2011; Regoes and Hehl, 2005), and in cell culture (Maurel et al., 2008), but not in worms. It could provide us with a method of assessing cohesin turnover in the germline. I have shown that we can successfully label REC-8::SNAP on meiotic chromosomes in *C. elegans.* Further work optimising the best conditions for delivery of the ligands to the germline is required, but following this, it should be possible to carry out a fluorescent pulse-chase experiment, as has been done in yeast to determine the rate of protein turnover (Bodor et al., 2012). Briefly, a first ligand would be introduced to the germline, some time later a second different ligand would be delivered. By varying the time between the first and second exposes and assess the difference between their levels it should be possible to determine whether cohesin turnover occurs and its rate. There are disadvantages to using this system: it is technically challenging and labour intensive. Also if the cohesin molecules removed from chromatin can be reloaded without synthesis, as might be suggested by the localisation of *REC-8::GFP fbf-2* 3'UTR, detecting protein

turnover might not be possible. Having said that, this is the technique that I developed furthest and shows a great deal of potential not only in this project, but also for scrutinizing other processes within the worm.

Figure 53. Model of the role of cohesin in CO formation

A Co-oriented sister linear loop array

B Recombining DNAs in chromatin loops are tethered to axes via axis/recombinosome contacts in ‘‘tethered-loop axis complexes’’ (Blat et al., 2002)

1. DSB formation: Cohesin removal required for resection
2. Single-end invasion: Cohesin removal on invading strand but cohesin maintenance (Kim et al., 2010b).
3. Double Holliday Junction formation: Cohesin removal required for second-end invasion (Kim et al., 2010b)

C Homologous recombination repair pathway

4. Cohesin reloading onto single-stranded interhomologue DNA molecules to prevent convergent branch migration and dHJ dissolution.

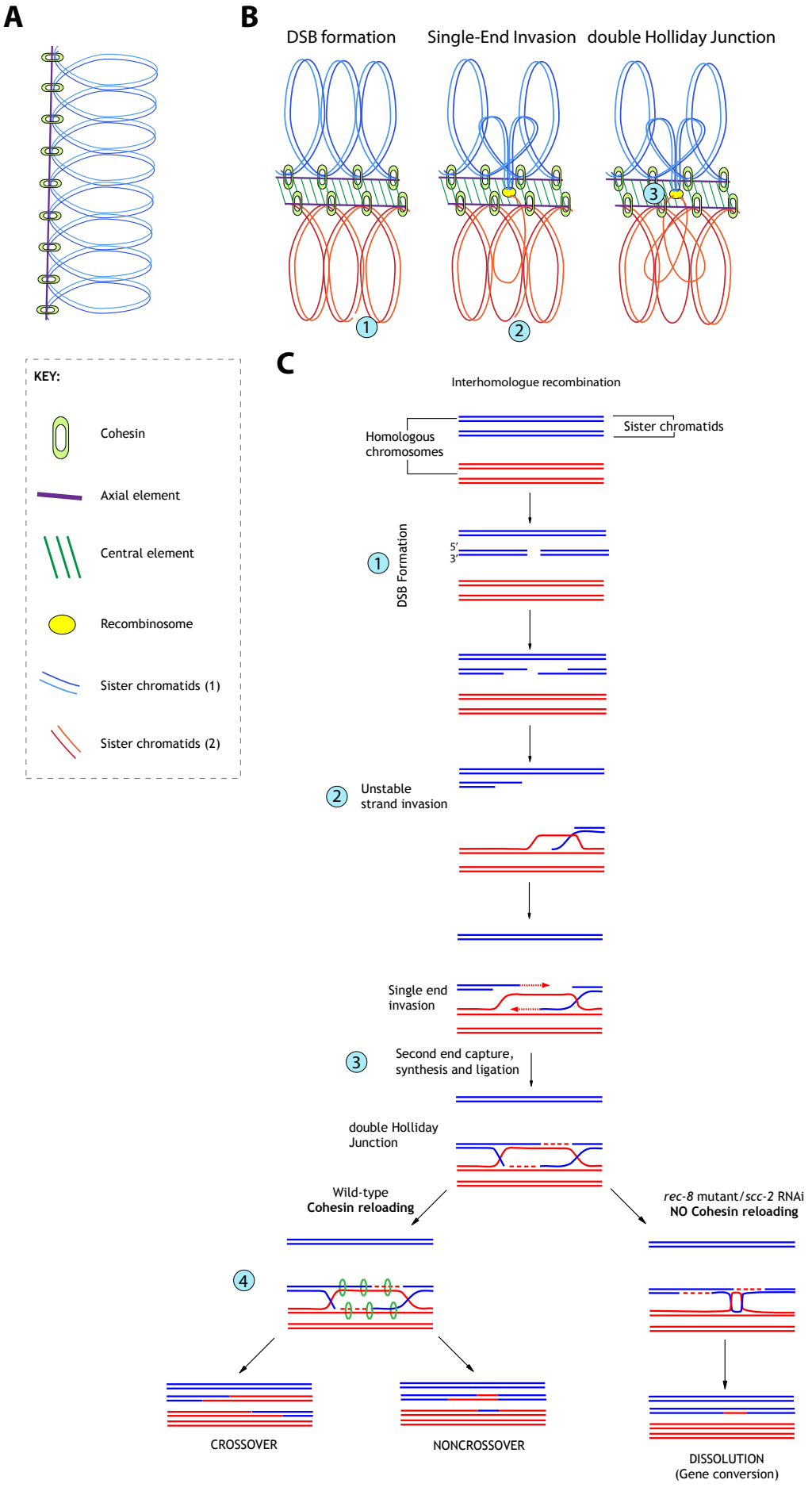
A
B
DSB formation
Single-End Invasion
double Holliday Junction
1
2
3
KEY:
Cohesin
Axial element
Central element
Recombinosome
Sister chromatids (1)
Sister chromatids (2)
C
Interhomologue recombination
Homologous chromosomes
Sister chromatids
1
DSB Formation
5'
3'
2
Unstable strand invasion
Single end invasion
3
Second end capture, synthesis and ligation
double Holliday Junction
Wild-type
Cohesin reloading
rec-8 mutant/scc-2 RNAi
NO Cohesin reloading
4
CROSSOVER
NONCROSSOVER
DISSOLUTION
(Gene conversion)

REFERENCES

Aboussekhra, A., Chanet, R., Adjiri, A., and Fabre, F. (1992). Semidominant suppressors of Srs2 helicase mutations of Saccharomyces cerevisiae map in the RAD51 gene, whose sequence predicts a protein with similarities to procaryotic RecA proteins. Molecular and cellular biology *12*, 3224-3234.

Adamo, A., Collis, S.J., Adelman, C.A., Silva, N., Horejsi, Z., Ward, J.D., Martinez-Perez, E., Boulton, S.J., and La Volpe, A. (2010). Preventing nonhomologous end joining suppresses DNA repair defects of Fanconi anemia. Mol Cell *39*, 25-35.

Alani, E., Padmore, R., and Kleckner, N. (1990). Analysis of wild-type and rad50 mutants of yeast suggests an intimate relationship between meiotic chromosome synapsis and recombination. Cell *61*, 419-436.

Alexandru, G., Uhlmann, F., Mechtler, K., Poupart, M.A., and Nasmyth, K. (2001). Phosphorylation of the cohesin subunit Scc1 by Polo/Cdc5 kinase regulates sister chromatid separation in yeast. Cell *105*, 459-472.

Allard, J.B., Kamei, H., and Duan, C. (2013). Inducible transgenic expression in the short-lived fish Nothobranchius furzeri. J Fish Biol *82*, 1733-1738.

Allers, T., and Lichten, M. (2001). Intermediates of yeast meiotic recombination contain heteroduplex DNA. Mol Cell *8*, 225-231.

Alpi, A., Pasierbek, P., Gartner, A., and Loidl, J. (2003). Genetic and cytological characterization of the recombination protein RAD-51 in Caenorhabditis elegans. Chromosoma *112*, 6-16.

Anderson, D.E., Losada, A., Erickson, H.P., and Hirano, T. (2002). Condensin and cohesin display different arm conformations with characteristic hinge angles. The Journal of cell biology *156*, 419-424.

Arumugam, P., Gruber, S., Tanaka, K., Haering, C.H., Mechtler, K., and Nasmyth, K. (2003). ATP hydrolysis is required for cohesin's association with chromosomes. Current biology : CB *13*, 1941-1953.

Bai, X., Peirson, B.N., Dong, F., Xue, C., and Makaroff, C.A. (1999). Isolation and characterization of SYN1, a RAD21-like gene essential for meiosis in Arabidopsis. Plant Cell *11*, 417-430.

Barber, L.J., Youds, J.L., Ward, J.D., McIlwraith, M.J., O'Neil, N.J., Petalcorin, M.I., Martin, J.S., Collis, S.J., Cantor, S.B., Auclair, M.*, et al.* (2008). RTEL1 maintains genomic stability by suppressing homologous recombination. Cell *135*, 261-271.

Barbosa, V., Kimm, N., and Lehmann, R. (2007). A maternal screen for genes regulating Drosophila oocyte polarity uncovers new steps in meiotic progression. Genetics *176*, 1967-1977.

Bardhan, A. (2010). Many functions of the meiotic cohesin. Chromosome Res *18*, 909-924.

Baudat, F., Buard, J., Grey, C., Fledel-Alon, A., Ober, C., Przeworski, M., Coop, G., and de Massy, B. (2010). PRDM9 is a major determinant of meiotic recombination hotspots in humans and mice. Science *327*, 836-840.

Beard, J.H., Desai, S., Haag, R., Esumi, N., Surney, L.D., Parker, S., Richardson, C., and Rex, T.S. (2013). Identification of a therapeutic dose of continuously delivered erythropoietin in the eye using an inducible promoter system. Curr Gene Ther.

Beckouet, F., Hu, B., Roig, M.B., Sutani, T., Komata, M., Uluocak, P., Katis, V.L., Shirahige, K., and Nasmyth, K. (2010). An Smc3 Acetylation Cycle Is Essential for Establishment of Sister Chromatid Cohesion. Molecular cell *39*, 689-699.

Bergerat, A., de Massy, B., Gadelle, D., Varoutas, P.C., Nicolas, A., and Forterre, P. (1997). An atypical topoisomerase II from Archaea with implications for meiotic recombination. Nature *386*, 414-417.

Bhalla, N., Wynne, D.J., Jantsch, V., and Dernburg, A.F. (2008). ZHP-3 acts at crossovers to couple meiotic recombination with synaptonemal complex disassembly and bivalent formation in C. elegans. PLoS genetics *4*, e1000235.

Bishop, D.K., Park, D., Xu, L., and Kleckner, N. (1992). DMC1: a meiosis-specific yeast homolog of E. coli recA required for recombination, synaptonemal complex formation, and cell cycle progression. Cell *69*, 439-456.

Blat, Y., and Kleckner, N. (1999). Cohesins bind to preferential sites along yeast chromosome III, with differential regulation along arms versus the centric region. Cell *98*, 249-259.

Blat, Y., Protacio, R.U., Hunter, N., and Kleckner, N. (2002). Physical and functional interactions among basic chromosome organizational features govern early steps of meiotic chiasma formation. Cell *111*, 791-802.

Boddy, M.N., Gaillard, P.H., McDonald, W.H., Shanahan, P., Yates, J.R., 3rd, and Russell, P. (2001). Mus81-Eme1 are essential components of a Holliday junction resolvase. Cell *107*, 537-548.

Bodor, D.L., Rodriguez, M.G., Moreno, N., and Jansen, L.E. (2012). Analysis of protein turnover by quantitative SNAP-based pulse-chase imaging. Curr Protoc Cell Biol *Chapter 8*, Unit8 8.

Borde, V., Goldman, A.S., and Lichten, M. (2000). Direct coupling between meiotic DNA replication and recombination initiation. Science *290*, 806-809.

Borges, V., Lehane, C., Lopez-Serra, L., Flynn, H., Skehel, M., Ben-Shahar, T.R., and Uhlmann, F. (2010). Hos1 Deacetylates Smc3 to Close the Cohesin Acetylation Cycle. Molecular cell *39*, 677-688.

Borner, G.V., Kleckner, N., and Hunter, N. (2004). Crossover/noncrossover differentiation, synaptonemal complex formation, and regulatory surveillance at the leptotene/zygotene transition of meiosis. Cell *117*, 29-45.

Bowles, J., Knight, D., Smith, C., Wilhelm, D., Richman, J., Mamiya, S., Yashiro, K., Chawengsaksophak, K., Wilson, M.J., Rossant, J.*, et al.* (2006). Retinoid signaling determines germ cell fate in mice. Science *312*, 596-600.

Brar, G.A., Hochwagen, A., Ee, L.S., and Amon, A. (2009). The multiple roles of cohesin in meiotic chromosome morphogenesis and pairing. Molecular biology of the cell *20*, 1030-1047.

Brenner, S. (1974). The genetics of Caenorhabditis elegans. Genetics *77*, 71-94.

Buard, J., Barthes, P., Grey, C., and de Massy, B. (2009). Distinct histone modifications define initiation and repair of meiotic recombination in the mouse. The EMBO journal *28*, 2616-2624.

Buonomo, S.B., Clyne, R.K., Fuchs, J., Loidl, J., Uhlmann, F., and Nasmyth, K. (2000). Disjunction of homologous chromosomes in meiosis I depends on proteolytic cleavage of the meiotic cohesin Rec8 by separin. Cell *103*, 387-398.

Cai, X., Dong, F.G., Edelmann, R.E., and Makaroff, C.A. (2003). The Arabidopsis SYN1 cohesin protein is required for sister chromatid arm cohesion and homologous chromosome pairing. Journal of cell science *116*, 2999-3007.

Campos, C., Kamiya, M., Banala, S., Johnsson, K., and Gonzalez-Gaitan, M. (2011). Labelling cell structures and tracking cell lineage in zebrafish using SNAP-tag. Dev Dyn *240*, 820-827.

Carballo, J.A., Johnson, A.L., Sedgwick, S.G., and Cha, R.S. (2008). Phosphorylation of the axial element protein Hop1 by Mec1/Tel1 ensures meiotic interhomolog recombination. Cell *132*, 758-770.

Cha, R.S., Weiner, B.M., Keeney, S., Dekker, J., and Kleckner, N. (2000). Progression of meiotic DNA replication is modulated by interchromosomal interaction proteins, negatively by Spo11p and positively by Rec8p. Genes & development *14*, 493-503.

Chan, R.C., Chan, A., Jeon, M., Wu, T.F., Pasqualone, D., Rougvie, A.E., and Meyer, B.J. (2003). Chromosome cohesion is regulated by a clock gene paralogue TIM-1. Nature *423*, 1002-1009.

Chelysheva, L., Diallo, S., Vezon, D., Gendrot, G., Vrielynck, N., Belcram, K., Rocques, N., Marquez-Lema, A., Bhatt, A.M., Horlow, C.*, et al.* (2005). AtREC8 and AtSCC3 are essential to the monopolar orientation of the kinetochores during meiosis. Journal of cell science *118*, 4621-4632.

Chiang, T., Duncan, F.E., Schindler, K., Schultz, R.M., and Lampson, M.A. (2010). Evidence that weakened centromere cohesion is a leading cause of age-related aneuploidy in oocytes. Current biology : CB *20*, 1522-1528.

Ciosk, R., Shirayama, M., Shevchenko, A., Tanaka, T., Toth, A., and Nasmyth, K. (2000). Cohesin's binding to chromosomes depends on a separate complex consisting of Scc2 and Scc4 proteins. Mol Cell *5*, 243-254.

Ciosk, R., Zachariae, W., Michaelis, C., Shevchenko, A., Mann, M., and Nasmyth, K. (1998). An ESP1/PDS1 complex regulates loss of sister chromatid cohesion at the metaphase to anaphase transition in yeast. Cell *93*, 1067-1076.

Clejan, I., Boerckel, J., and Ahmed, S. (2006). Developmental modulation of nonhomologous end joining in Caenorhabditis elegans. Genetics *173*, 1301-1317.

Cohen-Fix, O., Peters, J.M., Kirschner, M.W., and Koshland, D. (1996). Anaphase initiation in Saccharomyces cerevisiae is controlled by the APC-dependent degradation of the anaphase inhibitor Pds1p. Genes & development *10*, 3081-3093.

Colaiacovo, M.P., MacQueen, A.J., Martinez-Perez, E., McDonald, K., Adamo, A., La Volpe, A., and Villeneuve, A.M. (2003). Synaptonemal complex assembly in C.

elegans is dispensable for loading strand-exchange proteins but critical for proper completion of recombination. Developmental cell *5*, 463-474.

Cortes-Ledesma, F., and Aguilera, A. (2006). Double-strand breaks arising by replication through a nick are repaired by cohesin-dependent sister-chromatid exchange. Embo Rep *7*, 919-926.

Couteau, F., and Zetka, M. (2005). HTP-1 coordinates synaptonemal complex assembly with homolog alignment during meiosis in C. elegans. Genes & development *19*, 2744-2756.

Covo, S., Westmoreland, J.W., Gordenin, D.A., and Resnick, M.A. (2010). Cohesin Is Limiting for the Suppression of DNA Damage-Induced Recombination between Homologous Chromosomes. PLoS genetics *6*, -.

Crittenden, S.L., Eckmann, C.R., Wang, L., Bernstein, D.S., Wickens, M., and Kimble, J. (2003). Regulation of the mitosis/meiosis decision in the Caenorhabditis elegans germline. Philosophical transactions of the Royal Society of London Series B, Biological sciences *358*, 1359-1362.

D'Ambrosio, C., Schmidt, C.K., Katou, Y., Kelly, G., Itoh, T., Shirahige, K., and Uhlmann, F. (2008). Identification of cis-acting sites for condensin loading onto budding yeast chromosomes. Genes & development *22*, 2215-2227.

Daley, J.M., Palmbos, P.L., Wu, D., and Wilson, T.E. (2005). Nonhomologous end joining in yeast. Annu Rev Genet *39*, 431-451.

Davis, L., and Smith, G.R. (2006). The meiotic bouquet promotes homolog interactions and restricts ectopic recombination in Schizosaccharomyces pombe. Genetics *174*, 167-177.

de Carvalho, C.E., Zaaijer, S., Smolikov, S., Gu, Y., Schumacher, J.M., and Colaiacovo, M.P. (2008). LAB-1 antagonizes the Aurora B kinase in C. elegans. Genes & development *22*, 2869-2885.

de los Santos, T., Hunter, N., Lee, C., Larkin, B., Loidl, J., and Hollingsworth, N.M. (2003). The Mus81/Mms4 endonuclease acts independently of double-Holliday junction resolution to promote a distinct subset of crossovers during meiosis in budding yeast. Genetics *164*, 81-94.

Deardorff, M.A., Bando, M., Nakato, R., Watrin, E., Itoh, T., Minamino, M., Saitoh, K., Komata, M., Katou, Y., Clark, D.*, et al.* (2012). HDAC8 mutations in Cornelia de Lange syndrome affect the cohesin acetylation cycle. Nature *489*, 313-317.

Degner, S.C., Wong, T.P., Jankevicius, G., and Feeney, A.J. (2009). Cutting edge: developmental stage-specific recruitment of cohesin to CTCF sites throughout immunoglobulin loci during B lymphocyte development. J Immunol *182*, 44-48.

Dernburg, A.F., McDonald, K., Moulder, G., Barstead, R., Dresser, M., and Villeneuve, A.M. (1998). Meiotic recombination in C. elegans initiates by a conserved mechanism and is dispensable for homologous chromosome synapsis. Cell *94*, 387-398.

Diaz-Martinez, L.A., Gimenez-Abian, J.F., and Clarke, D.J. (2007). Cohesin is dispensable for centromere cohesion in human cells. PloS one *2*, e318.

Doherty, A.J., and Jackson, S.P. (2001). DNA repair: how Ku makes ends meet. Curr Biol *11*, R920-924.

Dreier, M.R., Bekier, M.E., 2nd, and Taylor, W.R. (2011). Regulation of sororin by Cdk1-mediated phosphorylation. Journal of cell science *124*, 2976-2987.

Dutrillaux, B., Couturier, J., Richer, C.L., and Viegas-Pequignot, E. (1976). Sequence of DNA replication in 277 R- and Q-bands of human chromosomes using a BrdU treatment. Chromosoma *58*, 51-61.

Eckert, C.A., Gravdahl, D.J., and Megee, P.C. (2007). The enhancement of pericentromeric cohesin association by conserved kinetochore components promotes high-fidelity chromosome segregation and is sensitive to microtubule-based tension. Genes & development *21*, 278-291.

Eijpe, M., Heyting, C., Gross, B., and Jessberger, R. (2000). Association of mammalian SMC1 and SMC3 proteins with meiotic chromosomes and synaptonemal complexes. Journal of cell science *113 (Pt 4)*, 673-682.

Eijpe, M., Offenberg, H., Jessberger, R., Revenkova, E., and Heyting, C. (2003). Meiotic cohesin REC8 marks the axial elements of rat synaptonemal complexes before cohesins SMC1beta and SMC3. The Journal of cell biology *160*, 657-670.

Fernius, J., Nerusheva, O.O., Galander, S., Alves Fde, L., Rappsilber, J., and Marston, A.L. (2013). Cohesin-dependent association of scc2/4 with the centromere initiates pericentromeric cohesion establishment. Curr Biol *23*, 599-606.

Fire, A., Xu, S., Montgomery, M.K., Kostas, S.A., Driver, S.E., and Mello, C.C. (1998). Potent and specific genetic interference by double-stranded RNA in Caenorhabditis elegans. Nature *391*, 806-811.

Funabiki, H., Yamano, H., Kumada, K., Nagao, K., Hunt, T., and Yanagida, M. (1996). Cut2 proteolysis required for sister-chromatid seperation in fission yeast. Nature *381*, 438-441.

Fung, J.C., Rockmill, B., Odell, M., and Roeder, G.S. (2004). Imposition of crossover interference through the nonrandom distribution of synapsis initiation complexes. Cell *116*, 795-802.

Gandhi, R., Gillespie, P.J., and Hirano, T. (2006). Human Wapl is a cohesin-binding protein that promotes sister-chromatid resolution in mitotic prophase. Current Biology *16*, 2406-2417.

Garcia-Cruz, R., Brieno, M.A., Roig, I., Grossmann, M., Velilla, E., Pujol, A., Cabero, L., Pessarrodona, A., Barbero, J.L., and Garcia Caldes, M. (2010). Dynamics of cohesin proteins REC8, STAG3, SMC1 beta and SMC3 are consistent with a role in sister chromatid cohesion during meiosis in human oocytes. Hum Reprod *25*, 2316-2327.

Gause, M., Misulovin, Z., Bilyeu, A., and Dorsett, D. (2010). Dosage-sensitive regulation of cohesin chromosome binding and dynamics by Nipped-B, Pds5, and Wapl. Molecular and cellular biology *30*, 4940-4951.

Gerlich, D., Koch, B., Dupeux, F., Peters, J.M., and Ellenberg, J. (2006). Live-cell imaging reveals a stable cohesin-chromatin interaction after but not before DNA replication. Current biology : CB *16*, 1571-1578.

Gerton, J.L., DeRisi, J., Shroff, R., Lichten, M., Brown, P.O., and Petes, T.D. (2000). Global mapping of meiotic recombination hotspots and coldspots in the yeast Saccharomyces cerevisiae. Proceedings of the National Academy of Sciences of the United States of America *97*, 11383-11390.

Gillespie, P.J., and Hirano, T. (2004). Scc2 couples replication licensing to sister chromatid cohesion in Xenopus egg extracts. Current biology : CB *14*, 1598-1603.

Goodyer, W., Kaitna, S., Couteau, F., Ward, J.D., Boulton, S.J., and Zetka, M. (2008). HTP-3 links DSB formation with homolog pairing and crossing over during C. elegans meiosis. Developmental cell *14*, 263-274.

Gray, M., Piccirillo, S., Purnapatre, K., Schneider, B.L., and Honigberg, S.M. (2008). Glucose induction pathway regulates meiosis in Saccharomyces cerevisiae in part by controlling turnover of Ime2p meiotic kinase. FEMS yeast research *8*, 676-684.

Gruber, S., Arumugam, P., Katou, Y., Kuglitsch, D., Helmhart, W., Shirahige, K., and Nasmyth, K. (2006). Evidence that loading of cohesin onto chromosomes involves opening of its SMC hinge. Cell *127*, 523-537.

Gruber, S., Haering, C.H., and Nasmyth, K. (2003). Chromosomal cohesin forms a ring. Cell *112*, 765-777.

Gumienny, T.L., Lambie, E., Hartwieg, E., Horvitz, H.R., and Hengartner, M.O. (1999). Genetic control of programmed cell death in the Caenorhabditis elegans hermaphrodite germline. Development *126*, 1011-1022.

Hadjur, S., Williams, L.M., Ryan, N.K., Cobb, B.S., Sexton, T., Fraser, P., Fisher, A.G., and Merkenschlager, M. (2009). Cohesins form chromosomal cis-interactions at the developmentally regulated IFNG locus. Nature *460*, 410-413.

Haering, C.H., Farcas, A.M., Arumugam, P., Metson, J., and Nasmyth, K. (2008). The cohesin ring concatenates sister DNA molecules. Nature *454*, 297-301.

Haering, C.H., Lowe, J., Hochwagen, A., and Nasmyth, K. (2002). Molecular architecture of SMC proteins and the yeast cohesin complex. Molecular cell *9*, 773-788.

Haering, C.H., Schoffnegger, D., Nishino, T., Helmhart, W., Nasmyth, K., and Lowe, J. (2004). Structure and stability of cohesin's Smc1-kleisin interaction. Molecular cell *15*, 951-964.

Harper, N.C., Rillo, R., Jover-Gil, S., Assaf, Z.J., Bhalla, N., and Dernburg, A.F. (2011). Pairing centers recruit a Polo-like kinase to orchestrate meiotic chromosome dynamics in C. elegans. Developmental cell *21*, 934-947.

Hartman, T., Stead, K., Koshland, D., and Guacci, V. (2000). Pds5p is an essential chromosomal protein required for both sister chromatid cohesion and condensation in Saccharomyces cerevisiae. The Journal of cell biology *151*, 613-626.

Hassold, T., Hall, H., and Hunt, P. (2007). The origin of human aneuploidy: where we have been, where we are going. Human molecular genetics *16 Spec No. 2*, R203-208.

Hassold, T., and Hunt, P. (2001). To err (meiotically) is human: the genesis of human aneuploidy. Nature reviews Genetics *2*, 280-291.

Hassold, T.J., Burrage, L.C., Chan, E.R., Judis, L.M., Schwartz, S., James, S.J., Jacobs, P.A., and Thomas, N.S. (2001). Maternal folate polymorphisms and the etiology of human nondisjunction. American journal of human genetics *69*, 434-439.

Hauf, S., Roitinger, E., Koch, B., Dittrich, C.M., Mechtler, K., and Peters, J.M. (2005). Dissociation of cohesin from chromosome arms and loss of arm cohesion during early mitosis depends on phosphorylation of SA2. PLoS Biol *3*, e69.

Hauf, S., and Watanabe, Y. (2004). Kinetochore orientation in mitosis and meiosis. Cell *119*, 317-327.

Heidinger-Pauli, J.M., Mert, O., Davenport, C., Guacci, V., and Koshland, D. (2010). Systematic reduction of cohesin differentially affects chromosome segregation, condensation, and DNA repair. Curr Biol *20*, 957-963.

Heidinger-Pauli, J.M., Unal, E., Guacci, V., and Koshland, D. (2008). The kleisin subunit of cohesin dictates damage-induced cohesion. Molecular cell *31*, 47-56.

Heidinger-Pauli, J.M., Unal, E., and Koshland, D. (2009). Distinct targets of the Eco1 acetyltransferase modulate cohesion in S phase and in response to DNA damage. Mol Cell *34*, 311-321.

Henry, J.M., Camahort, R., Rice, D.A., Florens, L., Swanson, S.K., Washburn, M.P., and Gerton, J.L. (2006). Mnd1/Hop2 facilitates Dmc1-dependent interhomolog crossover formation in meiosis of budding yeast. Molecular and cellular biology *26*, 2913-2923.

Higashi, T.L., Ikeda, M., Tanaka, H., Nakagawa, T., Bando, M., Shirahige, K., Kubota, Y., Takisawa, H., Masukata, H., and Takahashi, T.S. (2012). The prereplication complex recruits XEco2 to chromatin to promote cohesin acetylation in Xenopus egg extracts. Current biology : CB *22*, 977-988.

Hirano, M., and Hirano, T. (2002). Hinge-mediated dimerization of SMC protein is essential for its dynamic interaction with DNA. The EMBO journal *21*, 5733-5744.

Hodges, C.A., Revenkova, E., Jessberger, R., Hassold, T.J., and Hunt, P.A. (2005). SMC1beta-deficient female mice provide evidence that cohesins are a missing link in age-related nondisjunction. Nature genetics *37*, 1351-1355.

Hofmann, E.R., Milstein, S., Boulton, S.J., Ye, M., Hofmann, J.J., Stergiou, L., Gartner, A., Vidal, M., and Hengartner, M.O. (2002). Caenorhabditis elegans HUS-1 is a DNA damage checkpoint protein required for genome stability and EGL-1-mediated apoptosis. Curr Biol *12*, 1908-1918.

Hollingsworth, N.M., Goetsch, L., and Byers, B. (1990). The HOP1 gene encodes a meiosis-specific component of yeast chromosomes. Cell *61*, 73-84.

Holloway, J.K., Booth, J., Edelmann, W., McGowan, C.H., and Cohen, P.E. (2008). MUS81 generates a subset of MLH1-MLH3-independent crossovers in mammalian meiosis. PLoS Genet *4*, e1000186.

Holmquist, G., Gray, M., Porter, T., and Jordan, J. (1982). Characterization of Giemsa dark- and light-band DNA. Cell *31*, 121-129.

Honigberg, S.M., and Purnapatre, K. (2003). Signal pathway integration in the switch from the mitotic cell cycle to meiosis in yeast. Journal of cell science *116*, 2137-2147.

Hu, B., Itoh, T., Mishra, A., Katoh, Y., Chan, K.L., Upcher, W., Godlee, C., Roig, M.B., Shirahige, K., and Nasmyth, K. (2011). ATP hydrolysis is required for relocating cohesin from sites occupied by its Scc2/4 loading complex. Curr Biol *21*, 12-24.

Hunter, N., and Kleckner, N. (2001). The single-end invasion: an asymmetric intermediate at the double-strand break to double-holliday junction transition of meiotic recombination. Cell *106*, 59-70.

Ishiguro, K., Kim, J., Fujiyama-Nakamura, S., Kato, S., and Watanabe, Y. (2011). A new meiosis-specific cohesin complex implicated in the cohesin code for homologous pairing. Embo Rep *12*, 267-275.

Ishiguro, T., Tanaka, K., Sakuno, T., and Watanabe, Y. (2010). Shugoshin-PP2A counteracts casein-kinase-1-dependent cleavage of Rec8 by separase. Nature cell biology *12*, 500-506.

Ivanov, D., and Nasmyth, K. (2005). A topological interaction between cohesin rings and a circular minichromosome. Cell *122*, 849-860.

Jaramillo-Lambert, A., Ellefson, M., Villeneuve, A.M., and Engebrecht, J. (2007). Differential timing of S phases, X chromosome replication, and meiotic prophase in the C. elegans germ line. Developmental biology *308*, 206-221.

Jin, H., Guacci, V., and Yu, H.G. (2009). Pds5 is required for homologue pairing and inhibits synapsis of sister chromatids during yeast meiosis. J Cell Biol *186*, 713-725.

Jones, G.H., and Franklin, F.C. (2006). Meiotic crossing-over: obligation and interference. Cell *126*, 246-248.

Kagami, A., Sakuno, T., Yamagishi, Y., Ishiguro, T., Tsukahara, T., Shirahige, K., Tanaka, K., and Watanabe, Y. (2011). Acetylation regulates monopolar attachment at multiple levels during meiosis I in fission yeast. Embo Rep *12*, 1189-1195.

Kassir, Y., Granot, D., and Simchen, G. (1988). IME1, a positive regulator gene of meiosis in S. cerevisiae. Cell *52*, 853-862.

Katis, V.L., Lipp, J.J., Imre, R., Bogdanova, A., Okaz, E., Habermann, B., Mechtler, K., Nasmyth, K., and Zachariae, W. (2010). Rec8 phosphorylation by casein kinase 1 and Cdc7-Dbf4 kinase regulates cohesin cleavage by separase during meiosis. Dev Cell *18*, 397-409.

Keeney, S., Giroux, C.N., and Kleckner, N. (1997). Meiosis-specific DNA double-strand breaks are catalyzed by Spo11, a member of a widely conserved protein family. Cell *88*, 375-384.

Keeney, S., and Neale, M.J. (2006). Initiation of meiotic recombination by formation of DNA double-strand breaks: mechanism and regulation. Biochemical Society transactions *34*, 523-525.

Kim, B.J., Li, Y.H., Zhang, J.L., Xi, Y.X., Li, Y.M., Yang, T., Jung, S.Y., Pan, X.W., Chen, R., Li, W*., et al.* (2010a). Genome-wide Reinforcement of Cohesin Binding at Pre-existing Cohesin Sites in Response to Ionizing Radiation in Human Cells. J Biol Chem *285*, 22782-22790.

Kim, K.P., Weiner, B.M., Zhang, L., Jordan, A., Dekker, J., and Kleckner, N. (2010b). Sister cohesion and structural axis components mediate homolog bias of meiotic recombination. Cell *143*, 924-937.

Kitajima, T.S., Kawashima, S.A., and Watanabe, Y. (2004). The conserved kinetochore protein shugoshin protects centromeric cohesion during meiosis. Nature *427*, 510-517.

Kitajima, T.S., Miyazaki, Y., Yamamoto, M., and Watanabe, Y. (2003). Rec8 cleavage by separase is required for meiotic nuclear divisions in fission yeast. The EMBO journal *22*, 5643-5653.

Kitajima, T.S., Sakuno, T., Ishiguro, K., Iemura, S., Natsume, T., Kawashima, S.A., and Watanabe, Y. (2006). Shugoshin collaborates with protein phosphatase 2A to protect cohesin. Nature *441*, 46-52.

Kleckner, N. (2006). Chiasma formation: chromatin/axis interplay and the role(s) of the synaptonemal complex. Chromosoma *115*, 175-194.

Klein, F., Mahr, P., Galova, M., Buonomo, S.B., Michaelis, C., Nairz, K., and Nasmyth, K. (1999). A central role for cohesins in sister chromatid cohesion, formation of axial elements, and recombination during yeast meiosis. Cell *98*, 91-103.

Kogut, I., Wang, J., Guacci, V., Mistry, R.K., and Megee, P.C. (2009). The Scc2/Scc4 cohesin loader determines the distribution of cohesin on budding yeast chromosomes. Genes & development *23*, 2345-2357.

Kudo, N.R., Anger, M., Peters, A.H., Stemmann, O., Theussl, H.C., Helmhart, W., Kudo, H., Heyting, C., and Nasmyth, K. (2009). Role of cleavage by separase of the Rec8 kleisin subunit of cohesin during mammalian meiosis I. Journal of cell science *122*, 2686-2698.

Kueng, S., Hegemann, B., Peters, B.H., Lipp, J.J., Schleiffer, A., Mechtler, K., and Peters, J.M. (2006). Wapl controls the dynamic association of cohesin with chromatin. Cell *127*, 955-967.

Kugou, K., Fukuda, T., Yamada, S., Ito, M., Sasanuma, H., Mori, S., Katou, Y., Itoh, T., Matsumoto, K., Shibata, T*., et al.* (2009). Rec8 Guides Canonical Spo11 Distribution along Yeast Meiotic Chromosomes. Molecular biology of the cell *20*, 3064-3076.

Latypov, V., Rothenberg, M., Lorenz, A., Octobre, G., Csutak, O., Lehmann, E., Loidl, J., and Kohli, J. (2010). Roles of Hop1 and Mek1 in meiotic chromosome pairing and recombination partner choice in Schizosaccharomyces pombe. Molecular and cellular biology *30*, 1570-1581.

Lee, C.Y., Conrad, M.N., and Dresser, M.E. (2012). Meiotic chromosome pairing is promoted by telomere-led chromosome movements independent of bouquet formation. PLoS Genet *8*, e1002730.

Lee, J. (2013). Hypoxia-inducible Factor-1 (HIF-1)-independent hypoxia response of the small heat shock protein hsp-16.1 gene regulated by chromatin-remodeling factors in the nematode Caenorhabditis elegans. J Biol Chem *288*, 1582-1589.

Lee, J., and Hirano, T. (2011). RAD21L, a novel cohesin subunit implicated in linking homologous chromosomes in mammalian meiosis. J Cell Biol *192*, 263-276.

Lengronne, A., Katou, Y., Mori, S., Yokobayashi, S., Kelly, G.P., Itoh, T., Watanabe, Y., Shirahige, K., and Uhlmann, F. (2004). Cohesin relocation from sites of chromosomal loading to places of convergent transcription. Nature *430*, 573-578.

Lengronne, A., McIntyre, J., Katou, Y., Kanoh, Y., Hopfner, K.P., Shirahige, K., and Uhlmann, F. (2006). Establishment of sister chromatid cohesion at the S. cerevisiae replication fork. Molecular cell *23*, 787-799.

Lichten, M. (2001). Meiotic recombination: breaking the genome to save it. Curr Biol *11*, R253-256.

Lightfoot, J., Testori, S., Barroso, C., and Martinez-Perez, E. (2011). Loading of meiotic cohesin by SCC-2 is required for early processing of DSBs and for the DNA damage checkpoint. Current biology : CB *21*, 1421-1430.

Lin, Y., Gill, M.E., Koubova, J., and Page, D.C. (2008). Germ cell-intrinsic and -extrinsic factors govern meiotic initiation in mouse embryos. Science *322*, 1685-1687.

Lindroos, H.B., Strom, L., Itoh, T., Katou, Y., Shirahige, K., and Sjogren, C. (2006). Chromosomal association of the Smc5/6 complex reveals that it functions in differently regulated pathways. Molecular cell *22*, 755-767.

Lister, L.M., Kouznetsova, A., Hyslop, L.A., Kalleas, D., Pace, S.L., Barel, J.C., Nathan, A., Floros, V., Adelfalk, C., Watanabe, Y.*, et al.* (2010). Age-related meiotic segregation errors in mammalian oocytes are preceded by depletion of cohesin and Sgo2. Current biology : CB *20*, 1511-1521.

Liu, H., Rankin, S., and Yu, H. (2013). Phosphorylation-enabled binding of SGO1-PP2A to cohesin protects sororin and centromeric cohesion during mitosis. Nature cell biology *15*, 40-49.

Llano, E., Herran, Y., Garcia-Tunon, I., Gutierrez-Caballero, C., de Alava, E., Barbero, J.L., Schimenti, J., de Rooij, D.G., Sanchez-Martin, M., and Pendas, A.M. (2012). Meiotic cohesin complexes are essential for the formation of the axial element in mice. J Cell Biol *197*, 877-885.

Loidl, J., Klein, F., and Scherthan, H. (1994). Homologous pairing is reduced but not abolished in asynaptic mutants of yeast. The Journal of cell biology *125*, 1191-1200.

Lopez-Serra, L., Lengronne, A., Borges, V., Kelly, G., and Uhlmann, F. (2013). Budding yeast Wapl controls sister chromatid cohesion maintenance and chromosome condensation. Current biology : CB *23*, 64-69.

Losada, A., Hirano, M., and Hirano, T. (1998). Identification of Xenopus SMC protein complexes required for sister chromatid cohesion. Genes & development *12*, 1986-1997.

Losada, A., Hirano, M., and Hirano, T. (2002). Cohesin release is required for sister chromatid resolution, but not for condensin-mediated compaction, at the onset of mitosis. Genes & development *16*, 3004-3016.

Losada, A., Yokochi, T., and Hirano, T. (2005). Functional contribution of Pds5 to cohesin-mediated cohesion in human cells and Xenopus egg extracts. Journal of cell science *118*, 2133-2141.

Lu, N., Yu, X., He, X., and Zhou, Z. (2009). Detecting apoptotic cells and monitoring their clearance in the nematode Caenorhabditis elegans. Methods Mol Biol *559*, 357-370.

MacQueen, A.J., Colaiacovo, M.P., McDonald, K., and Villeneuve, A.M. (2002). Synapsis-dependent and -independent mechanisms stabilize homolog pairing during meiotic prophase in C. elegans. Genes & development *16*, 2428-2442.

MacQueen, A.J., Phillips, C.M., Bhalla, N., Weiser, P., Villeneuve, A.M., and Dernburg, A.F. (2005). Chromosome sites play dual roles to establish homologous synapsis during meiosis in C. elegans. Cell *123*, 1037-1050.

MacQueen, A.J., and Villeneuve, A.M. (2001). Nuclear reorganization and homologous chromosome pairing during meiotic prophase require C. elegans chk-2. Genes & development *15*, 1674-1687.

Maller, J.L., and Krebs, E.G. (1980). Regulation of oocyte maturation. Curr Top Cell Regul *16*, 271-311.

Martin, J.S., Winkelmann, N., Petalcorin, M.I., McIlwraith, M.J., and Boulton, S.J. (2005). RAD-51-dependent and -independent roles of a Caenorhabditis elegans BRCA2-related protein during DNA double-strand break repair. Molecular and cellular biology *25*, 3127-3139.

Martinez-Perez, E., Schvarzstein, M., Barroso, C., Lightfoot, J., Dernburg, A.F., and Villeneuve, A.M. (2008). Crossovers trigger a remodeling of meiotic chromosome axis composition that is linked to two-step loss of sister chromatid cohesion. Genes & development *22*, 2886-2901.

Martinez-Perez, E., and Villeneuve, A.M. (2005). HTP-1-dependent constraints coordinate homolog pairing and synapsis and promote chiasma formation during C. elegans meiosis. Genes & development *19*, 2727-2743.

Maurel, D., Comps-Agrar, L., Brock, C., Rives, M.L., Bourrier, E., Ayoub, M.A., Bazin, H., Tinel, N., Durroux, T., Prezeau, L.*, et al.* (2008). Cell-surface protein-protein interaction analysis with time-resolved FRET and snap-tag technologies: application to GPCR oligomerization. Nat Methods *5*, 561-567.

Mazina, O.M., Mazin, A.V., Nakagawa, T., Kolodner, R.D., and Kowalczykowski, S.C. (2004). Saccharomyces cerevisiae Mer3 helicase stimulates 3'-5' heteroduplex extension by Rad51; implications for crossover control in meiotic recombination. Cell *117*, 47-56.

McAleenan, A., Clemente-Blanco, A., Cordon-Preciado, V., Sen, N., Esteras, M., Jarmuz, A., and Aragon, L. (2013). Post-replicative repair involves separase-dependent removal of the kleisin subunit of cohesin. Nature *493*, 250-254.

McAleenan, A., Cordon-Preciado, V., Clemente-Blanco, A., Liu, I.C., Sen, N., Leonard, J., Jarmuz, A., and Aragon, L. (2012). SUMOylation of the alpha-kleisin subunit of cohesin is required for DNA damage-induced cohesion. Curr Biol *22*, 1564-1575.

McKee, A.H., and Kleckner, N. (1997). A general method for identifying recessive diploid-specific mutations in Saccharomyces cerevisiae, its application to the isolation of mutants blocked at intermediate stages of meiotic prophase and characterization of a new gene SAE2. Genetics *146*, 797-816.

Melby, T.E., Ciampaglio, C.N., Briscoe, G., and Erickson, H.P. (1998). The symmetrical structure of structural maintenance of chromosomes (SMC) and MukB proteins: long, antiparallel coiled coils, folded at a flexible hinge. J Cell Biol *142*, 1595-1604.

Mercier, R., Jolivet, S., Vezon, D., Huppe, E., Chelysheva, L., Giovanni, M., Nogue, F., Doutriaux, M.P., Horlow, C., Grelon, M.*, et al.* (2005). Two meiotic crossover classes cohabit in Arabidopsis: one is dependent on MER3,whereas the other one is not. Curr Biol *15*, 692-701.

Merritt, C., Rasoloson, D., Ko, D., and Seydoux, G. (2008). 3' UTRs are the primary regulators of gene expression in the C. elegans germline. Curr Biol *18*, 1476-1482.

Mets, D.G., and Meyer, B.J. (2009). Condensins regulate meiotic DNA break distribution, thus crossover frequency, by controlling chromosome structure. Cell *139*, 73-86.

Michaelis, C., Ciosk, R., and Nasmyth, K. (1997). Cohesins: Chromosomal proteins that prevent premature separation of sister chromatids. Cell *91*, 35-45.

Minn, I.L., Rolls, M.M., Hanna-Rose, W., and Malone, C.J. (2009). SUN-1 and ZYG-12, mediators of centrosome-nucleus attachment, are a functional SUN/KASH pair in Caenorhabditis elegans. Molecular biology of the cell *20*, 4586-4595.

Misulovin, Z., Schwartz, Y.B., Li, X.Y., Kahn, T.G., Gause, M., MacArthur, S., Fay, J.C., Eisen, M.B., Pirrotta, V., Biggin, M.D.*, et al.* (2008). Association of cohesin and Nipped-B with transcriptionally active regions of the Drosophila melanogaster genome. Chromosoma *117*, 89-102.

Mito, Y., Sugimoto, A., and Yamamoto, M. (2003). Distinct developmental function of two Caenorhabditis elegans homologs of the cohesin subunit Scc1/Rad21. Mol Biol Cell *14*, 2399-2409.

Molnar, M., Bahler, J., Sipiczki, M., and Kohli, J. (1995). The rec8 gene of Schizosaccharomyces pombe is involved in linear element formation, chromosome pairing and sister-chromatid cohesion during meiosis. Genetics *141*, 61-73.

Moore, J.K., and Haber, J.E. (1996). Cell cycle and genetic requirements of two pathways of nonhomologous end-joining repair of double-strand breaks in Saccharomyces cerevisiae. Molecular and cellular biology *16*, 2164-2173.

Moses, M.J., Counce, S.J., and Paulson, D.F. (1975). Synaptonemal complex complement of man in spreads of spermatocytes, with details of the sex chromosome pair. Science *187*, 363-365.

Murakami, H., and Nurse, P. (2001). Regulation of premeiotic S phase and recombination-related double-strand DNA breaks during meiosis in fission yeast. Nature genetics *28*, 290-293.

Nabeshima, K., Villeneuve, A.M., and Colaiacovo, M.P. (2005). Crossing over is coupled to late meiotic prophase bivalent differentiation through asymmetric disassembly of the SC. J Cell Biol *168*, 683-689.

Nasmyth, K. (2011). Cohesin: a catenase with separate entry and exit gates? Nature cell biology *13*, 1170-1177.

Nasmyth, K., and Haering, C.H. (2009). Cohesin: Its Roles and Mechanisms. Annual review of genetics *43*, 525-558.

Nasmyth, K., and Schleiffer, A. (2004). From a single double helix to paired double helices and back. Philos T Roy Soc B *359*, 99-108.

Navadgi-Patil, V.M., and Burgers, P.M. (2009). A tale of two tails: activation of DNA damage checkpoint kinase Mec1/ATR by the 9-1-1 clamp and by Dpb11/TopBP1. DNA Repair (Amst) *8*, 996-1003.

Neale, M.J., Pan, J., and Keeney, S. (2005). Endonucleolytic processing of covalent protein-linked DNA double-strand breaks. Nature *436*, 1053-1057.

Nicklas, R.B. (1988). The forces that move chromosomes in mitosis. Annual review of biophysics and biophysical chemistry *17*, 431-449.

Nicklas, R.B. (1997). How cells get the right chromosomes. Science *275*, 632-637.

Nishimura, K., Fukagawa, T., Takisawa, H., Kakimoto, T., and Kanemaki, M. (2009). An auxin-based degron system for the rapid depletion of proteins in nonplant cells. Nat Methods *6*, 917-922.

Nishiyama, T., Ladurner, R., Schmitz, J., Kreidl, E., Schleiffer, A., Bhaskara, V., Bando, M., Shirahige, K., Hyman, A.A., Mechtler, K.*, et al.* (2010). Sororin Mediates Sister Chromatid Cohesion by Antagonizing Wapl. Cell *143*, 737-749.

Panizza, S., Tanaka, T., Hochwagen, A., Eisenhaber, F., and Nasmyth, K. (2000). Pds5 cooperates with cohesin in maintaining sister chromatid cohesion. Current biology : CB *10*, 1557-1564.

Parelho, V., Hadjur, S., Spivakov, M., Leleu, M., Sauer, S., Gregson, H.C., Jarmuz, A., Canzonetta, C., Webster, Z., Nesterova, T.*, et al.* (2008). Cohesins functionally associate with CTCF on mammalian chromosome arms. Cell *132*, 422-433.

Pasierbek, P., Fodermayr, M., Jantsch, V., Jantsch, M., Schweizer, D., and Loidl, J. (2003). The Caenorhabditis elegans SCC-3 homologue is required for meiotic synapsis and for proper chromosome disjunction in mitosis and meiosis. Experimental cell research *289*, 245-255.

Pasierbek, P., Jantsch, M., Melcher, M., Schleiffer, A., Schweizer, D., and Loidl, J. (2001). A Caenorhabditis elegans cohesion protein with functions in meiotic chromosome pairing and disjunction. Genes & development *15*, 1349-1360.

Pauli, A., Althoff, F., Oliveira, R.A., Heidmann, S., Schuldiner, O., Lehner, C.F., Dickson, B.J., and Nasmyth, K. (2008). Cell-type-specific TEV protease cleavage reveals cohesin functions in Drosophila neurons. Developmental cell *14*, 239-251.

Pauli, A., van Bemmel, J.G., Oliveira, R.A., Itoh, T., Shirahige, K., van Steensel, B., and Nasmyth, K. (2010). A direct role for cohesin in gene regulation and ecdysone response in Drosophila salivary glands. Current biology : CB *20*, 1787-1798.

Penkner, A.M., Fridkin, A., Gloggnitzer, J., Baudrimont, A., Machacek, T., Woglar, A., Csaszar, E., Pasierbek, P., Ammerer, G., Gruenbaum, Y.*, et al.* (2009). Meiotic chromosome homology search involves modifications of the nuclear envelope protein Matefin/SUN-1. Cell *139*, 920-933.

Phillips, C.M., Meng, X., Zhang, L., Chretien, J.H., Urnov, F.D., and Dernburg, A.F. (2009). Identification of chromosome sequence motifs that mediate meiotic pairing and synapsis in C. elegans. Nature cell biology *11*, 934-942.

Prinz, S., Amon, A., and Klein, F. (1997). Isolation of COM1, a new gene required to complete meiotic double-strand break-induced recombination in Saccharomyces cerevisiae. Genetics *146*, 781-795.

Regoes, A., and Hehl, A.B. (2005). SNAP-tag mediated live cell labeling as an alternative to GFP in anaerobic organisms. Biotechniques *39*, 809-810, 812.

Remeseiro, S., and Losada, A. (2013). Cohesin, a chromatin engagement ring. Current opinion in cell biology *25*, 63-71.

Resnick, T.D., Satinover, D.L., MacIsaac, F., Stukenberg, P.T., Earnshaw, W.C., Orr-Weaver, T.L., and Carmena, M. (2006). INCENP and Aurora B promote meiotic sister chromatid cohesion through localization of the Shugoshin MEI-S332 in Drosophila. Dev Cell *11*, 57-68.

Revenkova, E., Eijpe, M., Heyting, C., Gross, B., and Jessberger, R. (2001). Novel meiosis-specific isoform of mammalian SMC1. Molecular and cellular biology *21*, 6984-6998.

Revenkova, E., Eijpe, M., Heyting, C., Hodges, C.A., Hunt, P.A., Liebe, B., Scherthan, H., and Jessberger, R. (2004). Cohesin SMC1 beta is required for meiotic chromosome dynamics, sister chromatid cohesion and DNA recombination. Nature cell biology *6*, 555-562.

Revenkova, E., Herrmann, K., Adelfalk, C., and Jessberger, R. (2010). Oocyte cohesin expression restricted to predictyate stages provides full fertility and prevents aneuploidy. Current biology : CB *20*, 1529-1533.

Riedel, C.G., Katis, V.L., Katou, Y., Mori, S., Itoh, T., Helmhart, W., Galova, M., Petronczki, M., Gregan, J., Cetin, B.*, et al.* (2006). Protein phosphatase 2A protects centromeric sister chromatid cohesion during meiosis I. Nature *441*, 53-61.

Rinaldo, C., Ederle, S., Rocco, V., and La Volpe, A. (1998). The Caenorhabditis elegans RAD51 homolog is transcribed into two alternative mRNAs potentially encoding proteins of different sizes. Molecular & general genetics : MGG *260*, 289-294.

Robine, N., Uematsu, N., Amiot, F., Gidrol, X., Barillot, E., Nicolas, A., and Borde, V. (2007). Genome-wide redistribution of meiotic double-strand breaks in Saccharomyces cerevisiae. Molecular and cellular biology *27*, 1868-1880.

Rockmill, B., and Roeder, G.S. (1998). Telomere-mediated chromosome pairing during meiosis in budding yeast. Genes & development *12*, 2574-2586.

Rogers, E., Bishop, J.D., Waddle, J.A., Schumacher, J.M., and Lin, R. (2002). The aurora kinase AIR-2 functions in the release of chromosome cohesion in Caenorhabditis elegans meiosis. J Cell Biol *157*, 219-229.

Rolef Ben-Shahar, T., Heeger, S., Lehane, C., East, P., Flynn, H., Skehel, M., and Uhlmann, F. (2008). Eco1-dependent cohesin acetylation during establishment of sister chromatid cohesion. Science *321*, 563-566.

Rollins, R.A., Morcillo, P., and Dorsett, D. (1999). Nipped-B, a Drosophila homologue of chromosomal adherins, participates in activation by remote enhancers in the cut and Ultrabithorax genes. Genetics *152*, 577-593.

Rowland, B.D., Roig, M.B., Nishino, T., Kurze, A., Uluocak, P., Mishra, A., Beckouet, F., Underwood, P., Metson, J., Imre, R.*, et al.* (2009). Building sister chromatid cohesion: smc3 acetylation counteracts an antiestablishment activity. Molecular cell *33*, 763-774.

Rubio, E.D., Reiss, D.J., Welcsh, P.L., Disteche, C.M., Filippova, G.N., Baliga, N.S., Aebersold, R., Ranish, J.A., and Krumm, A. (2008). CTCF physically links cohesin to chromatin. Proceedings of the National Academy of Sciences of the United States of America *105*, 8309-8314.

Rumpf, C., Cipak, L., Dudas, A., Benko, Z., Pozgajova, M., Riedel, C.G., Ammerer, G., Mechtler, K., and Gregan, J. (2010). Casein kinase 1 is required for efficient removal of Rec8 during meiosis I. Cell Cycle *9*, 2657-2662.

Sato, A., Isaac, B., Phillips, C.M., Rillo, R., Carlton, P.M., Wynne, D.J., Kasad, R.A., and Dernburg, A.F. (2009). Cytoskeletal forces span the nuclear envelope to coordinate meiotic chromosome pairing and synapsis. Cell *139*, 907-919.

Schaaf, C.A., Misulovin, Z., Sahota, G., Siddiqui, A.M., Schwartz, Y.B., Kahn, T.G., Pirrotta, V., Gause, M., and Dorsett, D. (2009). Regulation of the Drosophila Enhancer of split and invected-engrailed gene complexes by sister chromatid cohesion proteins. PloS one *4*, e6202.

Scherthan, H., Weich, S., Schwegler, H., Heyting, C., Harle, M., and Cremer, T. (1996). Centromere and telomere movements during early meiotic prophase of mouse and man are associated with the onset of chromosome pairing. The Journal of cell biology *134*, 1109-1125.

Schwacha, A., and Kleckner, N. (1995). Identification of double Holliday junctions as intermediates in meiotic recombination. Cell *83*, 783-791.

Schwacha, A., and Kleckner, N. (1997). Interhomolog bias during meiotic recombination: meiotic functions promote a highly differentiated interhomolog-only pathway. Cell *90*, 1123-1135.

Seitan, V.C., Hao, B., Tachibana-Konwalski, K., Lavagnolli, T., Mira-Bontenbal, H., Brown, K.E., Teng, G., Carroll, T., Terry, A., Horan, K.*, et al.* (2011). A role for

cohesin in T-cell-receptor rearrangement and thymocyte differentiation. Nature *476*, 467-471.

Severson, A.F., Ling, L., Van Zuylen, V., and Meyer, B.J. (2009). The axial element protein HTP-3 promotes cohesin loading and meiotic axis assembly in C. elegans to implement the meiotic program of chromosome segregation. Genes & development *23*, 1763-1778.

Shinohara, A., Ogawa, H., and Ogawa, T. (1992). Rad51 protein involved in repair and recombination in S. cerevisiae is a RecA-like protein. Cell *69*, 457-470.

Shinohara, M., Sakai, K., Shinohara, A., and Bishop, D.K. (2003). Crossover interference in Saccharomyces cerevisiae requires a TID1/RDH54- and DMC1-dependent pathway. Genetics *163*, 1273-1286.

Siomos, M.F., Badrinath, A., Pasierbek, P., Livingstone, D., White, J., Glotzer, M., and Nasmyth, K. (2001). Separase is required for chromosome segregation during meiosis I in Caenorhabditis elegans. Curr Biol *11*, 1825-1835.

Sjogren, C., and Nasmyth, K. (2001). Sister chromatid cohesion is required for postreplicative double-strand break repair in Saccharomyces cerevisiae. Current Biology *11*, 991-995.

Slimko, E.M., and Lester, H.A. (2003). Codon optimization of Caenorhabditis elegans GluCl ion channel genes for mammalian cells dramatically improves expression levels. J Neurosci Methods *124*, 75-81.

Smith, A.V., and Roeder, G.S. (1997). The yeast Red1 protein localizes to the cores of meiotic chromosomes. The Journal of cell biology *136*, 957-967.

Smolikov, S., Eizinger, A., Schild-Prufert, K., Hurlburt, A., McDonald, K., Engebrecht, J., Villeneuve, A.M., and Colaiacovo, M.P. (2007). SYP-3 restricts synaptonemal complex assembly to bridge paired chromosome axes during meiosis in Caenorhabditis elegans. Genetics *176*, 2015-2025.

Smolikov, S., Schild-Prufert, K., and Colaiacovo, M.P. (2009). A yeast two-hybrid screen for SYP-3 interactors identifies SYP-4, a component required for synaptonemal complex assembly and chiasma formation in Caenorhabditis elegans meiosis. PLoS genetics *5*, e1000669.

Snowden, T., Acharya, S., Butz, C., Berardini, M., and Fishel, R. (2004). hMSH4-hMSH5 recognizes Holliday Junctions and forms a meiosis-specific sliding clamp that embraces homologous chromosomes. Molecular cell *15*, 437-451.

Strachan, T. (2005). Cornelia de Lange Syndrome and the link between chromosomal function, DNA repair and developmental gene regulation. Current opinion in genetics & development *15*, 258-264.

Strom, L., Lindroos, H.B., Shirahige, K., and Sjogren, C. (2004). Postreplicative recruitment of cohesin to double-strand breaks is required for DNA repair. Mol Cell *16*, 1003-1015.

Strom, L., and Sjogren, C. (2005). DNA damage-induced cohesion. Cell Cycle *4*, 536-539.

Sullivan, M., Hornig, N.C., Porstmann, T., and Uhlmann, F. (2004). Studies on substrate recognition by the budding yeast separase. J Biol Chem *279*, 1191-1196.

Sumara, I., Vorlaufer, E., Gieffers, C., Peters, B.H., and Peters, J.M. (2000). Characterization of vertebrate cohesin complexes and their regulation in prophase. J Cell Biol *151*, 749-762.

Sumara, I., Vorlaufer, E., Stukenberg, P.T., Kelm, O., Redemann, N., Nigg, E.A., and Peters, J.M. (2002). The dissociation of cohesin from chromosomes in prophase is regulated by Polo-like kinase. Mol Cell *9*, 515-525.

Sun, H., Treco, D., Schultes, N.P., and Szostak, J.W. (1989). Double-strand breaks at an initiation site for meiotic gene conversion. Nature *338*, 87-90.

Sung, P., and Robberson, D.L. (1995). DNA strand exchange mediated by a RAD51-ssDNA nucleoprotein filament with polarity opposite to that of RecA. Cell *82*, 453-461.

Sung, W.K., Van't Hof, J., and Jagiello, G. (1986). DNA synthesis studies in pre-meiotic mouse oogenesis. Experimental cell research *163*, 370-380.

Sym, M., Engebrecht, J.A., and Roeder, G.S. (1993). ZIP1 is a synaptonemal complex protein required for meiotic chromosome synapsis. Cell *72*, 365-378.

Symington, L.S., Brown, A., Oliver, S.G., Greenwell, P., and Petes, T.D. (1991). Genetic analysis of a meiotic recombination hotspot on chromosome III of Saccharomyces cerevisiae. Genetics *128*, 717-727.

Szostak, J.W., Orr-Weaver, T.L., Rothstein, R.J., and Stahl, F.W. (1983). The double-strand-break repair model for recombination. Cell *33*, 25-35.

Tachibana-Konwalski, K., Godwin, J., van der Weyden, L., Champion, L., Kudo, N.R., Adams, D.J., and Nasmyth, K. (2010). Rec8-containing cohesin maintains bivalents without turnover during the growing phase of mouse oocytes. Genes & development *24*, 2505-2516.

Takahashi, T.S., Basu, A., Bermudez, V., Hurwitz, J., and Walter, J.C. (2008). Cdc7-Drf1 kinase links chromosome cohesion to the initiation of DNA replication in Xenopus egg extracts. Genes & development *22*, 1894-1905.

Tanaka, T., Cosma, M.P., Wirth, K., and Nasmyth, K. (1999). Identification of cohesin association sites at centromeres and along chromosome arms. Cell *98*, 847-858.

Tanno, Y., Kitajima, T.S., Honda, T., Ando, Y., Ishiguro, K., and Watanabe, Y. (2010). Phosphorylation of mammalian Sgo2 by Aurora B recruits PP2A and MCAK to centromeres. Genes & development *24*, 2169-2179.

Toth, A., Ciosk, R., Uhlmann, F., Galova, M., Schleiffer, A., and Nasmyth, K. (1999). Yeast cohesin complex requires a conserved protein, Eco1p(Ctf7), to establish cohesion between sister chromatids during DNA replication. Genes & development *13*, 320-333.

Tsai, C.J., Mets, D.G., Albrecht, M.R., Nix, P., Chan, A., and Meyer, B.J. (2008). Meiotic crossover number and distribution are regulated by a dosage

compensation protein that resembles a condensin subunit. Genes & development *22*, 194-211.

Tsubouchi, H., and Ogawa, H. (1998). A novel mre11 mutation impairs processing of double-strand breaks of DNA during both mitosis and meiosis. Molecular and cellular biology *18*, 260-268.

Tsubouchi, H., and Ogawa, H. (2000). Exo1 roles for repair of DNA double-strand breaks and meiotic crossing over in Saccharomyces cerevisiae. Molecular biology of the cell *11*, 2221-2233.

Tzur, Y.B., Egydio de Carvalho, C., Nadarajan, S., Van Bostelen, I., Gu, Y., Chu, D.S., Cheeseman, I.M., and Colaiacovo, M.P. (2012). LAB-1 targets PP1 and restricts Aurora B kinase upon entrance into meiosis to promote sister chromatid cohesion. PLoS Biol *10*, e1001378.

Uhlmann, F., Lottspeich, F., and Nasmyth, K. (1999). Sister-chromatid separation at anaphase onset is promoted by cleavage of the cohesin subunit Scc1. Nature *400*, 37-42.

Uhlmann, F., and Nasmyth, K. (1998). Cohesion between sister chromatids must be established during DNA replication. Curr Biol *8*, 1095-1101.

Uhlmann, F., Wernic, D., Poupart, M.A., Koonin, E.V., and Nasmyth, K. (2000). Cleavage of cohesin by the CD clan protease separin triggers anaphase in yeast. Cell *103*, 375-386.

Unal, E., Arbel-Eden, A., Sattler, U., Shroff, R., Lichten, M., Haber, J.E., and Koshland, D. (2004). DNA damage response pathway uses histone modification to assemble a double-strand break-specific cohesin domain. Mol Cell *16*, 991-1002.

Unal, E., Heidinger-Pauli, J.M., Kim, W., Guacci, V., Onn, I., Gygi, S.P., and Koshland, D.E. (2008). A molecular determinant for the establishment of sister chromatid cohesion. Science *321*, 566-569.

Unal, E., Heidinger-Pauli, J.M., and Koshland, D. (2007). DNA double-strand breaks trigger genome-wide sister-chromatid cohesion through Eco1 (Ctf7). Science *317*, 245-248.

Vaur, S., Feytout, A., Vazquez, S., and Javerzat, J.P. (2012). Pds5 promotes cohesin acetylation and stable cohesin-chromosome interaction. Embo Rep *13*, 645-652.

Vega, H., Waisfisz, Q., Gordillo, M., Sakai, N., Yanagihara, I., Yamada, M., van Gosliga, D., Kayserili, H., Xu, C., Ozono, K.*, et al.* (2005). Roberts syndrome is caused by mutations in ESCO2, a human homolog of yeast ECO1 that is essential for the establishment of sister chromatid cohesion. Nature genetics *37*, 468-470.

Verni, F., Gandhi, R., Goldberg, M.L., and Gatti, M. (2000). Genetic and molecular analysis of wings apart-like (wapl), a gene controlling heterochromatin organization in Drosophila melanogaster. Genetics *154*, 1693-1710.

Wagner, C.R., Kuervers, L., Baillie, D.L., and Yanowitz, J.L. (2010). xnd-1 regulates the global recombination landscape in Caenorhabditis elegans. Nature *467*, 839-843.

Waizenegger, I.C., Hauf, S., Meinke, A., and Peters, J.M. (2000). Two distinct pathways remove mammalian cohesin from chromosome arms in prophase and from centromeres in anaphase. Cell *103*, 399-410.

Wang, F., Ulyanova, N.P., van der Waal, M.S., Patnaik, D., Lens, S.M., and Higgins, J.M. (2011). A positive feedback loop involving Haspin and Aurora B promotes CPC accumulation at centromeres in mitosis. Curr Biol *21*, 1061-1069.

Wang, F., Yoder, J., Antoshechkin, I., and Han, M. (2003). Caenorhabditis elegans EVL-14/PDS-5 and SCC-3 are essential for sister chromatid cohesion in meiosis and mitosis. Molecular and cellular biology *23*, 7698-7707.

Watrin, E., Schleiffer, A., Tanaka, K., Eisenhaber, F., Nasmyth, K., and Peters, J.M. (2006). Human Scc4 is required for cohesin binding to chromatin, sister-chromatid cohesion, and mitotic progression. Curr Biol *16*, 863-874.

Wendt, K.S., Yoshida, K., Itoh, T., Bando, M., Koch, B., Schirghuber, E., Tsutsumi, S., Nagae, G., Ishihara, K., Mishiro, T.*, et al.* (2008). Cohesin mediates transcriptional insulation by CCCTC-binding factor. Nature *451*, 796-801.

Williamson, D.H., Johnston, L.H., Fennell, D.J., and Simchen, G. (1983). The timing of the S phase and other nuclear events in yeast meiosis. Experimental cell research *145*, 209-217.

Wilson, T.E., Grawunder, U., and Lieber, M.R. (1997). Yeast DNA ligase IV mediates non-homologous DNA end joining. Nature *388*, 495-498.

Wood, A.J., Lo, T.W., Zeitler, B., Pickle, C.S., Ralston, E.J., Lee, A.H., Amora, R., Miller, J.C., Leung, E., Meng, X.*, et al.* (2011). Targeted genome editing across species using ZFNs and TALENs. Science *333*, 307.

Wu, L., and Hickson, I.D. (2003). The Bloom's syndrome helicase suppresses crossing over during homologous recombination. Nature *426*, 870-874.

Wynne, D.J., Rog, O., Carlton, P.M., and Dernburg, A.F. (2012). Dynein-dependent processive chromosome motions promote homologous pairing in C. elegans meiosis. The Journal of cell biology *196*, 47-64.

Xu, H., Beasley, M.D., Warren, W.D., van der Horst, G.T., and McKay, M.J. (2005). Absence of mouse REC8 cohesin promotes synapsis of sister chromatids in meiosis. Dev Cell *8*, 949-961.

Xu, H.L., Beasley, M., Verschoor, S., Inselman, A., Handel, M.A., and McKay, M.J. (2004). A new role for the mitotic RAD21/SCC1 cohesin in meiotic chromosome cohesion and segregation in the mouse. Embo Rep *5*, 378-384.

Yazdi, P.T., Wang, Y., Zhao, S., Patel, N., Lee, E.Y.H.P., and Qin, J. (2002). SMC1 is a downstream effector in the ATM/NBS1 branch of the human S-phase checkpoint. Genes & development *16*, 571-582.

Yokoo, R., Zawadzki, K.A., Nabeshima, K., Drake, M., Arur, S., and Villeneuve, A.M. (2012). COSA-1 reveals robust homeostasis and separable licensing and reinforcement steps governing meiotic crossovers. Cell *149*, 75-87.

Yoon, P.W., Freeman, S.B., Sherman, S.L., Taft, L.F., Gu, Y., Pettay, D., Flanders, W.D., Khoury, M.J., and Hassold, T.J. (1996). Advanced maternal age and the risk

of Down syndrome characterized by the meiotic stage of chromosomal error: a population-based study. American journal of human genetics *58*, 628-633.

Youds, J.L., Mets, D.G., McIlwraith, M.J., Martin, J.S., Ward, J.D., NJ, O.N., Rose, A.M., West, S.C., Meyer, B.J., and Boulton, S.J. (2010). RTEL-1 enforces meiotic crossover interference and homeostasis. Science *327*, 1254-1258.

Yu, H.G., and Koshland, D. (2005). Chromosome morphogenesis: condensin-dependent cohesin removal during meiosis. Cell *123*, 397-407.

Zakharyevich, K., Ma, Y., Tang, S., Hwang, P.Y., Boiteux, S., and Hunter, N. (2010). Temporally and biochemically distinct activities of Exo1 during meiosis: double-strand break resection and resolution of double Holliday junctions. Molecular cell *40*, 1001-1015.

Zalevsky, J., MacQueen, A.J., Duffy, J.B., Kemphues, K.J., and Villeneuve, A.M. (1999). Crossing over during Caenorhabditis elegans meiosis requires a conserved MutS-based pathway that is partially dispensable in budding yeast. Genetics *153*, 1271-1283.

Zeiser, E., Frokjaer-Jensen, C., Jorgensen, E., and Ahringer, J. (2011). MosSCI and gateway compatible plasmid toolkit for constitutive and inducible expression of transgenes in the C. elegans germline. PloS one *6*, e20082.

Zetka, M.C., Kawasaki, I., Strome, S., and Muller, F. (1999). Synapsis and chiasma formation in Caenorhabditis elegans require HIM-3, a meiotic chromosome core component that functions in chromosome segregation. Genes & development *13*, 2258-2270.

Zhang, B., Chang, J., Fu, M., Huang, J., Kashyap, R., Salavaggione, E., Jain, S., Kulkarni, S., Deardorff, M.A., Uzielli, M.L.*, et al.* (2009). Dosage effects of cohesin regulatory factor PDS5 on mammalian development: implications for cohesinopathies. PloS one *4*, e5232.

Zhang, J., Hakansson, H., Kuroda, M., and Yuan, L. (2008a). Wapl localization on the synaptonemal complex, a meiosis-specific proteinaceous structure that binds homologous chromosomes, in the female mouse. Reprod Domest Anim *43*, 124-126.

Zhang, J., Shi, X., Li, Y., Kim, B.J., Jia, J., Huang, Z., Yang, T., Fu, X., Jung, S.Y., Wang, Y.*, et al.* (2008b). Acetylation of Smc3 by Eco1 is required for S phase sister chromatid cohesion in both human and yeast. Molecular cell *31*, 143-151.

Zhang, M., and Xia, G. (2012). Hormonal control of mammalian oocyte meiosis at diplotene stage. Cell Mol Life Sci *69*, 1279-1288.

Zhang, Z., Ren, Q., Yang, H., Conrad, M.N., Guacci, V., Kateneva, A., and Dresser, M.E. (2005). Budding yeast PDS5 plays an important role in meiosis and is required for sister chromatid cohesion. Mol Microbiol *56*, 670-680.

Zickler, D., and Kleckner, N. (1999). Meiotic chromosomes: integrating structure and function. Annual review of genetics *33*, 603-754.

Zou, H., McGarry, T.J., Bernal, T., and Kirschner, M.W. (1999). Identification of a vertebrate sister-chromatid separation inhibitor involved in transformation and tumorigenesis. Science *285*, 418-422.